



HAL
open science

Wet granulation of cohesive powders: Rheology, growth mechanisms and granule strength

Toma-Mihai Chitu

► **To cite this version:**

Toma-Mihai Chitu. Wet granulation of cohesive powders: Rheology, growth mechanisms and granule strength. Chemical and Process Engineering. Institut National Polytechnique de Toulouse - INPT, 2009. English. NNT: 2009INPT040G . tel-04400740

HAL Id: tel-04400740

<https://theses.hal.science/tel-04400740>

Submitted on 17 Jan 2024

HAL is a multi-disciplinary open access archive for the deposit and dissemination of scientific research documents, whether they are published or not. The documents may come from teaching and research institutions in France or abroad, or from public or private research centers.

L'archive ouverte pluridisciplinaire **HAL**, est destinée au dépôt et à la diffusion de documents scientifiques de niveau recherche, publiés ou non, émanant des établissements d'enseignement et de recherche français ou étrangers, des laboratoires publics ou privés.



THÈSE

En vue de l'obtention du

DOCTORAT DE L'UNIVERSITÉ DE TOULOUSE

Délivré par *Institut National Polytechnique de Toulouse*
Discipline ou spécialité : Génie des procédés

Présentée et soutenue par *M. Toma-Mihai CHITU*
Le 10 Décembre 2009

Titre : *GRANULATION HUMIDE DES POUDRES COHESIVES: RHEOLOGIE, MECANISMES DE CROISSANCE ET TENUE MECANIQUE DES GRANULES*

JURY

MM. CHULIA Dominique, Professeur, Université de LimogesMembre
M. CHAOUKI Jamal, Professeur, Université Polytechnique Montréal.....Rapporteur
M. SALEH Khashayar, Professeur, Université de Compiègne..... Rapporteur
M. DIGUET Sylvain, Dr Ing, DSM Nutritional Products Suisse.....Membre
M. DE RYCK Alain, Professeur, EMAC, Albi.....Membre
M. HEMATI Mehrdji, Professeur, INP Toulouse.....Co-directeur de thèse
M. OULAHNA Driss, Maitre Assistant HDR, EMAC, Albi Directeur de thèse

Ecole doctorale : *Mécanique, Energétique, Génie civil et Procédés*
Unité de recherche : *RAPSODEE (centre de Recherches d'Albi en génie des Procédés, des Solides Divisés, de l'Energie et de l'Environnement)*
Directeur(s) de Thèse : *Driss OULAHNA et Mehrdji HEMATI*

*A mes parents et ma famille,
A mes amis,
A Rodi*

Remerciements

Cette thèse a été le fruit d'une collaboration entre le centre de recherche Rapsodee d'Albi et le Laboratoire de Génie Chimique de Toulouse et ce travail a été réalisé au sein du Laboratoire de Poudres et Procédés à l'École des Mines d'Albi.

J'aimerais tout d'abord remercier M. Driss Oulahna pour m'avoir confié ce sujet de thèse qui m'a permis de découvrir ce domaine fascinant du milieu granulaire. Je tiens particulièrement à le remercier pour sa direction et ses encouragements, pour nos discussions scientifiques et amicales pour lesquelles il a consacré beaucoup de son temps et aussi pour m'avoir toujours poussé à ouvrir des portes, notamment en termes de collaborations.

Je remercie sincèrement M. Mehrdji Hemati pour son soutien tout au long de cette thèse et son enthousiasme, pour nos discussions, toujours enrichissantes, autour des résultats et pour sa pédagogie.

J'adresse mes remerciements à M. Alain de Ryck pour avoir accepté de présider le jury soutenance de ce mémoire et aux rapporteurs M. Khashayar Saleh et M. Jamal Chaouki pour leurs remarques constructives et pertinentes.

Je tiens aussi à remercier à M^{me} Dominique Chulia et M. Sylvain Diguët qui ont bien voulu juger ce travail et examiner en détail mon manuscrit.

J'exprime mes remerciements au personnel administratif de l'École des Mines d'Albi (M^{me} Ghislaine Reynes et M^{me} Claudette Loubatière, M^{me} Sylvaine Ponthus et M^{me} Cathy Mauriès), aux enseignants chercheurs du centre Rapsodee, M. Radu Barna, M^{me} Fabienne Espitalier, M. Abder Michrafy, M. O. Lecoq, M^{elle} Patricia Arlabosse, M. Martial Sauceau et aux techniciens : M^{me} Séverine Patry, M^{me} Sylvie Delconfeto, M. Laurent Devriendt, M. Philippe Accart, M. Denis Marty et M^{me} Christine Rolland.

Je remercie mes amis et mes collègues, surtout Romain et Guillaume mais aussi les autres doctorants de l'Emac et ailleurs avec qui j'ai passé des moments joyeux : Radu J, Marius, Cristina S, Cristina D, Francisco, Harona...

Finalement, je remercie mon épouse Rodi, mes parents et mes amis pour leur soutien, affection et confiance.

TABLE OF CONTENTS

	Page
Introduction	12/16
Chapter I. Essentials of High Shear Wet Granulation	19
1. Introduction	20
2. Inter-particle Forces	22
3. Theory of Granulation	24
3.1 Introduction	24
3.2 Nucleation Mechanisms	26
3.3 Granule Growth	28
3.4 Breakage and Attrition	35
4. Granule Strength	37
4.1 Equipment variables and operating conditions	38
4.2 Binder viscosity	39
4.3 Binder surface tension, contact angle, primary particle shape	40
5. Wet Mass Rheology	40
6. Scaling	44
7. Conclusion	46
Chapter II. Materials and Methods	53
1. Materials	54
1.1 Microcrystalline Cellulose	54
1.2 Lactose	58
1.3 Binder Properties	59
2. Characterization Methods	62
2.1 Morphological Characterization Methods	62
2.2 Rheological Characterization Methods	65
2.2.1 Flowability of the Starting Powders	65
2.2.2 Characterization of Binder Powder Interactions	67
2.3 Mechanical Characterization Methods	69

2.3.1 Preliminary Tests	71
3. Wet Granulation Protocol and Equipment	74
3.1 Introduction	74
3.2 Wet Granulation Protocol	76
3.3 The Mi-Pro HSM	77
3.4 The Diosna P1-6 HSM	79
4. Conclusion	80
Chapter III. Effect of Operating Conditions and Material Properties on the Wet Granulation in a Laboratory HSG	82
III.1 Typical Example	83
1. Introduction	83
2. Granulation Mechanisms	84
3. Optimum Liquid Requirement	89
4. Granule Strength	91
4.1 Wet Granule Strength	91
4.2 Dry Granule Strength	93
5. Conclusion	97
III.2 Effect of Operating Conditions	100
1. Effect of Fill Ratio	101
1.1. Introduction	101
1.2. Effect of Fill Ratio	101
2. Effect of Chopper Presence and Design and Impeller Speed	114
2.1. Introduction	114
2.2. Effect of Chopper Presence and Design and Impeller Speed	115
3. Effect of Equipment Geometry	130
4. Conclusion	134
III.3 Effect of Formulation:	
Effect of Binder Nature and Properties	137
1. Introduction	137
2. Effect of Binder Nature and Properties	139
2.1 Rheological Properties of the Powder-Binder Couple	139
2.2 Granulation Kinetics for the Studied Binders	141
2.3 Granule Strength	147
2.4 Effect of Mixer Design	151
3. Conclusion	154

III.4 Effect of Formulation:	
Granulation of Soluble and Insoluble Powders	156
1. Introduction	156
2. Effect of Formulation: Granulation of Soluble and Insoluble Powders	158
2.1 Characterization of the Starting Materials	158
2.2 Powder Mixtures Characterization	162
2.2.1 Rheological Characterization	162
2.2.2 Granulation Kinetics	164
2.2.3 Morphology Evolution	169
2.3 Granule Strength	172
2.4 Effect of Mixer Design	173
3. Conclusion	177
Synopsis et Points Clés de L'Etude	181
Conclusions and Perspectives	196
List of Appendices	200
I. Dry Binders Datasheets	201
II. Methods	203
II.1 Contact Angle Measurement for MCC Avicel 105	203
II.2 Viscosity Determination	206
II.3 Flow Function Determination	208
III. Roundness Curves in Histograms	212
List of Symbols	215
List of General Alphanumeric References	219
Abstract/Résumé	227

**Communications Orales et Actes de Congrès
(Comité de Sélection et de Lecture)**

Effect of binder type on wet mass rheology and mechanical properties of granule in high shear mixer granulation. Chitu T-M., Oulahna D., Hemati M. XII SFGP, Marseille, France, Oct.2009. (Oral Conference)

Wet granulation in a laboratory scale high shear mixer: Effect of chopper presence, design and impeller speed". Chitu T-M., Oulahna D., Hemati M. 9th Int. Symp. on Agglomeration, Sheffield, UK, June 2009. (Prix du Meilleur Poster avec Relevance Pharmaceutique)

Wet granulation in laboratory high shear mixers : effect of physico-chemical properties. Chitu T-M., Oulahna D., Hemati M. 9th Int. Symp. on Agglomeration, Sheffield, UK, June 2009. (Oral Conference)

Rhéologie, Croissance Granulaire et Résistance Mécanique des Granules: Application au transfert d'échelle. Chitu T-M., Oulahna D., Hemati M. Congrès STPMF Science et technologie des Poudres et Matériaux Frittés, Montpellier, Mai 2009. (Poster)

Wet granulation in a Mi-Pro high shear mixer granulator: Effect of agitation. Chitu T-M., Oulahna D., Hemati M. PSA, Particulate System Analysis, Stratford, UK, Sept. 2008, (Oral Conference)

Prediction of granulation mechanisms in high shear mixing granulation for soluble and insoluble substrates using rheological characterization and moisture sorption isotherms. Chitu T-M., Oulahna D., Hemati M. CHISA, 18th International Congress of Chemical and Process Engineering, Prague, CZ, August 2008. (Oral Conference)

Articles soumis à publication:

Rheology, granule growth and strength : Application to the wet granulation of lactose-MCC mixtures, Chitu T-M., Oulahna D., Hemati M., Powder Technology, Accepté (2009).

Wet granulation in laboratory scale high shear mixers : Effect of chopper presence, design and impeller speed, Chitu T-M., Oulahna D., Hemati M., Powder Technology, Sous review, (2009).

Wet granulation in laboratory scale high shear mixers: Effect of binder properties, Chitu T-M., Oulahna D., Hemati M., Powder Technology, Sous review, (2009).

INTRODUCTION GENERALE

La granulation en voie humide est un procédé courant dans diverses industries (chimie fine, pharmacie, alimentaire et minérale). Plusieurs travaux de recherche depuis ces 20 dernières années portent sur l'étude et la compréhension des processus mis en jeu au niveau des poudres et des liants utilisés et au niveau des procédés mis en œuvre.

Les approches de formulation solide (avec choix de phases liantes) sont basées sur des modèles et des essais expérimentaux qui restent à valider pour chaque type de fonctionnalité recherchée (tailles, formes, propriétés mécaniques des granules, etc.).

Une difficulté souvent rencontrée est le contrôle du procédé du point de vue de la quantité optimale du liant et qui dépend essentiellement de l'opérateur et des propriétés finales des granules recherchées. Les difficultés se manifestent le plus souvent pour le contrôle d'un procédé de granulation avec de nouveaux produits. C'est aussi le cas où on souhaite prendre en compte un changement dans la formulation ou établir un changement d'échelle du procédé.

Au plan microstructural, la mise en forme par croissance granulaire humide trouve actuellement des bases scientifiques et des lois de comportement granulaire qui justifient leurs adaptations aux poudres usuellement utilisées. Les connaissances pratiques dans l'industrie pharmaceutique permettent d'ajuster les différents paramètres (poudres, liants, agglomérats et variables du procédé), mais nécessitent une étude systémique lourde allant des propriétés intrinsèques des poudres aux propriétés finales des granules.

Un des cas généralement rencontré dans les poudres pharmaceutiques (excipients) est l'impact des solubilités des substrats solides et son influence sur les approches énergie de surface, choix des liants, et finalement la procédure d'identification de mécanismes de croissance.

Comme nous allons le développer dans ce manuscrit, la complémentarité des modèles d'énergie de surface et des modèles visqueux de croissance peuvent donner des critères

de choix entre l'analyse en phase humide (solide-liquide) et l'évolution des tenues mécaniques.

Notre étude porte donc sur des poudres largement rencontrées dans la formulation solide pharmaceutique (Lactose et deux variétés de cellulose microcristalline). Ces poudres présentent néanmoins des difficultés liés à leur solubilité (lactose), au mélange (poudres cohésives) et en termes de suivi de la cinétique de croissance granulaire (collage sur les parois).

Parmi nos objectifs, on peut citer les points suivants:

1. Mettre en place une méthodologie d'identification des mécanismes de granulation et contrôle des taux de liant en tenant compte des variables intrinsèques des poudres.
2. Corréler les paramètres physico-chimiques (solide-liant), la rhéologie de la masse humide et la tenue mécanique des agglomérats (granules) secs obtenus.
3. Identifier l'évolution des structures granulaires (via l'approche rhéologie) des mécanismes de croissance des mélanges de poudres hydro-soluble / hydro-insoluble et spécialement (MCC + Lactose).
4. Corréler les profils rhéologiques de granulation humide issus de deux approches et contraintes différentes (cas du mélangeur à haut cisaillement Mi-Pro Procept® et du rhéomètre MTR Caléva®). Ceci devra nous permettre de revenir sur les liens entre la nature des pontages liquides mise en jeu dans la granulation humide et l'évolution d'un profil rhéologique général.

Nous avons fait le choix de présenter une thèse de doctorat rédigée en anglais avec les parties introductives et conclusions en français et anglais.

En fin de manuscrit, nous avons souhaité présenter un rappel, en français, de données clés de cette étude sous forme de « Synopsis ».

Ce manuscrit s'articule autour de 3 Chapitres. Le premier est dédié à un rappel succinct des connaissances actuelles dans le domaine de la granulation humide à fort taux de cisaillement. Nous avons volontairement réduit ce parcours bibliographique car plusieurs références et thèses de doctorat avaient développé cet aspect. Une liste bibliographique est donnée à la fin de chaque chapitre du manuscrit ainsi qu'une liste alphabétique (en

annexe) des auteurs cités dans ce travail. Nous décrirons, néanmoins, les connaissances à ce jour au niveau de l'influence des paramètres opératoires et matières premières ainsi que les outils de contrôle généralement appliqués.

Le deuxième chapitre regroupe l'ensemble des techniques et procédés utilisés dans ce travail et présente les données et caractérisations des matériaux et liants utilisés. On y présente aussi les méthodes mises en place pour l'identification des résistances mécaniques des granules.

Le troisième chapitre (découpé en 4 sous chapitres) regroupe l'essentiel de nos résultats expérimentaux et analyses et synthèses des données. Les 4 parties de ce chapitre développent :

- la méthodologie mise en place pour granuler nos matériaux ainsi que l'approche mécanique pour la résistance à la compression de nos granules. Nous présentons cette méthodologie sous forme d'un exemple type de granulation humide,
- l'effet des variables opératoires, comme le taux de remplissage, la vitesse d'agitation de la pale, la présence et la dimension de l'émetteur ainsi que la dépendance entre ces variables. Une place importante est donnée à l'effet du taux de remplissage à différentes vitesses d'agitation,
- l'effet des propriétés des phases liantes et des approche physico-chimie des interfaces (mouillabilité, angle de contact, travail d'adhésion, viscosité),
- l'effet de la formulation solide lors de la granulation des mélanges (binaires) des poudres hydro-solubles / hydro-insolubles.

Ainsi, dans cette étude, on se propose de développer des démarches permettant d'associer le comportement lors de la granulation (mécanismes, cinétiques de croissance, etc.) et les notions de consistance des granules humides et rhéologie avec la tenue mécanique à l'échelle du grain sec.

INTRODUCTION

Wet granulation is a process encountered in many industries (chemical, pharmaceutical, food and mining). A multitude of research papers of the last 20 years have tried to bring more understanding to the process in terms of binders and powders used and the equipments used.

The solid formulation approach and the choice of the binding agent are based on models and experimental work that must be validated for each type of desired end-product property (size, shape, mechanical properties) etc.

An often encountered difficulty is the control/monitoring of the process for an optimum binder requirement. This requirement depends largely on the operator and the desired end-granule properties. Difficulties arise for the control of the process when new products are involved. It is also the case when a new formulation is developed or the scale of the process has to be changed.

At the micro scale size enlargement by wet granulation finds a scientific background and models that justify their adaptations for the more common powders. Practical knowledge within the pharmaceutical research allows adjusting the different influencing factors (starting materials, operating conditions) but they require systematic study ranging from starting materials characterization to end-granule properties.

An often encountered case in the granulation of pharmaceutical excipients is the influence of soluble powders and their impact on the binder surface energy, binder choice and the identification of growth mechanisms.

As it will be developed in this study the complementarity of the surface energy and the viscous growth models can give criteria of choice between the characterization in the wet state (solid-liquid) and the evolution of granule strength.

Our study deals with the wet granulation of fine, cohesive excipients generally used in the pharmaceutical industry (lactose and two grades of microcrystalline cellulose). These powders present however difficulties from a mixing point of view, solubility and granule growth kinetics.

The objectives of this study include:

1. Defining a methodology allowing the identification of granule growth mechanisms and optimum binder requirement control taking into account the physico-chemical properties of the starting materials.
2. Relating physico-chemical properties of the starting materials (powder, binder solution), rheology and dry granule strength.
3. Identifying the evolution of granule growth mechanisms by rheological approach of binary mixtures of water soluble / water insoluble powders.
4. Comparison of torque curves obtained under different constraints (Mi-Pro Procept® high shear mixer and MTR Caleva® mixer torque rheometer) which should allow relating the nature of liquid bridges and the evolution of torque.

We chose to present a PhD thesis written in english with introductive and concluding remarks in both english and french. At the end of the paper a reminder of objectives, approach, results and conclusions is given in french under the title "Synopsis".

The thesis contains three chapters. The first is dedicated to short introduction into the world of wet granulation research. We kept this part short and concise on purpose since this aspect is generally well covered in literature (Handbooks) as well as other PhD thesis. We describe the knowledge to date as well as the means of control usually encountered. For convenience references are given at the end of each chapter and a general alphabetic list is given at the end of the thesis.

The second chapter gives a description of the materials and methods used in this study as well as the equipment used. The experimental method used to describe granule strength and its optimization is also described.

The third chapter contains the results and discussions related to the investigated parameters. The 4 sub-chapters describe:

- the methodology allowing the characterization of the wet granulation process runs as well as the characterization of the granules mechanical strength. We present this methodology as a typical example of wet granulation,
- the effect of operating conditions like fill ratio, impeller speed, chopper presence and design (size) as well as the interaction between these factors. A special focus is set on the granulation at different impeller speeds for different fill ratios,
- the effect of binder physico-chemical properties and the approach of wetting thermodynamics (wettability, contact angle, work of adhesion) and kinetics (viscosity),
- the effect of solid formulation on the granulation of binary mixtures of water soluble / water insoluble powders.

In this study we wish to develop techniques that allow relating the behavior observed during granulation (mechanisms, kinetics etc.) and the notions of wet mass consistency and rheology to the dry granule strength at the scale of the dry agglomerate.

CHAPTER I

Essentials of High Shear Wet Granulation

Chapter I: Essentials of High Shear Wet Granulation

1. Introduction

The agglomeration of particulate solids in order to enlarge their size is an old technique encountered in many of today's industries. For each case be it the pharmaceutical, food or mining industry the substitution of the powder with agglomerated material presents certain advantages: the improvement of flow properties allowing an easier handling, the reduction of dust quantity in the work environment reducing inhalation risks and explosion hazard, improving on the products aspect and strength, segregation can be reduced while other properties like solubility and chemical reactivity can be improved. When an agglomeration technique implies agitation it is usually called granulation. Granulation is an agglomeration technique that allows obtaining granules with desired characteristics and functionality and can also be referred to as balling, pelletisation or coating.

Granulation can be achieved by dry or wet methods depending on the initial powder properties and the required final granule properties. Dry granulation can be preferable when the product is sensitive to moisture. It can be achieved with small highly cohesive particles with sizes smaller than several microns only by applying pressure by extruding/compacting, fluidizing or tumbling [1,2] with another important aspect being the avoidance of a drying step. Subsequently dry granulation can be achieved in extruders, roller compactors, fluid or tumbling beds.

Wet granulation is achieved by bringing in an intimate contact the initial powder particles with a binder solution. This can be done in high or low shear mixers, fluid bed granulators, tumbling drums or extruders. A variation of the wet granulation technique is the melt granulation - here the binder is added as a dry powder to the initial powder and

upon heating and melting allows the creation of material bridges between the initial particles in a similar manner to the wet granulation.

The focus of this thesis is set on the study of granulation done in high shear mixers. This is a batch process consisting of a bowl equipped with a multi blade impeller and a chopper. This type of mixers can be found in the pharmaceutical, agrochemical and detergent industry because of their capacity to handle difficult initial powder formulations. The feed powder is usually dry mixed before the process starts so as to break up any dry agglomerates that may be already present in the mix and ensure homogenous starting conditions of each batch. Binder is then added either at the beginning or gradually during the process. Binder added gradually can be added in a drop by drop fashion or sprayed on. In the wet massing stage the impeller ensures the mixing of powder and binder as well as the densification by shearing and impacting while the chopper is used to break up large agglomerates ensuring a redistribution of the material and obtaining a higher homogeneity in the final product. Finally the wet massing stage is followed by a drying stage. The advantages presented by the high shear granulation process are that they can process wet sticky materials, can spread viscous binders, can handle cohesive powders, are less sensitive to operating conditions than tumbling granulators and can produce small high density granules [3].

The formation of granules in wet high shear mixing can be viewed as a succession of stages:

1. Wetting: the initial particles are wetted by the liquid binder (solvent alone, solution or molten) and no bridges are formed between the initial particles;
2. Growth of the particles: occurs first by nucleation, a process that when sufficient liquid is present at the granule surface allows for two or more granules to stick together. Under impact with the impeller, chopper, bowl walls and other particles these nuclei are densified squeezing more liquid to the surface and allowing to bind more particles.
3. Breakage of granules: can also take place at the same time as growth and depending on the ratio between breakage and growth an equilibrium phase can be reached in granule growth.

2. Inter-particular Forces

The forces that hold granules together were first approached by Rumpf [4,5] distinguishing between bonds with and without material bonds, followed by other researchers (Israelachvili [6] Schubert [7]; Tomas and Schubert [8]; Tomas [9]):

With material bonds:

- solid bridges created by mass transfer by sinter bridges because of high temperatures, partial melting, chemical reaction, hardening binders or crystal bridges because of recrystallization;
- liquid bridges:
 - low mobility liquid bridges given by highly viscous binders that create strong bonds close in terms of strength to the solid bridges;
 - mobile liquid bridges created by surface tension and capillary pressure

Without material bonds:

- molecular forces (Van-der-Waals forces, free chemical bonds or valence forces, hydrogen bridges), electric and magnetic forces are forces that work at short range ($<1\mu\text{m}$) and depend on the roughness and size ($<100\mu\text{m}$) of the initial particles
- interlocking bonds if the particles present a certain shape like fibers or threads that can twist and bend around each other or entangle during agglomeration.

Figure 1 gives a graphic representation of these forces as given by Tomas [10] while Figure 2 shows the relative force of these types of bonds as a function of particle size [11,12]. Schubert [7] has shown that the Van der Waals forces are dominant between the forces without material bridge when the particle sizes are smaller than 100 microns.

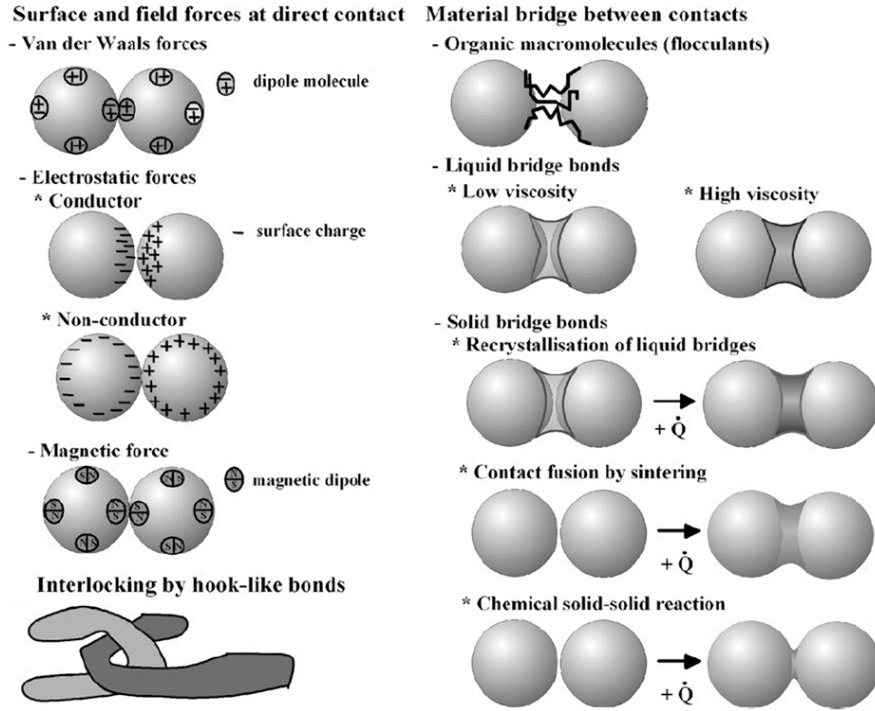


Figure 1. Bonds between particles as seen by Tomas [10]

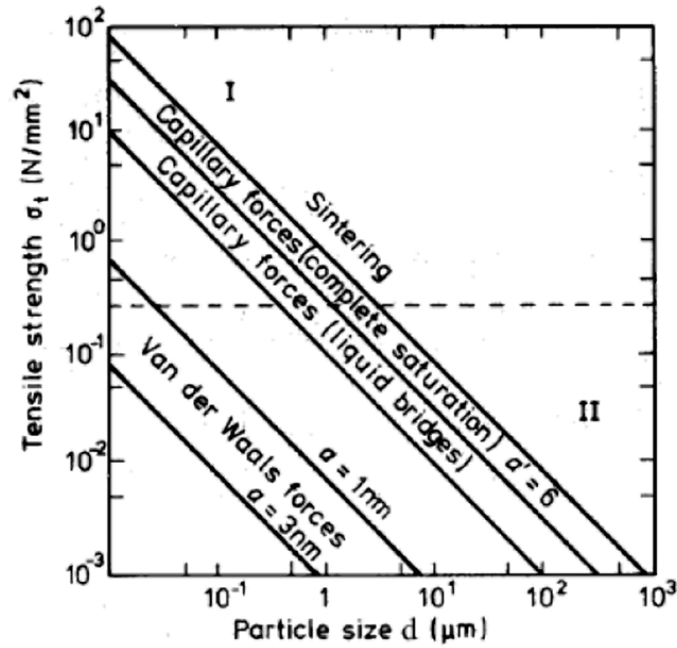


Figure 2. Tensile strength as a function of interparticle bonding mechanism and particle size (Rumpf [11], Pietsch [12])

3. Theory of Granulation

3.1 Introduction

Newitt and Conway-Jones [13] described the different stages of liquid bonding in granules and defined four stages: the pendular, the funicular, the capillary and the droplet stage (Figure 3).

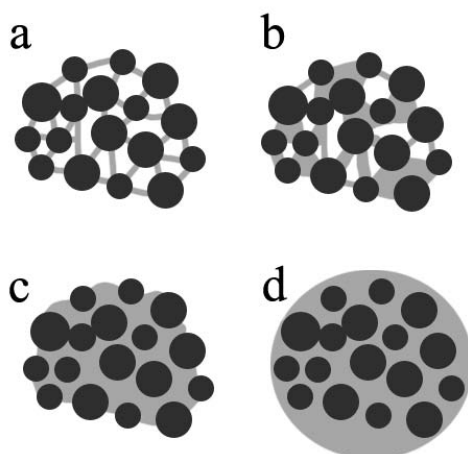


Figure 3. Granule saturation stages: a-pendular, b-funicular, c-capillary and d-droplet

Before the addition of liquid to the dry powder mix agglomerates only exist due to attractive forces like the Van der Waals forces. The pendular stage is the first saturation stage - here particles are kept together by few liquid bridges present only at the contact points between the initial particles. The funicular stage is an intermediary stage between the capillary and the pendular stage - the amount of liquid has now increased and the bridges can bind more particles with the voids between the liquid bridges partly saturated with liquid. In the capillary stage this voids are saturated with liquid. The capillary stage is supposed to give the highest granule strength. At the surface of the agglomerate the liquid is drawn back into the pores under capillary action while inside the agglomerate the voids are completely filled with liquid. The droplet stage corresponds to what is generally called in granulation as over-wetting, the wetted mass loses most of its strength and turns into a paste and upon further liquid addition to a suspension. In high shear wet granulation the passage between these states can be a result of continued binder

addition as well as consolidation of the granules as a result of collisions with impeller, other granules or bowl walls increasing the saturation of the granules by reducing the interparticular voids.

The modern theory of granulation [14] retains three granulation mechanisms (Figure 4) defined as:

1. Wetting and Nucleation,
2. Consolidation and Growth
3. Attrition and Breakage

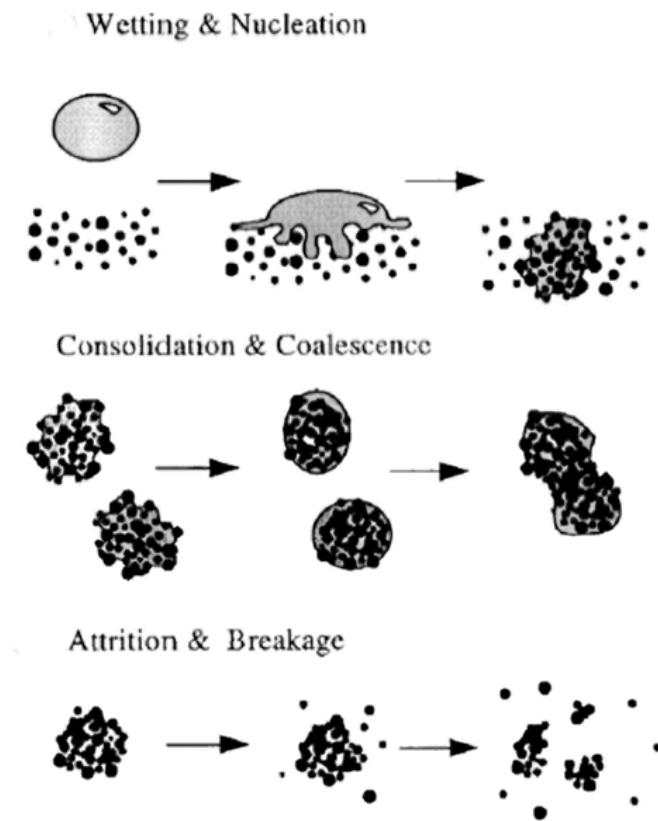


Figure 4. Mechanisms of granulation Iveson et al [14]

3.2 Nucleation Mechanisms

After being wetted by the liquid binder, granules start to agglomerate to form initial nuclei of two or more particles in the nucleation stage. Of special importance in this initial stage is the wetting zone which is defined as the zone where powder and liquid first come into contact. The nucleation stage is influenced by the wetting thermodynamics, drop penetration kinetics and binder dispersion. This initial stage is very important for the outcome of the granulation process. A choice of powder and binder that can lead to poor wetting or a choice of operating conditions like an increased liquid flow rate combined with an insufficiently high mixing speed can both lead to granulation runs with low reproducibility and small yields. Wetting thermodynamics establish if wetting is energetically favorable or not with the contact angle (θ) between solid and binder and the spreading coefficient (λ) of the liquid on the powder surface as main parameters to be controlled.

The spreading coefficient λ shows the tendency of a powder-binder couple to spread over each other and depends on the works of cohesion and adhesion:

$$\text{Work of cohesion for the solid: } W_{CS} = 2\gamma_{SV} \quad (\text{I-1})$$

$$\text{Work of cohesion for the liquid: } W_{CL} = 2\gamma_{LV} \quad (\text{I-2})$$

$$\text{Work of adhesion between liquid and solid: } W_a = \gamma_{LV} (\cos \theta + 1) \quad (\text{I-3})$$

$$\text{Liquid-solid spreading coefficient: } \lambda_{LS} = W_a - W_{CL} \quad (\text{I-4})$$

$$\text{Solid-liquid spreading coefficient: } \lambda_{SL} = W_a - W_{CS} \quad (\text{I-5})$$

Where θ is the contact angle, λ the spreading coefficient, γ the surface free energy and L, S and V show the state as being liquid, solid and vapor respectively. Equation I-3 is only valid for $\theta > 0$ which is a common case in wet granulation experiments. According to Rowe [15] two situations may be encountered as a function of λ_{LS} and λ_{SL} :

-When $\lambda_{LS} > 0$ and $\lambda_{SL} < 0$ the binder forms a strong film around the solid particles and granule properties depend on the binder properties,

-When $\lambda_{LS} < 0$ and $\lambda_{SL} > 0$ the binder does not form a film around the particles and only isolated parts are covered with liquid.

Aulton and Banks [16] have shown that increasing contact angle, by changing the ratio of hydrophobic and hydrophilic powders (salicylic acid, $\theta=103^\circ$ and lactose, $\theta=30^\circ$) in the powder mix, while granulating with a 5% PVP aqueous solution in a fluid bed granulator, reduces the size of the final granulated product. Tüske et al. [17] have shown that by changing the nature of the powder (microcrystalline cellulose, lactose and starch) if the work of cohesion of the binder (hydroxypropylcellulose) is inferior to the work of cohesion of the powder and the work of adhesion binder/powder the binder coats the particles in a uniform layer. They also showed that a positive spreading coefficient for a two component system (binder+powder) can lead to dense, non-friable pellets but that certain limitations exist when trying to predict granule properties from spreading coefficients alone for more complex systems where the work of cohesion of the binder can also play an important role.

The nucleation mechanism is highly dependant on the drop size relative to the primary powder particles. Shaefer and Mathiesen [18] proposed the following scenarios (Figure 5) for the case of melt granulation and were later on extended by Scott et al [19] to cover wet granulation.:

- If the drops are relatively small nucleation will occur by distribution of the drops on the particle surface which will then coalesce to form nuclei.
- If the drop is much larger than the initial particles nucleation will take place by immersion of the particles into the drop producing nuclei with saturated pores.

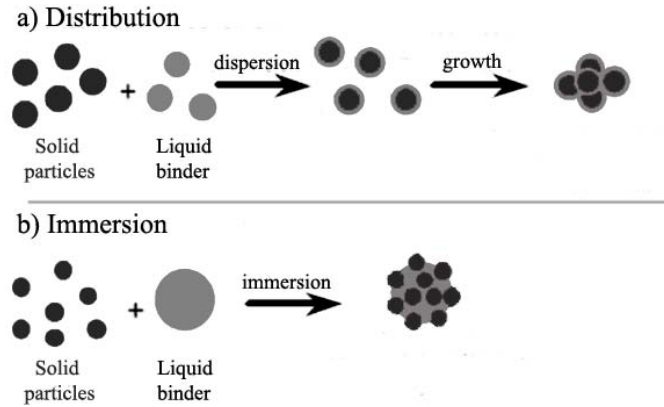


Figure 5. Mechanisms of nucleation after Schaefer and Mathiesen [18]

In the case of immersion the theory proposed by Denesuk et al [20] for the penetration of a single drop into a porous surface applies the Washburn equation where flow is promoted by the capillary pressure and opposed by viscous dissipation giving a theoretical penetration time described by the following equation:

$$\tau = \frac{2V_0^2}{\pi^2 \varepsilon^2 r_d^4 R_{pore}} \frac{\mu}{\gamma_{LV} \cos \theta} \quad (\text{I-6})$$

Where V_0 is the total drop volume, ε the external porosity, r_d the radius of the drop footprint on the surface, R_{pore} the effective pore radius based on cylindrical pores, μ is the liquid viscosity, γ_{LV} the liquid surface tension and θ the contact angle. This equation shows the direct dependence between nucleation kinetics and the adhesion tension on one side and the adverse affect on kinetics of liquid viscosity. The slowing effect of high viscosity on nucleation has been discussed by many authors (Kristensen et al [21], Hoornaert et al [22], Knight and Seville [23]) showing an increase in nucleation time and in nuclei diameter with increasing viscosity.

3.3 Granule Growth

Granule growth occurs when material in the granulator sticks together upon impact. The mechanism is called coalescence if two similarly sized granules are involved and layering or snowballing when collisions between coarse and fine particles take place. The distinction between the two is however dependant on the size intervals used to define

coarse and fine particles and therefore arbitrary. Granule growth modeling has been approached by many authors. We will present in the following the main models depending on the main forces involved in their development.

a) Rumpf's Theory

The model proposed by Rumpf [2] estimates the force of the bond between two particles, which depends on the amount of binder between the two spherical particles relative to their volume and the size of the particles among others, to be the result of mainly static forces with the maximum value of this force given by the expression:

$$F_{cap} = \alpha \gamma d_p \quad (I-7)$$

Where $1.9 < \alpha < \pi$ depending on the moisture content (ratio between liquid volume and particle volume), γ relates to the surface tension of the liquid and d_p to the particle diameter.

The failure mechanism proposed by Rumpf was taken to be the strength required to break all bridges between every particle along the fracture plane with the tensile strength for the funicular or capillary saturation stage given by:

$$\sigma = C \cdot S \cdot \frac{(1-\varepsilon)}{\varepsilon} \cdot \frac{\gamma}{d_{pi}} \cdot \cos(\theta) \quad (I-8)$$

Where C is the coordination number depending on the particle shape, S is the liquid saturation, ε the intragranular porosity, θ the contact angle, γ the liquid surface tension and d_{pi} the initial particle diameter. The liquid saturation is defined as:

$$S = H \cdot \frac{(1-\varepsilon)}{\varepsilon} \cdot \frac{\rho_s}{\rho_l} \quad (I-9)$$

Where H is the moisture content, calculated as the ratio between the liquid mass introduced and the initial dry solid mass, ρ_s and ρ_l the solid and liquid density respectively.

Rumpf's equation states that granule strength is proportional to the binding force being inversely proportional with the initial particle size and increasing with decreasing porosity. Schubert [24] investigated the dependence between granule strength and liquid saturation state (Figure 6). In the figure S_p indicates the end of the pendular state and S_c the start of the capillary state where the granule is completely saturated. In the funicular state between the pendular and capillary state granule strength shows a steady increase which is expected as interparticular voids are replaced by liquid bridges.

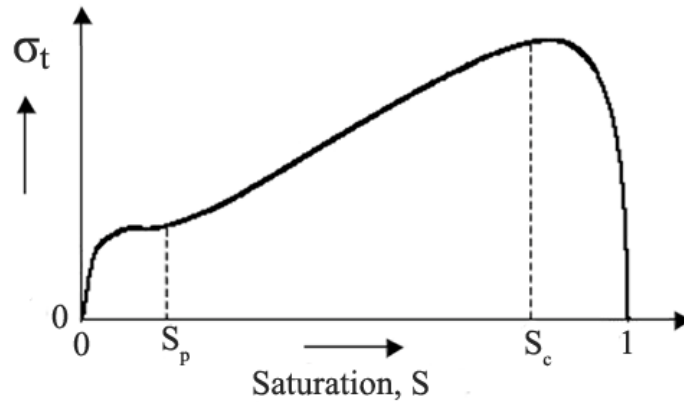


Figure 6. Relationship proposed by Schubert[24] between granule tensile strength and granule saturation states

b) Ennis and Liu Theory

Ennis et al [25, 26] developed a model for granule growth based on the dynamic liquid bridge. They defined the dimensionless viscous number in order to predict if collisions between two spherical granules will result in either coalescence or rebound depending on their kinetic energy and the energy dissipated during the collision:

$$St_v = \frac{8 \cdot \rho \cdot v_0 \cdot r}{9 \cdot \mu} \quad (\text{I-10})$$

Where ρ is the granule density, μ the viscosity of the binder liquid and v_0 the relative velocity between the two spheres estimated to be close to the impeller tip speed in high shear granulation.

The model predicts that collisions will be successful (result in coalescence) if the viscous Stokes number has a higher value than a critical viscous Stokes number defined as:

$$St_v^* = \left(1 + \frac{1}{e}\right) \ln\left(\frac{h}{h_a}\right) \quad (I-11)$$

Where e is the coefficient of restitution h is the thickness of the liquid surface layer and h_a is the characteristic height of surface asperities (Figure 7)

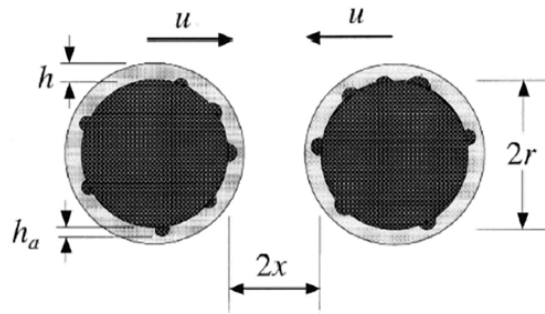


Figure 7. Collision of two pellets as described by Ennis [25]

Ennis et al defined three regimes as granules grow in size in the granulator in terms of magnitude of the viscous Stokes number compared to the critical Stokes number:

$St_v \ll St_v^*$ non-inertial regime all collisions are successful regardless of size of colliding granules;

$St_v = St_v^*$ inertial regime, some collisions are successful, collisions between two large granules are less likely to succeed;

$St_v \gg St_v^*$ coating regime, no collisions are successful.

However, this model can be useful in predicting the size of granules for which successful coalescence is possible. Since in granulators the collision velocity can only be described as a range of values it imposes a range of Stokes viscous numbers to be considered. This makes that the passage from growth to no growth can only be described by a decrease in the proportion of collisions that result in successful coalescence. Granule growth is promoted by low values of the viscous Stokes number and high values of the critical Stokes number. The probability of successful coalescence increases with decreasing

particle density, impeller speed and granule size and increasing surface liquid layer and binder liquid viscosity.

Thielmann et al [27] granulated in fluid bed a hydrophilic and hydrophobic powder (glass beads). They found the binder to spread better on the surface of hydrophilic particles giving a smaller liquid layer thickness than for the hydrophobic particles where the binder concentrated at the contact points between particles. This resulted in granules that were larger and rounder for the hydrophobic particles however this was accompanied by a wider final granule size distribution presenting significantly more fines than the hydrophilic particles.

One difficulty in the model proposed by Ennis resides in the estimation of the coefficient of restitution, liquid layer thickness and the height of the asperities as they dependent on time and binder content.

Liu et al [28] developed a model starting from the work of Ennis allowing to take into account the plastic deformation of granules on impact. Granules were supposed to have a strain rate independent elastic modulus and plastic yield stress. They studied two cases: when the granules present a liquid layer at granule surface and when the granule surface is dry and liquid is squeezed to the surface upon collision. The model defines conditions for two types of coalescence:

- type I: when granules coalesce by viscous dissipation in the surface liquid layer before their surfaces touch (elastic deformation)
- type II: when granules are stopped to a halt during rebound after their surface have made contact (plastic deformation)

The regime diagrams proposed by these authors (Figures 8 and 9) are based on the viscous Stokes number as defined by Ennis and a Stokes deformation number that relates impact kinetic energy to the plastic deformation of the granule. Figure 8 shows the possible interpretations of this model. At low St_{def} coalescence success depends only on the critical Stokes number as defined by Ennis. Different from the Ennis model is the prediction that at high plastic deformation increasing impact velocity can improve the probability of coalescence. For the dry surface case (Figure 9) at low St_{def} no plastic

deformation occurs while for values above a critical value of St_{def} the probability of coalescence becomes similar to the probability in the wet surface case.

$$St_{def} = \frac{\rho \cdot U_0^2}{2Y_d} \quad (I-12)$$

Where ρ represents the granules density (calculated as ratio between harmonic mean mass and cube diameter), U_0 the collision velocity and Y_d the granule dynamic yield stress.

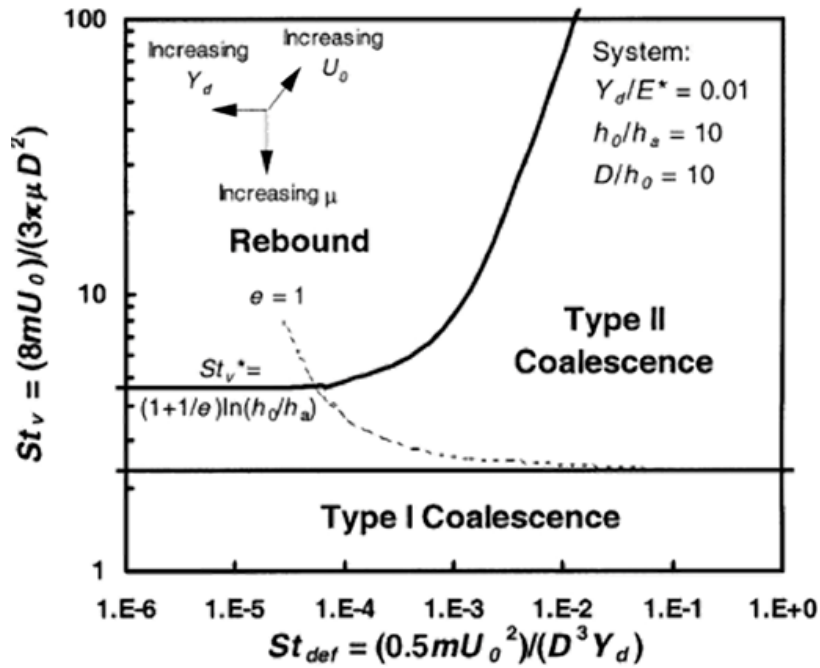


Figure 8. St_v vs St_{def} for the wet surface case Liu [28]

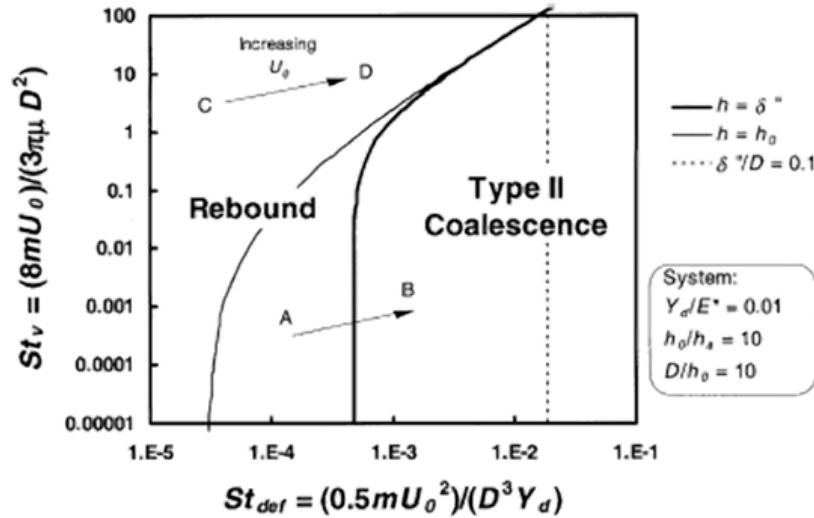


Figure 9. St_v vs. St_{def} for the dry surface case Liu [28]

c) Granule Growth Regime Map

Iveson and Litster [29] introduced a granule growth regime map (Figure 10) taking into account the Stokes deformation number as a function of pore saturation (i.e. the amount of liquid present in the pores inside the granules as a fraction of the total pores). When not enough liquid binder is present we are in the dry, free flowing powder regime. With increasing binder content nucleation occurs while the induction growth corresponds to a low deformability of the material not leading to successful coalescence. Upon further increase of the pore saturation granules become deformable enough for successful coalescence and we are said to be in the steady growth regime in which granules grow linearly with time. Further wetting causes the granules to be too deformable and thus too weak to withstand impact with the granulation equipment and upon even further liquid addition a suspension is formed/the mass becomes over-wetted.

Certain limitations of the granule growth regime map have been noted by Bouwman [30]. They show that difficulties in accurate measurement of the Stokes deformation number for visco-elastic materials can be encountered and due to large variations the results can overlap all growth regions.

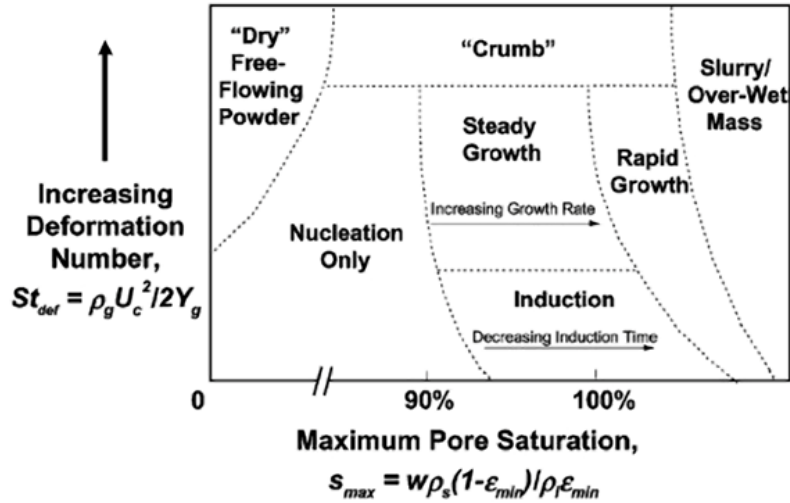


Figure 10. Granule growth regime map updated by Iveson and Litster [31] to the Stokes deformation number

3.4 Breakage and Attrition

Breakage of wet agglomerates in the granulator and attrition of dry agglomerates are both phenomena that affect the final product size distribution. Knight identified breakage as a function of impeller speed [32] in a process of melt granulation in a high shear mixer giving as proof of breakage the bimodal size distribution as well as the decrease in mean granule size when increasing the impeller speed from 800 to 1500 rpm at the end of an 800 rpm batch (Figure 11) and a reduction of granule sphericity with increasing impeller speed due to fragmentation. Ramaker et al [33] replaced 5 to 10% of the mixers contents with fresh prepared colored granules in two high shear mixers (a coffee mixer and a Gral 10) and calculated conversion rates as a function of color concentration at different processing times. They found that the conversion rate constants of smaller pellets were higher than those of the larger ones which indicated a faster formation of smaller pellets due to the break up of larger pellets. At higher impeller speeds they found an increase in the conversion rate constants indicating a faster break up of granules. Pearson et al [34] investigated breakage in a similar manner in a 30 L high shear mixer and found that the dye was distributed more from the larger particles to the finer particles than the other way around indicating that larger granules seem to be weaker. Vonk et al [35] approached the

breakage during growth from the early stages of the granulation process proposing a destructive nucleation growth mechanism where nuclei are broken down, densified and followed by further growth. An equilibrium between growth and breakage is found as fragmented parts are used to form new granules (Figure 12). It should be noted that in the experiments of Ramaker and Vonk all liquid was introduced at the beginning of the granulation process and not gradually which explains the simultaneity of nucleation, breakage and growth. Vonk et al also found that for increasing values of the impeller speed breakage of nuclei occurs when the impact pressure (Equation I-13) value increases above the calculated tensile strength of the nuclei.

$$\sigma_{\text{impact}} = \frac{F_a}{A} = \frac{4ma}{\pi D_g^2} = \frac{2}{3} \rho \omega^2 \quad (\text{I-13})$$

Where σ_{impact} is the impact pressure, F the acceleration force, A the cross sectional area of the granule, m the mass of the nucleus/agglomerate, a the acceleration of the agglomerate, D_g the agglomerate diameter, ρ the agglomerate density and ω the impeller tip speed ($=\pi ND$, where N is the impeller speed in rpm and D the impeller diameter).

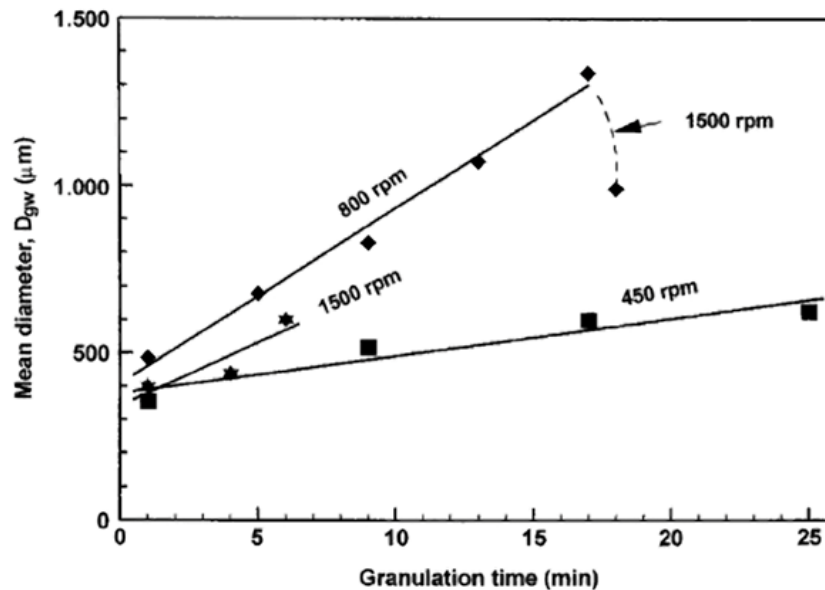


Figure 11. Mean granule diameter vs granulation time and impeller speed by Knight et al[32]

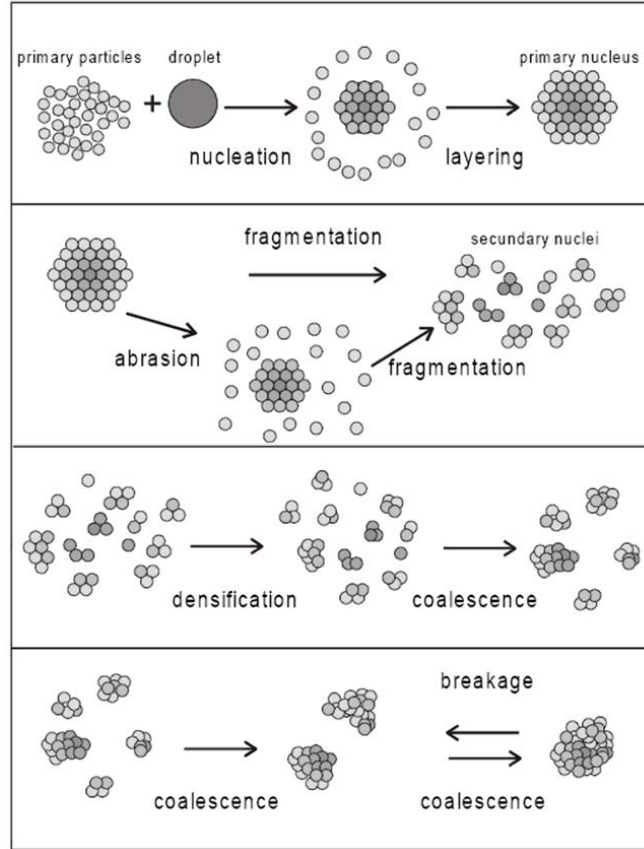


Figure12. The growth mechanism proposed by Vonk et al[35]

4. Granule Strength

The equation proposed by Rumpf (Equation I-8) that enables a prediction of wet granule strength has been argued by Kendall [36] because of the assumption that all the bridges between the particles in the fracture plain fail suddenly. Kendall suggested that the fracture is more likely a result of crack propagation through the flaws in the granule structure. He applied a fracture mechanics approach to the sequential fracture of bonds rather than simultaneous bond rupture proposed by Rumpf deriving the following expression for granule strength:

$$\sigma_t = 15.6\phi^4\Gamma_c^{5/6}\Gamma^{1/6}(d_p c)^{-1/2} \quad (\text{I-14})$$

Where ϕ is the solid fraction of the granular assembly, Γ_c is the fracture surface energy, Γ is the equilibrium surface energy, d_p is the constituent particle diameter and c is the flaw size in the assembly.

Bika et al [37] point out that due to the heterogeneity characteristic to agglomerated material such continuum descriptions applicable to metals, ceramics and other conventional solids are not obvious but that agglomerate deformation is fundamentally similar to other solids.

Factors affecting granule strength are: equipment variables and operating conditions like agitation intensity, equipment design and binder addition method and content; binder and feed powder properties like binder viscosity and surface tension, contact angle, feed powder nature and primary particle size.

4.1 Equipment variables and operating conditions

Increasing impeller speeds when a low viscosity binder is involved tends to lead to breakage (Schaefer [38], Knight [32]) while the agglomerate sphericity is decreased (Knight [32], Eliassen[39]). Impeller design has been found to give more spherical granules when the impeller blades are curved than when they are plane (Schaefer [40]). High impeller speeds are usually accompanied with a reduction in porosity and increase in compaction and consolidation which would typically lead to an increase in granule strength. A similar reasoning can be applied to the effect of increasing binder content that also reduces porosity and increasing granulation time that would lead to increased compaction and densification. Chopper speed influence is highly dependant on equipment design and deformability of the feed material as some authors found that chopper size and rotation can have an influence on granule strength by reducing the proportion of coarse granules and promoting densification (Holm[41]) while others reported that although the chopper slightly reduced granule size without having a significant effect on granule size distribution and intragranular porosity (Schaefer [42]). Holm et al [43] found that atomization improved the binder distribution at low impeller and chopper speeds while Knight et al [44] found that in high shear mixer granulation although initial differences exist between pour in, melt in and atomization, longer granulation times can ensure good binder distribution and uniform results. The influence

of increasing impeller speed has also been shown to improve liquid distribution and give narrower granule size distributions (Saleh [45], Oulahna [46]).

4.2 Binder viscosity

Keningley et al [47] showed that for a given particle size a minimum viscosity of the binder was necessary in order to promote growth. This minimum viscosity was found to increase with increasing particle size. Eliassen et al [48] found that for the granulation of lactose higher viscosity binders produce stronger granules presenting less comminution during the granulation process.

Ennis et al [25] defined a viscous capillary number expressed as:

$$Ca_{vis} = \frac{\mu U}{\gamma_L} \quad (I-15)$$

Where U is the speed of the particles, μ is the binder viscosity and γ_L is the liquid surface tension. They state that:

- If $Ca_{vis} < 10^{-3}$ the energy dissipation due to the viscosity can be neglected compared to the capillary forces and that adhesion is the product of static forces
- If $Ca_{vis} > 1$ the viscous force is dominant over the static forces. The viscous force expressed as:

$$F_v = \frac{3}{8} \pi \mu d_p^2 \frac{U}{L} \quad (I-16)$$

Where L is the distance between two particles and d_p the particle diameter. Ennis also showed that increasing binder viscosity reduces binder mobility in granules limiting compaction by resisting binder migration to the surface.

In a similar manner Knight et al [44] define a critical viscosity of 1Pa.s above which binder viscosity is dominant and below which surface tension forces dominate. However, these boundaries have to be put however in the context of the materials on which they were obtained as material properties like nature, primary particle size and shape also play an important role. Iveson et al [49] showed that granule consolidation is a function of

both interparticle friction and viscous dissipation and that increasing binder viscosity reduces the deformability of granules reducing the consolidation rate. Van den Dries et al [50] found that increasing binder viscosity increases the heterogeneity of the agglomeration while also producing stronger granules and less breakage.

4.3 Binder surface tension, contact angle, primary particle shape

Capes and Danckwerts [51] found that a minimal surface tension was necessary to obtain agglomerates of a certain size in the drum granulation of sand. Iveson et al [52] found that a decrease in binder surface tension decreases the dynamic yield stress of granules. However for a more viscous binder they found that binder viscosity dominated the yield stress behavior. Frictional forces also depend on the contact angle between liquid binder and powder particles. Knight et al [53] found that for contact angles above 90° granules present lower granule strength and wider granule size distributions. Johansen and Schaefer [54] showed that rounder particles with narrow particle size distribution give smaller granule strengths due to reduced particle interlocking.

5. Wet Mass Rheology

Measuring either the torque developed by the impeller or the power draw of the granulator was among the first methods attempted to follow the wet granulation process (Lindberg et al. [55], Travers et al. [56]). Leuenberger et al [57] showed that both can be related to changes in the cohesive force or the tensile strength of the wet agglomerates. Figure 13 shows the evolution of mean granule size and torque evolution as a function of binder saturation as found by Leuenberger et al [57]. Leuenberger et al [58] defined stages in granulation corresponding to the liquid saturation stages of the wet mass (See section 1.3.1) by drawing tangents to the torque profile (Figure 14). This typical profile consists out of five phases as defined by the authors:

- Phase I (up to S_2): The components take up the binder to saturate the moisture content (equilibrium moisture content at 100% relative humidity of air).

- Phase II (S_2 to S_3): Corresponds to the formation of liquid bridges (pendular state) between the primary particles.
- Phase III (S_3 to S_4): Plateau phase, the inter-particulate void space is filled by the binder, the liquid bridges are mobile (corresponds to the transition from pendular to funicular saturation state).
- Phase IV (S_4 to S_5): Corresponds to the funicular saturation state with some particles already in the capillary state.
- Phase V (above S_5): Transition from the capillary state to a suspension.

They stated that usable granules for tableting can be obtained from granules produced between S_3 and S_4 .

A π value has been defined by Imanidis et al.[59] (Equation I-17) which corresponds to a well defined point on the plateau (between S_3 and S_4). The calculation of π depends on the detection of the steepest ascent (S-shaped ascent in the power consumption curve) and adding a constant amount of liquid:

$$\pi = \frac{S - S_2}{S_5 - S_2} \quad (\text{I-17})$$

Where S is the amount of granulating liquid, S_2 is the amount of liquid necessary which corresponds to moisture equilibrium at about 100% relative humidity, S_5 is the amount for which complete saturation of inter-particulate void space before a suspension is formed.

This method has been successfully implemented in an automated process (Betz et al. [60]) and allowed the operators to obtain a higher homogeneity of granule size distribution than in the case of adding a constant amount of granulating liquid. It allowed minimizing the effect of varying initial particle size distributions and seasonal effects like differences in relative humidities between winter and summer.

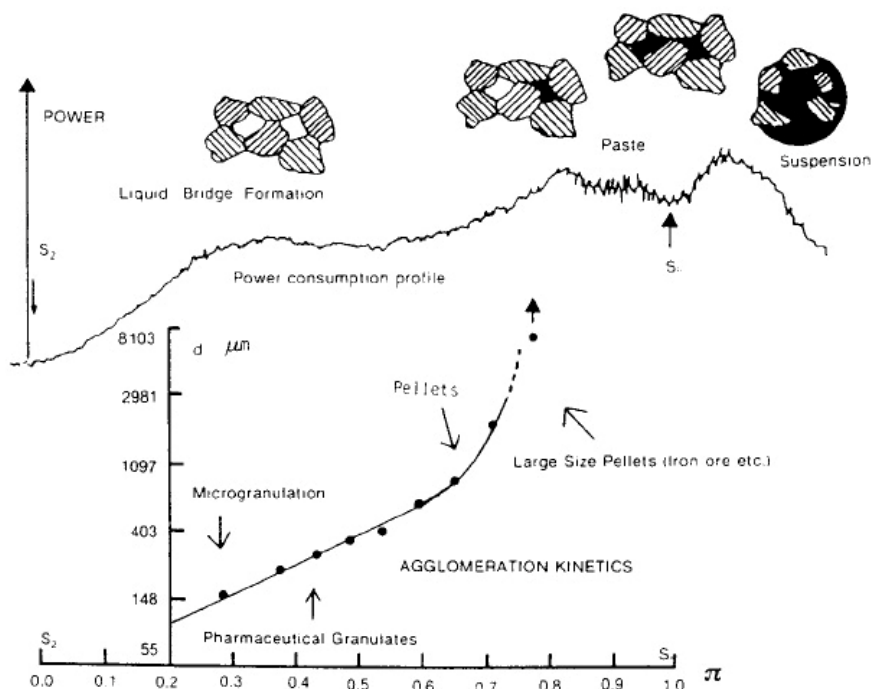


Figure 13. Granule saturation as a function of added binder and torque profile Leuenberger[57]

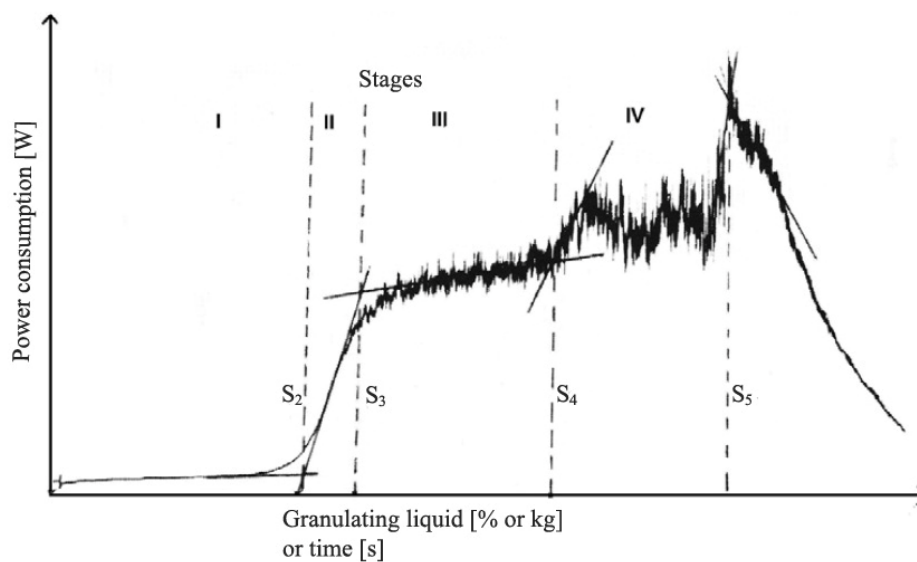


Figure 14. Power consumption profile Leuenberger [58]

Torque/power consumption curves present the advantage of in-line control of the granulation process if the granulator is instrumented in this respect. Some limitations

however, need to be taken into account if torque/power consumptions are to be used for control purposes:

- the solid formulation should present a limited dissolution in the binder liquid
- low viscosity binders are preferable and if possible a dry binder should be added to the powder mix and using a low viscosity binder (like water) as the binder liquid
- hydration is also a phenomenon to be avoided as is gelation at higher temperatures
- the liquid binder should be added gradually and not as poured in, all at the beginning

Mackaplow et al. [61] describe encountering limitations in the usability of torque curves for very cohesive powders (high shear wet granulation of fine lactose particles).

Instrumented granulators allow a comparison of torque/power consumptions curves for different starting materials. Other equipments that allow the assessment of the wet massing behavior of different powder-binder combinations have also been studied. One such equipment is the mixer torque rheometer (Figure 15) which has two contra-rotating intermeshing blades that mix the wet mass. Torque is recorded via a torque arm fixed to the reactor and linked to a calibrated dynamometer. It can be used to assess the changes in the wet mass when continually adding liquid but it can also be used to determine a pseudo-viscosity named wet mass consistency by introducing wet granules in the rheometer and recording the equilibrium torque. The mixer torque rheometer has been used for the estimation of the optimum water level for extrusion spherulization by Souto et al [62], Luukonen [63], to study source variation of MCC grades (Parker and Rowe [64]), to study binder - powder interactions (Parker [65], [66]) as well as control in regards to scale-up (Landin [67], Faure [68]). By introducing the wet mass in the mixer torque rheometer and mixing for a certain amount of time a pseudo-viscosity can be defined. This pseudo viscosity, also called wet mass consistency, can be introduced as the viscosity term in the Reynolds number enabling the comparison of different scales with regards to a measurable wet mass property. If using the mixer torque rheometer as a scaled down high shear granulator one has to be careful in considering the differences in geometry and impeller speed in order to subject the wet mass to constraints of a similar magnitude order.

Even though the use of torque curves/power consumption profiles in order to describe the wet granulation process goes back a long time it's still an active subject of research because of the complex nature of agglomeration. The characteristic profile has been related to agglomerate tensile strength (Betz [60]), to liquid saturation (Holm et al [69]), to interparticle friction forces (Pepin et al [70]) and intragranular porosity (Ritala [71]).

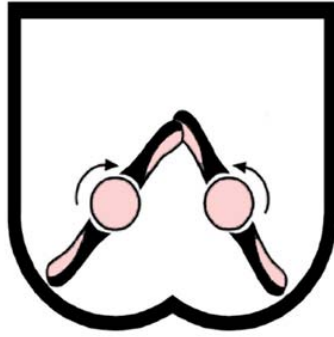


Figure 15. Schematic of the Caleva[®] mixer torque rheometer

6. Scaling

Recent PhD thesis by Giry [72] and Camara [73] as well as recent publications by Leuenberger and Betz [74] and Mort [75] give good overview of the wet granulation scale-up research knowledge to date. In this subchapter we will only be presenting some basic strategies regarding scale-up. High shear mixers come in a variety of designs; while some can be instrumented others may not. Given that high shear mixer granulation is a batch process scale-up to higher capacities has always presented an important research interest. There are several dimensionless groups that can be used for scale-up purposes and according to Buckingham's theorem they are:

$$\text{- Power number } \pi_1 = \frac{P}{r^5 N^3 \rho} \quad (\text{I-18})$$

$$\text{- Specific amount of granulating liquid } \pi_2 = \frac{qt}{V\rho} \quad (\text{I-19})$$

$$\text{- Fraction of volume loaded with particles } \pi_3 = \frac{V}{V^*} \quad (\text{I-20})$$

- Geometric number $\pi_4 = \frac{r}{D_v}$ (I-21)

- Froude number $\pi_5 = \frac{rN^2}{g}$ (I-22)

Where P is the power consumption, r is the radius of the impeller, ρ is the specific density, q is the mass of granulating liquid added per unit of time, N is the impeller speed in revolutions per second, t is the process time, V the volume loaded with particles, V^* is the total volume of the mixer, g is the gravitational acceleration and D_v the diameter of the vessel. If viscous binders are to be used the inclusion of the viscous Stokes number is recommended (Leuenberger et al [76]).

Other dimensionless numbers are:

- the impeller tip speed that can be used in order to maintain a constant maximal shear rate - the relative swept volume that represents the fractional volume of the total batch size which is displaced by the impeller in a specific time range and can be expressed as:

$$RSV = \frac{\frac{\pi}{4} \cdot r^2 \cdot h_b \cdot n}{T_R \cdot V^*} \cdot N \quad (I-23)$$

Where N is the impeller speed in rpm, n the number of blades, r the radius of impeller, h_b the height of the blade, T_R the fill ratio and V^* the mixer volume.

-the Reynolds number which can use instead of the viscosity term the pseudo-viscosity obtained from the wet mass consistency measurements done in a mixer torque rheometer (Landin [67]):

$$Re = \frac{\rho_w N r^2}{\mu^*} \quad (I-24)$$

Where ρ_w is the wet mass bulk density, N is the impeller speed in rpm, r the impeller radius and μ^* the wet mass consistency.

-constant shear stress investigated by Tardos et al [77] and Michaels et al [78] showed that adjusting impeller speed to match the maximum shear stress at each scale of

investigation allowed them to obtain good agreement upon scale-up in terms of mean granule size, granule dissolution and tensile strength. In their case constant shear was obtained for a scaling index n of 0.8 to 0.85 in the expression:

$$\frac{N_x}{N_y} = \left(\frac{D_y}{D_x} \right)^n \quad (\text{I-25})$$

Impeller tip speed, Froude number or the relative swept volume can not be kept constant at the same time during scale-up. Also as neither contains elements relative to the wet mass they should be considered a means for the scale-up of the machine rather than the process (Faure [79]). Rahmanian et al [80] tested some of the most common dimensionless numbers: constant shear, constant impeller tip speed and constant Froude number for the scale-up from a 1L Hosokawa Cyclomix high shear mixer to a 250L (going through 5 and 50L) and used granule strength in order to quantify scale-up efficiency. They found that constant impeller tip speed allowed them to obtain granules of comparable strength across the scales while the differences increased when using constant shear stress or constant Froude number.

Scale-up of the wet granulation process is a complicated issue due to the complex nature of agglomeration but it can be further complicated by the lack of geometric similarity between scales even in granulators coming from the same manufacturer. Scale-up must also compensate for such effects like the effect of the chopper especially since it can affect differently granulation at different scales or the effect of the wall on which granules can stick and which can also slow down the granules. Such effects are more present at the small laboratory scale where new formulations and processes are developed but where extensive testing is far less expensive.

7. Conclusion

The most important goal in the research of the wet granulation process is the understanding of the underlying mechanisms and controlling the final granule properties. This introduction has shown that granulation presents complex interactions between

equipment variables as well as material properties making the outcome of a granulation hard to predict.

This literature review has shown the great wealth of information available for the wet granulation agglomeration technique. The results presented allow us to draw the following conclusions:

- The mechanisms occurring in a wet granulation process can be generally divided into three categories: wetting and nucleation, densification and growth and breakage and attrition. However the predominance of one mechanism over the other remains relatively poorly understood with the majority of the studies investigating just one of the categories usually under a small variation of operating conditions and physico-chemical properties of the powder-binder couple.
- Systematic studies (Vialatte [2], Oulahna [46], Rahmanian[80], Benali [81]) allow to relate the effect of operating conditions and physico-chemical properties of the starting materials to agglomerate quality (size, size distribution, porosity, shape, strength)
- The definition of the optimum binder requirement is a key issue in high shear wet granulation. As it depends mainly on the operator, the definition and optimization of the optimum binder requirement is of crucial importance for the subsequent product characterization. However, it is also a parameter that is often neglected making the generalization of the results presented in literature difficult.
- The use of torque/power consumption curves to control wet granulation is a fairly established technique. It allows controlling the binder saturation of the wet mass. However the definition that the optimal binder requirement for pharmaceutical granulation purposes is situated on the plateau region remains somewhat vague. Also the relationship between the wet mass properties, granulation mechanisms and torque curves is still a subject of actuality with reports in literature showing little agreement.
- Torque rheometers can be employed in order to offer additional information about the granulation behavior of powder-binder couples. They offer a refinement in the use of torque for scale-up of the wet granulation process. The connection between the information obtained in the rheometer and the wet granulation process is limited to the

measure of a pseudo-viscosity called wet mass consistency that allows verifying scale-up efficiency.

- The influence of mixer scale is usually done by keeping one or more dimensionless groups constant, however these groups don't usually take into account the physico-chemical properties of the starting materials representing the scale-up of the machine rather than the process mechanisms.

The aim of this thesis is to bring more insight to the relationships between torque curves and changes in operating conditions and physico-chemical properties of the starting materials on one hand as well as the effects that these changes can have on the mechanical properties of the wet and dry granules. We will also investigate the effect of technology by changing mixer design and investigate the effect on mean granule size, granule size distribution, growth mechanisms and granule strength.

Chapter II presents the materials and the equipment as well as the characterization methods used in this study.

Chapter III will be divided in four subchapters each presenting one important aspect of granulation. Subchapter III.1 presents a typical example of granulation showing a granulation run and the methodology used to characterize the results. Subchapter III.2 deals with the influence of operating conditions like fill level, impeller speed and chopper influence while also investigating the effect of mixer design for two geometrically similar granulators. In subchapter III-3 the influence of binder properties like viscosity, binder surface tension and powder binder interactions are discussed as well as the influence of binder choice. Finally subchapter III-4 shows the influence of varying substrate nature as well as granulation of mixes of two different components at two scales.

References

- [1] K. Niishi, M. Horio, Handbook of Powder Technology Chapter 6 Dry Granulation, Elsevier (2006) 289-323
- [2] M. Jacob, Handbook of Powder Technology Chapter 9 Granulation Equipment, Elsevier (2006) 417-477
- [3] G.K. Reynolds, P.K. Le, A.M. Nilpawar, Handbook of Powder Technology Chapter 1 High Shear Granulation, Elsevier (2006) 1-23
- [4] H. Rumpf, Grundlagen und Methoden des Granulierens, Chemie-Ingenieur-Technik 30 (1958) 144–158
- [5] H. Rumpf, Die Wissenschaft des Agglomerierens., Chemie-Ingenieur-Technik 46 (1974) 1–11
- [6] J.N. Israelachvili, D. Tabor, Van der Waals forces: theory and experiment, Progress of Surface and Membrane Science 7 (1973) 1–55
- [7] H. Schubert, Grundlagen des Agglomerierens. Chemie-Ingenieur-Technik 51 (1979) 266–277
- [8] J. Tomas, H. Schubert, Modeling of the strength and flow properties of moist soluble bulk materials, Proceedings of International Symposium on Powder Technology '81 Kyoto (1981), 118–124
- [9] J. Tomas, Zum Verfestigungsprozeß von Schüttgütern - Mikroprozesse, Kinetik-modelle und Anwendungen., Chemie-Ingenieur-Technik 69 (1997) 455–467
- [10] J. Tomas, Adhesion of ultra fine particles-A micromechanical approach, Chemical Engineering Science 62 (2007) 1997-2010
- [11] H. Rumpf, Agglomeration: the strength of granules and agglomerates, W.A. Keppner (1962)
- [12] W. Pietsch, Size enlargement by agglomeration, Wiley (1991)
- [13] D.M. Newitt, J.M.A. Conway-Jones, A contribution to the theory and practice of granulation Trans.Instn.Chem.Engrs. 36 (1958) 422-442.
- [14] S. M. Iveson, J. D. Litster, K. Hapgood, B. J. Ennis, Nucleation, growth and breakage phenomena in agitated wet granulation processes: a review, Powder Technol. 117 (2001) 3–39
- [15] R.C. Rowe, Adhesion of film coating to tablet surfaces: a theoretical approach based on solubility parameters, International Journal of Pharmaceutics 41 (1988a) 219-222
- [16] M.E. Aulton, M. Banks, Influence of the hydrophobicity of the powder mix on fluidised bed granulation, International Conference on Powder Technology in Pharmacy, Basel, Switzerland, Powder Advisory Centre, 1979
- [17] Z. Tüske, G. Regdon, Jr. Eris, I.S. Srčić, K. Pintye-Hódi, The role of the surface free energy in the selection of a suitable excipient in the course of wet-granulation method
Powder Technology 155 (2005) 139-144
- [18] T. Schäfer, C. Mathiesen, Melt pelletization in a high shear mixer: IX. Effects of binder particle size, Int. J. Pharm. 139 (1996) 139–148
- [19] A.C. Scott, M.J. Hounslow, T. Instone, Direct evidence of heterogeneity during high-shear granulation, Powder Technol. 113 (2000) 205–213
- [20] M. Denesuk, G.L. Smith, B.J.J. Zelinski, N.J. Kreidl, D.R. Uhlmann, Capillary penetration of liquid droplets into porous materials, J. Colloid Interface Sci. 158 (1993) 114–120.
- [21] H.G. Kristensen, T. Schäfer, Agglomeration with viscous binders, First International Particle Technology Forum Denver USA (1994)

- [22] F. Hoornaert, P.A.L. Wauters, G.M.H. Meesters, S.E. Pratsinis, B. Scarlett, Agglomeration behaviour of powders in a Lodige mixer granulator, *Powder Technol.* 96 (1998) 116–128.
- [23] P.C. Knight, J.P.K. Seville, Effect of binder viscosity on agglomeration processes, *World Congr. Part. Technol.* 3 (1998)
- [24] Schubert, H., Tensile strength of agglomerates, *Powder Technol.* 11 (1975) 107-119
- [25] Ennis, B.J., Tardos, G., Pfeffer, R., A microlevel-based characterization of granulation phenomena, *Powder Technol.* 65 (1991) 257-272
- [26] Ennis, B.J., Li, J., Tardos, G., Pfeffer, R., The influence of viscosity on the strength of an axially strained pendular liquid bridge, *Chem.Eng.Sci.* 45 (10) (1990) 3071-3088
- [27] F. Thielmann, M. Naderi, M. A. Ansari, F. Stepanek, The effect of primary particle surface energy on agglomeration rate in fluidised bed wet granulation, *Powder Technol.* 181 (2008) 160–168
- [28] L.X. Liu, S.M. Iveson, J.D. Litster, B.J. Ennis, Coalescence of deformable granules in wet granulation processes, *AIChE J.* 46 (2000) 529–539
- [29] S.M. Iveson, J.D. Litster, Growth regime map for liquid-bound granules, *AIChE J.* 44 (1998) 1510–1518
- [30] A.M. Bouwman, The influence of material properties and process conditions on the shape of granules produced by high shear granulation, PhD thesis Rijksuniversiteit Groningen (2005)
- [31] S. M. Iveson, P. A. L. Wauters, S. Forrest, J. D. Litster, G. M. H. Meesters, B. Scarlett, Growth regime map for liquid-bound granules: further development and experimental validation, *Powder Technol.* 117 (2001) 83-97
- [32] P. Knight, A. Johansen, H. Kristensen, T. Schaefer, J. Seville, An investigation of the effects on agglomeration of changing the speed of a mechanical mixer. *Powder Technol.* 110 (2000) 204–209.
- [33] J. Ramaker, M. Albada Jelgersma, P. Vonk, N. Kossen, Scaledown of a high shear pelletisation process: flow profile and growth kinetics. *International Journal of Pharmaceutics* 166 (1998) 89–97
- [34] J. Pearson, M. Hounslow, T. Instone, Tracer studies of high-shear granulation: I. Experimental results. *A.I.Ch.E. Journal* 47 (2001) 1978–1983
- [35] P. Vonk, C.P.F. Guillaume, J.S. Ramaker, H. Vromans, N. Kossen, Growth mechanisms of high-shear pelletisation, *Int.J.Pharm.* 157 (1997) 93-102
- [36] K. Kendall, Agglomerate strength, *Powder Metallurgy* 31 (1988) 28–31
- [37] D. Bika, M. Gentzler, J. Michaels, Mechanical properties of agglomerates, *Powder Technol.* 117 (2001) 98–112.
- [38] T. Schaefer, Growth mechanisms in melt agglomeration in high shear mixers, *Powder Technol.* 117 (2001) 68–82
- [39] H. Eliassen, H. Kristensen, T. Schaefer, Growth mechanisms in melt agglomeration with a low viscosity binder, *Int. J. Pharm.* 186 (1999) 149–159
- [40] T. Schaefer, B. Taagegaard, L. Thomsen, H. Kristensen, Melt pelletization in a high shear mixer. Part V. Effects of apparatus variables. *European J. Pharm. Science* 1 (1993) 133–141
- [41] P. Holm, Effect of impeller and chopper design on granulation in a high speed mixer *Drug Dev. and Ind. Pharm.* 13 (1987) 1675–1701
- [42] T. Schaefer, P. Holm, H. Kristensen, Melt pelletization in a high shear mixer. Part i. Effects of process variables and binder, *Acta Pharmaceutica Nordica* 4 (1992) 133–140
- [43] P. Holm, O. Jungersen, T. Schaefer, H. Kristensen, Granulation in high speed mixers. Part 1. Effects of process variables during kneading, *Pharmaceutical Industry* 46, (1983) 97–101

- [44] P. Knight, T. Instone, J. Pearson, M. Hounslow, An investigation into kinetics of liquid distribution and growth in high shear mixer agglomeration. *Powder Technol.* 97 (1998) 246–257
- [45] K. Saleh, L. Vialatte, P. Guigon, Wet granulation in a batch high shear mixer, *Chemical Engineering Science* 60 (2005), 3763-3775
- [46] D. Oulahna, F. Cordier, L. Galet, J. A. Dodds, Wet granulation: the effect of shear on granule properties, *Powder Technol.* 130 (2003) 238-246
- [47] S. Keningley, P. Knight, A. Marson, An investigation into the effects of binder viscosity on agglomeration behaviour, *Powder Technol.* 91 (1997) 95–103
- [48] H. Eliassen, T. Schaefer, H. Kristensen, Effects of binder rheology on melt agglomeration in a high shear mixer, *Int. J. Pharm.* 176 (1998) 73–83
- [49] S. M. Iveson, J.D. Litster, B. Ennis, Fundamental studies of granule consolidation. Part 1. Effects of binder content and binder viscosity, *Powder Technol.* 88 (1996) 15–20
- [50] K. van den Dries, O. de Vegt, V. Girard, H. Vromans, Granule breakage phenomena in a high shear mixer: influence of process and formulation variables and consequences on granule homogeneity, *Powder Technol.* 133 (2003) 228–236
- [51] C. Capes, P. Danckwerts, Granule formation by the agglomeration of damp powders. Part I: the mechanism of granule growth, *Transactions of the Institution of Chemical Engineers* 43 (1965) 116–124
- [52] S. M. Iveson, J.D. Litster, B. Ennis, Fundamental studies of granule consolidation. Part 2. Quantifying the effects of particle and binder properties. *Powder Technol.* 99 (1998) 243–250
- [53] P. Knight, Structuring agglomerated products for improved performance, *Powder Technol.* 119 (2001) 14–25
- [54] A. Johansen, T. Schaefer, Effects of interactions between powder particle size and binder viscosity on agglomerate growth mechanisms in a high shear mixer, *European J. of Pharm. Sciences* 12 (2001) 297–309
- [55] N-O Lindberg, L. Leander, L. Wenngren, H. Helgesen, R. Reenstierna, Granulation in a change can mixer. *Acta Pharm. Suec.* 11 (1974)
- [56] D.N. Travers, A.G. Rogerson, T.M. Jones, A torque arm mixer for studying wet massing, *J.Pharm.Pharmacol.* 27 Suppl. 3P (1975)
- [57] H. Leuenberger, H-P Bier, H. Sucker, Theory of the granulation-liquid requirement in the conventional granulation process, *Pharm.Tech.Int.* 3 (1979) 61-68.
- [58] H. Leuenberger, Granulation, New Techniques, *Pharm. Acta Helv.* 57(3) (1982) 72-82
- [59] G. Imanidis, Untersuchungen über die Agglomerierkinetik und die elektrische Leistungsaufnahme beim Granulierprozess im Schnellmischer, PhD thesis, University of Basel (1986)
- [60] G. Betz, P. J. Burgin, H. L. Leuenberger, Power consumption profile analysis and tensile strength measurements during moist agglomeration, *Int. J. Pharm.* 252 (2003)11–25
- [61] M. B. Mackaplow, L. A. Rosen, J. N. Michaels, Effect of primary particle size on granule growth and endpoint determination in high-shear wet granulation, *Powder Technol.* 108 (2000) 32-45
- [62] C. Souto, R. Alvarez, R. Duro, A. Concheiro, J.L. Gomez-Amoza, R. Martinez-Pacheco, Versatility of mixer torque rheometry predictions in extrusion-spheronization, *Proc. 2nd World Meeting APGI/APV* (1998), 447-448
- [63] P. Luukkonen, T. Schæfer, K. Mäkelä, U. Södergård, L. Hellén, J. Yliruusi, Evaluation of the optimum water level for pelletisation using a mixer torque rheometer. *AAPS PharmSci* 1148 (1999), New Orleans, USA
- [64] M.D. Parker, R.C. Rowe, Source variation in the wet massing (granulation) of some microcrystalline celluloses. *Powder Technol.* 65 (1991) 273-281

- [65] M.D. Parker, P. York, R.C. Rowe, Binder-substrate interactions in wet granulation 1: The effect of binder characteristics, *Int.J.Pharm.* 64 (1990) 207-216
- [66] M.D. Parker, P. York, R.C. Rowe, Binder-substrate interactions in wet granulation. 2: The effect of binder molecular weight, *Int.J.Pharm.* 72 (1991) 243-249
- [67] M. Landín, P. York, M.J. Cliff, R.C. Rowe, A.J. Wigmore, Scale-up of a pharmaceutical granulation in fixed bowl mixer-granulators, *Int.J.Pharm.* 133 (1996) 127-131
- [68] A. Faure, I. Grimsey, R. Rowe, P. York, M. Cliff, Process control in a high shear mixer-granulator using wet mass consistency: The effect of formulation variables, *J.Pharm.Sci.* 88 (1999) 191-195
- [69] P. Holm, T. Schæfer, H.G. Kristensen, Granulation in High-Speed Mixers. Part V. Power Consumption and Temperature Changes During Granulation. *Powder Technol.* 43 (1985) 213-223
- [70] X. Pepin, S. Blanchon, G. Couarraze, Power Consumption Profiles in High-Shear Wet granulation. I: Liquid distribution in Relation to Powder and Binder Properties, *J.Pharm.Sci.* 90 (2001) 322-331
- [71] M. Ritala, P. Holm, T. Schæfer, H.G. Kristensen, Influence of liquid bonding strength on power consumption during granulation in a high shear mixer, *Drug Dev.Ind.Pharm.* 14 (1988) 1041-1060
- [72] K. Giry, Impact du changement de procede de granulation humide sur les caracteristiques pharmacotechniques des grains et des comprimés : Procédé monophasique versus procédé séquentiel, PhD thesis, Université de Limoges (2007)
- [73] A.L. Camara, Intrapolation du procédé de granulation humide en mélangeurs à haute vitesse, PhD thesis, Institut National Polytechnique de Lorraine (2005)
- [74] H. Leuenberger, G. Betz, Handbook of Powder Technology Chapter 15 Granulation process control-Production of pharmaceutical Granules: The classical batch concept and the problem of scale-up, Elsevier (2006) 705-734
- [75] P.R. Mort, Handbook of Powder Technology Chapter 19 Scale-up of high shear binder-agglomerate processes, Elsevier (2006) 853-896
- [76] H. Leuenberger, M. Puchkov, E. Krausbauer, G. Betz, Manufacturing pharmaceutical granules: Is the granulation end-point a myth?, *Powder Technol.* 189 (2009) 141-148
- [77] G. Tardos, Wet-granulation research with application to scale-up, *China Particuology*, 3 (3) (2005) 191-195
- [78] J. N. Michaels, L. Farber, G. S. Wong, K. Hapgood, S. J. Heidel, J. Farabaugh, J-H Chou, G. I. Tardos, Steady states in granulation of pharmaceutical powders with application to scale-up, *Powder Technol.* 189 (2009) 295-303
- [79] A. Faure, P. York, R. Rowe, Process control and scale-up of pharmaceutical wet granulation processes: a review, *Eur. J. Pharm. and Biopharm.* 52 (2001) 269-277
- [80] N. Rahmanian, M. Ghadiri, Y. Ding, Effect of scale of operation on granule strength in high shear granulators, *Chemical Engineering Science* 63 (2008) 915 – 923
- [81] M. Benali, V. Gerbaud, M. Hemati, Effect of operating conditions and physico-chemical properties on the wet granulation kinetics in high shear mixer, *Powder Technol.* 190 (2009) 160-169

CHAPTER II

Materials and Methods

Chapter II: Materials and Methods

In this chapter we will be presenting:

- the powder and binder solutions physico-chemical properties,
- the main characterization methods employed
- the operating protocol for the wet granulation experiments,
- the equipment used in this study: the high shear mixers.

1. Materials

The principal starting powders used in this study were microcrystalline cellulose (MCC Avicel 105, FMC Biopolymer) and α -lactose monohydrate (Fischer-Bioblock, Acros Organics). The study of equipment variables and binder properties on granulation has been performed with 100% MCC while lactose was employed only for the study of varying proportions of MCC in MCC-lactose formulations. The binders used in this study were aqueous solutions of various concentrations of Polyvinylpyrrolidone (PVP, Sigma Aldrich) and Hydroxypropylmethylcellulose (HPMC, Sigma Aldrich). More detail on the solid state binder products used can be found Appendix I.

1.1 Microcrystalline Cellulose

The chosen MCC powder, MCC Avicel 105 (FMC Biopolymer), presents a high cohesion and poor flowing characteristics being an interesting candidate for size enlargement operations. This powder is usually encountered in direct compression operations. Figure 1 shows a scanning electron microscope image of the initial MCC particles. MCC presents itself as a fine, white, water insoluble powder showing particles with elongated, irregular form. This form makes the definition of a mean diameter difficult. The values reported here are the ones obtained using a laser particle size analyzer (Malvern Mastersizer). Figure 2 shows the X-ray diffraction spectrum allowing

us to measure the cristallinity index according to the relation proposed by Sidiras, Koullas, Vgenopoulos and Koukios [1]:

$$CrI = \frac{[(I_{002} - I_{am})]}{I_{002}} \cdot 100 \quad (\%) \quad (II-1)$$

Where I_{002} is the intensity peak at approximately $2\theta=23^\circ$ and I_{am} is the intensity corresponding to the peak at approximately $2\theta=16^\circ$. The cristallinity index of the powder has been found to be of the order of 66% (Table 1).

The properties of a more conventional MCC grade for high shear wet granulation, the Avicel 101, are also presented. Table 1 regroups the physical characteristics of the two MCC powders showing that both grades give similar cristallinity index values and leading us to believe that except for differences in mean particle size and density the two powders can be regarded as two different grades of the same product.

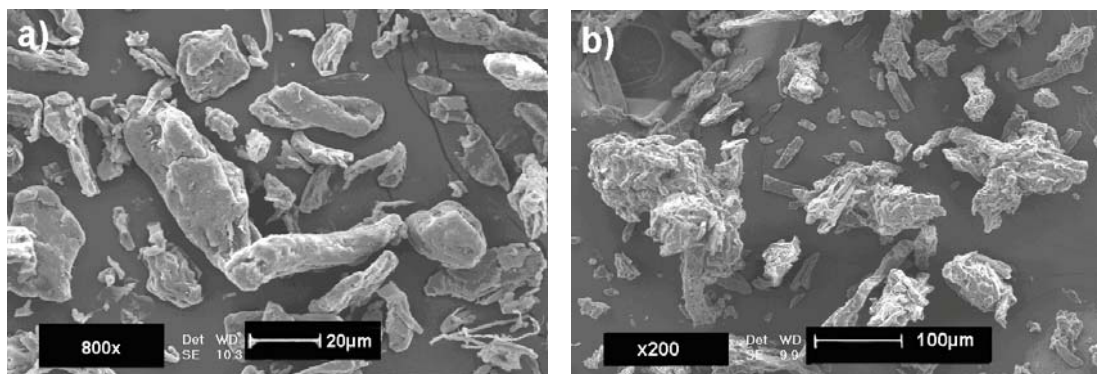


Figure 1. SEM image of initial MCC Avicel 105 particles(a) and Avicel 101 particles (b)

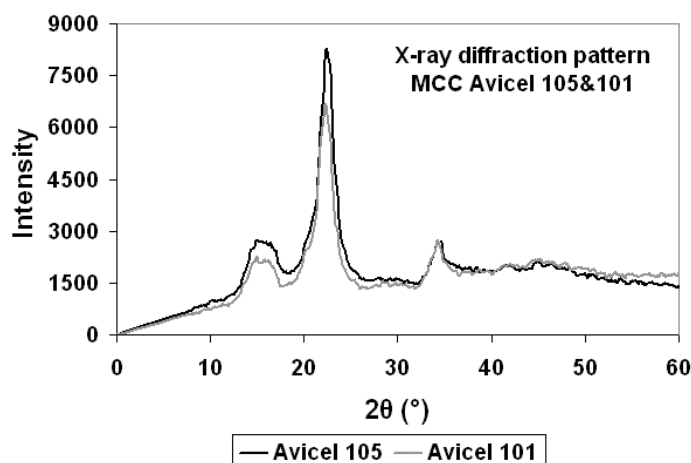


Figure 2. X-ray diffraction patterns for two MCC grades: MCC Avicel 105 and Avicel 101

Powder properties	D ₅₀ [μm]	Span (D ₉₀ -D ₁₀)/ D ₅₀	Bulk Density [kg/m ³]	True Density [kg/m ³]	Cristallinity Index [%]
Avicel 105	20	1.93	244	1514	66.33
Avicel 101	60	2.1	291	1540	66.41

Table 1. Physical characteristics of the MCC powders Avicel 105 and 101

Microcrystalline cellulose can be prepared from either cotton seed hair or wood with cotton being almost poor cellulose while wood contains varying degrees of cellulose (40-50%), hemicelluloses (20-30%) and lignin (20-30%). The cellulose polymer is made of cellobiose units that are linked by β -(1-4) glucosidic bonds. Figure 3 shows the cellobiose units (a) that form larger unit cells (b) which form crystallites (c). Crystallites that present crystalline and amorphous regions are combined into microfibrils (d) and fibrils (e) which form the cellulose fibers (Luukonen [2]). Figure 4 shows the amorphous and crystalline zones in microcrystalline cellulose fibrils (Ribet [3]).

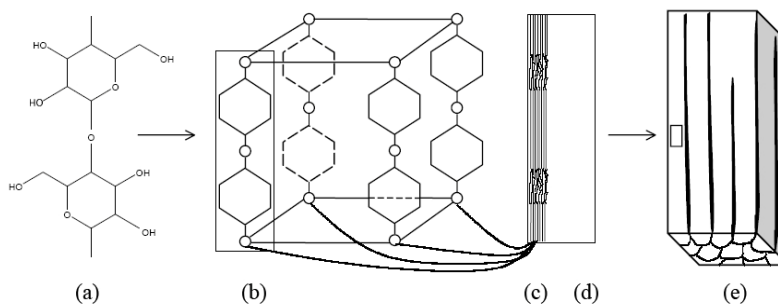


Figure 3. Microcrystalline cellulose structure [3]

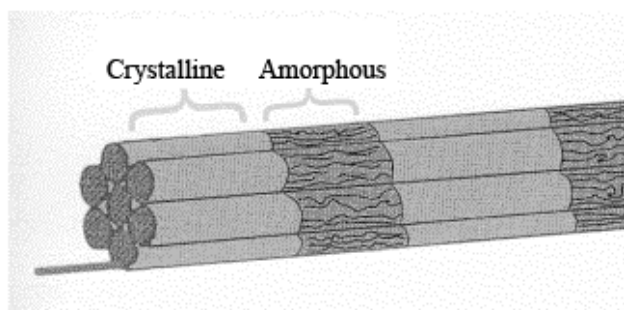


Figure 4. MCC microfibrils structure [4]

The manufacturing process of microcrystalline cellulose requires dissolving the pulp by acid hydrolysis shortening the cellulose chains and removing the soluble parts like hemicelluloses and lignin. After washing with water, the suspension is spray dried into microcrystalline cellulose particles with sizes ranging from 50 to 100 μ m. If the pulp is milled, powdered cellulose can be produced that presents a higher degree of polymerization (~500 vs ~200 for MCC) and a lower degree of crystallinity (15-45% vs 65-75% for MCC). Both types of celluloses are encountered in pharmaceutical applications.

Fielden et al [4] suggested based on thermal studies of the interaction between MCC and water that MCC can be considered a 'molecular sponge'. MCC can retain large amounts of water but also easily release it upon drying. The role of MCC is stated to be to control the movement of the water through the wet powder mass during extrusion and modify the rheology of the wet mass conferring it a certain degree of plasticity. In the extrusion process the sponges are compressed until water is squeezed out and lubricate the particle flow through the extruder.

Another model has presented by Kleinebudde [5] who proposes that a gel is produced during extrusion/granulation with MCC. In the presence of water the MCC particles are broken down into smaller subunits by the shear forces present in granulation/extrusion operations. The single particles with the size of a few microns turn into a 'crystallite gel' that immobilizes the liquid. The crystallites or their agglomerates can form a network by cross linking with hydrogen bonds at the amorphous ends.

The complexity of the models makes them difficult to be directly proven and studies that support both are available in literature ([6], [7], [8], [9]). Kleinebudde [10] suggested that the sponge model is more appropriate for the cellulose presenting a high degree of polymerization (powdered cellulose) while the crystallite gel model is more applicable to cellulose types with a lower degree of polymerization (MCC and silicified MCC).

1.2 Lactose

Alongside microcrystalline cellulose, lactose is another very widely used excipient. Sousa et al. [11] found when extruding/spheronizing different starting materials microcrystalline cellulose, glucose, mannitol, lactose, calcium phosphate, and barium sulphate that lactose was the material that did not present spherical pellets. This may be one of the reasons why MCC is often present in formulations together with lactose as it is known for its capacity to produce granules with high sphericity.

Lactose is a disaccharide that consists of β -D-galactose and α/β -D-glucose fragments bonded through a β 1-4 glycosidic linkage. Figure 5 presents the initial lactose particles that show large lactose crystals with finer lactose particles sticking to their surface. Table 2 regroups the main physical characteristics of the α -lactose monohydrate powder (Fischer Scientific) used in this study.

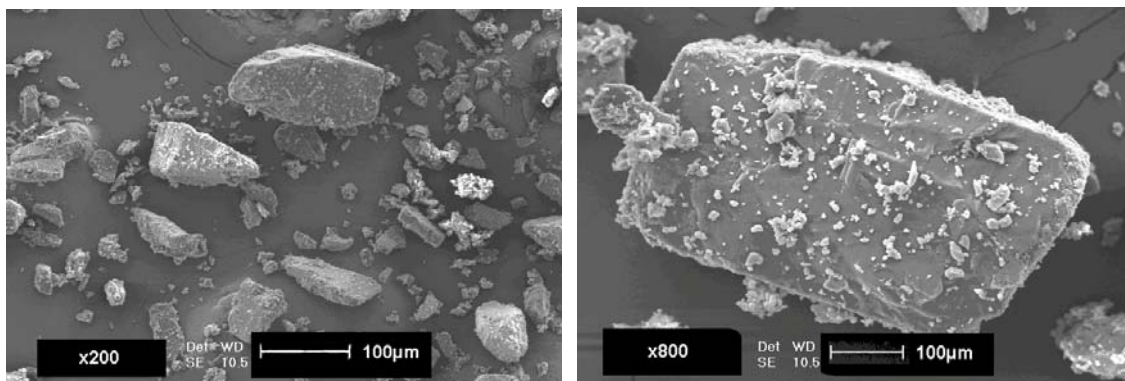


Figure 5. SEM image of initial α lactose monohydrate particles

Powder properties	D₅₀ [μm]	Span (D₉₀-D₁₀)/ D₅₀	Bulk Density [kg/m³]	True Density [kg/m³]	Solubility [g/100 cm³ water at 25°C]
α lactose monohydrate	60	2.28	465	1510	17

Table 2. Physical characteristics of lactose

1.3 Binder Properties

The binders used in this study were chosen so as not to chemically react with the solid and also to be of a certain practical importance for the wet granulation of the chosen excipients.

The influence of the operating conditions and changing initial formulations in this study have been studied using ultra-pure water as a binder. For the study of binder properties aqueous solutions of various concentrations of Polyvinylpyrrolidone (PVP) and Hydroxypropylmethylcellulose (HPMC) have been prepared. Contact angle values were obtained by the dynamic capillary rise method on a GBX Instrument balance (as described in Appendix II-1). Binder viscosity was obtained using a Haake Rheostress RS 600 rheometer (As described in Appendix II-2).

For the non-Newtonian binder solutions variations are observed in viscosity depending on shear rate. As it can be observed the higher concentration HPMC binder, HPMC 3%, presents Non-Newtonian behavior. The value chosen for representing viscosity for HPMC 3% was 1047 s⁻¹. An impeller speed of 800 rpm on the Mi-Pro 1.9L was imposed for all experiments when binder properties influence was studied.

Table 3 regroups the physico-chemical properties of the binders used in this study and the contact angle between them and the microcrystalline cellulose powder Avicel 105. Figure 6 shows the evolution of viscosity with increasing binder content while initially several concentrations were characterized only the ones allowing certain correlations between viscosity and work of adhesion (modification of viscosity for low variations of work of

adhesion and variation of work of adhesion for low variations in viscosity respectively) were chosen.

The binders chosen are binders commonly used in the pharmaceutical industry and as it can be observed while viscosity varies strongly with a factor of 100 contact angle values are pretty close between the different binders.

Binder properties	ρ (kg/m ³)	γ (mN/m)	μ (mPa·s at 25°C)	θ (°)
Water	1000	72.2	1.0	69.0 ± 1.2
Aqueous solution: PVP 3% (wt%)	1002	63.6	1.3	62.8 ± 4.3
Aqueous solution: PVP 13% (wt%)	998	53.8	3.1	63.8 ± 4.7
Aqueous solution: HPMC 0.5% (wt%)	986	47.6	3.1	76.3 ± 4.5
Aqueous solution: HPMC 1% (wt%)	993	47.1	8.1	79.0 ± 4.8
Aqueous solution: HPMC 3% (wt%)	1004	47.3	117.0	82.2 ± 5.0

Table 3. Binder solutions properties and contact angle with CMC Avicel 105 (viscosity determined at 1047 rpm for HPMC 3%)

	Wa	Ca*
Water	98.1	0.06
PVP 3%	92.8	0.08
PVP 13%	77.5	0.23
HPMC 0.5%	58.9	0.30
HPMC 1%	56.1	0.84
HPMC 3%	53.7	12.76

Table 4. Work of adhesion and modified capillary number values for the studied binder solutions (binder solutions and CMC Avicel 105)

Table 4 presents the values of the work of adhesion defined as:

$$W_a = \gamma (\cos \theta + 1) \quad (\text{II-2})$$

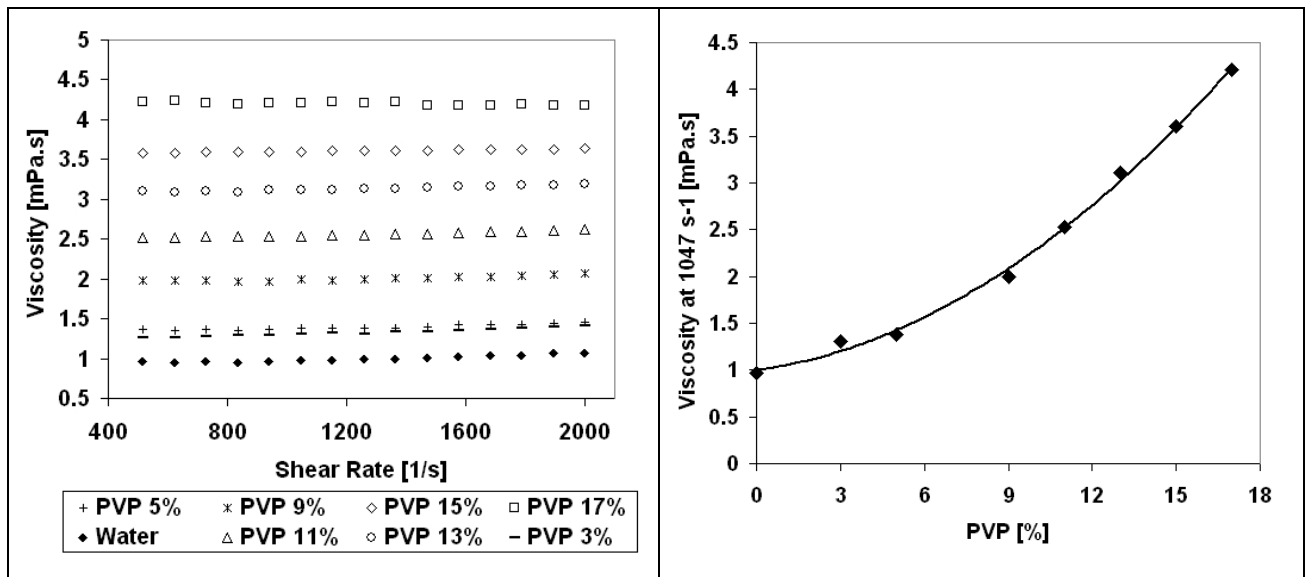
Where θ is the contact angle and γ_L the liquid surface tension,

and the modified capillary number allowing to take into account the contact angle between the powder and the liquid binder as proposed by Benali [12]:

$$Ca^* = \frac{\mu U}{\gamma(1 + \cos\theta)} \quad (\text{II-3})$$

Where U is the speed of the particles, μ is the binder viscosity, γ is the liquid surface tension and θ the contact angle.

As it can be seen in Tables 4 we can investigate the effect of interfacial forces for similar values of liquid viscosity (water and PVP 3%, and PVP13% and HPMC 0.5%) as well as the effect of viscosity for similar values of work of adhesion (the HPMC solutions), while varying the modified capillary number values between 0.06 and 12.76.



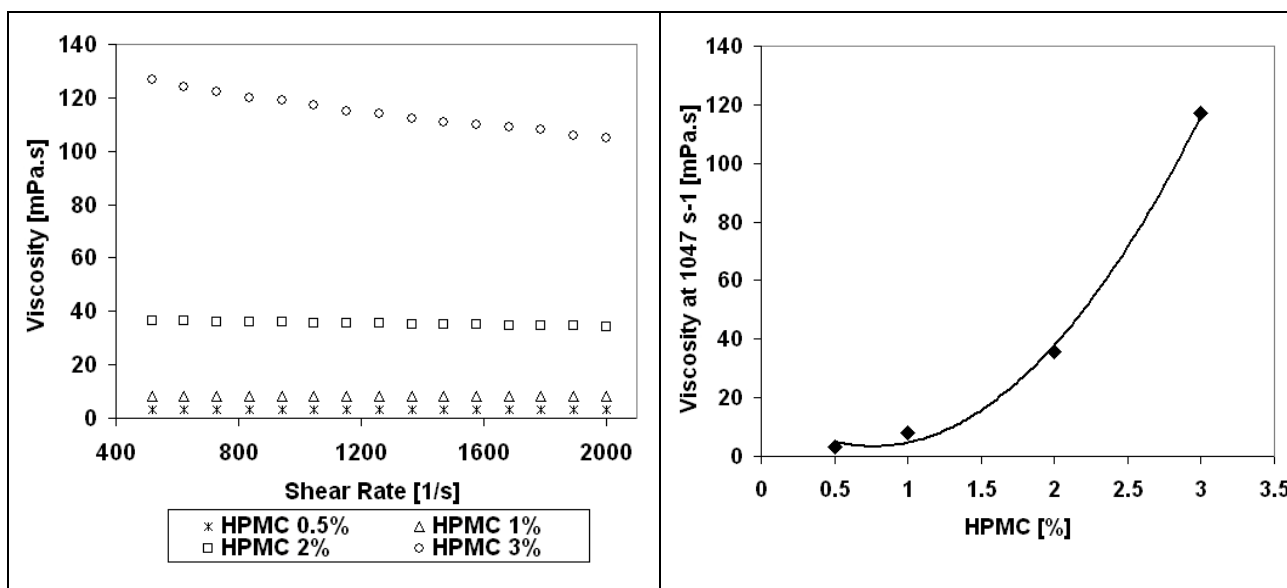


Figure 6. Viscosity evolution as a function of polymer concentration and shear rate

2. Characterization Methods

The characterization methods used in this study can be divided in morphological characterization methods, rheological and mechanical.

2.1. Morphological Characterization Methods

Morphological characterization methods include:

- the study of granule surface morphology achieved on a Scanning Electron Microscope,
- starting materials interaction with water was studied by water sorption isotherms,
- granule roundness characterization on a an automated microscopy and image analysis technique, true density on a helium pycnometer,
- mean granule size distribution by sieving,
- granule porosity by mercury porosimetry.

In order to assess granule growth and morphological properties representative samples of solid (15 to 30g) were removed from the bed and tray-dried at 40°C for 24 hours. Due to the small size of the Mi-Pro mixer bowl each sample was taken from a new batch with experiments being carried out twice. The dried granules were sieved and 15 size fractions were collected. Weight mean diameter was determined using the following equation:

$$\text{Mean diameter: } d_{\text{pm}} = \frac{\sum_i f_i d_i}{\sum_i f_i} \quad (\text{II-4})$$

Where f_i is the particle mass fraction of size interval i , d_i is the mean diameter of size interval i (μm). For a better understanding of agglomeration mechanisms, three characteristic granule classes were defined (Figure 7): fine (corresponding to the initial powder with granule diameters and dry agglomerates inferior to 200 μm), intermediate (weak granules with diameters between 200 μm and 800 μm) and coarse agglomerate (strong, dense granules with diameters greater than 800 μm but smaller than 5mm). Granules exceeding 5mm are defined as lumps. Figure 7 shows the defined classes at 50% liquid to solid ratio for an impeller speed of 800 rpm and chopper speed of 3000 rpm as well as the expected effect on the granule sizes of impeller and chopper, with the impeller promoting agglomeration of fine and intermediate particles and the chopper cutting up the larger coarse particles.

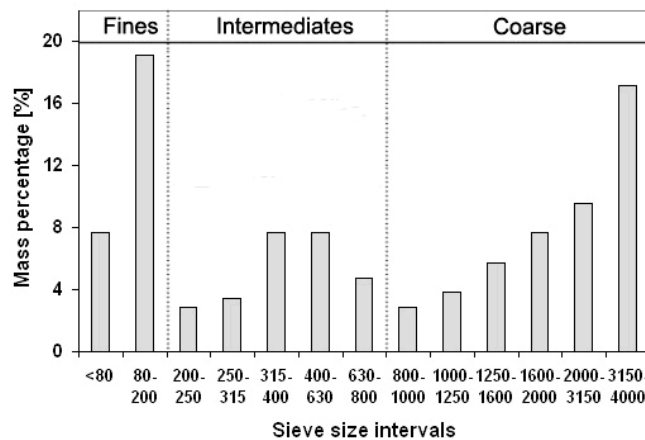


Figure 7. Sieving results for a L/S ratio of 50% (Mi-Pro $V=1.9L$, $w=800$ rpm, chopper=3000 rpm)

In our study the tapped and apparent density were evaluated using a tapped density tester (Erweka Ltd). The apparatus consists of two graduated cylinders placed on the tester platform. The tapping action is generated by a camshaft that lifts the platform and allows it to drop back onto its original position. The applied speed was of 300 taps per minutes and the number of taps applied was directly related to the changes observed by the operator in the volume occupied by the powder. Usually after ten minutes no further changes were observed in the volume occupied by the powder. The bulk density was the density obtained by dividing the mass of powder introduced to the volume occupied by the aerated powder in the cylinder. For the determination of the wet mass bulk density the wet granules were just slightly manually tapped in a graduated cylinder as the wet product could easily be deformed and densified on prolonged tapping.

The microcrystalline cellulose powder did not exhibit any intragranular porosity accessible by mercury porosimetry. The equation used to determine porosity is based on the tapped density of the powder and the true density determined by helium pycnometer:

$$\varepsilon = \left(1 - \frac{\rho_{tapped}}{\rho_s} \right) \cdot 100 \quad (\%) \quad (\text{II-5})$$

Granule roundness was determined by an automated microscopy and image analysis technique (PharmaVision 830, Malvern Instruments Inc. USA). Roundness is a measurement relating length to width and presenting values in the range of 0 to 1. A perfect circle would present a roundness of 1 while a needle shaped particle would have a roundness close to 0. The roundness is determined typically using the equation:

$$Roundness = \frac{4\pi A_g}{P_g^2} \quad (\text{II-6})$$

Where A_g is the measured area and P_g is the perimeter of the granules. The zoom objective was used at the 0.5 position at which it presents a resolution of 18 μm , a depth of field of 11 μm , a field of view of 4722x6166 μm and can analyze granules in the size range of 45 to 1908 μm . Granules investigated for roundness where granules in the range of 1000-1250 μm . Results can be expressed as a function of number or value distributions

however in our experiments both methods presented very similar values as well as nearly identical trends.

Adsorption isotherms, characterizing liquid to solid adsorption have been investigated for the starting materials. They represent the relationship between the amount of gas or liquid adsorbed by unit mass of solid and the equilibrium pressure (or relative pressure) at a known temperature.

The sorption characteristics of cellulose and lactose have been determined by a gravimetric method using a Surface Measurement Systems® automated Dynamic Vapor Sorption (DVS-1000) instrument which measures the uptake and loss of vapor using a controlled atmosphere microbalance with a mass resolution of $\pm 0.1 \mu\text{g}$ equipped with a video microscope system. The vapor partial pressure around the sample is controlled by mixing dry and saturated vapor gas flows using electronic mass flow controllers. In these experiments, the variation of mass of the sample was measured as a function of time over a range of values of relative humidity. The temperature is maintained constant at $25^{\circ}\text{C}\pm 0.1^{\circ}\text{C}$ by enclosing the system in a temperature-controlled incubator.

2.2 Rheological Characterization Methods

Rheological characterization methods include:

- characterization of starting materials flowability on an Hosokawa powder tester and - granule bulk and tapped density on a tapped density tester
- characterization of powder binder interaction by the multiple liquid addition method and and characterization of wet mass consistency on a mixer torque rheometer

2.2.1 Flowability of the Starting Powders

The flowability of the starting powders used in this study was assessed by calculating the Carr index (Table 5) and by tests carried out on a Freeman FT4 equipped with a shear cell (Appendix II.3). The tests on the shear cell allowed us to obtain the flow functions for our initial powders following the Jenike classification of flowability by flow index [13]

and allowed us to further describe the cohesion of our initial powders (Figure 8). The Hausner ratio gives a measure of the compressibility of the powder.

$$I_c = \left(\frac{\rho_{tapped} - \rho_{bulk}}{\rho_{tapped}} \right) \quad (II-7)$$

$$H_r = \frac{\rho_{tapped}}{\rho_{bulk}} \quad (II-8)$$

Carr Index (%)	Flowability	Powder State
5-15	Excellent	Sand like powder without fibres and fine particles
15-18	Good	Sand like powder without fibres and fine particles
18-22	Normal	Powder with small amounts of fine particles and high density particles
22-35	Not Good	Powder with fine particles
35-40	Poor	Cohesive powder
>40	Very Poor	Very cohesive powder

Table 5. Flowability of powders according to the Carr index

Hausner Ratio	Compressibility
<1.25	Low
1.25-1.4	Intermediate
>1.4	High

Table 6. Compressibility of powders as a function of the Hausner ratio

Powder	Carr Index	Hausner Ratio
α Lactose	48,89	1,95
MCC Avicel 101	32,37	1,48
MCC Avicel 105	51,47	2,06

Table 7. The Carr index and Hausner ratio for the starting materials

According to the values obtained for the Carr index and Hausner ratio (Table 7) we can observe the larger microcrystalline cellulose powder, MCC Avicel 101, showing a better flowability and somewhat lower compressibility than both of the main powders in this study: MCC Avicel 105 and lactose.

Figure 8 shows the obtained flow functions (measurement detailed in Appendix II.3) that confirm the predictions of the Carr index with the MCC Avicel 101 showing better flowability than both MCC Avicel 105 and Lactose that are in the cohesive region.

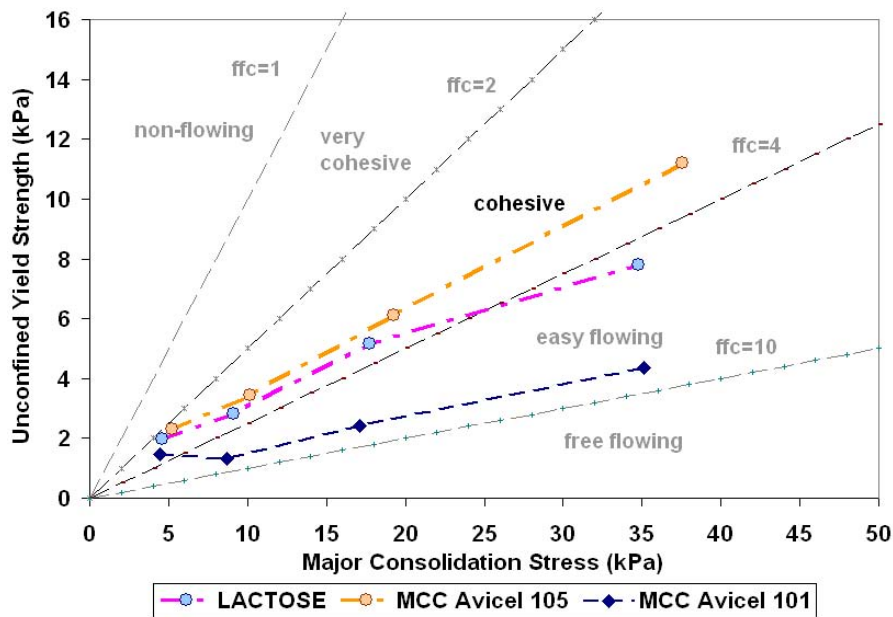


Figure 8. Flow functions for the studied materials

2.2.2 Characterization of Binder Powder Interactions

The characterization of binder powder interactions was achieved using a mixer torque rheometer (Model MTR, Caleva Ltd, Dorset, England) which allows recording of torque values while the wet mass is being mixed. Two types of measurements have been carried out in this study:

1. The MTR (Figure 9) was used as a tool for initial characterization of the powder binder couple by carrying out the multiple binder addition test. The binder is added to the powder with a certain liquid flow rate and then both binder and powder are mixed for a certain time. This step is repeated a certain number of times usually taking the powder

from the dry state to a suspension. The mixer torque rheometer measures two values in function of time and added liquid: the mean torque and the amplitude of the torque oscillations or torque range [14]. The mean torque is equivalent to the resistance of the wet mass to mixing and allows the monitoring of the different states of saturation of the agglomerate (Figure 10). The torque range describes the heterogeneity of the wet powder being a measure of mean torque standard deviation. In this study only the mean torque is represented as the mean range showed the same effects.

The dry powder was mixed in the rheometer for 30 seconds in order to obtain the baseline response. The quantity of dry powder was selected so as to cover the mixing blades which led to a fill ratio of about 40%. The binder was added by the multiple addition method, after each addition the wet mass is mixed and at the end of the mixing period a mean torque value is stored so that each point on the torque curve corresponds to an addition and so to a new saturation value of the wet mass. The torque values are expressed as normalized torque thus taking into account the fill level. For all our experiments on the mixer torque rheometer a target mixing time of 10 minutes has been sought in order to ensure the good distribution of the binder in the powder bed.

2. The wet mass consistency was determined on the MTR. The MTR (Figure 9) presents a great impeller surface in a confined bowl allowing an intense mixing of the wet mass. Samples of wet granules were mixed in the MTR and the torque response was recorded. A time of 480s was imposed for mixing of the wet granules. Granules are deformed under the action of the impellers and torque values evolve to a constant value named wet mass consistency.

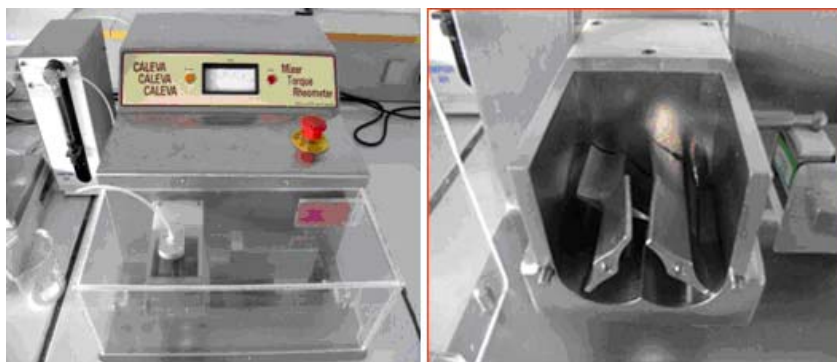


Figure 9. The mixer torque rheometer (MTR)

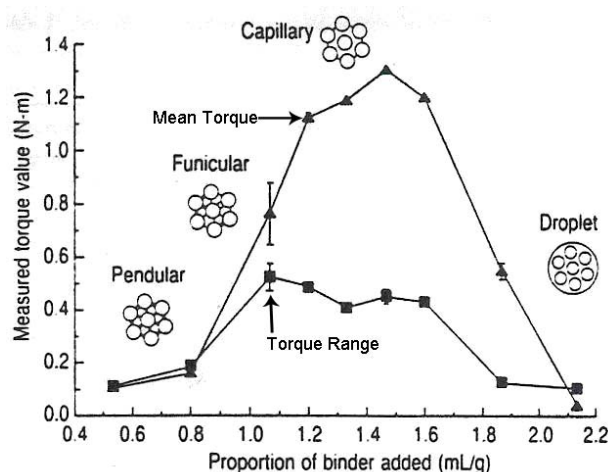


Figure 10. Mean torque as a function of added binder on the MTR [14]

2.3 Mechanical Characterization Methods

The mechanical characterization methods include the testing of the mechanical strength of the obtained granules.

Two units were used in order to assess dry granule strength: a Texture Analyser XT plus (Figure 11) from Stable MicroSystems and a Instron 5567 mechanical testing machine (Figure 12). The Instron testing machine allows recording a maximum force of 500N while the Texture Analyser equipped with a 5kg load cell only allows measuring forces up to 50N. Both values were, however sufficiently high to ensure the breakage of the granules. Due to availability issues of the Instron testing machine, the Texture Analyser had to be used for the characterization of granules obtained with different binders (Subchapter III-3). While the principle is the same results are not directly comparable due to the difference in load cells as well as probe surface size for the two machines. All other granule strength characterizations have been carried out on the Instron testing machine.

Single granules were compressed with a stainless steel probe with pictures were taken before and after compression. Granules tested had a diameter close to the mean diameter of the granulation run. Granule strength was assessed using the following equation proposed by Adams et al [15]:

$$\sigma_g = 4 \frac{F_{\max}}{\pi \cdot D_g^2} \quad (\text{II-9})$$

Where F_{\max} is the fracture force and D_g is the measured granule diameter.

Imposed velocity of the steel probe was of 1 mm/min unless otherwise stated.

Because granules are semi-brittle measuring the compression strength is possible. When the granule is subjected to compressive strain (displacement) a marked drop in the signal can be observed when the granule first cracks (Figure 13). The values recorded after this point on the load-displacement curve are of little practical use as they represent the compression of granule fragments and eventually powder particles.



Figure 11. The Texture Analyzer XT plus

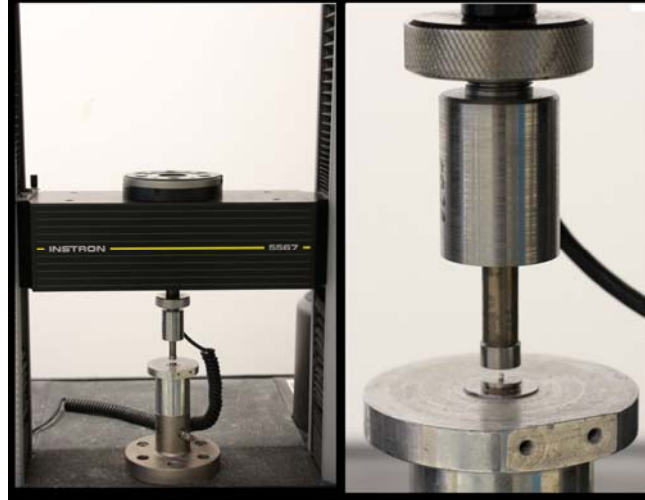


Figure 12. The Instron 5567 mechanical testing machine

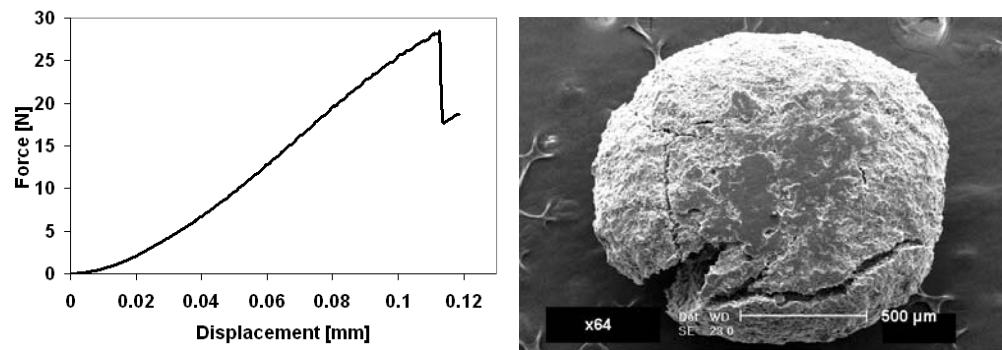


Figure 13. Load-displacement evolution for MCC Avicel 105 granulated with water, granule of 1.1 mm diameter under uniaxial compression at 1mm/min

2.3.1 Preliminary Tests

Figure 14 shows the evolution of the mean fracture force standard deviation as a function of the number of granules tested. There is only a very small difference in the mean value for the test of more than 30 granules. In our study the results expressed represent the mean deviation for at least 30 granules. The standard deviation calculated using Microsoft Office Excel was defined as:

$$St_{dev} = \sqrt{\frac{\sum (x - \bar{x})^2}{n - 1}} \quad (\text{II-10})$$

Where \bar{x} represents the arithmetic mean of the x values and n the number of values.

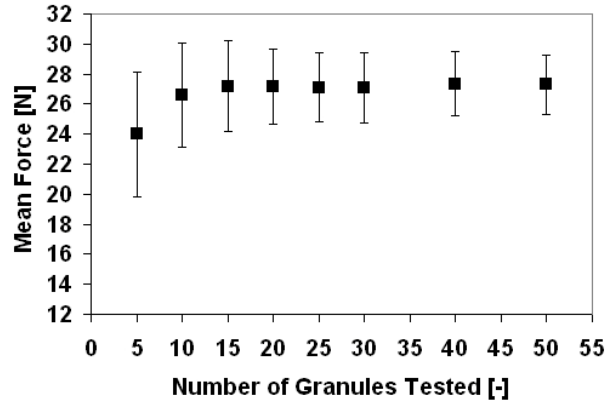


Figure 14. Mean value and standard deviation for granule strength measurements as a function of the number of tested granules (Avicel 105 granulated with water at 800 rpm in the Mi-Pro V=1.9L, granules in the size class 1000-1250 μ m)

The granules seem to exhibit elastoplastic deformation which led us to investigate also the evolution of the Young's modulus. We applied the methodology described by Mangwandi et al. [16] in finding the elastic limit by following the linearity of the equation at the beginning of the compression cycle, allowing us to determine the point up until which the Hertz equation is applicable (Figure 15). The Hertz equation [17] is described as:

$$F = \frac{\sqrt{2}}{3} R_g^{1/2} E_l^* \Delta^{3/2} \quad (\text{II-11})$$

where F is the force, R_g is the radius of the granule, E_l^* is the effective Young's modulus and Δ is the total displacement of the moving platen. They [16] simplified the effective modulus by considering it reasonable that the Young's modulus of the platens is much greater than that of the granules so that the effective Young's modulus becomes a function of Poisson's ratio considered to be 0.2 as a typical value for porous materials as described by Chun et al [18]:

$$E_l^* = \frac{E}{1-\nu^2} \quad (\text{II-12})$$

Where E is the Young's modulus and ν is the Poisson's ratio.

The energy required to be transmitted to the granule in order to induce macroscopic failure has been calculated from the area under the force displacement curve (Figure 16) up to the fracture peak using the OriginPro8[®] (Originlab) data analysis software. The fracture energy has been calculated as an absolute value but also as specific fracture energy as a function of the mean granule size by dividing the obtained surface by peak integration with the granule contact surface.

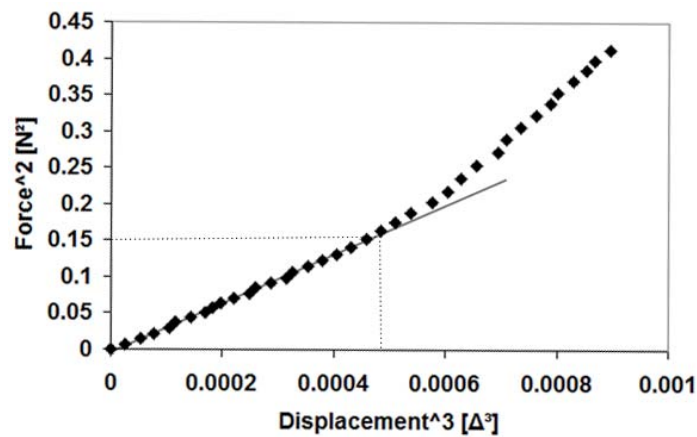


Figure 15. Identifying the elastic limit of the granules by linearizing the Hertz equation

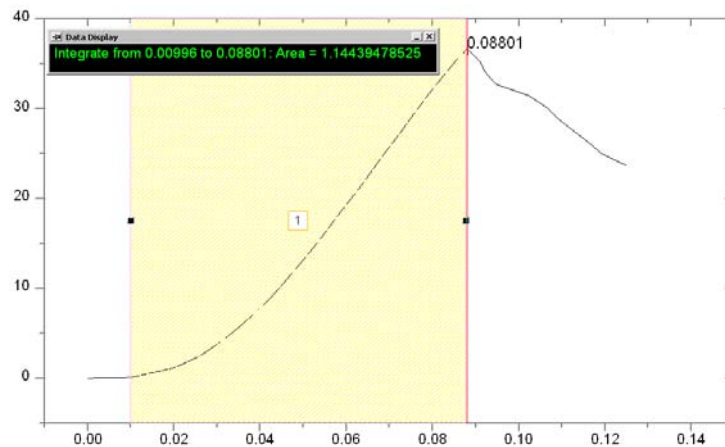


Figure 16. Force-displacement peak integration using the OriginPro 8 data analysis software

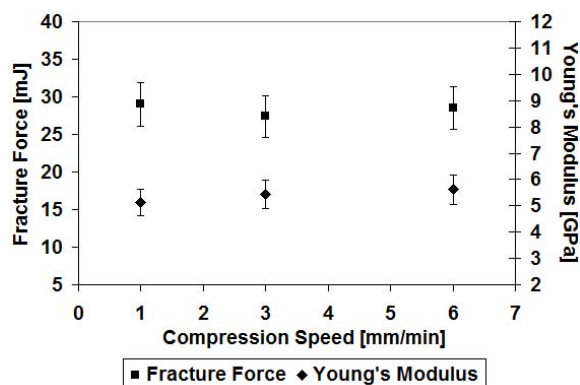


Figure 17. Fracture force and Young's modulus as a function of compression speed

Three compression speeds have been investigated: 1, 3 and 6 mm/min. Figure 17 shows the evolution of the Young's modulus and the fracture force as a function of compression speed for granules with mean granule sizes between 1000 and 1250 microns. We found that compression speed seems to have only a small influence on both parameters. However the loading Young's modulus can be more precisely identified at the smaller compression speeds, which is why the rest of our results correspond to a 1 mm/min compression speed.

3. Wet Granulation Protocol and Equipment

3.1 Introduction

High shear wet granulation can be achieved in a variety of mixer designs and can be instrumented or not. As a function of the high shear mixer design forces of different magnitude can be exerted on the powder bed. Figure 18 shows the forces that are subject to be influenced by the high shear mixer design according to Royce et al [19]: acceleration force (F1), resistance of the bowl (F2), centripetal force (F3), centrifugal force (F4), gravitational force (F5), and a fluidization force resulting from the angle of the impeller blade (F6).

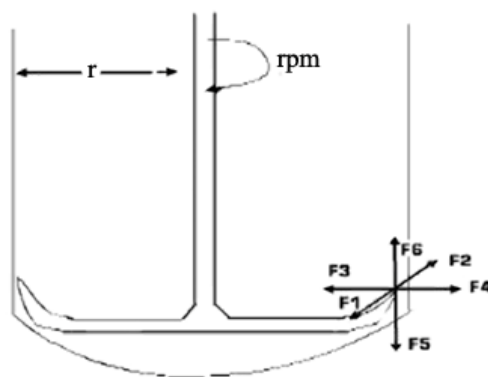


Figure 18. Forces developed by the equipment during the granulation process [19]

High shear mixers can be vertical or horizontal mixers (Figure 19) depending on the rotation plane of the impeller shaft. A special type of vertical high shear mixer is the high shear mixer with replaceable bowls where the chopper and the impeller are top driven and which allows the reduction of contamination since the seals do not come in contact with the product. In this thesis we focused on the wet granulation process performed in vertical high shear mixers.

A typical high shear granulation experiment implies the following steps:

- Premixing (usually done at high impeller and chopper speeds) of the initial dry powder
- Addition of the liquid binder, we distinguish:
 - when the binder is poured in, the binder requirement is known and all the binder is introduced in the beginning of the granulation process, usually at low impeller and chopper speeds and followed by wet massing at high impeller and chopper speeds
 - when the binder is added gradually, binder addition and wet massing are concomitant usually at high impeller and chopper speeds
- Drying stage

As this thesis also uses the torque as a means to control wet granulation, binder is always added gradually in order to study the changes in torque as a function of added binder amount. The first two steps are done inside the granulator while the drying of the granules is done on a tray in an oven.

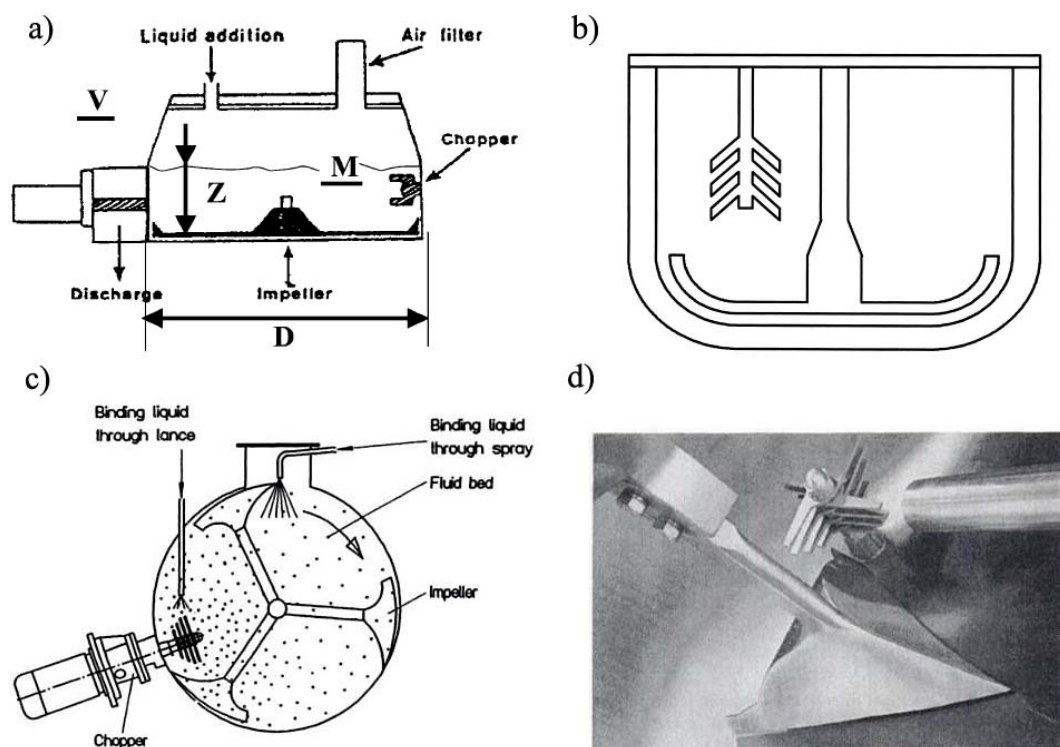


Figure 19. Two design philosophies for vertical high shear mixers: a) and b), schematic view of a horizontal high shear mixer c) and view inside an horizontal high shear mixer showing the ploughshare shovel, inlet lance for binder liquid and multibladed chopper

3.2 Wet Granulation Protocol

Granulation time for all experiments was of about 14 minutes: two minutes of dry mixing allowing for homogenization of the dry mass and allowing us to check torque stability and twelve minutes of wet mixing during which binder was added at a certain flow rate using a drop by drop system. The first granulation runs allowed us to establish the torque profiles for the studied operating conditions, powder and binder used. The results obtained are expressed in function of the fraction added liquid to initial dry powder mass named liquid to solid ratio:

$$L/S \text{ Ratio} = \text{Added Liquid Mass [kg]} / \text{Initial Powder Mass [kg]} (\%) \quad (\text{II-13})$$

Discussing kinetics as a function of added liquid will always present a certain degree of relativity as the added liquid may or may not correspond to the granule liquid saturation especially when poor liquid distribution is involved. However, as we will discuss when presenting the materials used in this study, the complex nature of liquid solid interactions between the chosen powders and binders makes calculating saturation difficult.

One of the most important parameters in wet granulation is the optimum liquid requirement. These first experiments allowed us to visually observe the evolution of the wet mass and obtain the torque curves which on analysis indicated the optimum liquid to solid ratio. These experiments were followed by new experiments where the granulation run was stopped at different liquid to solid ratios and samples were retrieved. These samples allowed us to characterize wet mass properties like wet bulk density, wet mass consistency and dry mass properties like mean granule size and morphology after drying. The drying of the granules was done overnight for about 24 hours at 40°C.

3.3 The Mi-Pro HSM

The Mi-Pro (Pro-C-Ept, Zelzate, Belgium) high shear mixer allows granulating while recording real time impeller torque values with 1 second intervals. This vertical axis high shear granulator can be equipped with differently sized glass bowls with corresponding three bladed impellers and choppers. They can range from 0.25 capacity to 1.9L through 0.5L and 0.9L. In this thesis the 1.9L capacity bowl was chosen as the reference scale with some granulation runs being carried out at the 0.9L scale. Figure 20 gives the schematic description of the 1.9L and 0.9L bowls the only difference between them being a slight inclination of the chopper on the 0.9L bowl. The mixer is composed from:

- An impeller that is close to the bottom of the bowl.
- A chopper that is closed to the wall of the bowl.
- The binder delivery system consists of an aspiration pump delivering the binder through a tube that intrudes in the mixer bowl. Binder addition was done at a constant rate using a Dosimat 760 syringe pump (Metrohm, Berchem, Belgium). The size of the capillary at

the end of the tube is of about 400 μ m and binder flow is directed towards the chopper in order to ensure better binder dispersion.

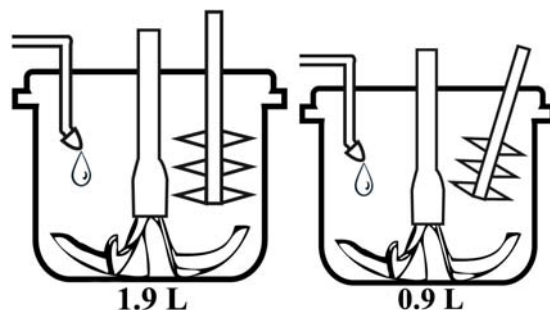


Figure 20. Schematic representation of the two Mi-Pro bowls employed

Figure 21 shows the whole setup including the computer whose software interface allows changing impeller, chopper and liquid dosing speed as well as allowing the operator to follow a real time evolution of the recorded torque and temperature.

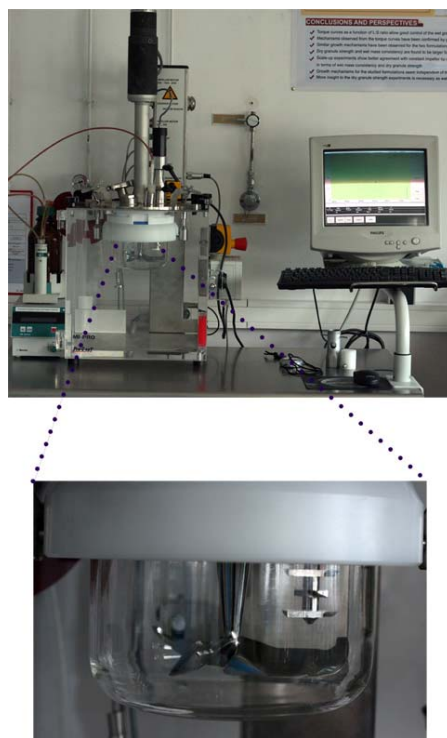


Figure 21. The Mi-Pro high shear mixer

3.4 The Diosna P 1-6 HSM

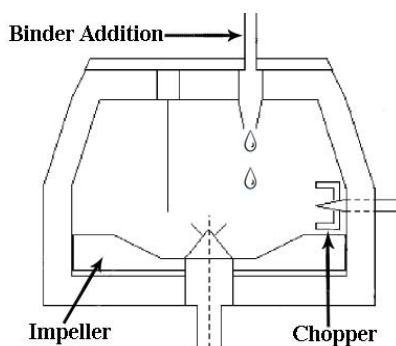


Figure 22. Schematic of the Diosna high shear mixer

The Diosna high shear mixer (Figure 22 and 23) is a 6L unit with a three bladed impeller and a tulip shaped chopper. Binder addition is done via a pump in a drop by drop manner with the size of the capillary of about $800\mu\text{m}$. The Diosna high shear mixer doesn't record torque or power consumption curves but it does represent the power consumption and temperature on the screen of the computer used to control impeller and chopper speed.



Figure 23. The Diosna high shear mixer

4. Conclusion

In this chapter we have presented the products on which this study is focused, the equipments and the methods used to characterize our results. The main powders in this study are: MCC Avicel 105 and Lactose both being very cohesive powders with poor flowability characteristics. MCC Avicel 101 which is more common for high shear wet granulation experiments is also present in this study but only for comparison purposes. Because it is not soluble and because of its strong cohesion the MCC Avicel 105 seems an interesting candidate in evaluating the relationship between torque curves and the main factors influencing high shear wet granulation. The influence of the main operating conditions and binder properties will be studied on the MCC Avicel 105 and from this point of view it should be considered the main powder in this study. Lactose is a product commonly found alongside MCC in granule formulations, it is soluble and allows for fast disintegrating tablets and is present in many of today's excipient formulations.

The main equipments for creating granules have also been presented. The Mi-Pro high shear granulator allows working with different sized bowls similar in terms of bowl, impeller and chopper geometry and allowing the recording of torque curves developed on the main impeller shaft. The main scale of study is the Mi-Pro equipped with a 1.9L bowl. The Mi-Pro 0.9L bowl allows us to investigate granulation on a lower scale while the 6L Diosna high shear mixer allows us to investigate the effect of mixer design on a larger scale.

Powder binder interaction will be assessed by means of contact angle measurements and rheology characterization on a mixer torque rheometer. Granule strength in the dry state will be evaluated by diametric single granule compression tests while wet granule strength will be assessed by using the same mixer torque rheometer in order to determine the wet mass consistency.

References

- [1] D. K. Sidiras, D. P. Koullas, A. G. Vgenopoulos, E. G. Koukios, Cellulose crystallinity as affected by various technical processes, *Cellulose Chemistry and Technology* 24 (1990) 309–317
- [2] P. Luukkonen, Rheological properties and the state of water of microcrystalline cellulose and silicified microcrystalline cellulose wet masses, Academic dissertation, Pharmaceutical Technology Division Department Pharmacy University Helsinki (2001)
- [3] J. Ribet, Fonctionnalisation des excipients : Application a la comprimabilité des celluloses et des saccharoses, Thèse Université de Limoges, Faculté de Pharmacie
- [4] K.E. Fielden, J.M. Newton, P. O'Brien, R.C. Rowe, Thermal studies of interaction of water and microcrystalline cellulose. *J. Pharm. Pharmacol.* 40 (1988) 674–678
- [5] P. Kleinebudde, The crystallite-gel-model for microcrystalline cellulose in wet granulation, extrusion and spheronization, *Pharm. Res.* 14 (1997) 804-809
- [6] P. W. S. Heng, O. M. Y. Koo, A Study of the Effects of the Physical Characteristics of Microcrystalline Cellulose on Performance in Extrusion Spheronization, *Pharm. Res.* 18 (4) (2001) 480-487
- [7] P. Luukkonen, T. Maloney, J. Rantanen, H. Paulapuro, J. Yliruusi, Microcrystalline Cellulose-Water Interaction—A Novel Approach Using Thermoporosimetry, *Pharm. Res.* 18 (11) (2001) 1562-1569
- [8] J. Kristensen, T. Schæfer, P. Kleinebudde, Direct Pelletization in a Rotary Processor Controlled by Torque Measurements. II: Effects of Changes in the Content of Microcrystalline Cellulose - AAPS Pharmsci 2(3) article 24 (2000)
- [9] T. Suzuki, H. Kikuchi, S. Yamamura, K. Terada, K. Yamamoto, The change in characteristics of microcrystalline cellulose during wet granulation using a high-shear mixer, *J. Pharm. Pharmacol.* 53 (2001) 609–616
- [10] P. Kleinebudde, M. Jumaa, F. El Saleh, Influence of degree of polymerization on behavior of cellulose during homogenization and extrusion/spheronisation, AAPS Pharmsci 2 (3) article 21 (2000)
- [11] J.J. Sousa, A. Sousa, F. Podczek, J.M. Newton, Factors influencing the physical characteristics of pellets obtained by extrusion-spheronization, *Int. J. Pharm.* 232 (2002) 91-106
- [12] M. Benali, V. Gerbaud, M. Hemati, Effect of operating conditions and physico-chemical properties on the wet granulation kinetics in high shear mixer, *Powder Technol.* 190 (2009) 160-169
- [13] J. Schwedes, Testers for measuring flow properties of particulate solids, *Powder Handling and Processing* 12 (4) (2000) 337-354
- [14] R. C. Rowe, Characterization of wet powder masses using a mixer torque rheometer. 4. Effect of blade orientation, *Int. J. Pharm.* 133 (1996) 133-138
- [15] M.J. Adams, M.A. Mullier, J.P.K. Seville, Agglomerate strength measurement using a uniaxial confined compression test, *Pow. Tech.* 78 (1994) 5-13
- [16] Mangwandi, C., Y.S. Cheong, M.J. Adams, M.J. Hounslow, A.D. Salman, The coefficient of restitution of different representative types of granules. *Chem. Eng. Sci.* 62 (2007), 437 - 450
- [17] K.L. Johnson, *Contact Mechanics*, Cambridge, Cambridge University Press (1985)
- [18] B.S. Chun, H.S.H.-S. Lim, M. Sagong, K. Kim, Development of a hyperbolic constitutive model for expanded polystyrene (EPS) geof foam under triaxial compression tests, *Geotextiles and Geomembranes*, 22(4) (2004) 223-237
- [19] A. Royce, M. Mecadon, J. Holinej, A. Karnachi, S. Valazza and W. Wei, Process control and scale-up of high shear wet granulation, *The Journal of Process Analytical Technology* 2 (2005) (2) 8–16

CHAPTER III

Effect of Operating Conditions and Material Properties on Wet Granulation

Chapter III.1: Typical Example

Because this study investigates variable operating conditions and varying binder band substrate natures we chose to begin the presentation of our wet granulation experiments with a typical example. It shows the granulation run for the case of Avicel 105 microcrystalline cellulose powder with ultra-pure water on the 1.9L Mi-Pro high shear mixer. The characterizations accessible to us for a typical high shear granulation run (impeller speed 800 rpm, chopper speed 3000 rpm) are presented.

1. Introduction

A typical wet granulation flux scheme can be observed Figure 1 as adapted from Ennis and Litster [1]. The main judging criterion of the wet granulation process is usually a particle size interval with anything not included in the researched size range being recycled into the process. Granule size depends on the starting material properties and the shear and impact forces developed in the granulator among others affecting the granule growth mechanisms. Newitt and Conway Jones in the 1950's [2] described the evolution of liquid bonding in the granule as the pendular, funicular, capillary and droplet stage. Many granulation mechanisms have been proposed for various mixer designs and starting materials. Predominance of one mechanism over the others depends on equipment variables and physico-chemical properties of the starting materials. The aim of this sub-chapter is to investigate the granulation of the MCC powder Avicel 105 on the Mi-Pro 1.9L bowl high shear mixer showing the granule growth mechanisms as well as the means to characterize the obtained product.

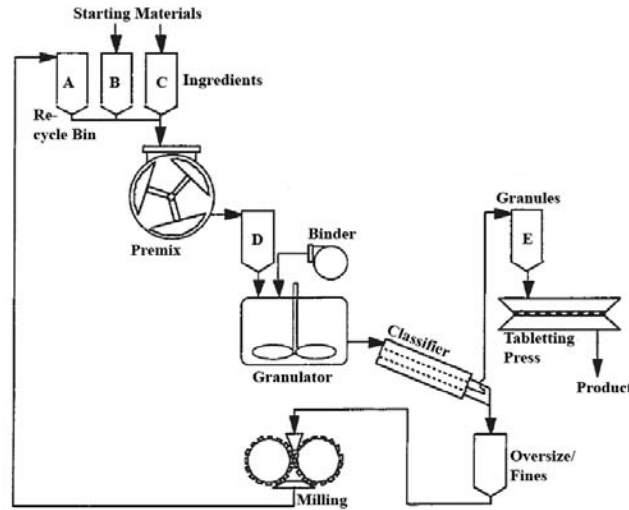


Figure 1. Typical agglomeration circuit adapted from Ennis and Litster [1]

2. Granulation Mechanisms

Before granulating the product in the Mi-Pro the mixer torque rheometer (MTR) was used to assess the interaction between the powder and the liquid binder. Table 1 shows the operating conditions for the runs on the mixer torque rheometer. Binder is added by multiple additions, for each addition the developed torque is recorded at 100 Hz and a mean point is calculated before another addition.

The curve obtained on the mixer torque rheometer (Figure 2) shows a slow evolution up to a liquid to solid (L/S) ratio of 20% corresponding to the wetting of the dry powder by the binder, for values between 20% and 43% an increase in torque is observed which might correspond to the formation of the first liquid bridges between the particles. For values between 43% and 85% a stark, almost linear increase in mean torque corresponding to the funicular stage. Beyond 85% the mass is very cohesive and evolves into a paste giving a maximum value at 150% L/S ratio. Beyond this point the paste transforms into a suspension and the torque values drop significantly. This preliminary test that takes little time and product allows us to predict the liquid requirement for the studied binder-powder couple and adjust the operating time on the Mi-Pro accordingly.

A typical granulation run in a high shear mixer consists of a succession of stages: a dry mixing stage, the wet massing stage when the granules are produced and liquid is added

gradually to the dry powder and a drying stage. Torque curves were recorded during granulation as well as the amount of added binder.

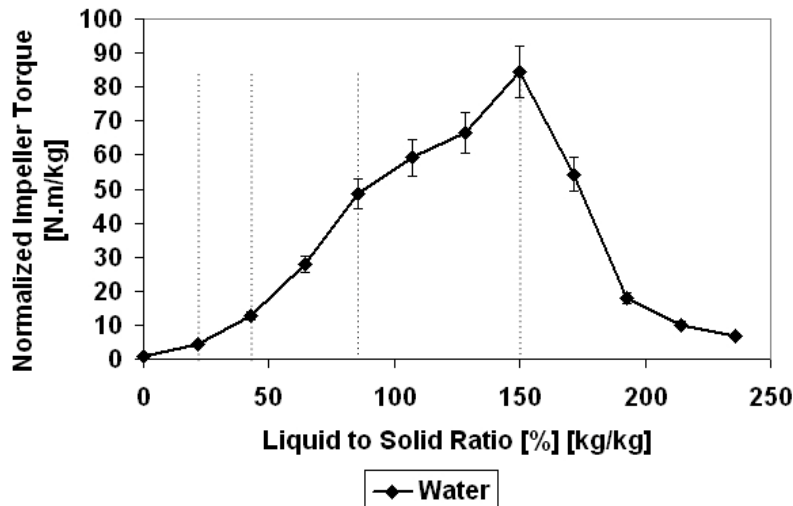


Figure 2. Normalized torque curve on the mixer torque rheometer (MTR) for the mixing of MCC Avicel 105 with ultra-pure water

Parameters	Mi-Pro	MTR
Binder	Ultra pure water	
Powder	MCC Avicel 105 ($d_{50}=20\mu\text{m}$)	
Mass (g)	120	14
Fill Ratio (% of Dry Powder Volume on Total Bowl Volume)	26%	40%
Liquid flow rate (ml/min)	10	3
Dry Massing Time [min]	2	0.5
Wet Massing Time [min]	12	1min/addition
Impeller speed (rpm)	800	42
Chopper speed (rpm)	3000	NA

Table 1. Operating conditions for the typical example on the Mi-Pro and on the MTR for the MCC Avicel 105 ultra-pure water couple

Figure 3 shows SEM pictures of the granules obtained. Figure 4 shows SEM pictures of granules obtained from microcrystalline cellulose and water on the Mi-Pro high shear mixer as a function of liquid to solid ratio and the corresponding torque curve. Figure 5 shows the evolution of the three characteristic classes, defined as fines for particles with a size below 200 microns, intermediates for particles between 200 and 800 microns and coarse for particles with a mean size between 800 microns and 4 mm. Based on these figures the observed growth mechanisms as a function of L/S ratio can be grouped as follows:

- for values of the S/L ratio between 0 and 20 % wetting occurs, SEM observations do not show any agglomerates. Only a very small percentage of fines is leading to intermediates, most probably because of the characterization method involved (sieving) and the very cohesive nature of the initial powder. Using a laser granulometry method for the initial stages of the granulation process might be a better solution than sieving.
- for values ranging from 20% to about 45% nucleation occurs with the fine particles agglomerating to intermediates in the 200-800 μm range,
- for L/S ratios exceeding 50% growth occurs by layering and coalescence, first with the fine particles being agglomerated into intermediate granules which achieve a maximum value at about 83% L/S ratio which also corresponds to the extinction of fines in the system and the apparition of the first coarse granules, secondly for values exceeding 83% when intermediate particles agglomerate to form coarse granules.
- for L/S ratios above 100% overwetting occurs, some usable granules could still be obtained up to 125% L/S ratio but the yield is low and the wet mass presents a high percentage of lumps. For values above 125% L/S ratio the wet mass evolves to highly cohesive paste where further binder addition for L/S ratios above 150% turns the paste into a suspension.

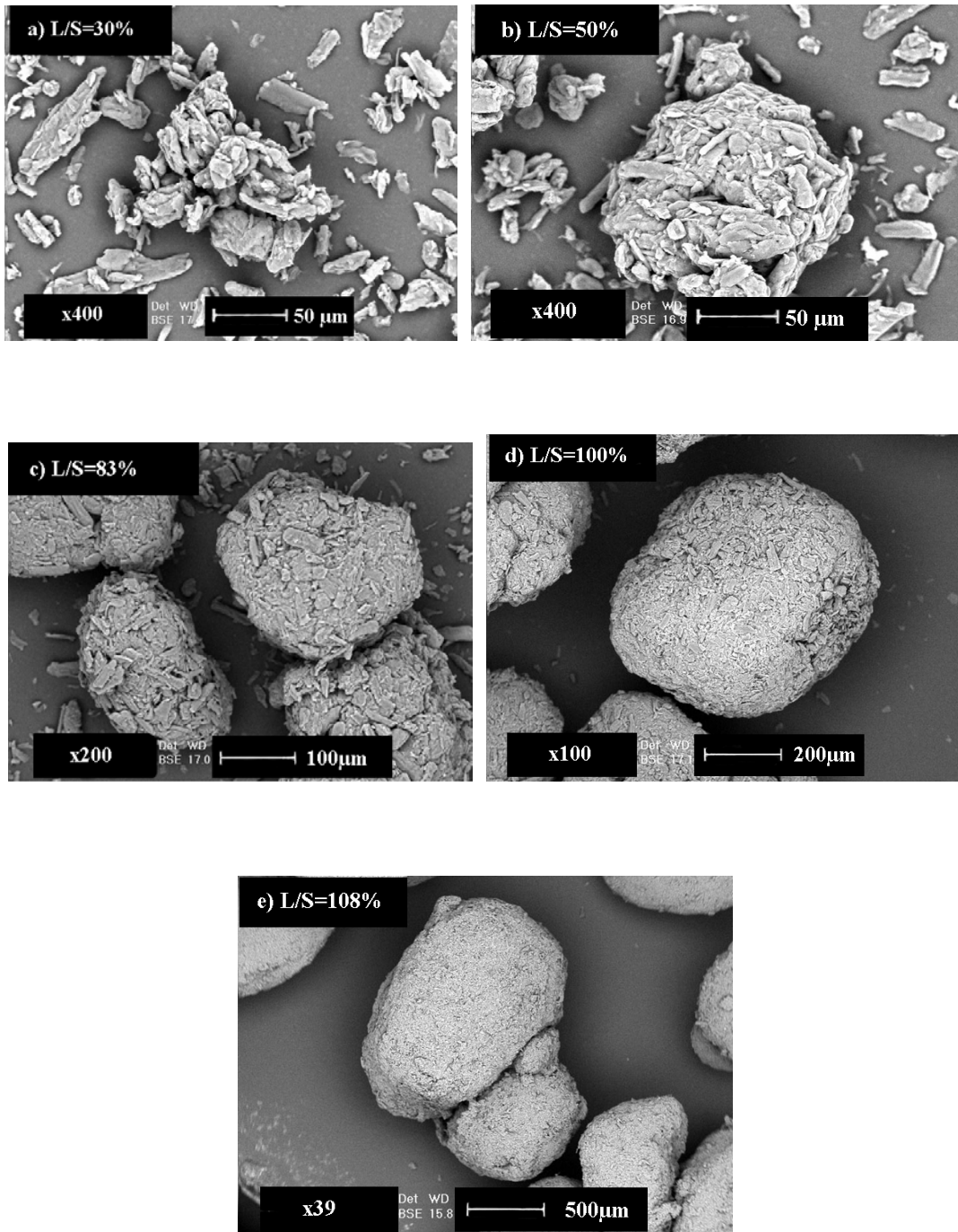


Figure 3. SEM images of the granules obtained in the Mi-Pro for the granulation of MCC Avicel 105 with ultra-pure water: Wetting (a), Nucleation (b), growth by coalescence/layering (c),(d), Over-wetting (e)

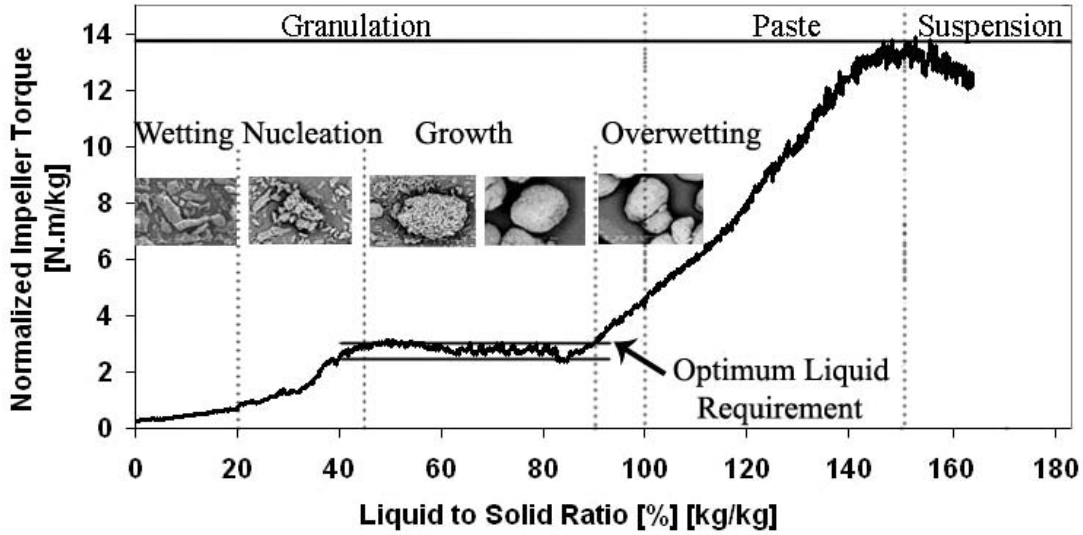


Figure 4. Torque curve obtained on the Mi-Pro HSM for the granulation of MCC Avicel 105 with ultra-pure water

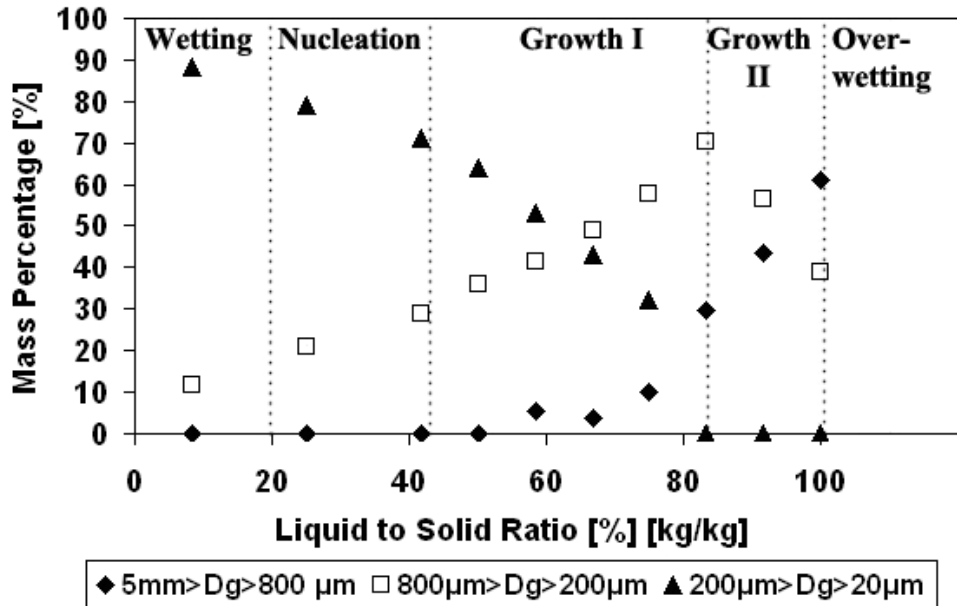


Figure 5. Evolution of the fine, intermediate and coarse size fractions obtained in the Mi-Pro for the granulation of MCC Avicel 105 with ultra-pure water

Figure 6 compares the torque curves obtained on the Mi-Pro and the MTR. What is immediately apparent is the much higher torque developed on the mixer torque rheometer which is clearly densifying more the wet mass and showing at the highest cohesion point

(150% L/S ratio) values roughly 6 times as high. Initially both start similarly: the wetting stages are almost identical while the nucleation stage seems to occur for similar values. From there on however differences become apparent: on the MTR granules are agglomerated much more quickly and liquid is more easily squeezed to the surface by the intense agitation taking place in the MTR and the mass evolves more quickly to a paste. Interestingly when the wet mass turns into a paste and no more differences exist between the structure of the product in either equipment we obtain the highest cohesion for the same L/S ratio. For values above 150% on the Mi-Pro the torque values (not represented) also drop however due to the stickiness of the paste it easily exits from the action range of the impeller sticking to the glass wall. This causes the torque curve to present great fluctuations and not be reproducible for values above 150% L/S ratio.

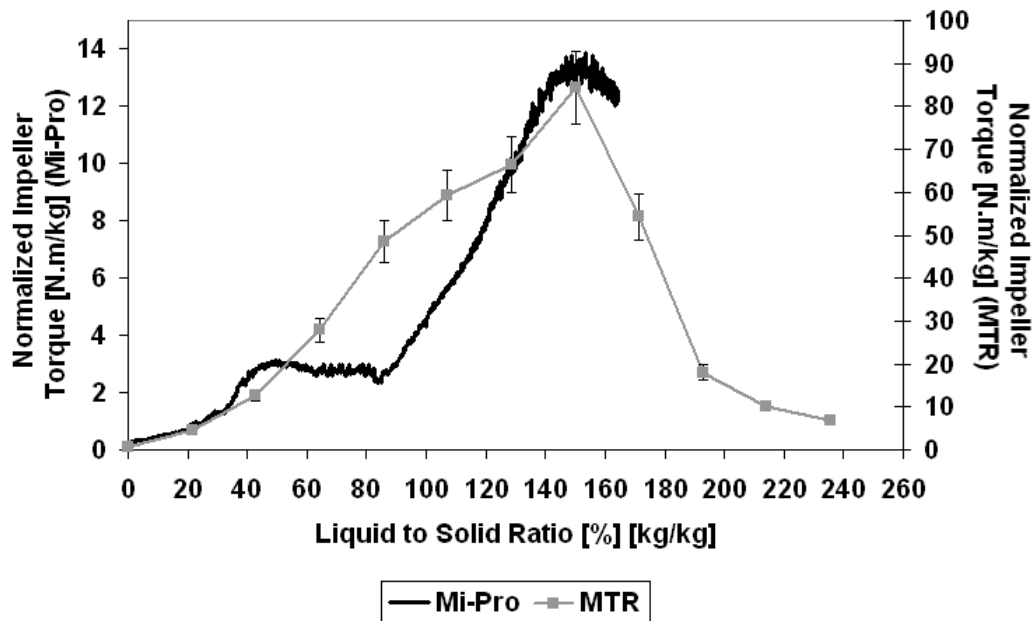


Figure 6. Comparison of the torque response for the granulation of MCC Avicel 105 in the Mi-Pro and the MTR with ultra-pure water

3. Optimum Liquid Requirement

Following the torque curve obtained on the mixer torque rheometer it is difficult to assess the optimum liquid requirement. The most reproducible point is the peak for which the wet mass in the Mi-Pro would correspond to a paste. On the Mi-Pro the growth zone is

represented by a plateau where the granule size is increasing (Figure 7) between 45 and 83-90% L/S ratio. So choosing an optimum L/S ratio near the end of the plateau would ensure bigger, denser granules. Following the evolution of the granule size fraction we can observe that the end of the plateau in the torque curve corresponds to the consumption of all the fine particles. This also explains the increase in torque values as with all the fines being consumed the collisions between similarly sized granules and between granules and impeller, chopper and walls squeezes more binder to the granule surface increasing their stickiness, which in turn increases torque (as shown by Bouwman et al [3]). Following the torque curves and the granule size fractions evolutions we defined an optimum L/S ratio of 100% allowing us to maximize the yield in coarse sized granules. It has to be mentioned that for 800 rpm the mean granule size is of 900 microns which is very close to the border chosen in order to separate the intermediates and coarse granules. So while the percentage of coarse particles might not seem that high the increase in mean granule size is evident and the limits between the different size classes have been chosen so as to cover a wide range of impeller speeds and binder viscosities.

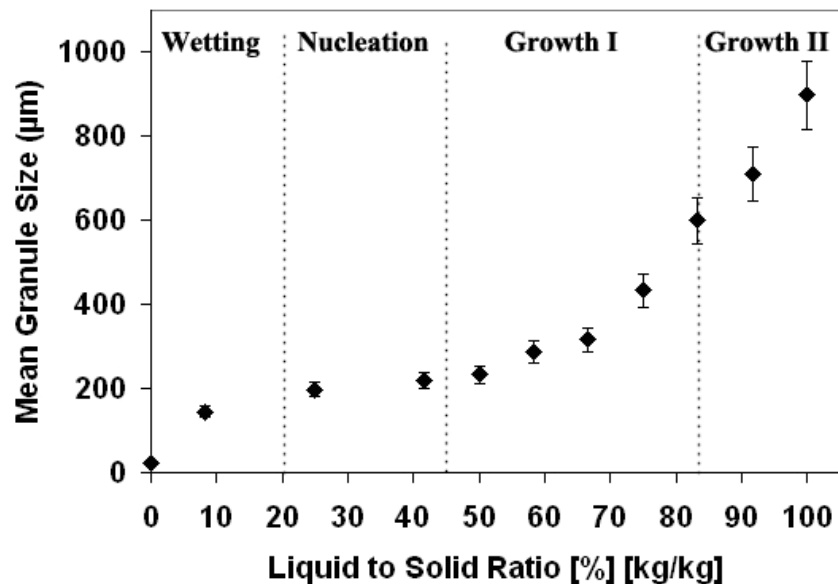


Figure 7. Evolution of mean granule size as a function of liquid to solid ratio obtained in the Mi-Pro for the granulation of MCC Avicel 105 with ultra-pure water

4. Granule Strength

4.1 Wet Granule Strength

Determining single granule strength as a function of added binder is difficult, when the binder is added gradually, as the granules in the early stages present low granule strengths and mean granule sizes and are difficult to get in the numbers needed so as to present statistically relevant results. This led us to investigate the bulk wet granule strength in the MTR, expressed as wet mass consistency.

While the values for the wet bulk density (Figure 8) are almost constant in the beginning of the process (between 0 and 50% L/S ratio) there are great differences when compared to the density at the end of the granulation. First there is a slight increase between 50 and 75% due to the apparition of dense coarse granules that are reflected in the density evolution followed by a strong increase in bulk density once the coarse fraction starts to increase (see also Figure 5). Because of this evolution the study of the wet mass consistency has been done at constant volume rather than constant mass with enough powder introduced in the mixer so as to cover the blades of the MTR.

Figure 9 shows the obtained the wet mass consistency measurements of the wet samples retrieved from the Mi-Pro high shear mixer. As it can be observed the technique is not very sensitive for low L/S ratios. Values increase as in the Mi-Pro only for values above 83% L/S ratio when all the fines in the system have been consumed the granules begin to exhibit liquid at their surface. This can also be observed through the glass bowl walls of the Mi-Pro where the fines covering the walls progressively disappear showing clear walls allowing the observation of the wet granules for values above 83% L/S ratio.

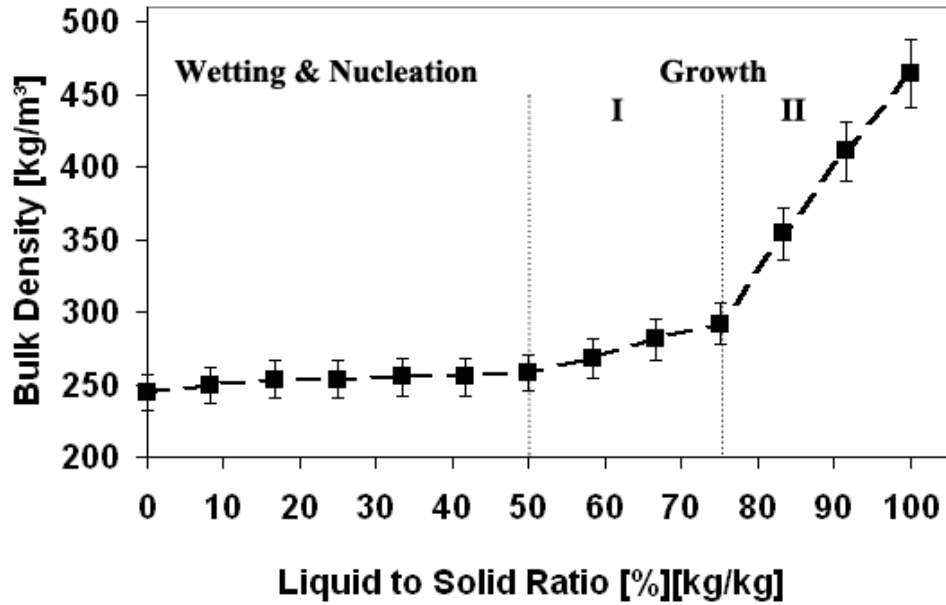


Figure 8. Evolution of the bulk density of the wet mass as a function of L/S ratio obtained in the Mi-Pro for the granulation of MCC Avicel 105 with ultra-pure water

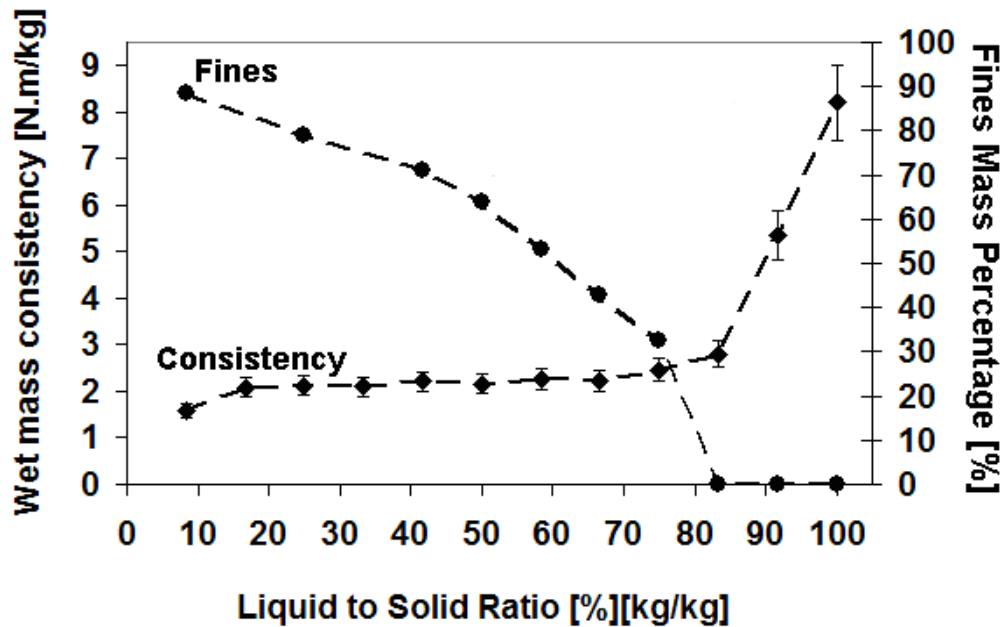


Figure 9. Evolution of wet mass consistency measurements as a function of L/S ratio obtained in the Mi-Pro for the granulation of MCC Avicel 105 with ultra-pure water

4.2 Dry Granule Strength

Figure 10 shows a typical granule size distribution for the typical experiment. Table 2 shows the obtained values for the fracture force, granule strength, loading Young's modulus, fracture energy and specific fracture energy as a function of mean granule size. Figures 11 to 13 show the graphical representation of these parameters as a function of mean granule size.

For the studied granulation run we investigated the evolution of the fracture force, granule strength, Young's modulus and fracture energy as a function of granule size. Based on the granule size distribution (Figure 10) we chose mean granule sizes between 400 and 1800 microns. 400 microns is found as a limit to successful single granule compression tests as even at that value most of the grains present a distinct irregular granule shape with small degree of sphericity being rather abrasions from larger granules. Also above 1800 microns the granules are actually grape like structures of larger granules being most probably a result of insufficient spreading surface in the drying stage of the granules.

The values of the Young's modulus and granule strength seem to be of the same order of magnitude as the ones presented by Nordstrom et al [4] for wet granulation granules of MCC Avicel 101. They obtained values of 24.4 MPa for the granule strength and 1.82 GPa for the Young modulus on the low porosity MCC granules (11% intragranular porosity determined as one minus the ratio between the effective and apparent densities). The differences might be explained by differences in starting material and granule preparation protocol (wet granulation followed by extrusion and spheronization and room temperature drying to name a few) translating in differences in final granule porosity. Similarly to the study of Nordstrom the first fracture point doesn't correspond to a catastrophic failure with the granule being broken up into fragments but in the apparition of the first crack in the granules and only upon further increase in the applied compression force did the granule break up.

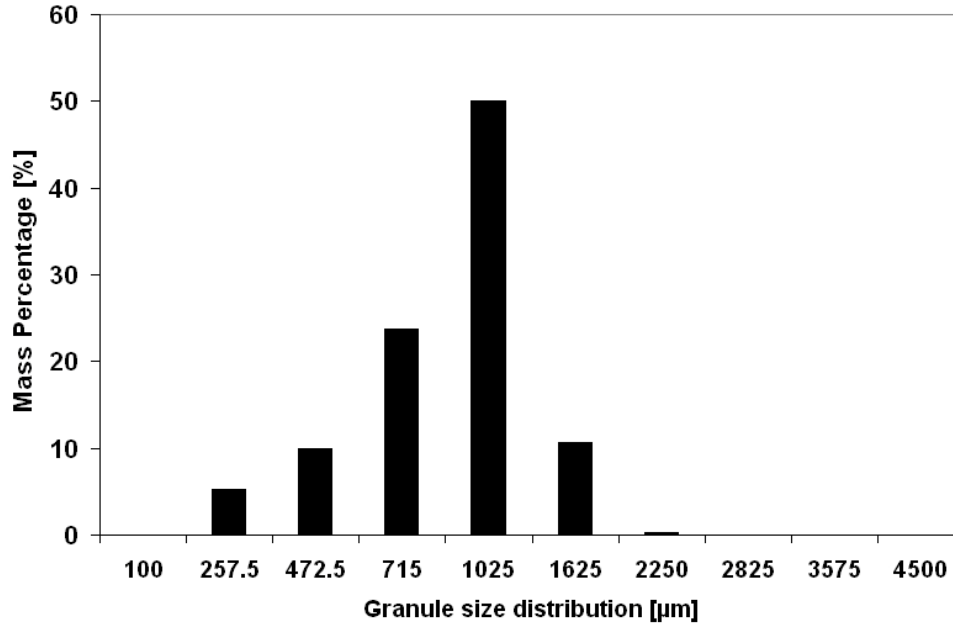


Figure 10. Granule size distribution for the end granules obtained in the Mi-Pro (granulation of MCC Avicel 105 with ultra-pure water)

Sieve Mean Granule Size [µm]	Fracture Force [N]	Granule Strength [MPa]	Young's Modulus [GPa]	Fracture Energy [mJ]	Specific Fracture Energy [mJ/mm ²]
450	1.2 ± 0.4	6.2 ± 2.1	0.7 ± 0.1	0.010 ± 0.003	0.18 ± 0.04
715	11 ± 0.9	25.0 ± 3.5	3.4 ± 0.3	0.5 ± 0.04	0.30 ± 0.02
900	20 ± 2.0	31.4 ± 4.5	4.8 ± 0.5	0.9 ± 0.07	0.34 ± 0.02
1125	29 ± 2.5	31.9 ± 4.6	5.1 ± 0.6	1.4 ± 0.12	0.35 ± 0.03
1425	40 ± 3.1	32.7 ± 4.8	5.6 ± 0.6	2.3 ± 0.18	0.32 ± 0.02
1800	59 ± 4.9	30.0 ± 4.5	5.5 ± 0.6	3.1 ± 0.22	0.34 ± 0.02

Table 2. Single granule strength and deformation parameters for the granulation of MCC Avicel 105 with ultra-pure water

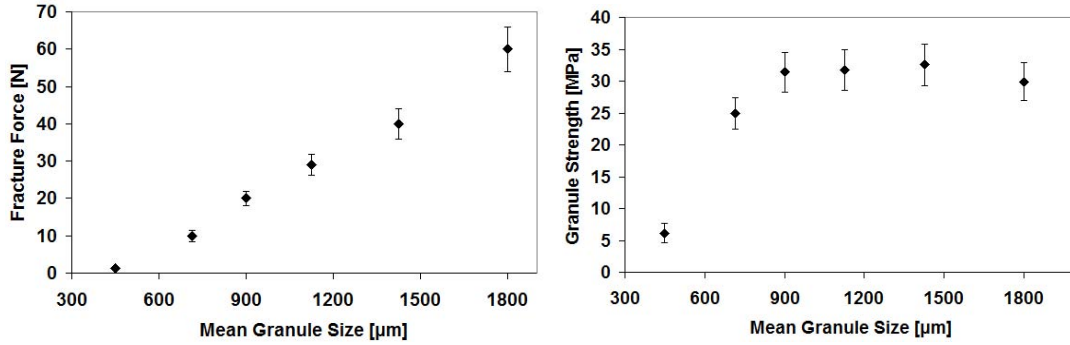


Figure 11. Mean fracture force and mean granule strength as a function of mean granule size for the granulation of MCC Avicel 105 with ultra-pure water

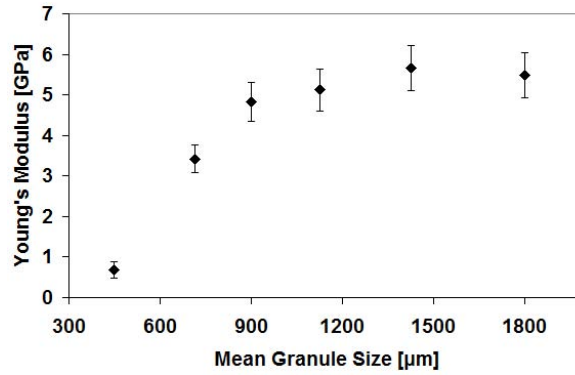


Figure 12. Mean Young's modulus as a function of mean granule size for the granulation of MCC Avicel 105 with ultra-pure water

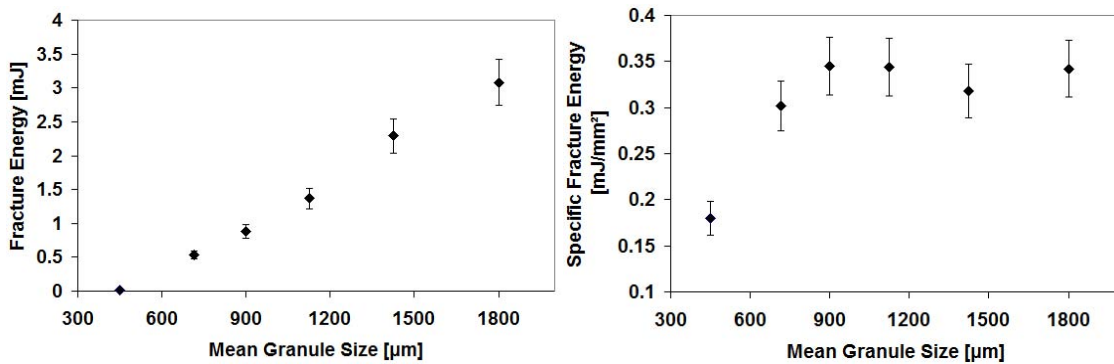


Figure 13. Mean fracture energy and mean specific fracture energy as a function of mean granule size for the granulation of MCC Avicel 105 with ultra-pure water

As it can be observed the fact that these measurements are all derived from the same basic information, that is the load – displacement curve, gives many similar evolutions of the different parameters. The parameters that also take into account the mean granule size (granule strength, Young's modulus, specific fracture energy) present similar evolutions and show a strong difference between the results obtained at 450 microns compared to the values obtained from mean granule sizes between 715 and 1800 microns. We believe this difference to come from the difference in shape parameters between the granule classes. While the similarity between granules between 715 and 1800 microns seem to indicate a similar internal structure.

Figure 14 shows the evolution of granule roundness as a function of granule size in the range accessible to the PharmaVision 830 Automated Microscopy System (45 to 1900 microns with a 0.5 zoom objective) showing the smallest granules to also present the lowest roundness values. From 715 μm onwards the roundness values present similar values with a peak being observed for granules with a mean granule size of about 1125 μm . This might be however related to sampling as the surface of the Pharmavision only allows testing a limited number of granules.

Parameters that do not take into account mean granule size like the fracture force and the fracture energy present a linearly growing relationship with mean granule size. For the further study of dry granule strength we will only present the fracture force and the mean granule strength knowing however that the Young's modulus, absolute and specific fracture energy can be calculated at any moment.

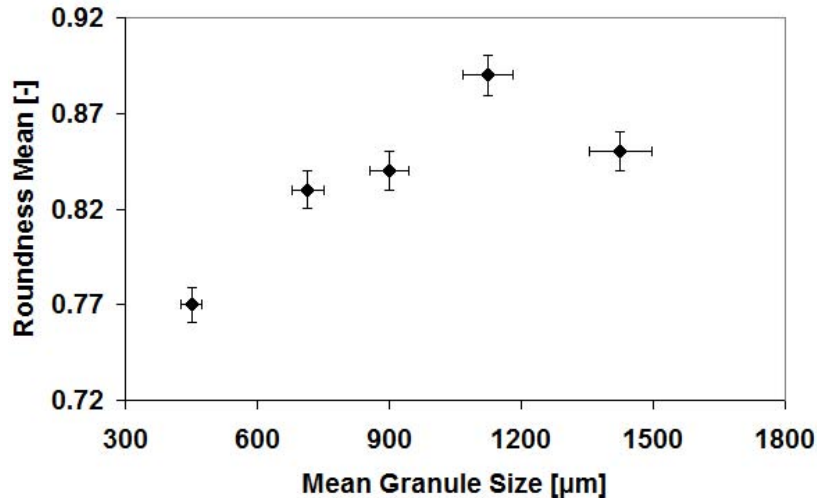


Figure 14. Roundness as a function of mean granule size for the granulation of MCC Avicel 105 with ultra-pure water

5. Conclusion

This first chapter described the wet granulation of the microcrystalline cellulose Avicel 105 on the Mi-Pro high shear mixer and the means allowing us to obtain information in order to further characterize the process.

Torque curves on the Mi-Pro have been found capable to ensure control of the granulation process without overwetting while following the granulation kinetics by retrieving samples, drying and sieving them allowed us to maximize the coarse fraction by slightly increasing the optimum liquid requirement. Comparisons between the torque curves obtained on the Mi-Pro and the mixer torque rheometer (MTR) show that the more intense mixing in the MTR (the normalized impeller torque is almost 6 times as high in the MTR than the Mi-Pro) makes it difficult to identify the growth zone (plateau phase on the Mi-Pro torque curve) while the wetting and nucleation stages and capillary peak as a function of added binder are common between the equipments.

The granulation of microcrystalline cellulose has been found by SEM observation to go through four characteristic stages: wetting, nucleation, growth and overwetting which could be related to changes observed in the torque curve. After the nucleation stage mean granule size increases only slowly between 50 and 75% L/S ratio as the granules are not

deformable enough to lead to successful coalescence between granules. For values above 80% L/S ratio mean granule size quickly grows as granules start to exhibit liquid on their surface.

Granule strength has been evaluated in both wet and dry conditions. For the wet granules granule strength has been assimilated to the wet mass consistency that can be measured in the mixer torque rheometer. As granule growth only occurs late in the process the wet mass consistency measurements show low sensitivity to changes in the wet mass between 20 and 83% L/S ratio as granules exhibiting liquid at the surface are covered with fine particles. The value of 83% corresponds to the extinction of the fines particles class and from here on more liquid needs to be squeezed to the surface in order for successful coalescence between intermediate and coarse granules to occur. This can also easily be observed on the Mi-Pro glass bowl walls where the fine particles covering them disappear showing a homogenous mass of granules while on the MTR the increased stickiness exhibited on granule surface increases wet mass consistency.

Dry granule strength has been assessed by single granule compression tests allowing us to describe strength, deformation characteristics through the Young modulus and assess the energy necessary in order to fracture the granule. Parameters taking into account the granule size have been found to exhibit a similar evolution. The lower sized particles with mean granule size of 450 microns have been found to exhibit lower values than granules between 715 and 1800 microns This is believed to be a function of a different formation mechanisms: as granules between 715 and 1800 microns are more spherical they seem to be the product of successful coalescence between granules while the smaller particles showing a lower degree of sphericity seem to be a result of granule breakage and attrition.

References

- [1] R.H. Snow, T.Allen, J.D. Litster, B.J. Ennis, Size Reduction Size Enlargement, in R.H. Perry, D.W. Green (Eds), Perry Chemical Engineers Handbook (1997) McGraw-Hill, USA
- [2] D.M. Newitt, J.M.A. Conway-Jones, A contribution to the theory and practice of granulation Trans.Instn.Chem.Engrs. 36 (1958) 422-442
- [3] A.M. Bouwman, The influence of material properties and process conditions on the shape of granules produced by high shear granulation, PhD thesis Rijksuniversiteit Groningen (2005)
- [4] J. Nordström, K. Welch, G. Frenning, G. Alderborn, On the physical interpretation of the Kawakita and Adams parameters derived from confined compression of granular solids, Pow. Tech. 182 (2008) 424–435

Chapter III.2: Effect of Operating Conditions and Equipment Geometry

The operating conditions and the equipment geometry can have a great impact on the growth and properties of granules. The Mi-Pro has made the object of studies regarding the influence of process parameters. Chevalier et al [1] investigated the effect of impeller speed, optimum liquid to solid (L/S) ratio and liquid flow rate as well as the effect of spheronization protocol on the wet granulation of a lactose – polyvinylpyrrolidone mixture with water. They found that increased impeller speed increases yield and reduces the fraction of fines and defined an optimum L/S ratio, liquid flow rate and spheronization protocol. Gomez et al [2] also studied the influence of liquid flow rate on the granulation of lactose in the Mi-Pro and found that an increase in liquid flow rate has an effect on the formation of liquid bridges but not on the optimum liquid requirement.

The Mi-Pro with a bowl of 1.9 L has been chosen as the reference scale and studies were conducted on the microcrystalline cellulose Avicel 105 granulated with ultra-pure water.

The parameters chosen for investigation in this subchapter are:

- Effect of operating conditions and equipment design. :

1. Effect of the fill ratio, defined as

$$\text{Fill Ratio} = \left(\frac{M_i}{\frac{\rho_{bulk}}{V^*}} \right) \cdot 100 \quad (\%) \quad (\text{III-2-1})$$

Where the volume of the initial dry powder is calculated by dividing the initial dry powder mass M_i with the bulk density of the dry powder ρ_{bulk} , and the result is divided with the empty bowl volume, V^* .

2. Effect of the impeller speed and chopper design,

3. Comparison between the 0.9L and the 1.9L bowls of the Mi-Pro.

1. Effect of fill ratio

1.1 Introduction

The fill ratio has been studied by Bock et al. [3] on a Diosna high shear mixer with 1.2L capacity by varying the load of initial dry powder in the mixer (calculated using the dry powder bulk density). They studied a formulation made from equal parts of microcrystalline cellulose, lactose and anhydrous calcium hydrogen phosphate and investigated fill ratios of 10, 20, 30, 40, 50, 60 and 70%. For a fill ratio of 80% granulation was not possible. They found the granule size distributions to be comparable between 10 and 20% and between 50 and 70% with the larger fill ratios presenting an increasing proportion of fine particles. Vialatte et al [4] studied the effect of increasing fill ratio from 25 to 42 and 59% in a system composed of alumina particles granulated with polyvinyl alcohol. They found that increasing fill ratio has no effect on the granulation mechanisms and granule growth and that for the same L/S ratio the amount of granulated product and granule porosity were not influenced by the fill ratio. They showed that increasing the fill ratio resulted in a higher mean granule size and wider granule size distributions. Schaefer et al [5], found that controlling the mixer load is crucial in controlling the movement of the mass in the bowl. They found that lower mixer loads give smaller mean granule sizes, a larger degree of lumps and small reproducibility.. Thies and Kleinebudde [6] state that for an increased mixer load an increase in mixing time is necessary in order to obtain pellets of a given size.

1.2 Effect of fill ratio

Three fill ratios were studied on the Mi-Pro using microcrystalline cellulose Avicel 105 as starting material and ultra-pure water as binder: 16%, 26% and 32%. For values above 32% slightly overwetting conditions lead to the impeller torque increasing above 110% of the maximum supported torque for more than three seconds leading to a halt of the mixing. As a result in order to protect the equipment we decided not to extend the study onto higher fill ratios.

The operating conditions associated to the study of the influence of the fill ratio are grouped in Table 1. The influence of the fill ratio has been studied with the chopper rotating at 3000 rpm, with the same specific liquid binder flow rate, the same optimum liquid requirement expressed as liquid to solid ratio (L/S ratio), the same mixing time and at three different impeller speeds: 100, 400 and 800 rpm corresponding to impeller tip speeds of 0.7, 2.9 and 5.8 m/s.

High Shear Mixer	Mi-Pro V=1.9L
$\text{Fill Ratio} = \left(\frac{M_i}{\frac{\rho_{bulk}}{V_{bowl}}} \right) \cdot 100 \quad (\%)$	16% (75g), 26% (120g) and 32% (150g)
Dry Mixing Time	2 min
Wet Mixing Time	12 min
Impeller Speed	100,400 and 800 rpm
Chopper Speed	3000 rpm
Specific Binder Flow Ratio	0.083(3) ml binder/ 1 g dry initial powder and minute
Optimum Liquid Requirement	100% L/S ratio

Table 1. Operating conditions on the Mi-Pro high shear mixer

Figures 1 and 2 show the obtained torque curves at the 100 and 800 rpm settings for the three fill ratios as well as the reproducibility for the lowest studied fill ratio of 16%. At the 400 rpm setting the torque curves present a certain peculiarity that will be presented in more detail when discussing the effect of impeller speed (Chapter III.2.3). There is little difference between the 26 and 32% fill ratio settings at 800 rpm. The 32% fill ratio gives a slightly higher torque response at both speeds which could be explained by the

fact that an increase in mass could lead to an increase in the densification of the granules squeezing more binder to the granule surface. However the wet mass consistency measurements (Figure 3) are not sensitive enough to differentiate between the 26 and 32% fill ratios both presenting similar wet mass consistencies.

The use of the 16% fill ratio at the 800 rpm impeller speed setting presents certain problems from an operator's point of view. Firstly, the reproducibility (Figure 2) of the torque curve at 800 rpm is low and can present certain artifacts that are not encountered at lower impeller speeds like the 100 rpm setting. Secondly, the low fill ratio coupled with strong affinity of the very cohesive MCC Avicel 105 to both walls and lid result in localized overwetting making results difficult to compare with the other fill ratios. The shorter growth zone observed on the torque curve for the 16% fill ratio at 800 rpm (Figure 1), the higher wet mass consistency (Figure 3, Table 2) and the higher mean granule sizes (Figure 6) are all proof that in this case overwetting occurs.

At 100 rpm the torque curves present different profiles for each fill ratio. While the 16 and 26% fill ratios are similar up to 30% for increased values the 26% fill ratio follows an evolution similar to the 32% fill ratio. The higher torque values in the beginning of the granulation for both 16 and 26% fill ratios could be explained by the combination of low fill ratio and low impeller speed not bringing the powder mass in contact with the chopper leading to a less than optimal binder distribution and the formation of lumps. The formation of lumps is however inherent to such a low impeller speed explaining the rather noisy evolution of the torque curves observed for all fill ratios.

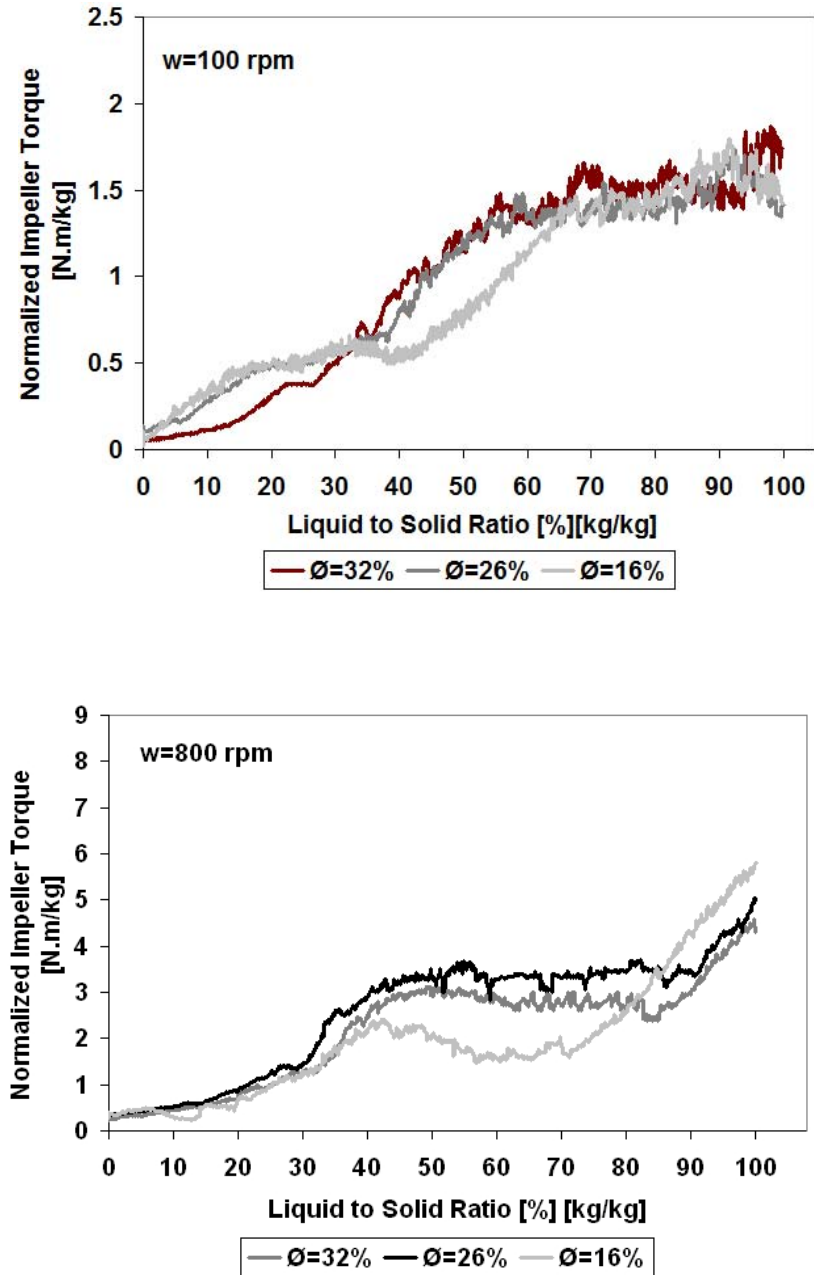


Figure 1. Torque curves evolution for different fill ratios at 100 and 800 rpm for the granulation of MCC Avicel 105 with ultra-pure water

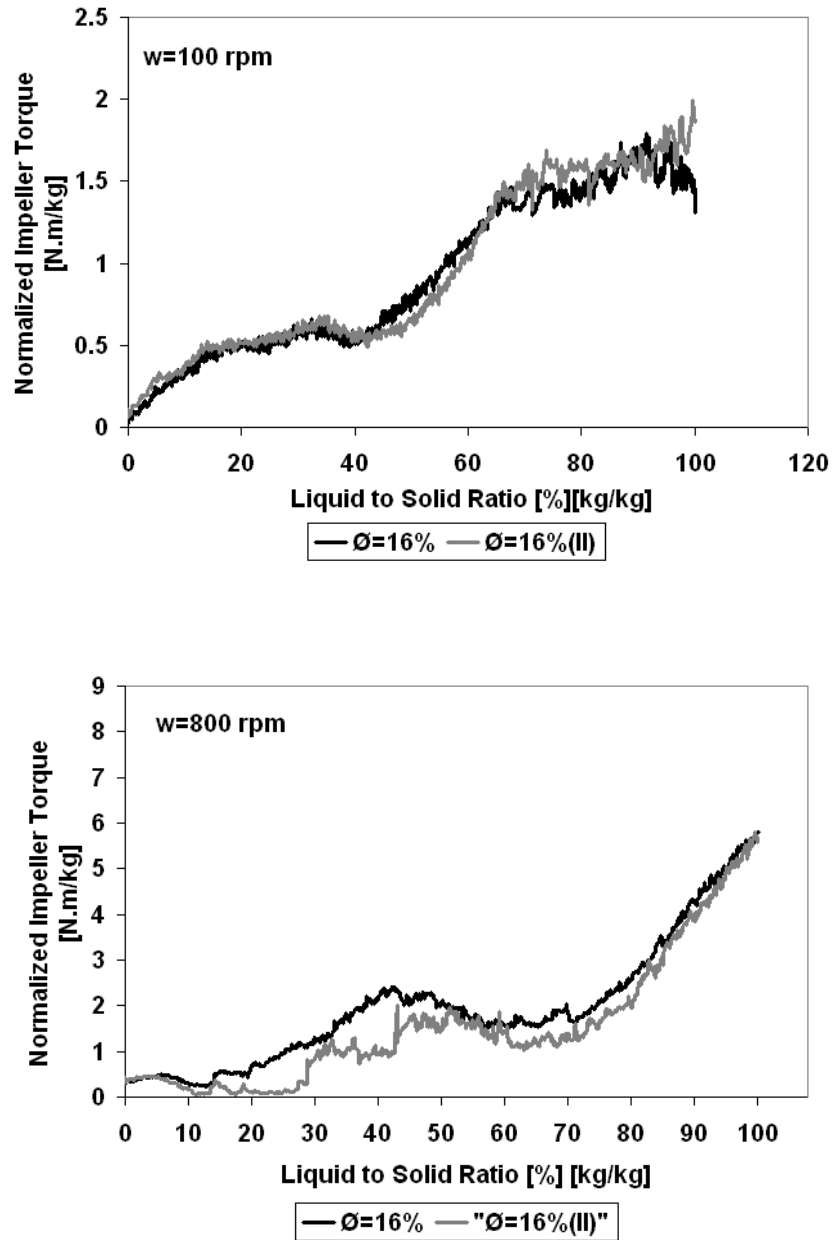


Figure 2. Reproducibility of the 16% fill ratio at 100 and 800rpm for the granulation of MCC Avicel 105 with ultra-pure water

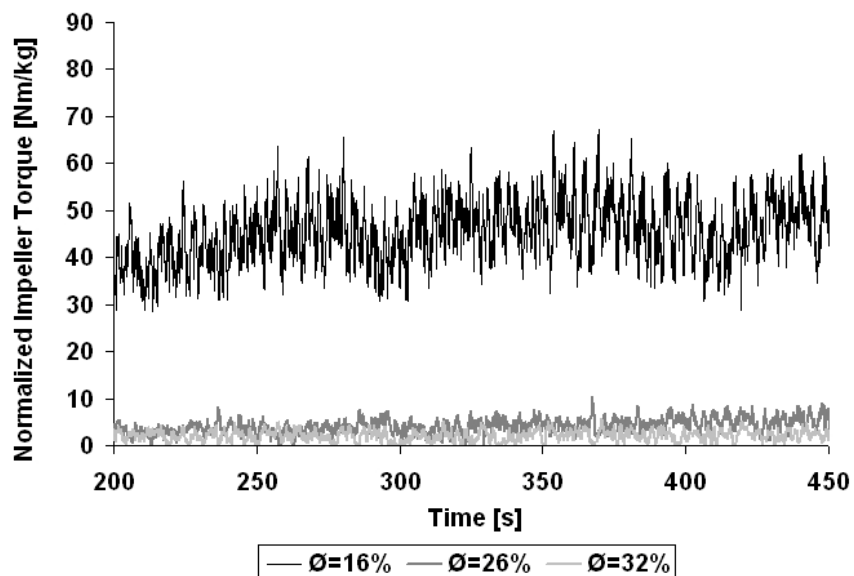


Figure 3. Wet mass consistency measurements for wet granules produced at different fill ratios at 800 rpm for the granulation of MCC Avicel 105 with ultra-pure water

Granule size distributions in the end of the granulation are presented in Figures 4 to 6 while Table 2 regroups the mean granule sizes and wet mass consistency measurements. Figure 6 confirms that the overwetting anticipated from the shorter growth zone and the higher wet mass consistency at 16% fill ratio and 800 rpm also translates into higher mean granule sizes. From a granule size distribution point of view no significant differences in modality between the different fill ratios have been observed at either 100 rpm or 400 rpm. However increasing impeller speed takes granule size distribution from pronounced bi-modal at 100 and 400 rpm to almost monomodal at 800 rpm for the 26 and 32% fill ratios. The mean granule size increases with increasing fill ratio at all speeds with the exception of 16% fill ratio at 800 rpm. In terms of granule size distribution wideness we could not find any notable differences. In our case this seemed to be more a function of impeller speed rather than fill ratio. The wet mass consistency measurements present values of the same order of magnitude, again, excepting the 16% fill ratio – 800 rpm impeller speed combination. Somewhat higher wet mass consistencies are obtained at 400 rpm than at 100 rpm however as granules are bigger in this case and sampling has

an important role in the outcome of the wet mass consistency we will consider the values to be of similar value.

Impeller Speed [rpm]	Fill Ratio [%]	Wet Mass Consistency [N.m/kg]	Mean Granule Size [μm] [$\pm 10\%$]
100	16	5.8 ± 1.2	2086
	26	6.2 ± 1.3	2254
	32	6.6 ± 1.5	2417
400	16	8.4 ± 1.9	1714
	26	8.9 ± 1.8	1880
	32	7.7 ± 1.7	2047
800	16	40 ± 6.3	2150
	26	8.2 ± 1.9	899
	32	6.4 ± 1.2	983

Table 2. Wet mass consistency and mean granule size as a function of fill ratio and impeller speed rpm for the granulation of MCC Avicel 105 with ultra-pure water

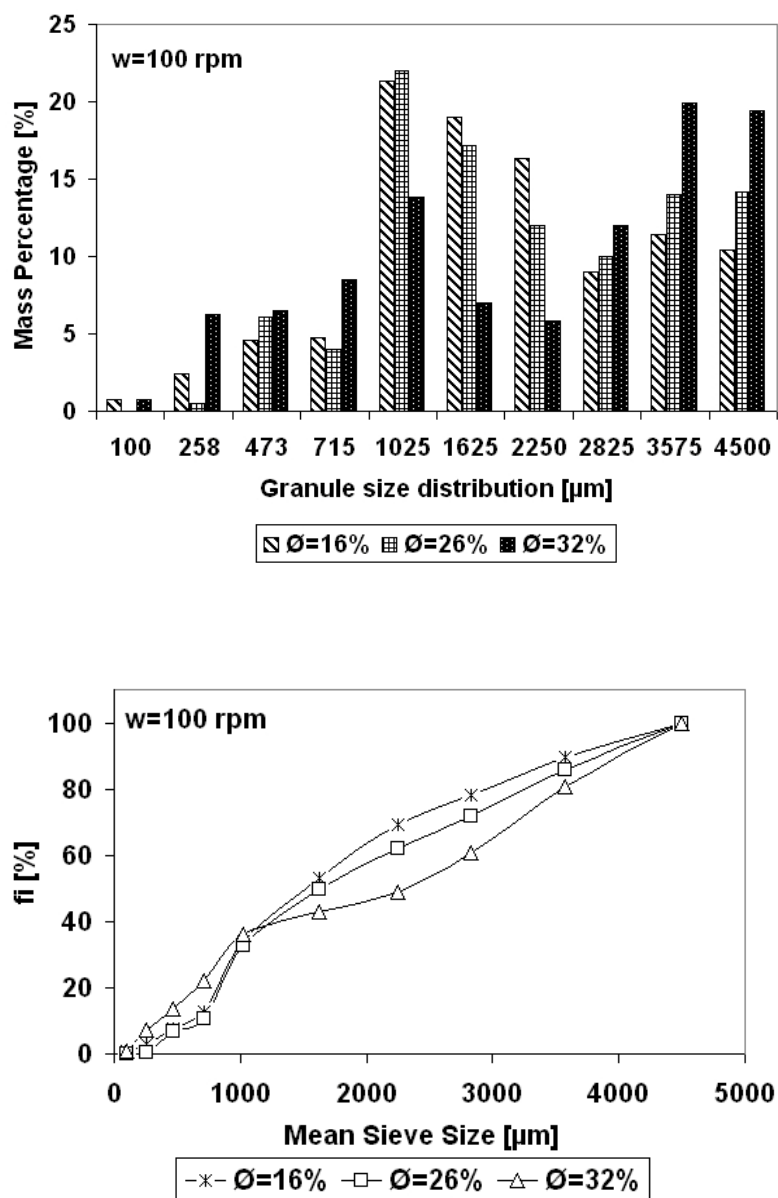


Figure 4. Granule size distributions (histogram and cumulative) as a function of fill ratio at 100 rpm for the granulation of MCC Avicel 105 with ultra-pure water (end product)

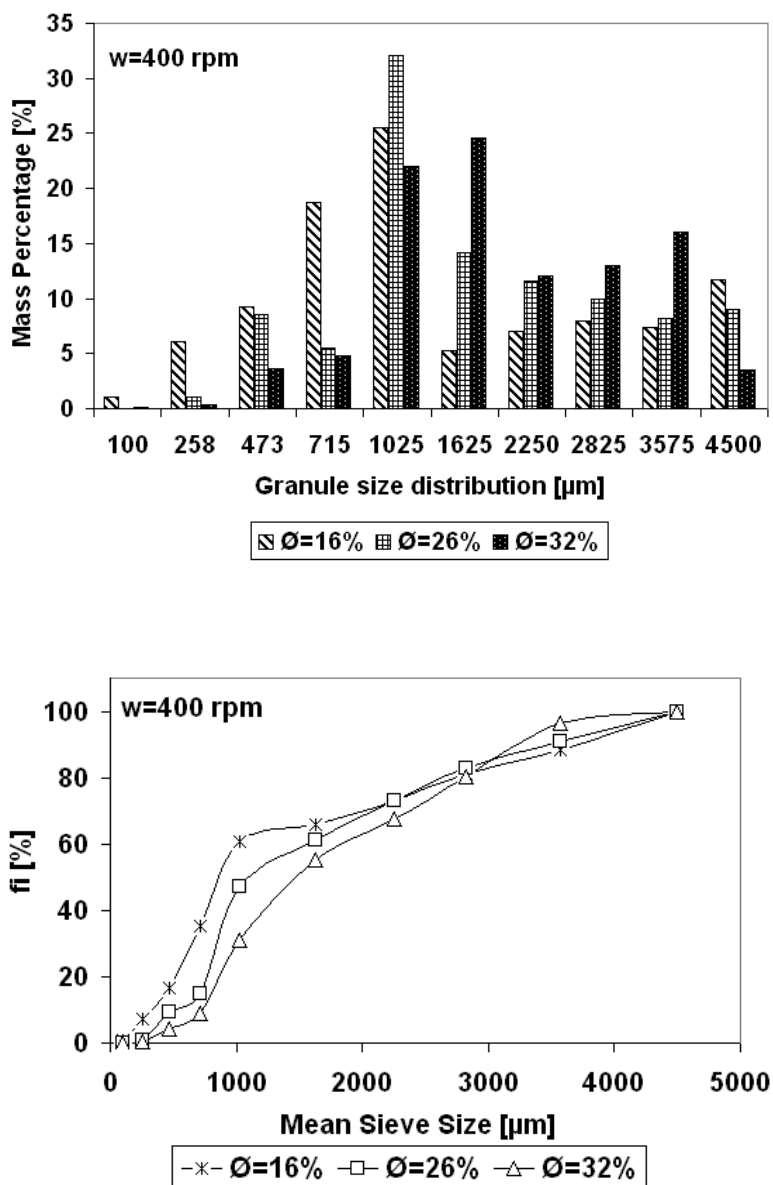


Figure 5. Granule size distributions (histogram and cumulative) as a function of fill ratio at 400 rpm for the granulation of MCC Avicel 105 with ultra-pure water (end product)

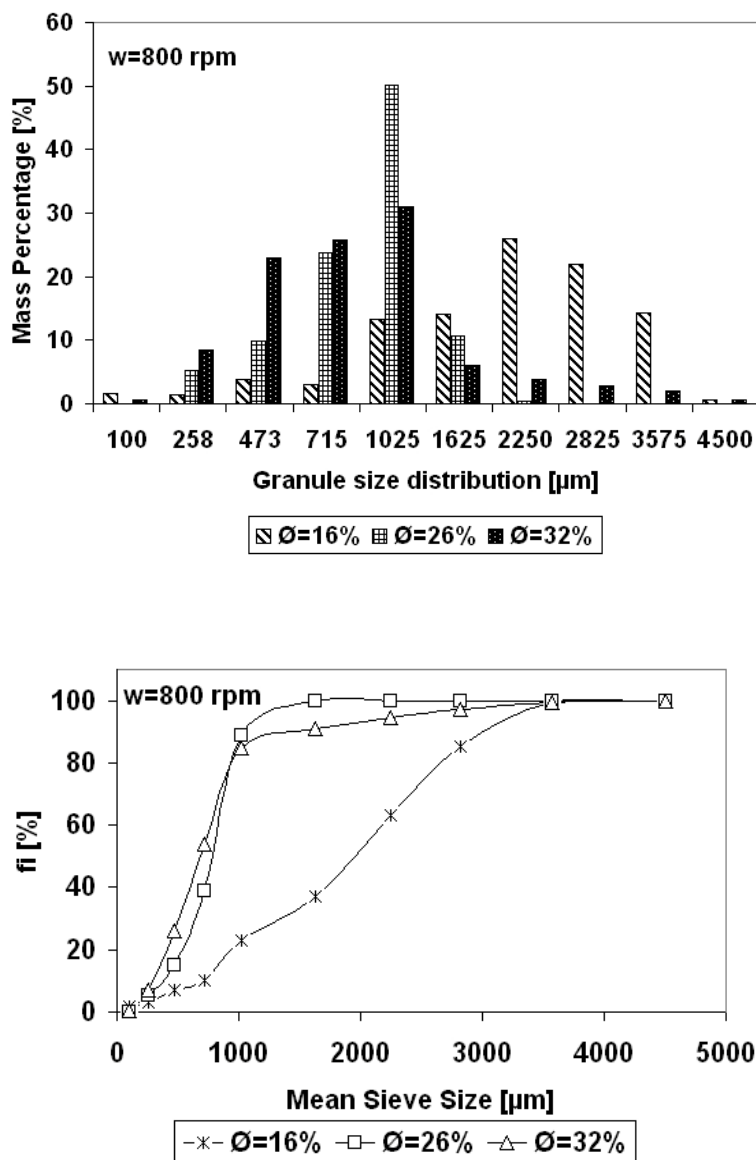


Figure 6. Granule size distributions (histogram and cumulative) as a function of fill ratio at 800 rpm for the granulation of MCC Avicel 105 with ultra-pure water (end product)

Table 3 shows the obtained roundness values from the number distributions as a function of fill ratio and impeller speed while Figure 7 shows a comparison between roundness distributions by number as a function of fill ratio for an impeller speed of 400 rpm (detailed as histograms in Appendix III). At 100 rpm a slight decrease in roundness can be observed which could be related to the higher fill ratios coming in more contact with the chopper at low speeds. The highest roundness values are observed for the 400 rpm impeller speed and the 26% fill ratio. At 400 rpm the roundness is found to increase with

fill ratio and the lowest span values are found at this value. At 100 rpm the span values are influenced by the low mechanical strength of the granules in the investigated size range (1000-1250 μm) producing fines during the manipulation while at 800 rpm the phenomenon most likely to produce a similarly high span is granule breakage causing a higher variability in granule shape. At 800 rpm the obtained values are too similar to allow making a distinction in terms of influence of the fill ratio on granule roundness.

Impeller Speed [rpm]	Fill Ratio [%]					
	16		26		32	
	D ₅₀	Span	D ₅₀	Span	D ₅₀	Span
100	0.72	0.61	0.67	0.70	0.69	0.70
400	0.76	0.47	0.86	0.45	0.83	0.41
800	0.73	0.58	0.72	0.54	0.73	0.6

Table 3. Roundness values based on number distribution obtained on the PharmaVision 830 Automated Microscopy System as a function of impeller speed and fill ratio (Span calculated as $D_{90}-D_{10}/D_{50}$) for the granulation of MCC Avicel 105 with ultra-pure water

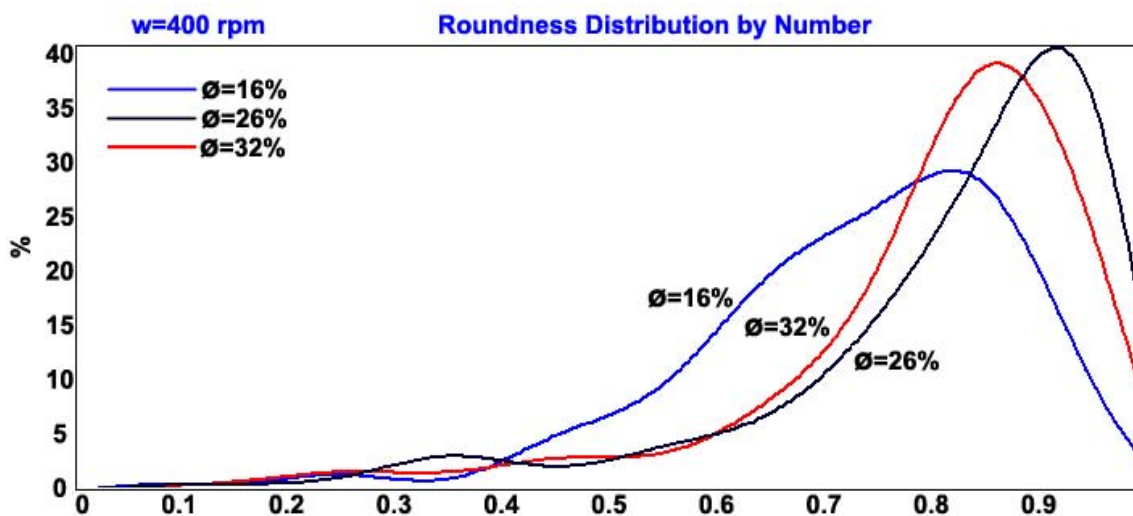
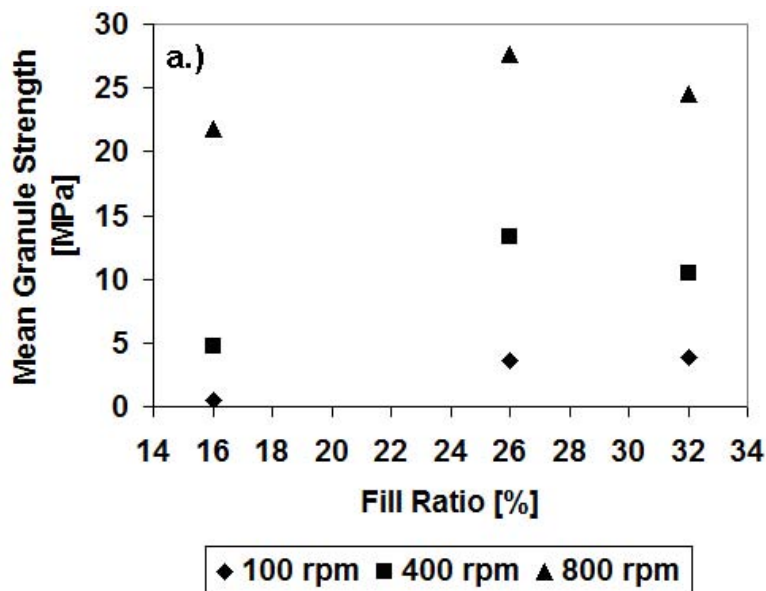


Figure 7. Roundness distributions by number obtained for the studied fill ratios at an impeller speed of 400 rpm for the granulation of MCC Avicel 105 with ultra-pure water

Dry granule strength measurements were performed on the Instron mechanical testing machine as a function of both fill ratio and impeller speed. The steel probe velocity was of 1mm/min while the maximum recordable force was of 500N. The studied granules were as for the roundness measurements in the 1000-1250 microns range at 400 and 800 rpm. At 100 rpm these granules were too fragile to give reproducible results which is why the size range of 2000 to 2500 microns was preferred. As a general rule increasing the fill ratio from 16 to 26% gives higher mean granule strengths at all impeller speeds (Figure 8a) with the difference being stronger at the lower (100 rpm) and medium (400 rpm) impeller speeds. Further increase in the fill ratio from 26 to 32% leads to weaker granules at 400 and 800 rpm while having no significant effect at 100 rpm.

At 800 rpm (Figure 8b) the values in terms of mean granule strength vary between 22 and 27.8 MPa with the 16% percent fill ratio presenting the lowest value (with a difference greater than the experimental uncertainty). At 400 rpm (Figure 8c) the same trend is observed however in this case the difference between the 16% fill ratio and the 26 and 32% presents greater values. The same has been observed at 100 rpm (Figure 8d) with the 26 and 32% fill ratios giving closer mean granule strength than the 16% fill ratio.



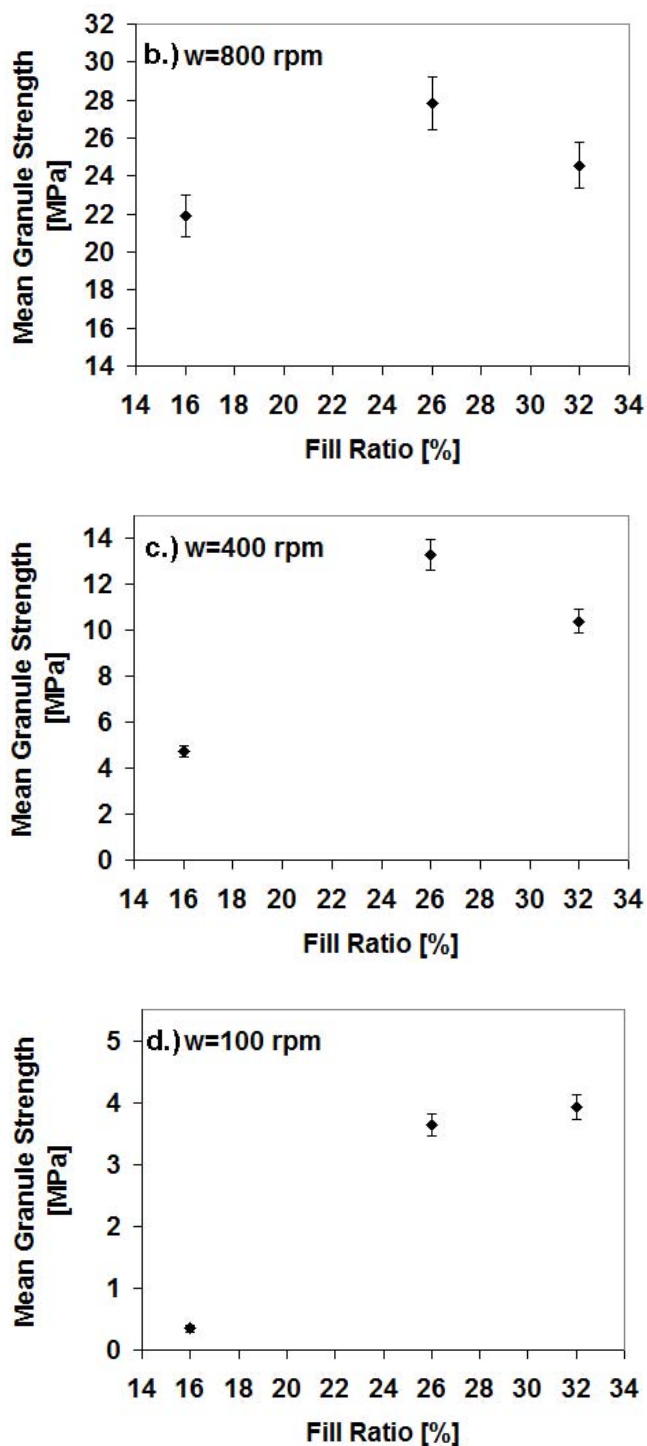


Figure 8. Mean granule strength as a function of fill ratio for the three studied impeller speeds: 100, 400 and 800 rpm for the granulation of MCC Avicel 105 with ultra-pure water (Strength determined on the 1000-1250 microns fraction for 400 and 800 rpm and 2000-2500 microns for 100 rpm)

2. Effect of Impeller Speed and Chopper Design

2.1 Introduction

In high shear granulation the role of the impeller is to distribute the binder and promote agglomeration by bringing into contact the wetted powder particles while the chopper is supposed to break up large agglomerates in order to ensure narrow granule size distributions. The effect of the chopper depends largely on the equipment used, while some authors like Michaels et al [7] find no effect of the chopper on the granule size distribution others have found that using the chopper slightly decreases the mean granule size, Schaefer et al [5] or narrows the granule size distribution, Knight et al [8]. Increasing the impeller speed generally leads to a decrease in granule size and an increase in growth rate while promoting breakage that also leads to a decrease in granule sphericity. On a Mi-Pro high shear mixer with a bowl volume of 1.7L Hamdani et al [9] showed that for the melt granulation of a lactose and phenylephrine hydrochloride formulation that lowering chopper speed from 4000 rpm to 130 rpm increased the weight mean diameter from 1240 to 1480 microns. They also reported that increasing the impeller speed from 400 to 800 rpm increases mean granule size by a factor of ~6 (230 to 1240 microns) while further increasing the impeller speed to 1000 rpm lead to overwetting due to excessive heat during granulation.

As most scale-up techniques usually imply finding the equivalence of impeller speeds between the scales following certain rules, reviewed by Faure et al [10], it seemed pertinent to investigate the effect of impeller speed on the Mi-Pro high shear mixer.

In situ monitoring and identification of granule growth kinetics are important aspects of the wet granulation process and transition between growth regimes can be influenced by changes in operating conditions as shown by Saleh et al [11] and Benali et al.[12]. Describing high shear mixer granulation is considered especially difficult as agglomeration (growth); breakage and attrition are often simultaneous. Breakage and attrition depend on the mechanical strength of the wet agglomerate and the impact and shear forces developed by the main means of agitation present in the mixer. It is reasonable to assume that both chopper and impeller impact the consolidation of the

granules while the high impeller tip speed of the chopper also ensures breakage of lumps. The granulation of fine microcrystalline cellulose powders has been shown to go through a typical four regime granulation: wetting, nucleation, growth and overwetting by Benali et al [12]. Bouwman et al [13] have shown that granules in the growth stage present a high deformability upon impact and shear with pieces of the main granules breaking off and coalescing with other granules followed by a new rearrangement to a sphere.

The aim of this chapter is to show the influence of impeller speed and chopper presence on the process and the ability of torque curves to control it.

2.2 Effect of Impeller Speed and Chopper Design

The main scale of operation was the Mi-Pro with a 1.9L bowl while the powder couple remains unchanged: microcrystalline cellulose MCC Avicel 105 as substrate and ultrapure water as a binder. The operating conditions are the same with the ones presented for the typical example except for the impeller speed that has been varied and the chopper that has been operated or not (as mentioned). The influence of chopper on mean granule size is discussed in Figure 9. Between 100 and 400 rpm lumps are found to increase with impeller speed when operating without a chopper (Figure 9a) leading to an inhomogenous product comprised of small fine undergranulated product and a large percentage of lumps which explains the high difference in mean granule size up to 600 rpm between operating with and without chopper (Figure 9b). The high value for mean granule size at 100 rpm can be explained by our choice in defining lumps only for granules exceeding 5mm as a mean granule size of 3.5mm is still high and indicative of less than perfect granulating conditions. From 600 rpm onwards the impeller speed becomes sufficiently high so as to break the lumps and reduce the percentage to a negligible value at 800 rpm and beyond. It should also be noted that the high impeller speed also distributes the liquid binder better. Because of the drop by drop binder addition method using the chopper and directing the binder flow towards the chopper is actually recommended to help ensure a better liquid distribution. The same behavior has been observed on the 0.9L Mi-Pro granulation bowl Figure 10 showing the representative

samples taken from the granulator at different speeds when granulating without a chopper.

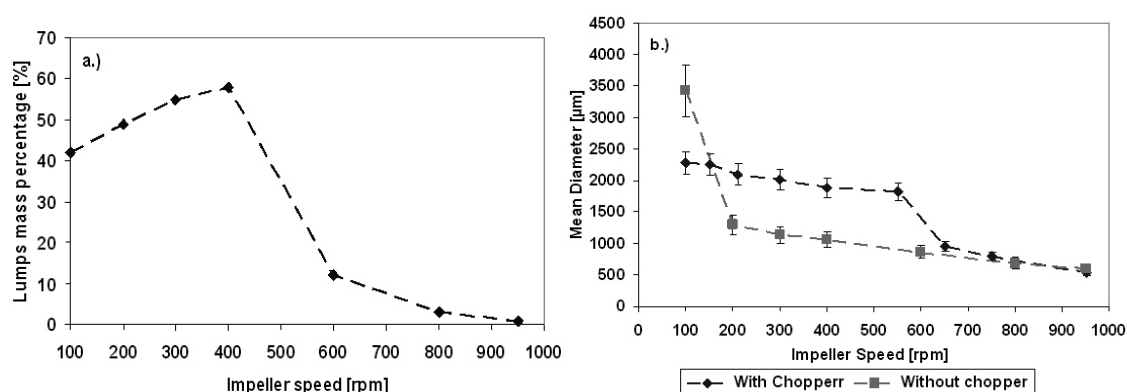


Figure 9. Evolution of the lumps fraction (granules with diameter above 5mm) as a function of impeller speed (a) and mean granule size evolution as a function of impeller speed (b) in the Mi-Pro HSM V=1.9 L

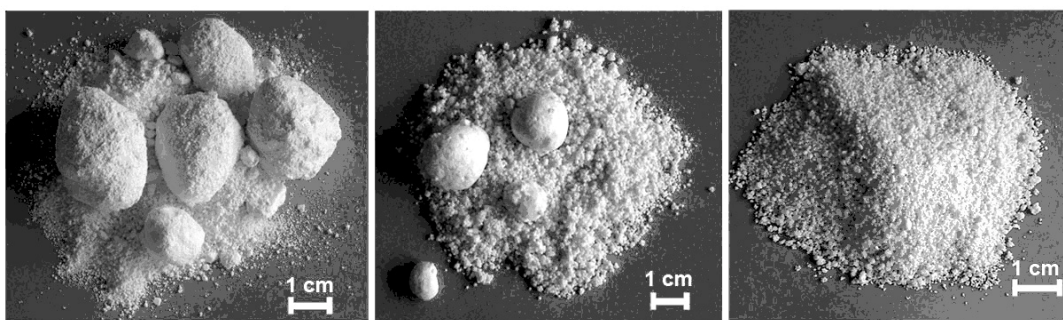
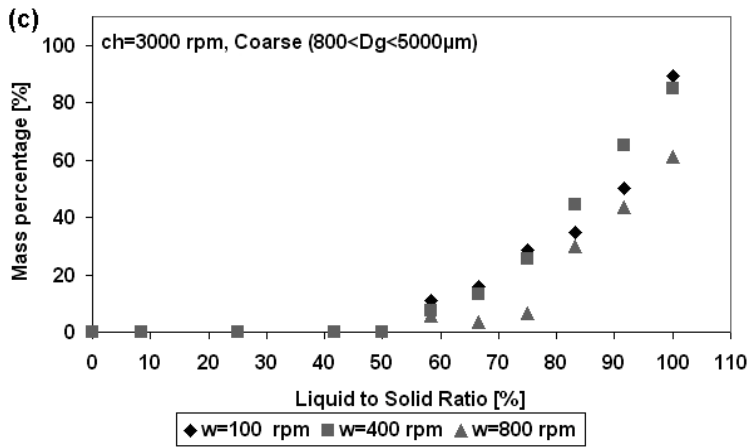
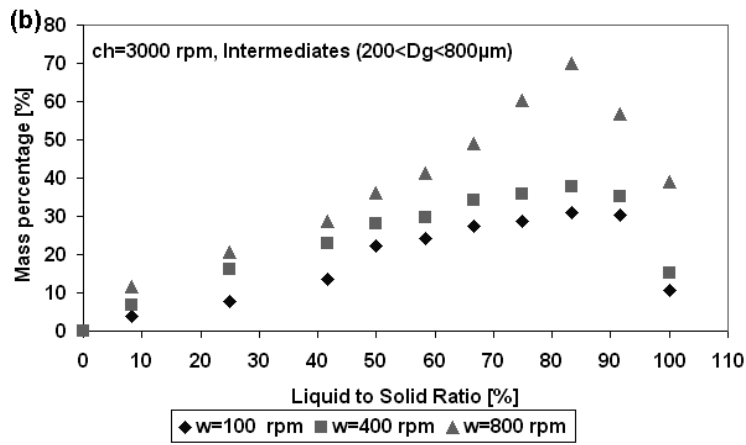
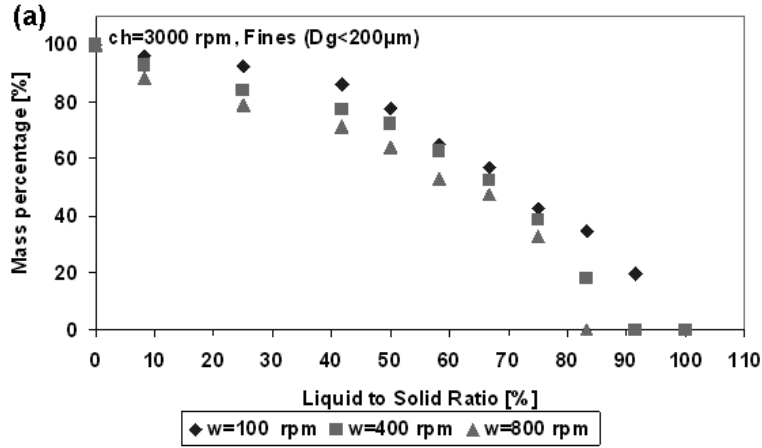


Figure 10. Evolution of final granulated product in the Mi-Pro HSM V=0.9 L without a chopper for three different speeds: 300, 650 and 950 rpm

Setting the chopper at a high rotating speed and regarding the influence of impeller speed at 100, 400 and 800 rpm on the growth kinetics we can observe that increasing impeller speed accelerates the consumption of fine particles and the formation of intermediates and coarse granules (Figure 11). While for the lower impeller speeds (<800rpm) a decrease in intermediate particles percentage is observed near the end of the granulation runs for 800 rpm the intermediate particles show the highest percentage and are still present at the end of the granulation. This can be explained by the fact that at 800 rpm breakage occurs and with a mean granule size of 900 microns the intermediate fraction 200-800µm does not contain low density, fragile granules, but rather high density broken down granules.



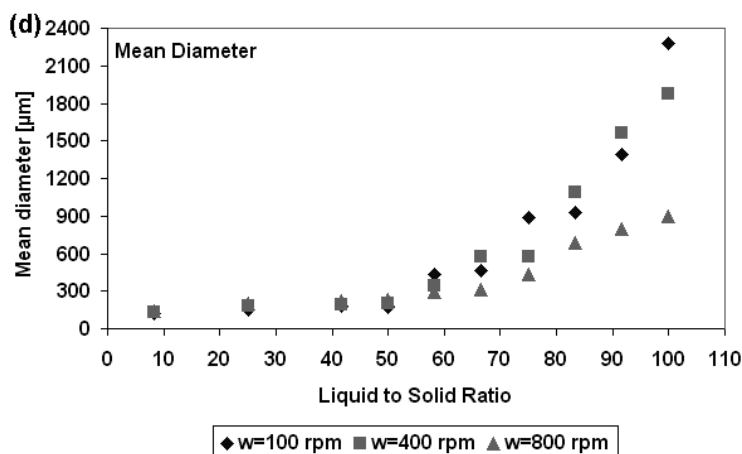
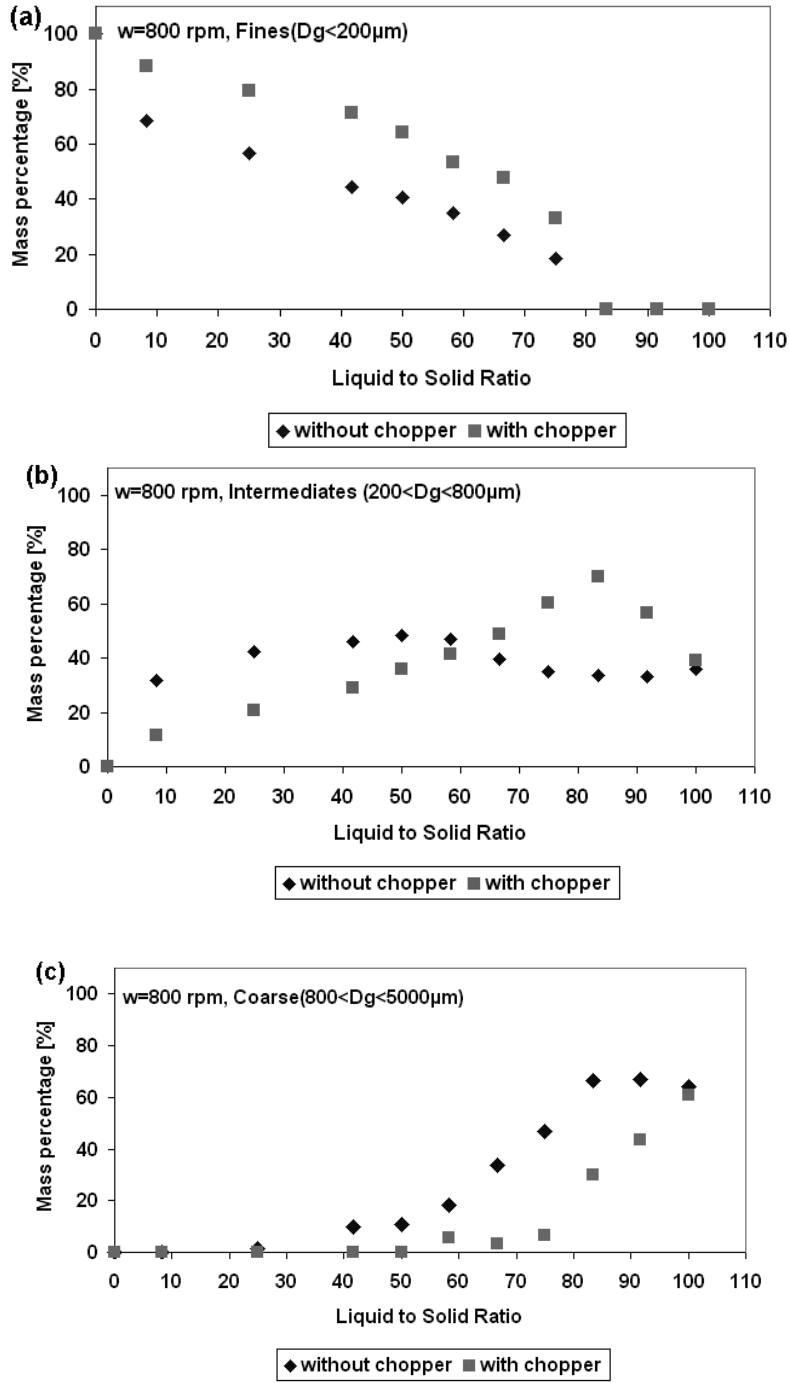


Figure 11. Evolution of the characteristic size fractions and mean granule size with chopper rotating at 3000 rpm for three impeller speeds in the Mi-Pro HSM V=1.9 L for the granulation of MCC Avicel 105 with ultra-pure water

When looking at what happens with or without chopper at 800 rpm, where the chopper wouldn't be necessary in regards to mean final granule size, we see a significant difference in terms of granule growth, with the chopper delaying the formation of coarse granules (Figure 12) and having a strong influence on the intermediate granule class. When no chopper is present the intermediate granule class increases uninhibited at lower liquid to solid ratios after which it remains constant with a slight decrease after adding a binder mass corresponding to 58% liquid to solid ratio. In contrast when the chopper is operated the intermediate fraction increases strongly in the growth region between 50 and 83-85% afterwards it seems that the chopper and less the impeller is responsible for the decrease observed in the descending evolution of intermediate particles above 85% L/S ratio and the agglomeration of these intermediate granules to coarse granules. Figure 12d shows the evolution of mean granule size showing best the influence of the chopper in delaying granule growth.



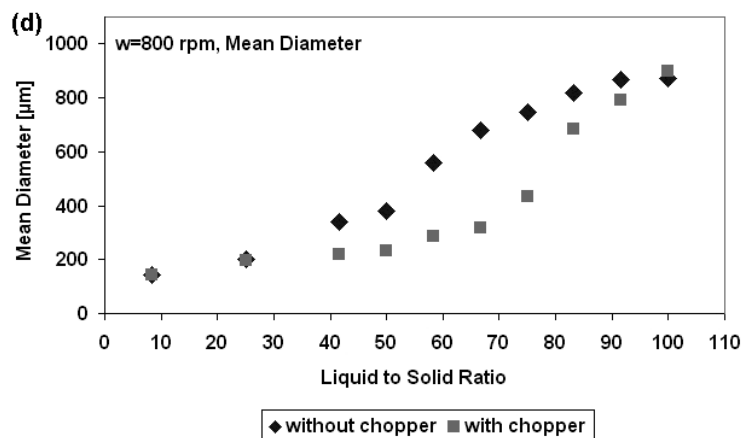
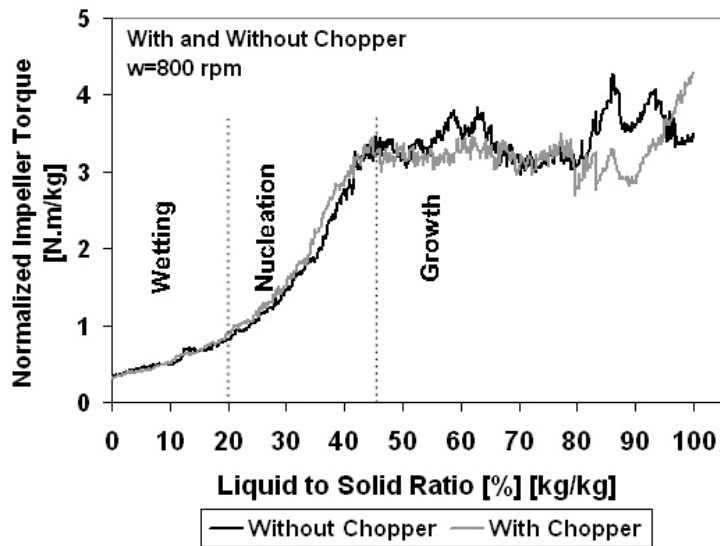
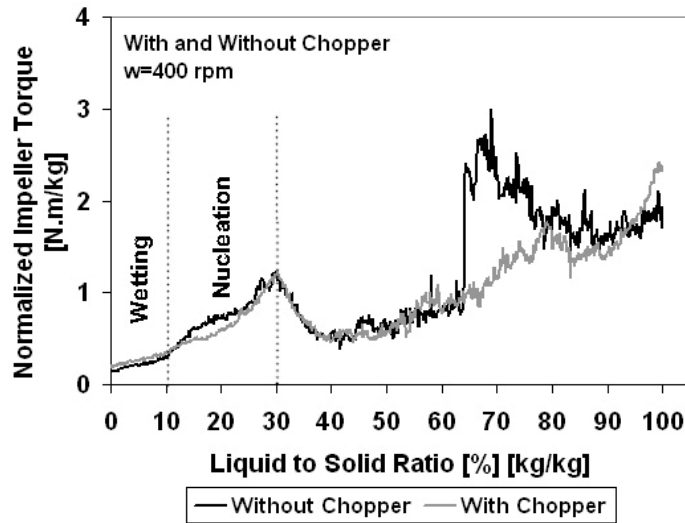
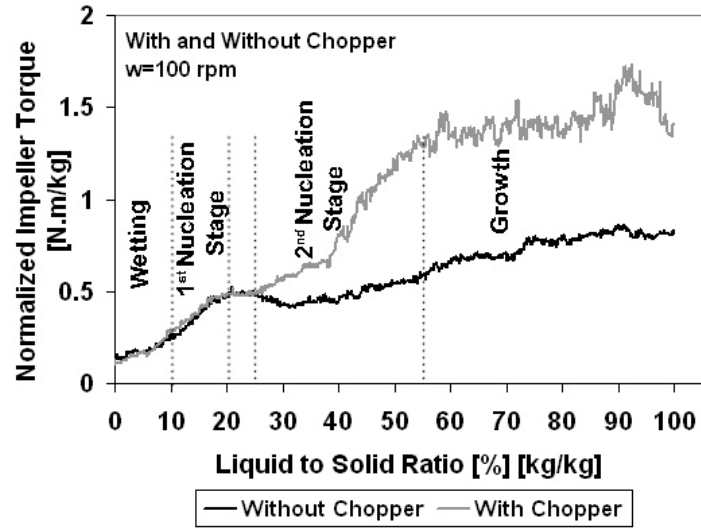


Figure 12 . Evolution of the characteristic size fractions and mean granule size with and without chopper at 800 rpm in the Mi-Pro HSM V=1.9 L for the granulation of MCC Avicel 105 with ultra-pure water

The effect of chopper presence on torque curves with the chopper turning at 3000 rpm shows only small differences between operating with or without chopper at medium and high impeller speeds (Figure 13) on the torque curves. On the 400 rpm curve after the wetting stage (up to 10% L/S ratio) a sharp drop in torque can be observed at 30% L/S ratio, it is characteristic for the granulation of MCC Avicel 105 at moderate speeds in the Mi-Pro and is independent of chopper operation: when sufficient liquid is added the powder sticks to the side walls exiting the impeller action causing a sharp drop in impeller torque. This seems to be related to the mechanical dispersion of the binder in the powder bed as well as the small particle size and high compressibility of the MCC Avicel 105. Figure 14 shows a torque comparison between MCC Avicel 105 ($D_{50}=20\mu\text{m}$) and MCC Avicel 101 ($D_{50}=60\mu\text{m}$) and the reproducibility for MCC Avicel 101 while Table 4 recalls the main differences between MCC Avicel 105 and MCC Avicel 101.



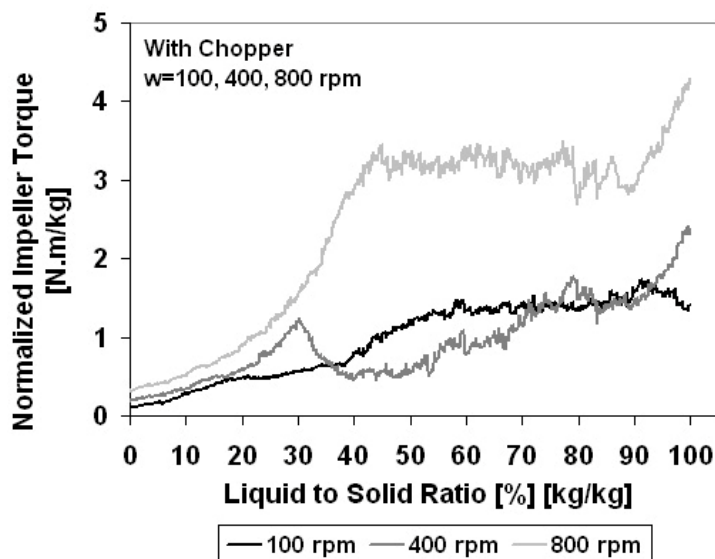
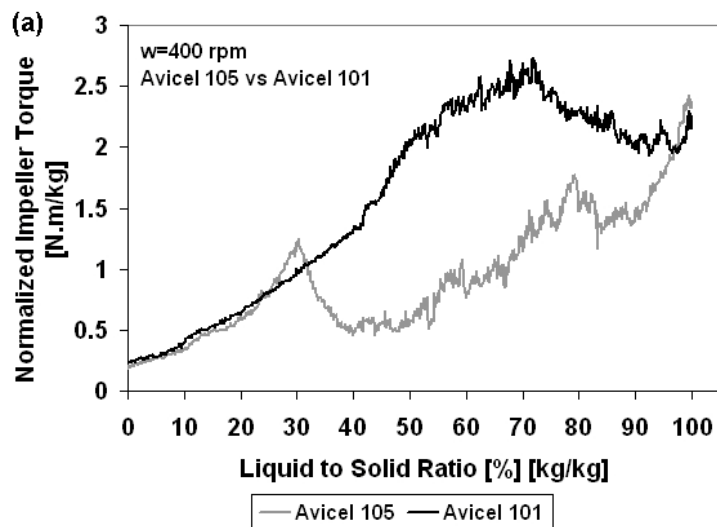


Figure 13. Torque curve comparison in the Mi-Pro $V=1.9$ L with and without chopper for three different impeller speeds: 100, 400 and 800 rpm and between speeds with chopper active for the granulation of MCC Avicel 105 with ultra-pure water



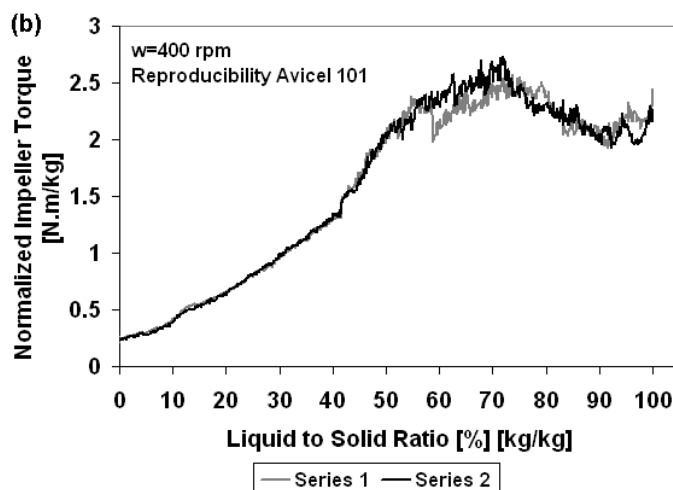


Figure 14. Comparison between torque curves at 400 rpm with chopper active for MCC Avicel 101 and 105 (a) and reproducibility for MCC Avicel 101 (b)

Powder properties	D ₅₀ [μm]	Span (D ₉₀ -D ₁₀)/ D ₅₀	Bulk Density [kg/m ³]	True Density [kg/m ³]	Cristallinity Index [%]
MCC Avicel 105	20	1.9	244	1514	66.3
MCC Avicel 101	60	2.1	291	1540	66.4

Table 4. Physical characteristics of the MCC powders Avicel 105 and 101

To better illustrate the difference in behavior between these two powders we performed a granulation run using water coloured with a red tracer. Figure 15 show the contents of the bowl for MCC Avicel 105 and Avicel 101. Figure 16 shows the bowl after the product has been emptied from the bowl. As it can be observed in Figure 15a there is a strong interaction between the MCC Avicel 105 powder and the glass walls of the Mi-Pro while the same cannot be observed for the MCC Avicel 101 where the product stays inside the bowl without sticking to the walls. When emptying the bowls we can observe that for both powders a certain amount of powder is being compressed to the glass wall in the space between impeller and wall. The red stains formed where the coloured water has been added show a much greater local overwetting for MCC Avicel 105 than for Avicel 101.

As noted by Hapgood et al [14] penetration times for different grades of excipients can vary greatly with mean particle size (Figure 17a) for different grades of lactose. The mean surface diameter varied between 26 and 69 microns and mean weight diameters between 67 and 200 microns (roughly 3 times as is the case for the difference between MCC Avicel 105 and Avicel 101). This phenomenon could account for the different behavior in the nucleation phase.

Hapgood et al [15] proposed a nucleation regime map (Figure 17b) describing a dimensionless penetration time parameter as a function of a dimensionless spray flux.

$$\tau_h = \frac{t_p}{t_c} \quad (\text{III-22})$$

$$\Psi_a = \frac{3V^*}{2A'd_d} \quad (\text{III-2-3})$$

Where t_p is the penetration time and t_c the circulation time of the powder in the nucleation zone, V' is the volumetric spray rate, A' the area flux of powder traversing the spray zone and d_d the droplet diameter.

While the penetration time is largely a function of formulation properties the adimensional spray flux ψ_a depends on the operating conditions. The regime map (Figure 17b) describes three regimes of nucleation:

- the drop controlled regime where each individual drop wets completely the powder bed to form a single nuclei granule and nuclei size distribution is controlled by the drop size distribution,
- shear controlled regime (or mechanical dispersion regime) where liquid pooling or caking occurs where the binder meets the bed and binder distribution occurs only by breakage of lumps due to shear forces inside the powder bed,
- and an intermediate regime between droplet and shear controlled where some agglomeration does occur near the spray zone without complete caking or pooling.

The presumable difference in penetration time difference for our two MCC grades could explain taking the powder from the drop controlled regime (or intermediate) to the

mechanical dispersion controlled regime where good binder dispersion requires good mechanical mixing. Given the binder “footprint” in Figure 16b it is reasonable to assume that granulation for MCC Avicel 101 at 400 rpm takes place in the intermediate regime while granulation for MCC Avicel 105 occurs in the shear controlled regime. In our case the same binder flow rate is imposed through the same binder addition method (same average drop size) which leaves the velocity of the powder surface as the only free variable in estimating ψ_a . We couldn't give an estimation for this velocity as the Mi-Pro lacks instrumentation with a high speed video camera and image analysis software or positron emission particle tracking technology, the two methods currently employed in order to measure powder surface velocity. However, as shown by Hapgood et al [15] for water pumped on a lactose bed the values for ψ_a would be close to a value of unity (in a 25L Fielder high shear mixer) which would make it borderline between the intermediate and the shear controlled regime.

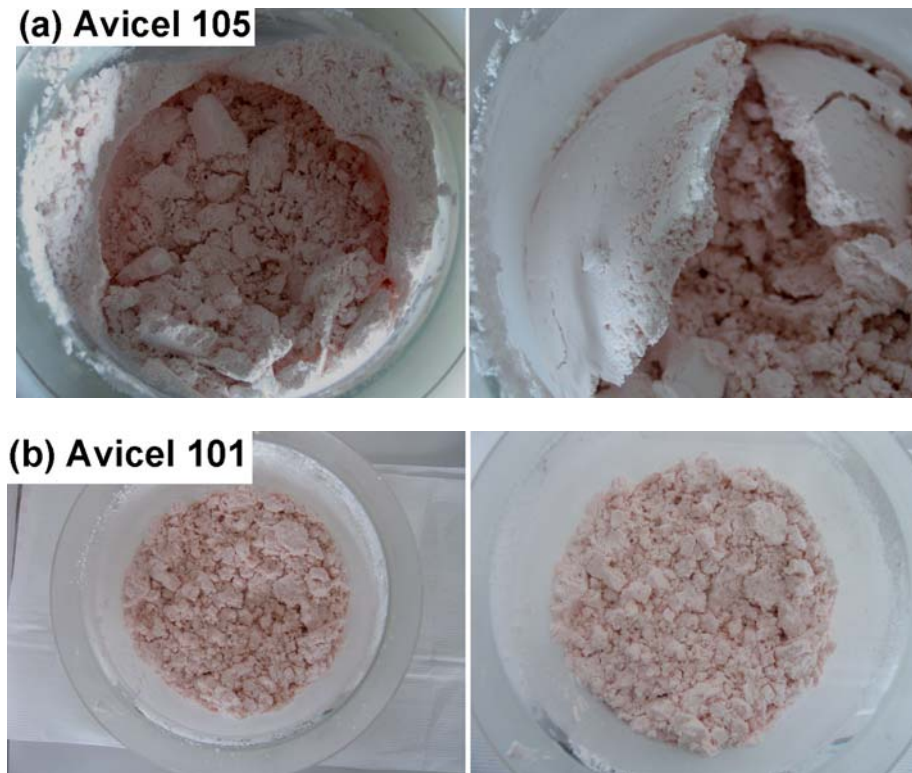


Figure 15. View of the full Mi-Pro 1.9L at 400 rpm with chopper active at 41% L/S ratio for MCC Avicel 105 (a) and Avicel 101 (b)

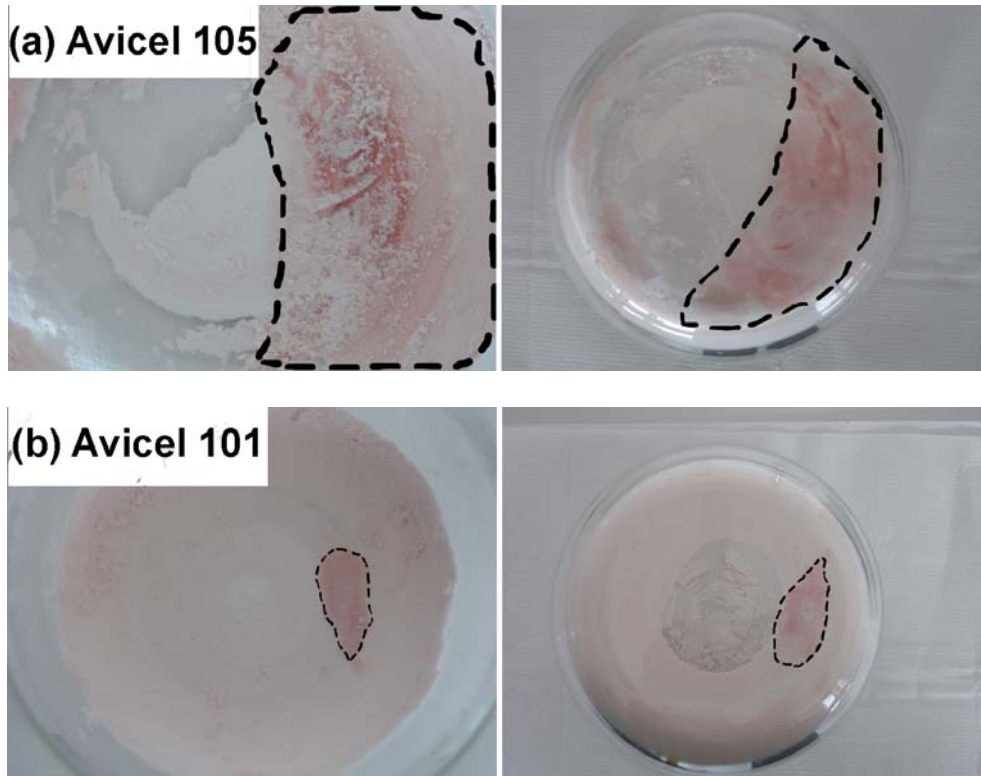


Figure 16. View of the empty Mi-Pro 1.9L at 400 rpm with chopper active at 41% L/S ratio for MCC Avicel 105 (a) and MCC Avicel 101 (b)

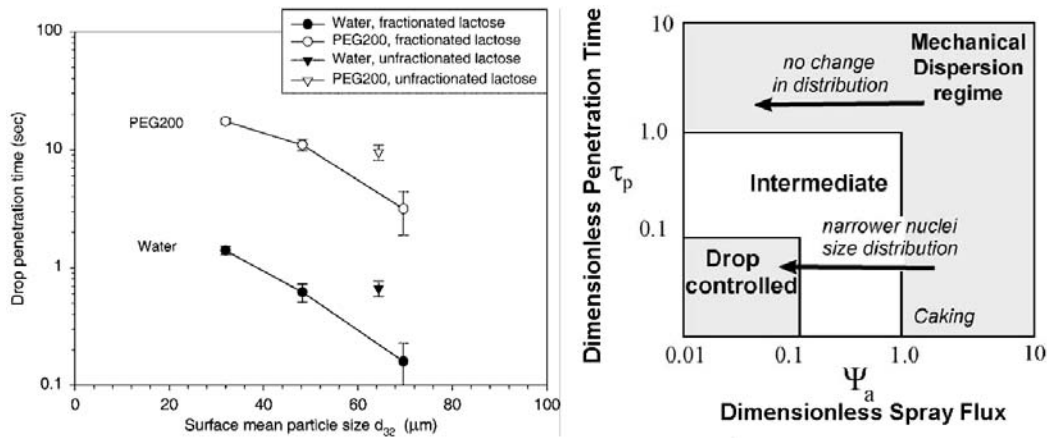


Figure 17. Drop penetration time as a function of lactose surface mean particle size from Hapgood et al [14] (a) and nucleation regime map from Hapgood et al [15] (b)

Where torque curves are continuous (100 and 800 rpm) we observe an evolution similar to that proposed by Leuenberger [16]. For the low impeller speed of 100 rpm we observed that the chopper turning at high speed can also lead to agglomeration. The granulation at

100 rpm with chopper active is characterised by an initial wetting stage up to 10% L/S ratio followed by a first stage of nucleation forming few but big low resistance agglomerates mainly by layering. Once granules are large enough they come in contact with the chopper and a secondary nucleation stage takes place with denser nuclei originated from the broken up larger agglomerates which ends at about 55% L/S ratio. For the granulation run without chopper at 100 rpm the second nucleation stage and redistribution of powder and binder doesn't take place and the end result corresponds to granules presenting a much larger mean granule size. At 400 and 800 rpm the chopper influence is not visible in the recorded torque curve showing the same inflexion points independent of chopper use.

An interesting feature to study has been the chopper design. The smaller and shorter chopper that equipped the 0.9 L bowl has been mounted on the 1.9 L bowl at an impeller speed of 650 rpm, considered sufficient so as to bring the powder mass in contact with both choppers (Figure 18). While in both cases no lumps have been observed the difference in mean granule size is quite stark: 1200 μm with the smaller chopper and 950 μm (20% difference) with the regular one showing the size reducing effect of the chopper for intermediate speeds.

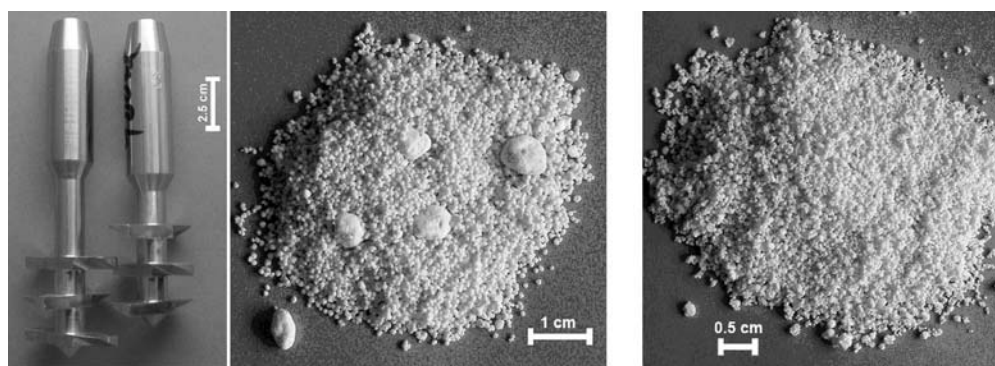


Figure 18. Choppers from the Mi-Pro HSM, 0.9 L and 1.9 L bowls and granules obtained in the 1.9 L bowl using the smaller chopper (left) and the regular chopper (right) for the granulation of MCC Avicel 105 with ultra-pure water

Using the granules in the 1000-1250 microns range the roundness of the obtained granules has been studied. Table 5 and Figure 19 show the evolution of roundness with

increasing impeller speed. Up to 400 rpm the roundness increases while for values above 400 rpm granules begin to decrease in roundness.

Impeller Speed [rpm]	Roundness	
	D_{50}	$\text{Span}=(D_{90}-D_{10})/D_{50}$
100	0.67	0.7
260	0.77	0.43
400	0.86	0.45
550	0.79	0.47
800	0.72	0.54

Table 5. Roundness as a function of impeller speed

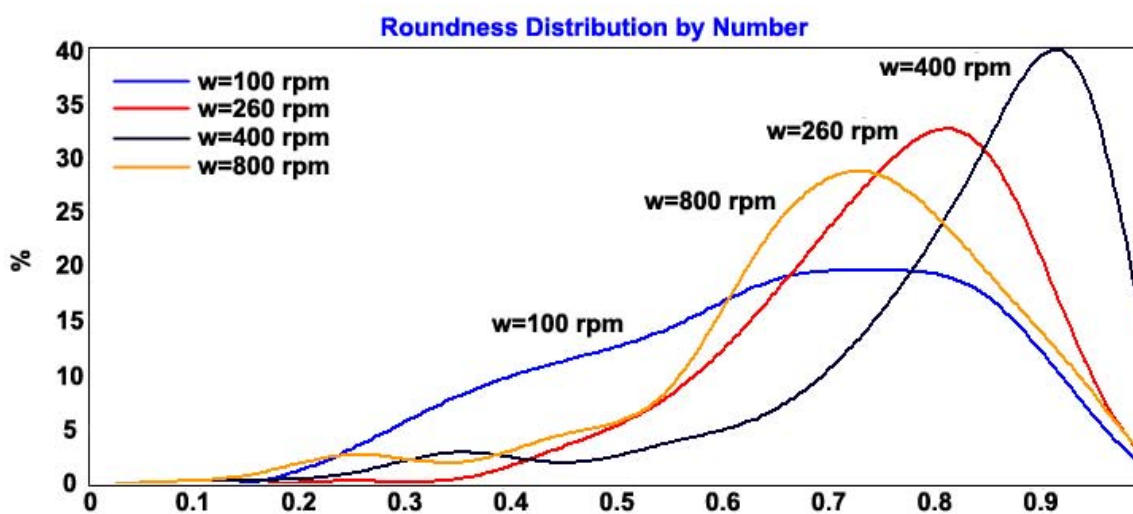


Figure 19. Roundness distributions by number as a function of impeller speed for the granulation of MCC Avicel 105 with ultra-pure water

Figure 20 shows the evolution of interparticular porosity with increasing impeller speed, as it is to expected the reduction in mean granule size also leads to a reduction in the volume occupied by the granules.

Dry granule strength measurements (Figure 21a) show that increasing the impeller speed leads to an increase in granule strength. Above 800 rpm however a slight decrease in

granule strength was also observed which could be related to granule breakage becoming dominant to such an extent that granule growth and consolidation are affected leading to less strong granules.

It should also be mentioned that the granules obtained at 100 rpm in the studied granule size range, 1000-1250 microns show a very low reproducibility (one in ten granules give an exploitable load-displacement curve). In order to obtain a better reproducibility granules in the size range 2000-2500 microns have also been studied for 100, 260 and 400 rpm. The results (Figure 21b) show the same trends with 100 rpm and 260 rpm showing similar dry granule strengths and a non-negligible increase in granule strength at 400 rpm.

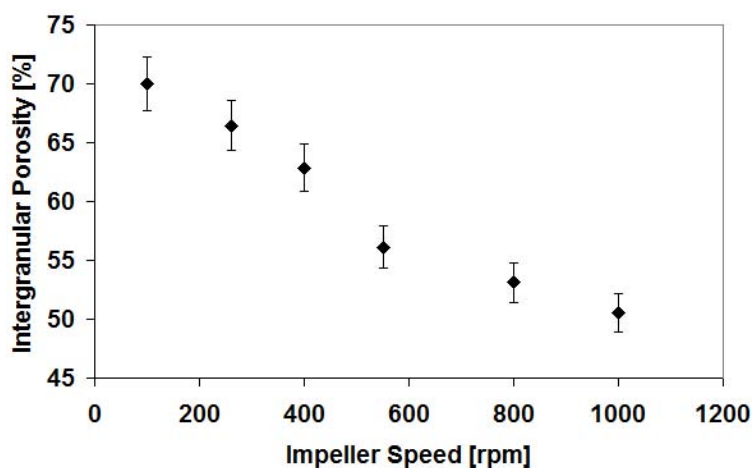


Figure 20. Evolution of intergranular porosity as a function of impeller speed for the granulation of MCC Avicel 105 with ultra-pure water

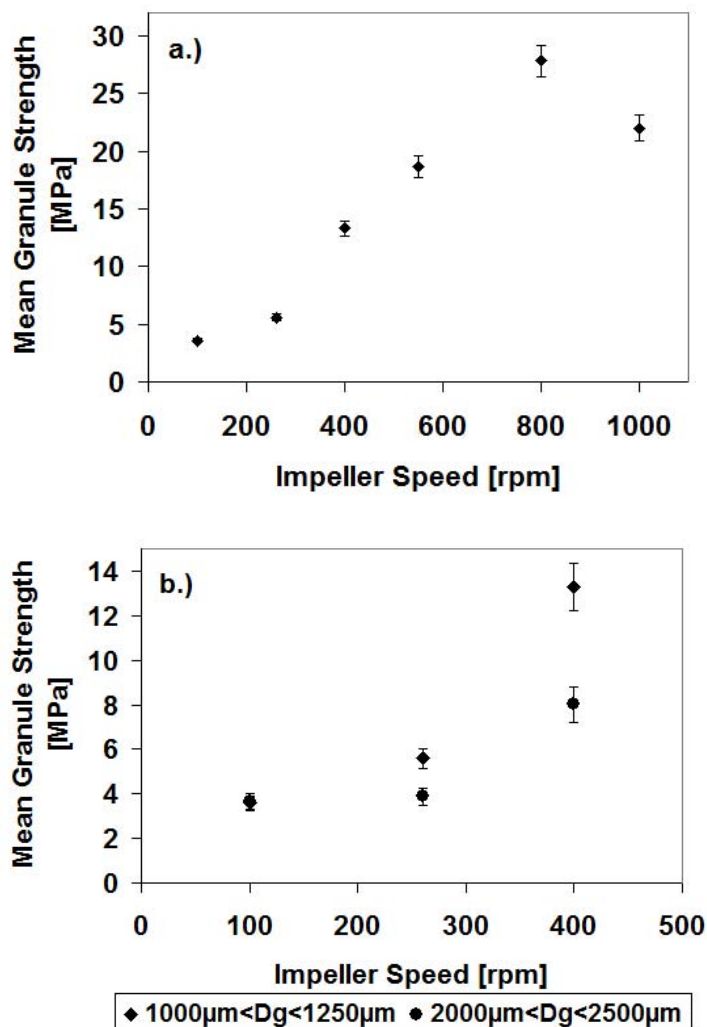


Figure 21. Evolution of dry granule strength as a function of impeller speed (a) and comparison between granule strength evolutions as a function of studied granule size (b) for the granulation of MCC Avicel 105 with ultra-pure water

3. Effect of Equipment Geometry

As we have shown when discussing chopper influence mean granule size depends largely on impeller speed, with sizes decreasing upon increasing impeller speed. Comparing final granule size between two scales of the Mi-Pro: 0.9 and 1.9L presenting similar geometric proportions in terms of bowl and impeller shape and expressing the impeller speed as impeller tip speed we found a greater granule size for speeds inferior to 1.5 m/s on the small scale (0.9L) as the liquid distribution is less than optimal and a high degree of

lumps are formed, while for speeds between 1.5 and 4.03 m/s granules are consistently larger on the larger scale (1.9L). The evolution of slowly decreasing mean granule sizes is common to both scales, for values above 4.03 m/s breakage occurs and for values of 4.7 m/s and above granule sizes become comparable (Figure 22).

Granule breakage is a result of impact pressure overcoming the strength of the wet granules. Figure 23 shows the evolution of impact pressure for the two setups calculated using the formula proposed by Vonk [17] in equation 5:

$$\sigma_{impact} \approx \frac{2}{3} \cdot \rho \cdot v^2 \quad (III-2-4)$$

Where ρ is the granule density and v the impact speed approximated as the impeller tip speed.

For both scales breakage is present from an impact pressure of approximately 6 kPa onwards corresponding to values above the theoretical static tensile strength calculated using the equation proposed by Rumpf [18]:

$$\sigma = C \cdot S \cdot \frac{(1-\varepsilon)}{\varepsilon} \cdot \frac{\gamma}{d_{pi}} \cdot \cos(\theta) \quad (III-2-5)$$

Where C is a material constant ($C=6$ for uniform spheres), ε is the granule porosity, d_i the initial particle diameter, θ is the liquid–solid contact angle, γ_L the liquid surface tension and S the liquid pore saturation.

In order to investigate differences between scales we chose to look in more detail at the growth mechanisms at nearly identical impeller tip speeds by analyzing the evolution of the three characteristic fractions (Figure 24). We chose the speed of 400 rpm at the 1.9 L scale and 460 rpm at the 0.9 L scale corresponding to impeller tip speeds of 2.93 and 2.89 m/s respectively. Fill ratio, binder flow per initial mass of dry powder, chopper speed, homogenization protocol and granulation time have been kept constant between scales. The wetting stage is similar occurring up until an S/L ratio of 30% is reached. Afterwards nucleation and growth start for the small scale, with coarse granules beginning to show at 30% L/S ratio, while for the larger scale coarse granules begin to form only from 50% L/S ratio onwards. This behavior can be explained by the more confined volume of the

0.9 L bowl causing an increase in contacts between granules which leads to an acceleration of growth mechanisms as well as the more inclined chopper that can interact more with the moving powder bed assuring a more intense mixing.

In terms of granulation mechanisms similar behavior to the one observed in the Mi-Pro have been observed in a 6L Diosna high shear mixer as described by Oulahna [19] and in the 10 L Zanchetta Roto as described by Benali [12].

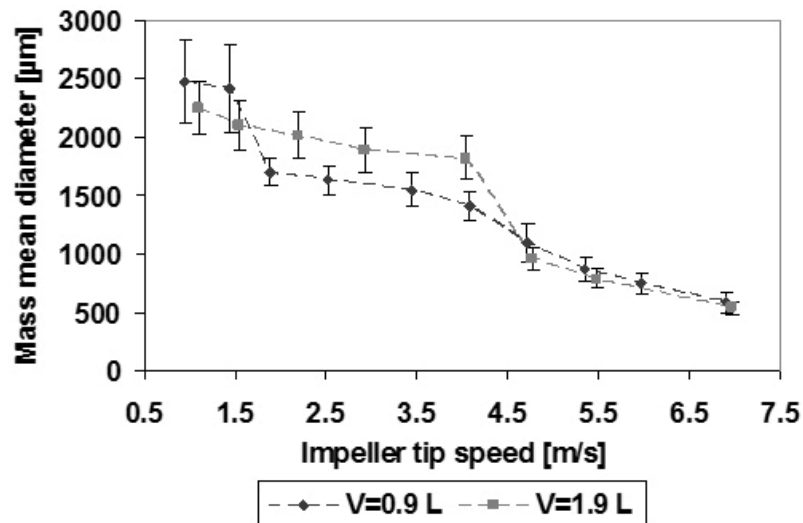


Figure 22. Evolution of mean granule size as function of impeller tip speed on two scales of the Mi-Pro HSM: 0.9L and 1.9L for the granulation of MCC Avicel 105 with ultra-pure water

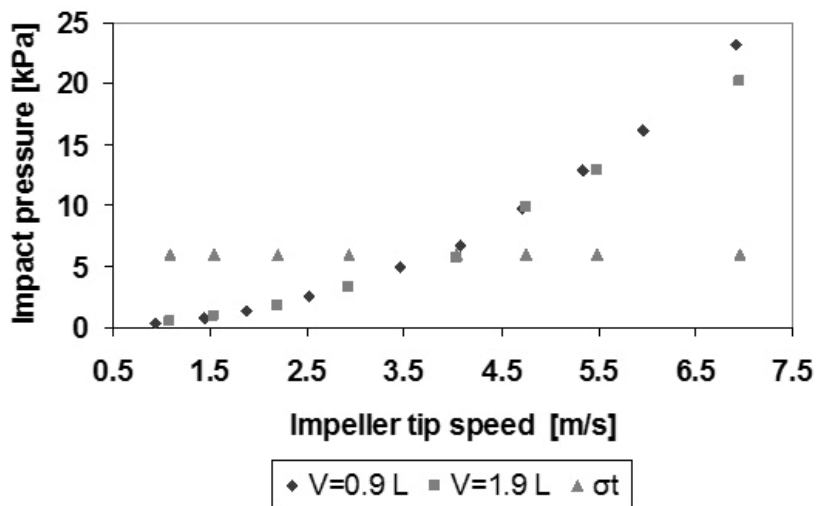


Figure 23. Evolution of Impact pressure and Rumpf's static tensile strength as a function of impeller tip speed for the granulation of MCC Avicel 105 with ultra-pure water

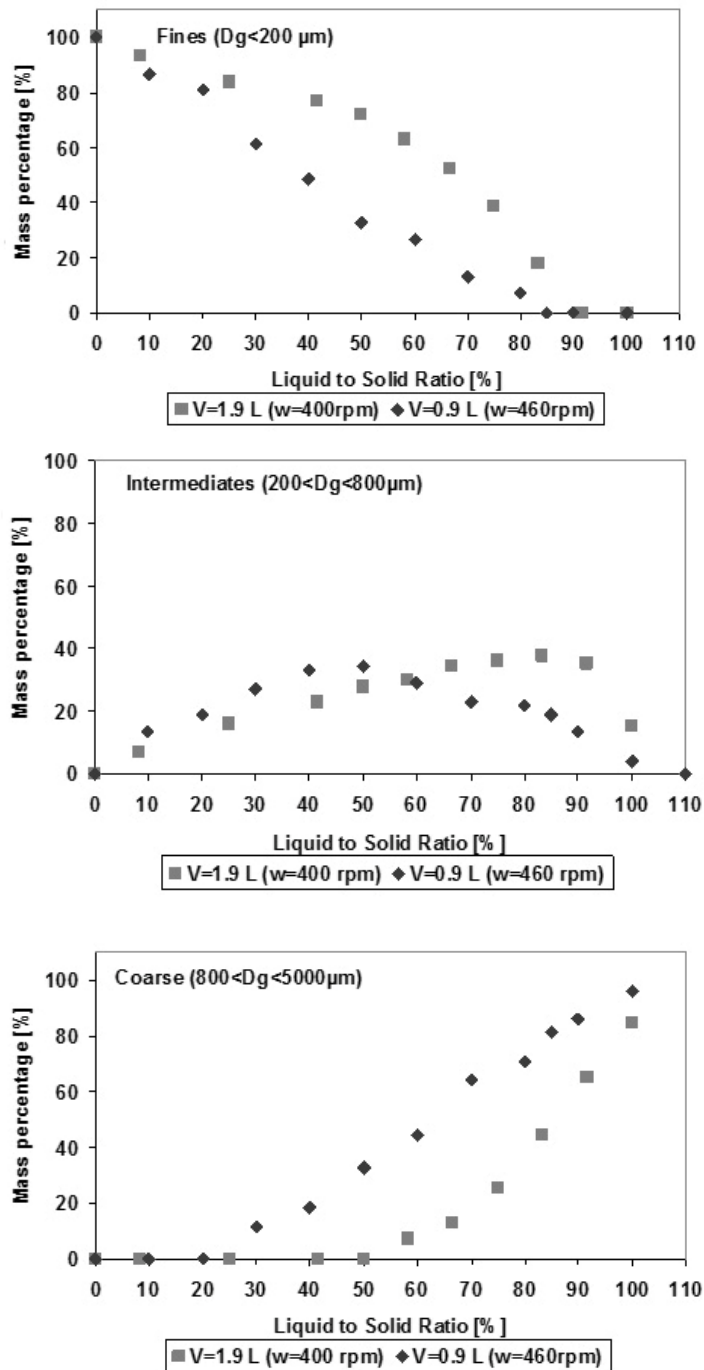


Figure 24. Evolution of the characteristic size fractions for the same impeller tip speed in the Mi-Pro HSM V=1.9 L and V=0.9 L

4. Conclusion

The effect of the fill ratio and the main means of agitation in a high shear mixer have been investigated in this study. Fill ratio has been found to increase mean granule size across all studied impeller speeds. While fill ratio has not been found to have a dramatic influence on granulation mechanisms two situations should be avoided:

- at low impeller speeds lower fill ratios will change the nucleation behavior of the powder as the particles might not be influenced by the chopper as a means of breaking up the early lumps that form at low impeller speeds,
- at high impeller speeds where the lower value of the fill ratio can lead to overwetting because of interactions between powder and wall/lid.

Fill ratio has been found to impact roundness of the obtained granules however this is more evident at low to medium impeller speeds, while at higher impeller speeds the roundness of the granules seemed independent of fill ratio. Mean dry granule strength has been shown to increase with fill ratio from 16 to 26% at all studied speeds with the phenomenon being more evident at lower to medium impeller speeds. A further increase of the fill ratio from 26 to 32% leads to lower dry granule strengths at lower to medium impeller speeds while at high impeller speeds no effect is observed.

We found that torque curves can allow a good control over the granulation process especially at high impeller speeds. At intermediate impeller speeds torque curves show a low reproducibility especially because of the strong cohesive nature of the employed grade of microcrystalline cellulose. We found that it is important to study the effect of chopper presence at more than just one speed as by increasing impeller speed lumps percentage will increase for low to medium impeller speeds and decrease when impeller speed alone can break up the lumps for high impeller speeds. As a general rule the chopper allows for better binder distribution in the Mi-Pro and is found to be necessary for successful granulation at low to moderate impeller speeds. For high impeller speeds in excess of 4.4 m/s with or without chopper similar granule sizes and growth mechanisms are observed.

Granule roundness was found to increase with impeller speed up to a certain speed after which granules roundness has been found to decrease with increasing impeller speed most probably because of increased breakage of the granules. Dry granule strength has been found to increase with increasing impeller speed presenting only a slight decrease at the highest impeller speed studied.

The effect of equipment geometry between the 0.9 and the 1.9 L Mi-pro high shear mixers has shown that at the lower scale accelerate granule growth takes place while keeping a constant impeller tip speed can give good agreement in terms of size between the scales.

References

- [1] E. Chevalier, M. Viana, C. Pouget, D. Chulia, Influence of process parameters on pellets elaborated in a Mi-Pro high-shear granulator, *Pharmaceutical development and technology* 12 (2007) 133-144
- [2] F. Gomez, K. Saleh, P. Guigon, Étude de la granulation humide en mélangeur à taux de cisaillement élevé par rhéométrie par couple de rotation, Congrès sur les Poudres, Nancy, France, 2001, Récents Progrès en Génie des Procédés, 15, 77, 317-322
- [3] T.K Bock, U. Kraas, Experience with the Diosna mini-granulator and assessment of process scalability, *Eur. J. of Pharm. and Biopharm.*, 52(3), (2001) 297-303
- [4] L. Vialatte, Mécanismes de granulation. Application à la granulation par agitation mécanique, PhD Thesis Université Technologique de Compiègne (1998)
- [5] T. Schaefer, B. Taagegard, L.J. Thomsen, H.G. Kristensen, Melt pelletization in a high shear mixer. V. Effects of apparatus variables, *Eur. J. Pharm. Sci.* (1993) 133-141
- [6] R. Thies, P. Kleinebudde, Melt pelletisation of a hygroscopic drug in a high shear mixer: Part 1. Influence of process variables, *Int. J. of Pharm.* 188(2) (1999) 131-143
- [7] J.N. Michaels, L. Farber, G. S. Wong, K. Hapgood, S. J. Heidel, J. Farabaugh, J-H. Chou, G. I. Tardos, Steady states in granulation of pharmaceutical powders with application to scale-up, *Powder Technol.* 189 (2009) 295-303
- [8] P.C. Knight, An investigation of the kinetics of granulation using a high shear mixer, *Powder Technol.* 77 (1993) 159-169
- [9] J. Hamdani, A.J. Moës, K. Amighi, Development and evaluation of prolonged release pellets obtained by the melt pelletization process, *Int. J. of Pharm.* 245(1-2) (2002) 167-177
- [10] A. Faure, P. York, R. Rowe, Process control and scale-up of pharmaceutical wet granulation processes: a review, *Eur. J. Pharm. and Biopharm.* 52 (2001) 269-277
- [11] K. Saleh, L. Vialatte, P. Guigon, Wet granulation in a batch high shear mixer, *Chemical Engineering Science* 60 (2005), 3763-3775
- [12] M. Benali, V. Gerbaud, M. Hemati, Effect of operating conditions and physico-chemical properties on the wet granulation kinetics in high shear mixer, *Powder Technol.* 190 (2009) 160-169
- [13] A.M. Bouwman, The influence of material properties and process conditions on the shape of granules produced by high shear granulation, PhD thesis Rijksuniversiteit Groningen (2005)
- [14] K. Hapgood, J. D. Litster, S. R. Biggs, T. Howes, Drop penetration into porous powder beds, *Journal of Colloid and Interface Science* 253, (2002) 353-366
- [15] K.P. Hapgood, J.D. Litster, R. Smith, Nucleation regime map for wet granulation, *AIChE J* 49 (2) (2003) 350-361
- [16] H. Leuenberger, H-P Bier, H. Sucker, Theory of the granulation-liquid requirement in the conventional granulation process, *Pharm.Tech.Int.* 3 (1979) 61-68
- [17] P. Vonk, C.P.F. Guillaume, J.S. Ramaker, H. Vromans, N.W.F. Kossen, Growth mechanisms of high shear pelletisation, *Int. J. Pharm.* 157 (1997) 93-102
- [18] H. Rumpf, Methoden des granulieren, *Chem. Eng. Technol.* 30 (1958) 144-158
- [19] D. Oulahna, F. Cordier, L. Galet, J. Dodds, Wet granulation the effect of shear on granule properties, *Powder Technol.* 130 (2003) 238-246

Chapter III.3 Effect of Formulation : Effect of Binder Nature and Properties

In this subchapter we have studied the influence of various aqueous polymer solutions on the wet granulation of microcrystalline cellulose MCC Avicel 105. We have investigated the influence of the binder properties (viscosity, work of adhesion) on the rheology, granulation kinetics, wet mass consistency and dry granule strength. In addition the influence of mixer design has also been studied for a low viscosity and a high viscosity system.

1. Introduction

Wet high shear granulation implies the addition of a binder. This can be achieved either by adding a liquid binder characterized by a certain viscosity, surface tension and contact angle or by adding a low viscosity liquid like water onto a powder mix comprised of the powder to granulate and a solid binder that dissolves in the low viscosity liquid changing its properties. Also the binder may be added as a dry powder in the powder mix and liquefied by increasing temperature up to its melting point. Adding the binder as a dry powder allows the granulation with high viscosity binders without using dedicated pumps or clogging the nozzles and for some high viscosities it might even be the only solution. We chose to work in the case of the first method where aqueous binder solutions are prepared and characterized before the granulation process. This limited the maximum viscosity to be studied to about 120 mPa.s as this was the upper limit for pump used by the liquid addition system used in this study.

The viscosity of the binder is important in understanding the granulation mechanisms involved and the strength of the resulting granules. Keningley et al [1] found a minimum binder viscosity associated with granulating non-porous calcium carbonate particles with silicone fluids. They found that in order to successfully form granules a minimum

viscosity of 10mPa.s was necessary for mean particle sizes of 8 microns, of 100 mPa.s for particles with a mean size of 50 to 80 microns and of 1Pa.s for particles presenting a mean particle size of 230 microns. Several authors have shown (Johansen and Schaefer [2], Mills et al [3]) that an increase in viscosity has a benefic effect on granulation up to a certain critical value above which the opposite effect is observed.

The influence of viscosity on granulation mechanisms has also been discussed by Mills et al [3]. The granulation: at low viscosities is believed to be controlled by layering growth mechanisms. At higher viscosities coalescence was the predominant mechanism based on the absence of layered material, a smaller sphericity and a slow growth consistent with growth by coalescence.

The influence of surface tension has been investigated by Capes and Danckwerts [4]. They found that a minimal surface tension was necessary in order to favor agglomeration. Iveson et al [5] found that:

- decreasing binder surface tension can lead to a decrease in the dynamic yield stress in the agglomerate
- but that for higher viscosities binder viscosity dominated the wet granule dynamic yield stress.

Ritala et al [6] found that power consumption of the granulator increases with increasing binder surface tension.

Ennis et al [7] studied the coupled effect of viscosity and surface tension. They found that the granulation mechanisms depend essentially on the competition between the capillary and viscous forces. They defined a viscous capillary number relating these forces:

$$Ca_{vis} = \frac{\mu U}{\gamma_L} \quad (\text{III-3-1})$$

Where U is the speed of the particles, μ is the binder viscosity and γ_L is the liquid surface tension.

They found that:

- If $Ca_{vis} < 10^{-3}$ the energy dissipation due to the viscosity can be neglected compared to the capillary forces and that adhesion is the product of interfacial forces
- If $Ca_{vis} > 1$ the viscous force is dominant over the static forces with the viscous force expressed as.

Like Ennis, Benali et al. [8] investigated the wet granulation of microcrystalline cellulose by defining a modified capillary number as:

$$Ca^* = \frac{\mu U}{\gamma_L (1 + \cos \theta)} \quad (\text{III-3-2})$$

Where the liquid surface tension is replaced by the work of adhesion. They found that for values of the modified capillary number above a value 1.62 the viscous forces predominate and control granule growth while for values below unity the interfacial forces are dominant since increasing the work of adhesion enhances the growth kinetics. They also found that granule friability increases with decreasing viscosity for values of the modified capillary number above unity. We chose to use this definition for our study.

The aim of this study is to better understand the relationship between the physico-chemical properties of the powder binder couple and their effects on wet mass rheology, granulation kinetics, wet mass consistency and dry granule strength.

2. Effect of Binder Nature and Properties

2.1 Rheological Properties of the Powder-Binder Couple

Figure 1 and Table 1 show the obtained torque curves on the MTR by the method of multiple liquid additions and the values corresponding to the peak of these curves respectively. As discussed in our previously (Chapter III-1) the peak torque on the MTR for the case of microcrystalline cellulose indicates the capillary state which in the Mi-Pro HSM corresponds to the granules uniting into a single paste like mass showing a maximum torque for the same L/S ratios. However when used comparatively to assess binder suitability we can observe similar behavior and cohesion for water and PVP 3% solution. PVP 13% develops a slightly higher cohesion than both water and PVP 3%

while using both PVP 3% and PVP 13% as binders lowers the L/S ratio necessary for achieving the capillary state. The HPMC 0.5% and 1% binder solutions are showing higher cohesions than those obtained with water while an abrupt increase in torque is observed for the more viscous binder solution of HPMC 3% indicating a greater risk in over wetting the powder bed. From a point of maximum developed cohesion HPMC 3% stands out from the rest of the polymer binders used.

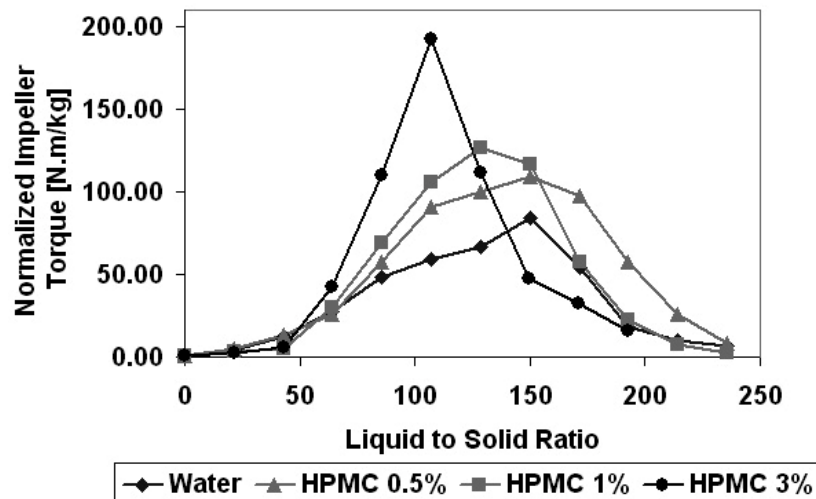
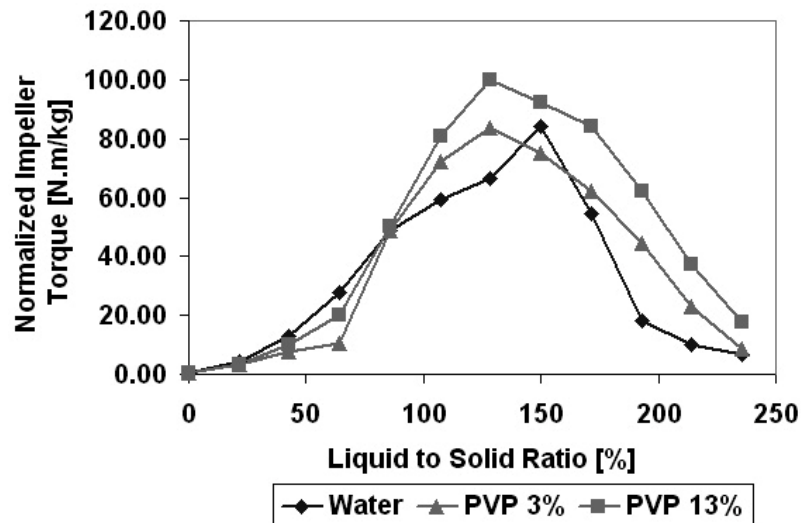


Figure 1. Mean torque curves on the MTR by the multiple addition method for the studied binder solutions using MCC Avicel 105 as powder

Binder type	γ (mN/m)	μ (mPa·s at 25°C)	Peak Torque [N.m/kg]	L/S Ratio corresponding to the Peak Torque [%]
Water	72.2	1.0	84.3 ± 4.3	150
PVP 3%	63.6	1.3	83.6 ± 4.8	128.5
PVP 13%	53.8	3.1	100.1 ± 5.1	128.5
HPMC 0.5%	47.6	3.1	109.3 ± 5.2	150
HPMC 1%	47.1	8.1	126.5 ± 5.3	128.5
HPMC 3%	47.3	117	192.9 ± 6.2	107

Table 1. Peak torque and corresponding L/S ratio for the studied aqueous solutions mixed by multiple addition method with MCC Avicel 105 on the MTR (as reminder from Chapter II for the differences between the binder solutions, the surface free energy and viscosity are also given)

2.2 Granulation Kinetics for the Studied Binders

Torque curves recorded on the Mi-Pro high shear mixer (Figure 2) have shown that different binder types present different liquid requirements. Table 2 regroups the optimal binder requirement and the L/S ratios for the transitions in the torque curve. The initial wetting and nucleation phases are similar for all binders the extent of the growth varies. For water a quantity of liquid equivalent to approximately 100% L/S ratio is necessary while even the slightest addition of a polymer (PVP 3%) lowers the optimum L/S ratio (Figure 2a). Low viscosity polymeric binders like PVP3% and PVP 13%, HPMC 0.5% and HPMC 1% show similar torque curves with the plateau phase ending at about 75 to 83% L/S ratios, lower than the 83-91% L/S ratio observed when granulating with water. It was also observed that both water and the PVP solutions give shorter wetting stages (20-22% L/S ratio) than the HPMC solutions (27% L/S ratio). For high viscosity binders like HPMC 3% we have observed even shorter growth zones with values around 75-78% L/S ratio (Figure 2b). The optimum liquid requirement corresponds largely with the end of the plateau. For water more water can be added as to maximize the yield in coarse granules without endangering overwetting. For the aqueous polymer solutions the end of the plateau is the maximum safe value for the L/S ratio. The polymer film on the granule surface favors coalescence and overwetting can easily occur. When granulating with

HPMC 3% granulation has to be closely watched because the passage from granules to paste occurs more rapidly for the more viscous binders and overwetting is easily obtained (Figure 3).

Binder type	Optimum L/S Ratio [%]	L/S ratio Wetting Stage [%]	L/S ratio Nucleation End[%]	L/S ratio Plateau region [%]				
Water	100	0-22	22-45	45→(83 to 91)				
PVP 3%	83	0-22	22-45	45→(75 to 83)				
PVP 13%	83	0-20	22-45	45→(75 to 83)				
HPMC 0.5%	83	0-27	27-45	45→(75 to 83)				
HPMC 1%	83	0-27	27-45 </tr <tr> <td>HPMC 3%</td> <td>77</td> <td>0-34</td> <td>34-50</td> <td>50→(75 to 77)</td> </tr>	HPMC 3%	77	0-34	34-50	50→(75 to 77)
HPMC 3%	77	0-34	34-50	50→(75 to 77)				

Table 2. Wet granulation characteristic results for the different binders employed

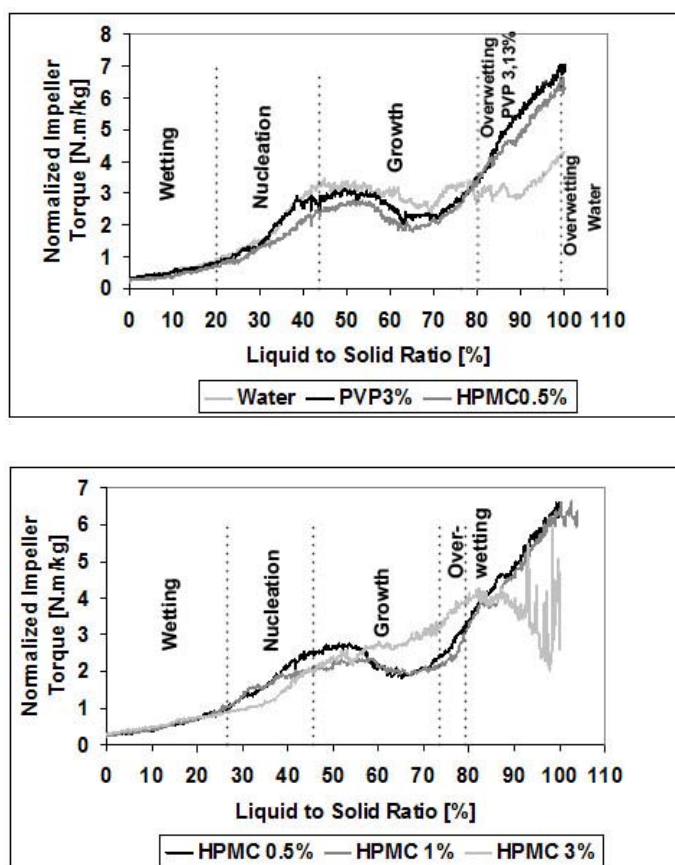


Figure 2. Representative torque curves for the studied binder solutions on the Mi-pro 1.9L HSM

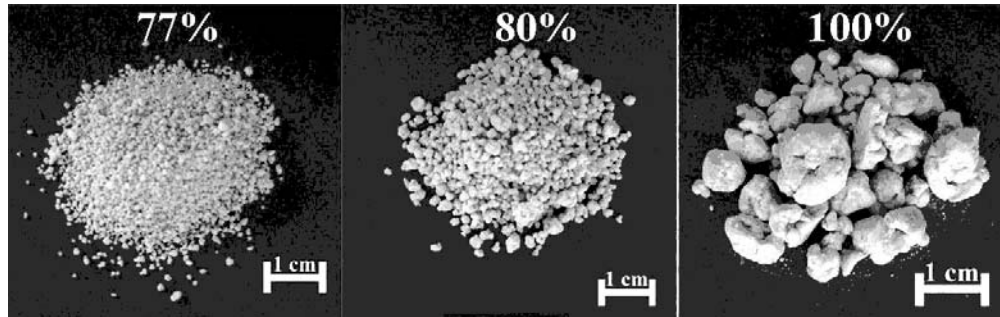
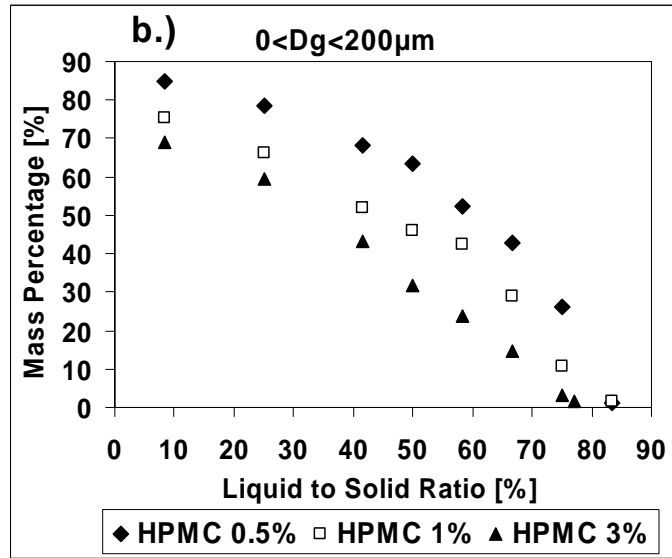
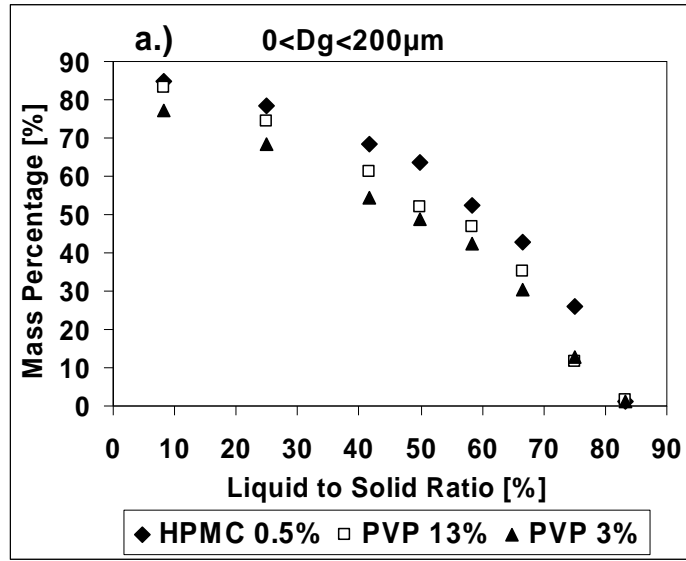


Figure 3. Final granules obtained in the Mi-Pro 1.L HSM for different L/S ratios of HPMC 3%

From the granule growth kinetics point of view we have observed that:

- for low viscosity binders like PVP 3%, PVP 13% and HPMC 0.5% for the same L/S ratio the interfacial forces are dominant (Figures 4a and 4c). The fine fraction decreasing more rapidly and mean granule size increasing with increasing work of adhesion in the order PVP 3%>PVP 13%> HPMC 0.5% as predicted from the wettability measurements,
- for different concentrations of HPMC increasing viscosity accelerates growth in the order HPMC 3%>HPMC 1%> HPMC 0.5% (Figures 4b and 4d),
- while the torque curve show little differences in the transitions between the wetting and nucleation stages the evolution of the fines particles class (Figures 4a and 4b) are more indicative for differences between the different aqueous solution binders,
- the evolution of the mean granule size (Figures 4c and 4d) does not allow us to interpret difference between the different binders up to 50% L/S ratio for the low viscosity binders and up to 25% for the higher viscosity binders.

The accelerated growth for more viscous binders, anticipated from the torque curves which indicated lower L/S ratios in order to achieve optimum liquid requirement, can be explained by the longer penetration time (as defined by Denesuk et al [9]) of the more viscous binders in the granules that form a film on the surface leading to successful coalescence between granules. This observation is further confirmed by the higher wet mass consistencies recorded.



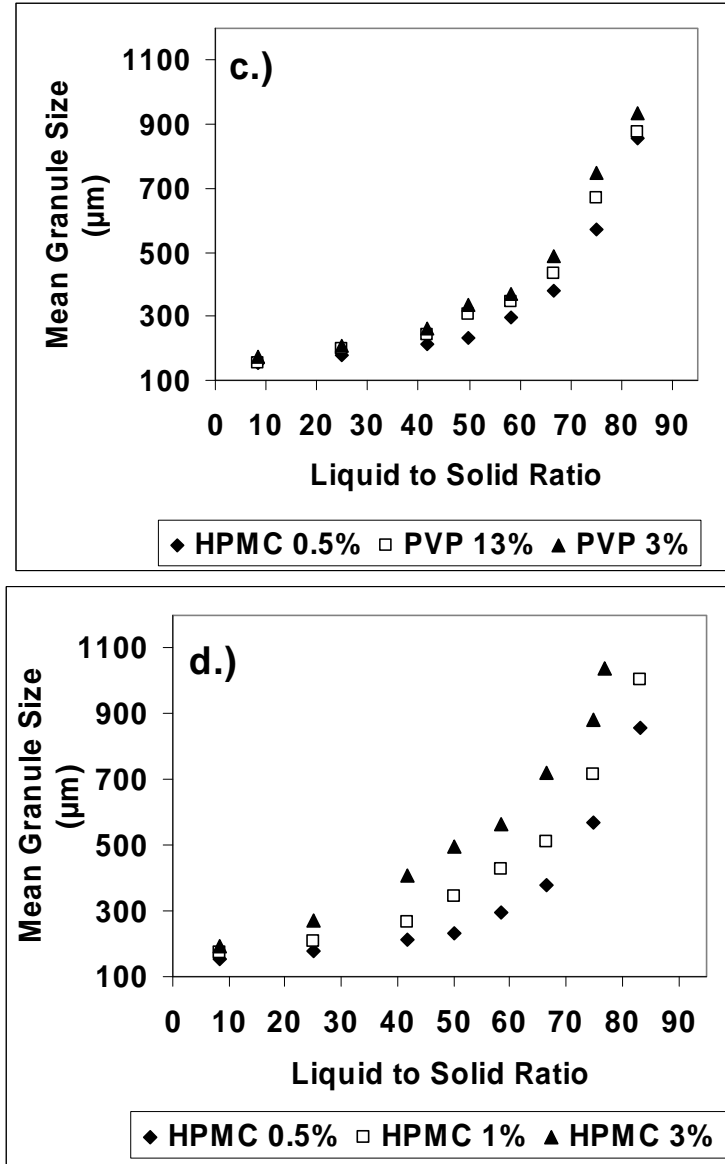


Figure 4. Evolution of fine particles(a,b) and mean granule size(c,d) for the wet granulation runs of MCC Avicel 105 with different binder solutions

We applied the same approximation of the granule growth kinetics as the one proposed by Benali et al [8] by assuming that granule growth can be described as a first order consecutive chemical reaction: $A \rightarrow B \rightarrow C$ (Figure 5). This allows defining an overall growth kinetic constant K by replacing the concentration of A by the percentage of the fine particles, and the time by the liquid to solid ratio in the chemical kinetic law:

$$K = \frac{d}{dL/S} \ln \left(\frac{x_{fines}^0}{x_{fines}} \right) \quad (\text{III-3-3})$$

Where X_{fines}^0 - initial ratio of fine particles and X_{fines} -the ratio of fine particles at a given L/S ratio.

Our results presented in Figure 6a confirm the observations of Benali et al [8] in that there seems to be a direct and linear correlation between growth and work of adhesion for the low viscosity binders (HPMC0.5%, PVP 3%, PVP 13%, water). A similar connection can be made drawn between the kinetic constant K and the capillary number (Figure 6b) using the HPMC aqueous binder solutions (HPMC 0.5%, HPMC 1%, HPMC 3%) however more points are necessary in order to establish the linearity of the dependence.

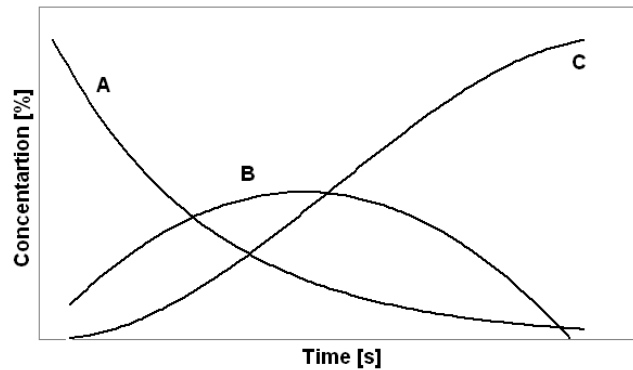
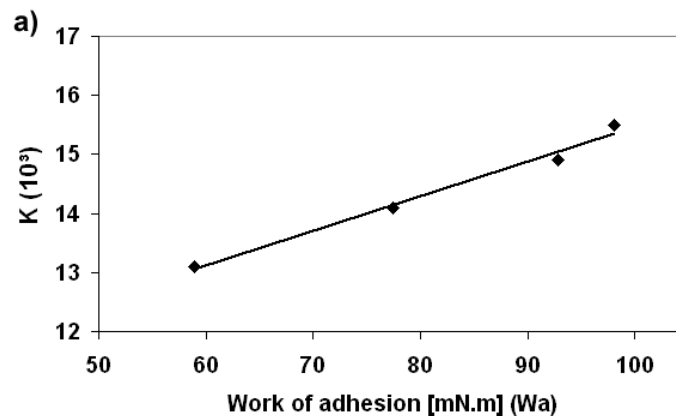


Figure 5. First order consecutive reaction kinetics



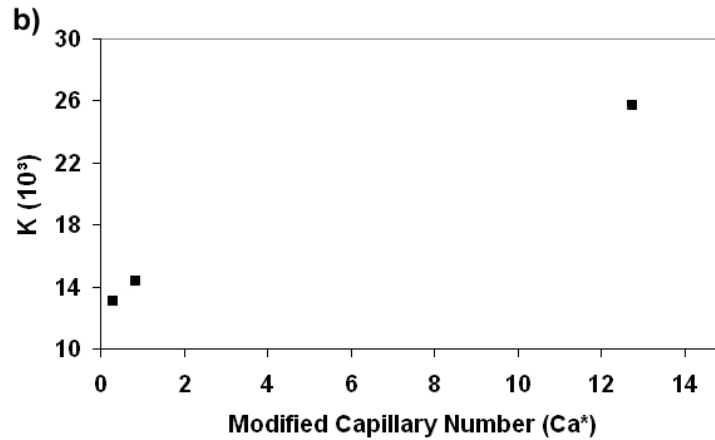


Figure 6. Kinetic constant vs work of adhesion for $Ca^* < 0.8$ (a) and kinetic constant vs Ca^* for the HPMC aqueous binder solutions used for the granulation of MCC Avicel 105 on the Mi-Pro 1.9L HSM

2.3 Granule Strength

Table 3 shows the results in terms of mean granule size, wet mass consistency and dry granule strength. Two situations can be identified:

- for the polymeric solutions with $Ca^* < 0.8$ a reduction of Wa leads to a reduction in mean granule size as well as a slight reduction of granule strength while the optimum L/S ratio remains constant
- for polymeric solutions with $Ca^* > 0.8$ we observe slightly larger mean granule sizes, lower granule strengths and an increase in wet mass consistency.

These results seem to be in line with the results obtained by Benali et al [8] with the decrease in the boundary condition (0.8 vs. 1) most probably affected by the lower viscosity necessary to agglomerate finer particles (20 microns mean granule size for MCC Avicel 105 versus 60 microns mean particle size for MCC Avicel 101) as also shown by Keningley et al [1].

Granulation with pure water is considered a special case as it demands much more liquid to granulate and interpretations on granule growth kinetics or final granule properties are

hard to correlate with just differences in physico-chemical properties between binder solutions.

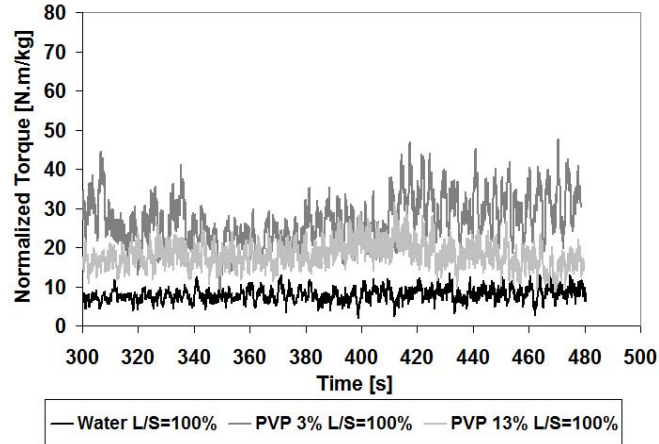
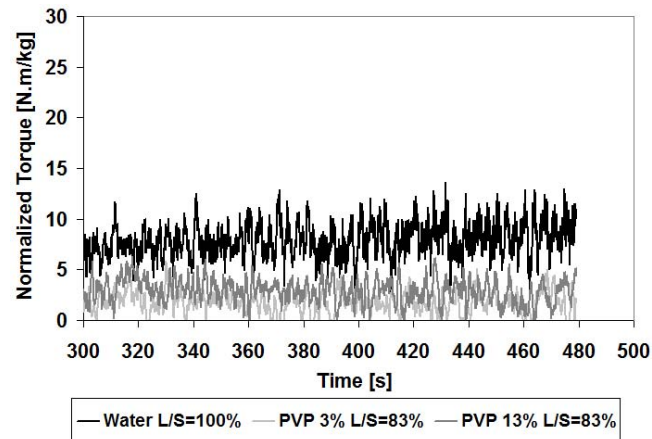
Binder type	Wa [mN/m]	Ca*	Mean Diameter [μm] [$\pm 10\%$]	Dry Granule Strength [MPa]	Wet Mass Consistency [N.m/kg]
Water	98.1	0.058	899	37.0 \pm 4.7	8.2 \pm 1.6
PVP 3%	92.8	0.082	936	29.2 \pm 4.3	2.6 \pm 0.6
PVP 13%	77.5	0.235	877	27.4 \pm 3.1	3.7 \pm 0.8
HPMC 0.5%	58.9	0.307	857	26.6 \pm 4.8	3.6 \pm 0.9
HPMC 1%	56.1	0.842	1006	13.7 \pm 2.7	5.2 \pm 1.3
HPMC 3%	53.7	12.76	1039	13.0 \pm 2.4	27.6 \pm 3.6

Table 3. Dry granule strength and wet mass consistency as a function of binder used for the granulation of MCC Avicel 105 on the Mi-Pro 1.9L HSM

Wet samples taken at the end of each granulation run of the Mi-Pro for the different aqueous solution binders at the optimum L/S ratios have been mixed in the MTR in order to determine wet mass consistency. This approach is based on the presumption that the intense mixing in the MTR can transform the granules to a homogenous mass. Figure 7 shows some typical wet mass consistency results from which the mean value has been calculated. For aqueous solution binders with a viscosity lower than 3.1 mPa.s the wet mass consistency depends on the added binder mass with the following evolution water > PVP 3% > PVP 13% (Figure 7a). At the same L/S ratio like water however both PVP solutions show higher wet mass consistencies than water (Figure 7b). For the HPMC solutions we can observe that only a high increase in viscosity as for HPMC 3% gives a much larger wet mass consistency compared to both HPMC 1% and HPMC 0.5%. (Figure 7c).

When regrouping the evolution of wet mass consistency as a function of the modified capillary number (Figure 8a) we can observe the following regions: for $Ca^* < 0.8$ we have lower viscosities which are followed by a weak change in wet mass consistency between 0.8 and 3.8 and by a strong increase for high values of Ca^* .

The mean dry granule strength was evaluated for granules with diameters between 1 and 1.25 mm considered as representative for our granulation runs in respect to the final mean granule sizes and granule size distributions. The dry granule strength measurements show that granule strength increases with increasing work of adhesion (Figure 8b) for low viscosity binders. It also shows a sharp drop in dry granule strength for the more viscous binders compared to the low viscosity binders.



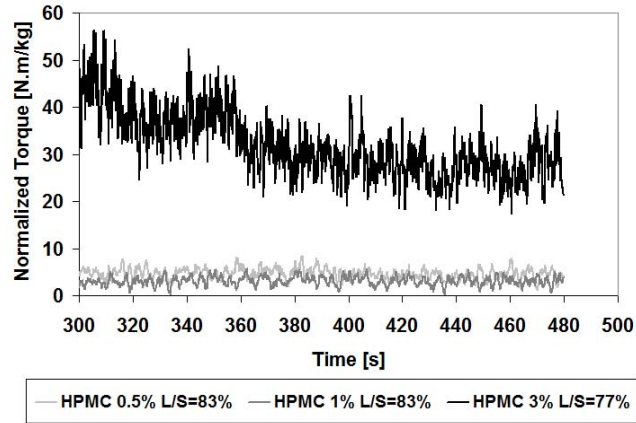
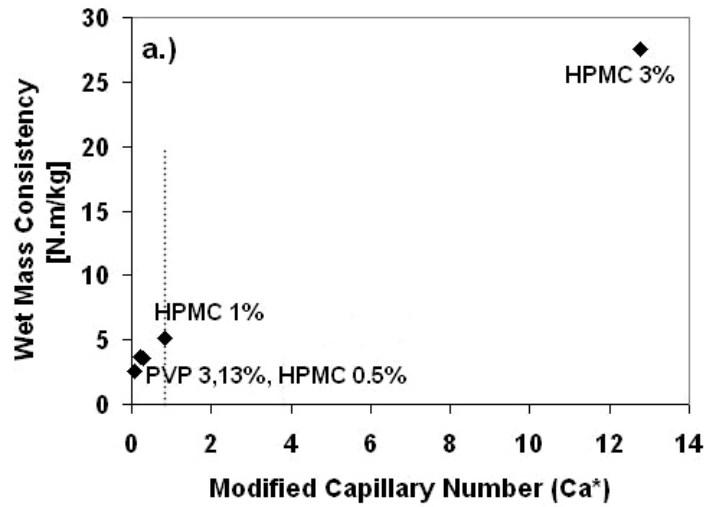


Figure 7. Wet mass consistency evolutions for the for PVP aqueous solutions and water at optimum binder requirement (a), at the same L/S Ratio =100% (b) and for the evolution of the HPMC aqueous binder solutions (c)



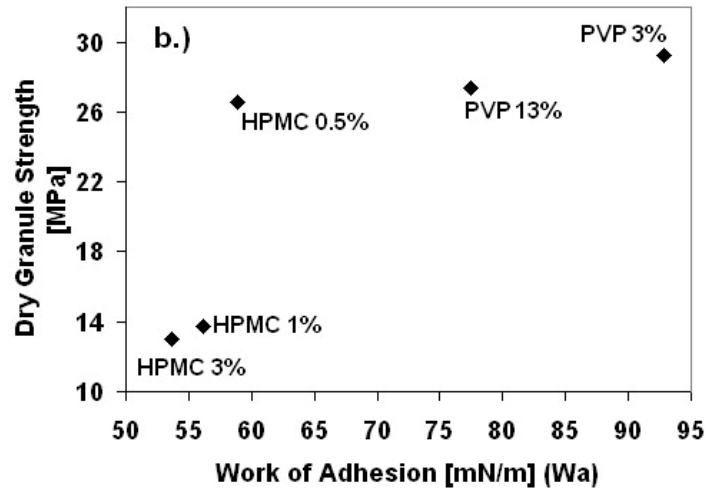


Figure 8. Evolution of wet mass consistency vs Ca^* (a) and dry granule strength vs work of adhesion (b)

2.4 Effect of Mixer Design

The results obtained on the 1.9L Mi-Pro were up scaled to a Diosna 6L high shear mixer in order to verify if the results previously described preserve their validity. We chose the two binders solution with significantly different properties from the ones tested: water with low viscosity and high binder surface tension and HPMC 3% with a high binder viscosity and a lower binder surface tension. Two scale-up criteria were investigated:

- constant impeller tip speed,
$$\omega = \frac{N}{60} \cdot \pi \cdot D \quad (\text{III-3-4})$$

- constant Froude number,
$$Fr = \frac{N^2 \cdot D}{g} \quad (\text{III-3-5})$$

Where N is the impeller speed, D the impeller diameter and g the gravitational acceleration constant.

Applying these rules gave two corresponding impeller speeds on the Diosna:

- 460 rpm for constant impeller tip speed,
- 605 rpm for constant Froude number.

The same fill ratios, granulation time, optimum L/S ratios have been kept while using the same manually controlled drop by drop pump on both high shear mixers. The chopper on the Diosna has been operated at 500 rpm while the chopper on the Mi-Pro was turning at 3000 rpm. Figure 9 shows the obtained granule size distributions.

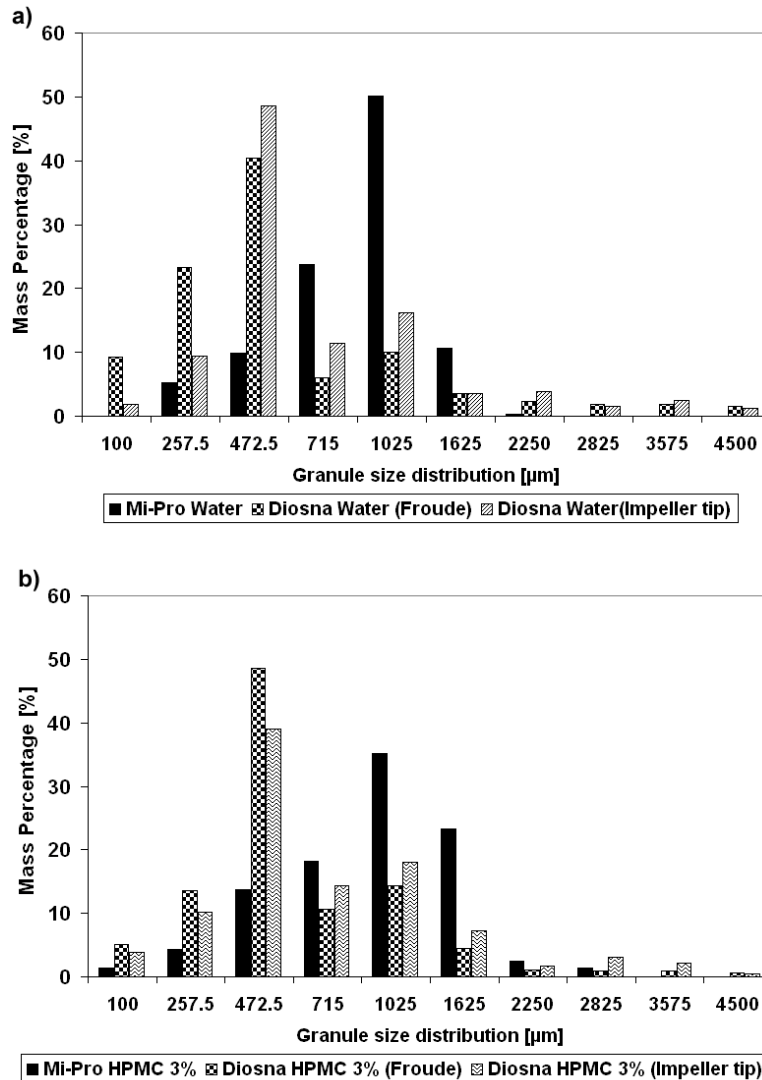


Figure 9. Granule size distributions on the studied high shear mixers: using water (a) and using HPMC 3% (b) for the granulation of MCC Avicel 105

Mean granule size analysis (Figure 9a and b) shows that both scale up criteria yield lower mean granule sizes on the Diosna. The constant impeller tip speed yields a closer result in

terms of granule sizes, it shears and impacts less, causing breakage to a lesser extent than when keeping the Froude number constant.

Dry granule strength (Table 4) shows again greater values for water as a binder than HPMC 3%. While dry granule strength has been determined for the same size interval as in the previous experiments we also tested some granules in the 2.5-3mm range. Figure 10 shows the load-displacements curve for two larger granules (2.5-3.15 mm) for water and HPMC. We observe that the water granulated granule doesn't break while the HPMC 3% granules is being crushed.

Binder type and Impeller speed	Dry Granule Strength [MPa]	Mean Granule Size [μm] [$\pm 10\%$]
Mi-Pro		
Water (800 rpm)	37.0 ± 4.7	899
HPMC 3% (800 rpm)	13.0 ± 2.4	1039
Diosna		
Water (460 rpm)	29.5 ± 5.0	840
Water (605 rpm)	24.1 ± 3.5	715
HPMC 3% (460 rpm)	10.6 ± 3.1	780
HPMC 3% (605 rpm)	10.8 ± 2.5	670

Table 4. Dry granule strength and mean granule size on the investigated mixers

Increasing impeller speed reduces dry granule strength on the low viscosity binder however on the high viscosity binder little variation in dry granule strength is observed. Granule strength compared between mixers shows lower values when granulating at the larger scale. This can be explained by the fact that at lower scales mixing is more intense and collisions between particles are more frequent leading to increased granule consolidation.

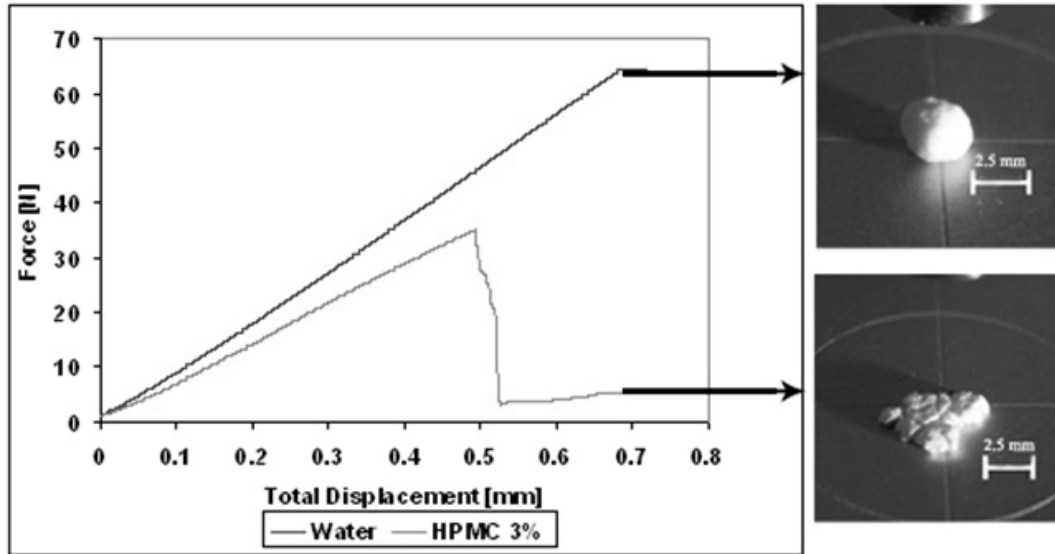


Figure 10. Typical load displacement curves for large granules from the Diosna HSM with constant impeller tip speed as scale-up rule and water and HPMC3% as binders for the granulation of MCC Avicel 105

3. Conclusion

We found that torque curves can allow a good control over the granulation process allowing us to define optimum binder requirements for the different binder solutions used, essential for obtaining similar granule size distributions. Optimum liquid requirement has been found to decrease with increasing viscosity, this indicating the accelerated growth due to more successful coalescence between granules, however this slower penetration of the binder has to very different effects on granule strength: it yields higher wet mass consistencies as the viscous binder is still at granule surface and sticks easily to the mixer torque rheometer blades but doesn't offer a great inner strength which is apparent from the dry granule uniaxial compression tests where the more viscous binders show lower granule strength. Recorded torque curves as well as granule growth kinetics and dry granule strength measurements show that granulation, at low viscosities, is dependant on the work of adhesion. The use of the capillary viscous number allowed us to define the boundaries for which the work of adhesion is the dominant parameter $Ca^* < 0.8$ and for which the viscosity is the controlling parameter $Ca^* \geq 0.8$.

References

- [1] S. Keningley, P. Knight, A. Marson, An investigation into the effects of binder viscosity on agglomeration behaviour, *Powder Technol.* 91 (1997) 95–103
- [2] A. Johansen, T. Schaefer, Effects of interactions between powder particle size and binder viscosity on agglomerate growth mechanisms in a high shear mixer, *European J. of Pharm. Sciences* 12 (2001) 297–309
- [3] P.J.T. Mills, J.P.K. Seville, P.C. Knight, M.J. Adams, The effect of binder viscosity on particle agglomeration in a low shear mixer/agglomerator, *Powder Technol.* 113 (2000) 140–147
- [4] C. Capes, P. Danckwerts, Granule formation by the agglomeration of damp powders. Part I: the mechanism of granule growth, *Transactions of the Institution of Chemical Engineers* 43 (1965) 116–124
- [5] S. M. Iveson, J.D. Litster, B. Ennis, Fundamental studies of granule consolidation. Part 2. Quantifying the effects of particle and binder properties. *Powder Technol.* 99 (1998) 243–250
- [6] M. Ritala, O. Jungersen, P. Holm, A comparison between binders in the wet phase of granulation in a high shear mixer, *Drug Dev. And Ind; Pharm.* 12 (1986) 1685-1700
- [7] Ennis, B.J., Tardos, G., Pfeffer, R., A microlevel-based characterization of granulation phenomena, *Powder Technol.* 65 (1991) 257-272
- [8] M. Benali, V. Gerbaud, M. Hemati, Effect of operating conditions and physico-chemical properties on the wet granulation kinetics in high shear mixer, *Powder Technol.* 190 (2009) 160-169
- [9] M. Denesuk, G.L. Smith, B.J.J. Zelinski, N.J. Kreidl, D.R. Uhlmann, Capillary penetration of liquid droplets into porous materials, *J. Colloid Interface Sci.* 158 (1993) 114–120.

Chapter III.4: Effect of Formulation: Granulation of Soluble and Insoluble Powders

On this subchapter we have studied the influence of microcrystalline cellulose content in lactose-MCC mixtures. The MCC grade chosen was MCC Avicel 105 while the lactose was a crystalline α -lactose monohydrate. The starting materials are characterized from a rheological standpoint as well as by their water sorption isotherms and their behavior during wet granulation on the Mi-Pro high shear mixer. Two formulations have been chosen one containing 7 parts lactose and 3 parts MCC Avicel 105 called "Lactose/MCC 7/3" and one containing 7 parts MCC and 3 parts lactose called "Lactose/MCC 3/7" and compared in terms of rheological characterization, granule growth kinetics, wet mass consistency and dry granule strength. Additionally we will try to relate the observations to the starting materials properties as well as attempt to validate our observations on two different scales.

1. Introduction

The manufacturing of granules often demands the granulation of powder mixtures in order to obtain specific product properties at the end of the granulation process. Favoring one component over the other in binary mixtures influences granule properties. Microcrystalline cellulose (MCC) is one of the most widely used pelletization agents, being highly hygroscopic and conferring a certain degree of plasticity to the mixture while lactose is commonly used as excipient in the pharmaceutical industry. The amount of granulation liquid required for granulation depends on the mass fraction of MCC in the formulation as shown by Kristensen et al [1] when describing the wet granulation of lactose-MCC mixtures in a rotary processor controlled by torque measurements. They show that increasing MCC content (between 10 and 100%) increases the water content at the end-point of binder addition, determined as a function of torque evolution.

Kristensen et al. [2] compared the growth mechanisms of water soluble lactose with that of water insoluble calcium hydrogen phosphate. They found that calcium hydrogen phosphate requires 1.8 times more binder for significant granule growth than lactose. This observation was related to the increased plasticity of the wetted mass given by the solubility (of about 20%) of lactose in water.

Different authors (Kristensen et al [1], Vecchio et al [3] and Holm et al [4]) recommend 10 to 45% mass percentage MCC for successful pelletization. However this amount depends largely on the other components present in the formulation as well as the grades of the components. Holm et al [4] found that MCC content was influential when paired with the water soluble lactose than with the insoluble calcium hydrogen phosphate. They also found that the lowest level of MCC content for which a controllable pelletization process could be obtained increased with the fineness lactose and calcium phosphate grades. They also underlined the greater sensitivity of lactose-MCC formulations to binder content: within 0.25% relative to dry material translating to ± 15 g of water in order to achieve a mean pellet size of 900 to 1100 μ m. Kleinebudde et al. also stress the importance binder requirement stating that if binder levels are to be kept constant for varying degrees of MCC content the results are not directly comparable. The studies of Leuenberger et al [5] and Betz et al [6] show that a ternary powder mixture composed of: 86% (of the dry mass) lactose, 10% corn starch and 4% Polyvinylpyrrolidone granulated with water can allow reliable control of the granulation process. Mackaplow et al. [7] showed that for wet high shear granulation of three different grades of lactose (fine, medium, and coarse) with water that torque curves become less reproducible and present more noise with decreasing mean granule size of the starting materials. They found the granulation process for the finer particles (mean particle size of 39 μ m) to be influenced by increased wall build-up affecting the torque curve in ways not related to intrinsic granule properties.

Even though many studies deal with the granulation of different pharmaceutical products mixtures there are still few systematic studies that allow characterizing the influence of formulation parameters (proportion of different components in the mixtures) and the influence of geometrical parameters (mixer design) on the granule growth kinetics, end-product granule strength and morphologic evolution of the obtained product.

We have set out to study the effect of microcrystalline cellulose content in lactose-MCC mixtures on wet mass rheology, high shear wet granulation kinetics, wet mass consistency and dry granule strength. Additionally we will try to relate the observations to the starting materials properties as well as attempt to validate our observations on two different scales. The powders chosen are fine (microcrystalline cellulose powder MCC Avicel 105 with mean granule size of 20 μm and a fine lactose grade, α lactose monohydrate with a mean granule size of 60 μm), very cohesive, presenting poor flowing characteristics. This makes them interesting candidates for size enlargement operations.

2. Effect of Formulation: Granulation of Soluble and Insoluble Powders

2.1 Characterization of the Starting Materials

SEM pictures of the starting materials can be found in Chapter II-1. We recall that:

- the MCC presents itself as a fine, white, water insoluble powder showing particles with elongated, irregular form,
- the initial lactose particles show large lactose crystals with finer lactose particles sticking to their surface.

Differences in liquid requirement between MCC and lactose have been apparent from the first preliminary characterization studies on the mixer torque rheometer and the water sorption isotherms. Water sorption isotherms are expressed as changes in sample mass as a function of water activity (or relative humidity) that can be defined as:

$$a_w = \frac{P}{P_0} \quad (\text{III-4-1})$$

$$RH = \frac{P}{P_0} \times 100\% = a_w \times 100\% \quad (\text{III-4-2})$$

Where a_w is the water activity, RH the relative humidity of the sample, p the partial pressure of water vapor in the mixture and p_0 the saturated vapor pressure of water at the temperature of the mixture.

Water sorption isotherms (Figures 1a and 1b) show type II sorption isotherms (Rouquerol et al [15]) where the adsorption of the first layer of water molecules on the particle surface can be identified by the first inflexion point in the sorption curve which with increasing water activity is followed by multiple layers being adsorbed to surface and as a second inflexion point appears in the curve water becomes loosely bound, mobile, with minimal water-solid interactions. MCC presents a much higher water affinity than lactose. For the same values of water activity, for instance for 0.8 when water is loosely bound MCC adsorbs about 8% while lactose adsorbs only about 0.04%. This result also implies that when granulating liquid would be present in a loose form at particle surface much quicker for the lactose particles than for the MCC particles. The observed hysteresis on desorption are comparatively low. They could be caused by intragranular porosity in the sample tested as well as the interaction between product and water molecules ([15]). As both products present interactions with water (as detailed in Chapter II for microcrystalline cellulose, while lactose is soluble) this could also explain the observed hysteresis.

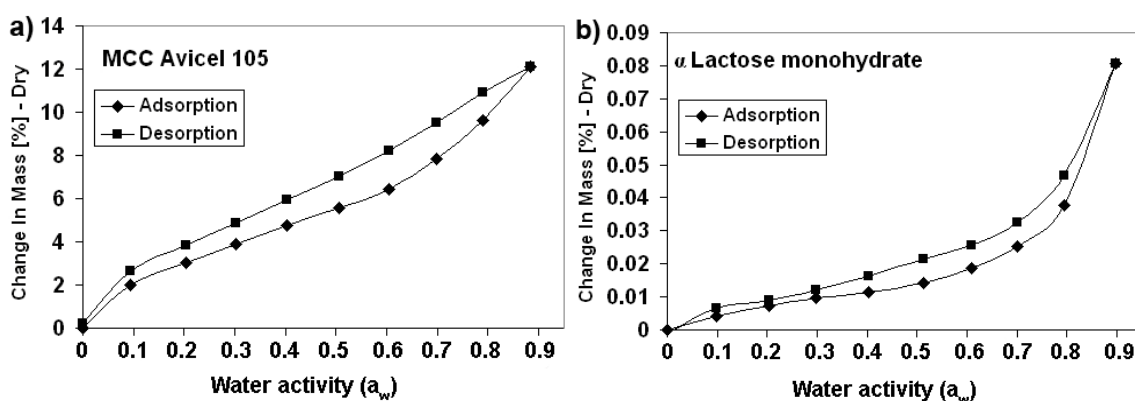
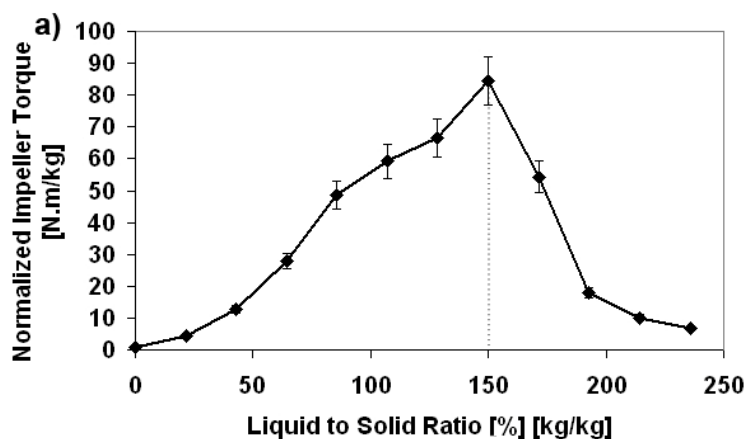


Figure 1. Water sorption isotherms for the starting materials: MCC (a) and Lactose (b)

Figure 2 shows the torque curve obtained on the MTR (Figure 2a) and the torque curve obtained on the Mi-Pro (Figure 2b) for the MCC Avicel 105 powder while Figure 3 gives the same information for lactose. The peak of the torque curve for the MCC powder corresponds to the wet powder mass turning to a highly cohesive paste in the Mi-Pro. The end of the plateau region on Figure 2b has been found to correspond to the total consumption of the fine particle class (Subchapter III-1) while granulation can still be

continued in order to maximize the coarse granules class up to a L/S ratio of 100% after which overwetting occurs. Growth mechanisms proposed on Figures 2b and 3b are based on characteristic granule class evolution and SEM observations. For the lactose MTR curve a shoulder is observed before the torque peak appearing at 16% L/S ratio. Benali [17] showed that for the same type of powder from the same source the optimum L/S ratio to be of 13% which would correspond to the end of the plateau region observed on the lactose MTR curve. Our experiments on the Mi-Pro with lactose have shown a very strong interaction between the wet mass and the mixer bowl leading to large wall build-ups for L/S ratios exceeding 4%. Stopping the granulation experiment and scraping the mixer bowls allows obtaining granules to the same L/S ratio as that observed by Benali [17]. With the gradual addition of binder, the end of the plateau region on the Mi-Pro (Figure 3b) corresponds to the majority of the wet mass exiting the impeller action and sticking to the mixer wall and a small fraction of product evolving to a suspension. It is our opinion that for the case of granulation of pure lactose a better granulation process can be achieved with the whole optimum water requirement should added over a short period of time in the beginning of the granulation. This would allow the formation of an initial homogenous paste like mass that would be further dispersed by the granulating equipment and shaped into granules.



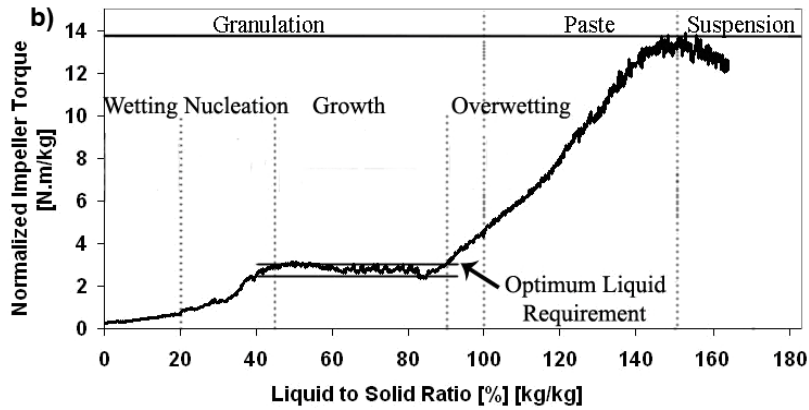


Figure 2. Torque curves developed upon gradual addition of binder on the (a) MTR and (b) Mi-Pro for MCC Avicel 105

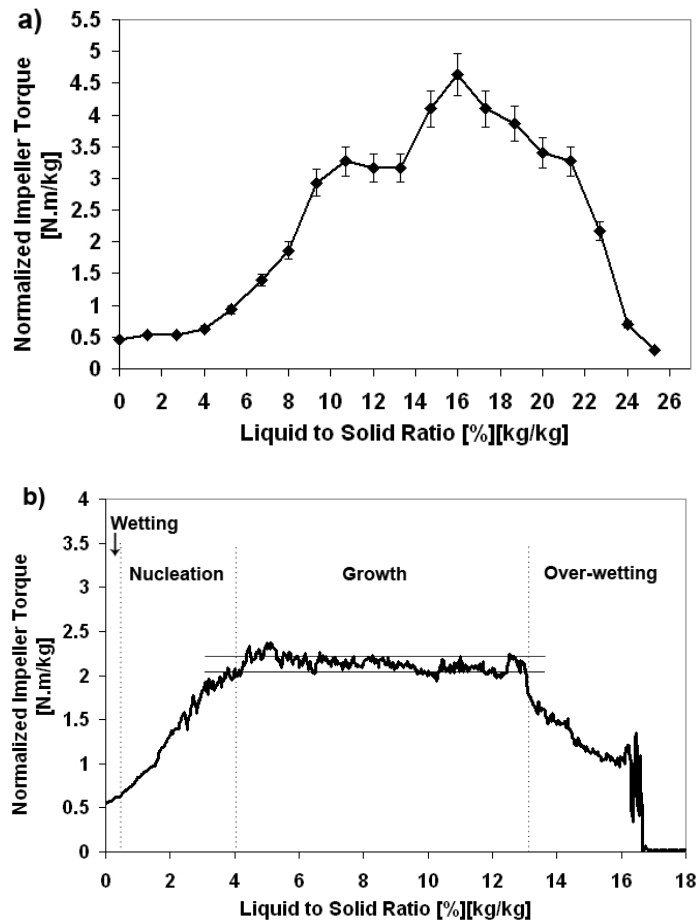


Figure 3. Torque curves developed upon gradual addition of binder on the (a) MTR and (b) Mi-Pro for lactose

Comparing the rheological data for the two starting materials we can conclude that:

- lactose requires less binder to granulate than microcrystalline cellulose (13% vs 100%),
- agglomerated MCC Avicel 105 particles develop a far greater cohesion than agglomerated lactose particles on the MTR (Figures 2a and 3a),
- torque curves on the Mi-Pro for MCC Avicel 105 and lactose are not completely comparable since the process is less than optimal for lactose granulation after the plateau region however what is evident is the much shorter wetting region for the lactose particles confirming our predictions from the water sorption isotherms that lactose presents binder on the surface for lower binder contents, which in turn will promote nucleation and growth.

2.2 Powder Mixtures Characterization

In order to study the granulation of powder mixtures we chose two different formulations, one containing 7 parts lactose and 3 parts MCC Avicel 105 called "**Lactose/MCC 7/3**" and one containing 7 parts MCC and 3 parts lactose called "**Lactose/MCC 3/7**" and compared them in terms of rheological characterization, granule growth kinetics, wet mass consistency and dry granule strength.

2.2.1 Rheological Characterization

It is apparent from the torque curves obtained on the MTR besides the difference in liquid requirement there also seems to be a huge difference in terms of developed torque. The torque values are almost 16 times higher for MCC Avicel 105 than lactose. Figure 4a shows the MTR curve for the two studied formulations as well as the curves for the pure starting materials. We find that increasing the percentage of microcrystalline cellulose increases linearly the liquid requirement for the mixture at the peak torque (Figure 4b). As expected from the findings of Kristensen et al [1] the liquid requirement and torque increase with increasing MCC percentage. MCC has a strong affinity for water and increasing MCC content increases the binder content necessary in order to promote granule growth. This behavior has also been observed on the granulation of MCC

Avicel 101 - Lactose mixtures (Figure 5): Increasing the percentage of microcrystalline cellulose increases linearly the liquid requirement for the mixture as well as the peak torque. This behavior seems to be independent of the grade of MCC used.

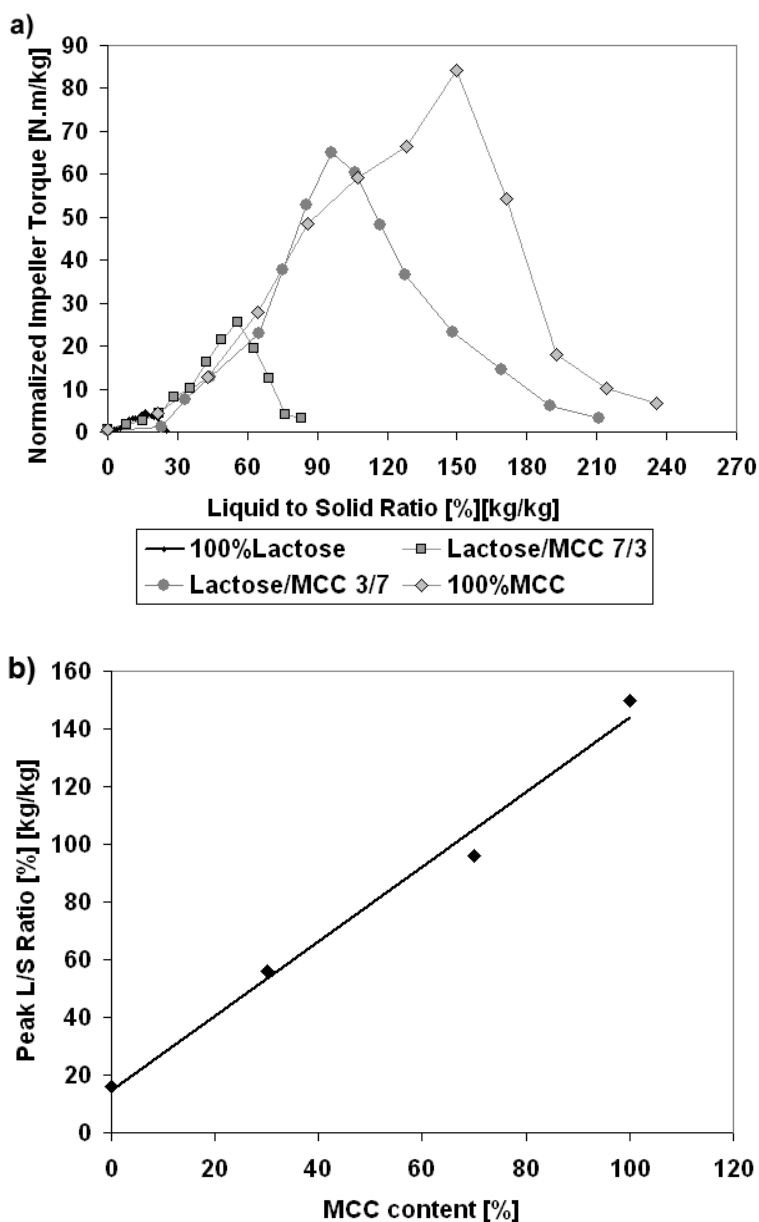


Figure 4. MTR torque curves developed upon gradual addition of binder for the pure starting materials and the studied formulations (a) and peak L/S ratio as a function of MCC Avicel 105 content (b)

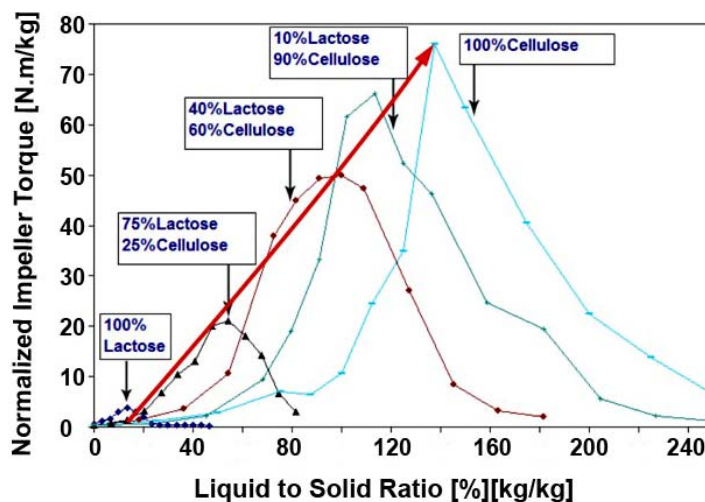


Figure 5. Mixer torque rheometer curves for different percentages of MCC Avicel 101 in MCC-Lactose mixtures

2.2.2 Granulation Kinetics

In order to obtain reproducible results granulation is best stopped in the passage from the pendular to the funicular saturation stage which is defined by the plateau region on the torque curves (Leuenberger [5]). Stopping liquid addition at L/S ratios closer to the end of the plateau allows obtaining denser granules, while slightly increased values allow a reduction of fines in the system but in the same time endanger overwetting. For the studied formulations values closest to the end of the plateau have been chosen as optimum liquid requirements for granulation: 38% for the granulation of the Lactose/MCC 7/3 formulation (Figure 6a) and 68% for the granulation of the Lactose/MCC 3/7 formulation (Figure 6b). From an optimum liquid requirement point of view this values fall as expected in between the liquid requirement for pure lactose granulation at 13% L/S ratio and pure MCC at 100% L/S ratio. It can also be observed that torque curves have a similar profile to the one presented for pure MCC in Figure 2b.

Torque profiles are similar for both formulations: after an initial wetting period longer for the Lactose/MCC 3/7 formulation the characteristic S-shaped "turning point" (as defined by Betz et al [6]) can be observed as a signal of the pendular saturation stage where

nucleation of initial particles usually occurs followed by the plateau region when growth of the particles occur in the funicular saturation stage (Goldszal and Bousquet [18]). Torque values on the plateau are slightly higher for the lactose/MCC 3/7 formulation reflecting the higher resistance to mixing of the MCC and indicating greater resistance to impact and shear of the agglomerates. It can also be observed that the Lactose/MCC 7/3 formulation torque curve is noisier as agglomerates containing more lactose are stickier and can easily adhere to the glass bowl causing inhomogeneous flow of the wetted material. This phenomenon has also been observed by Holm et al [4].

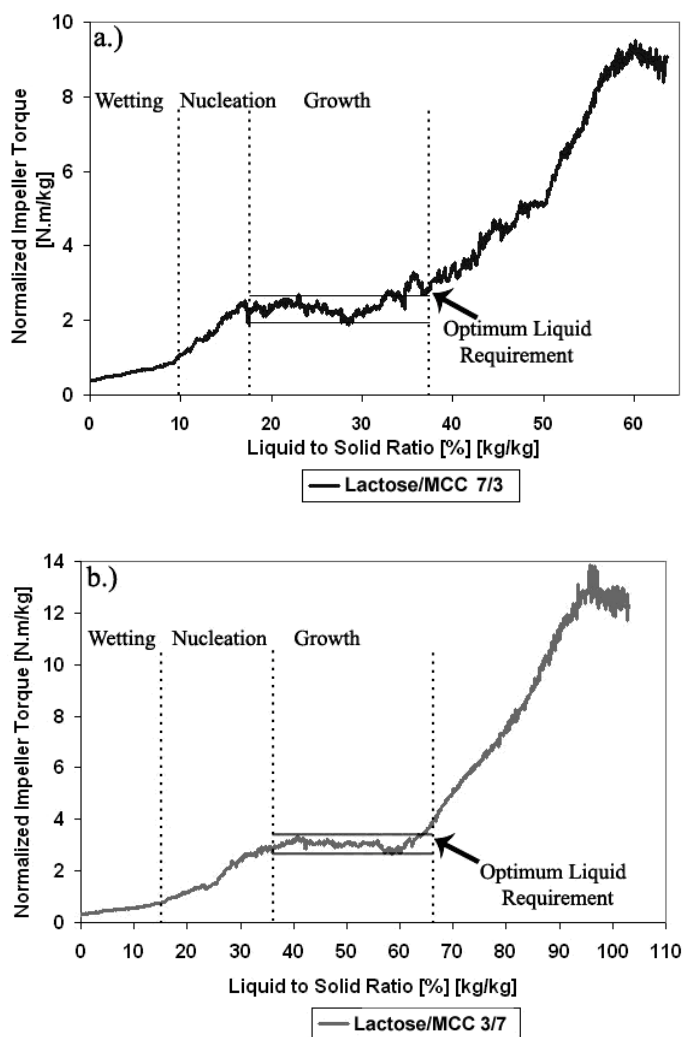
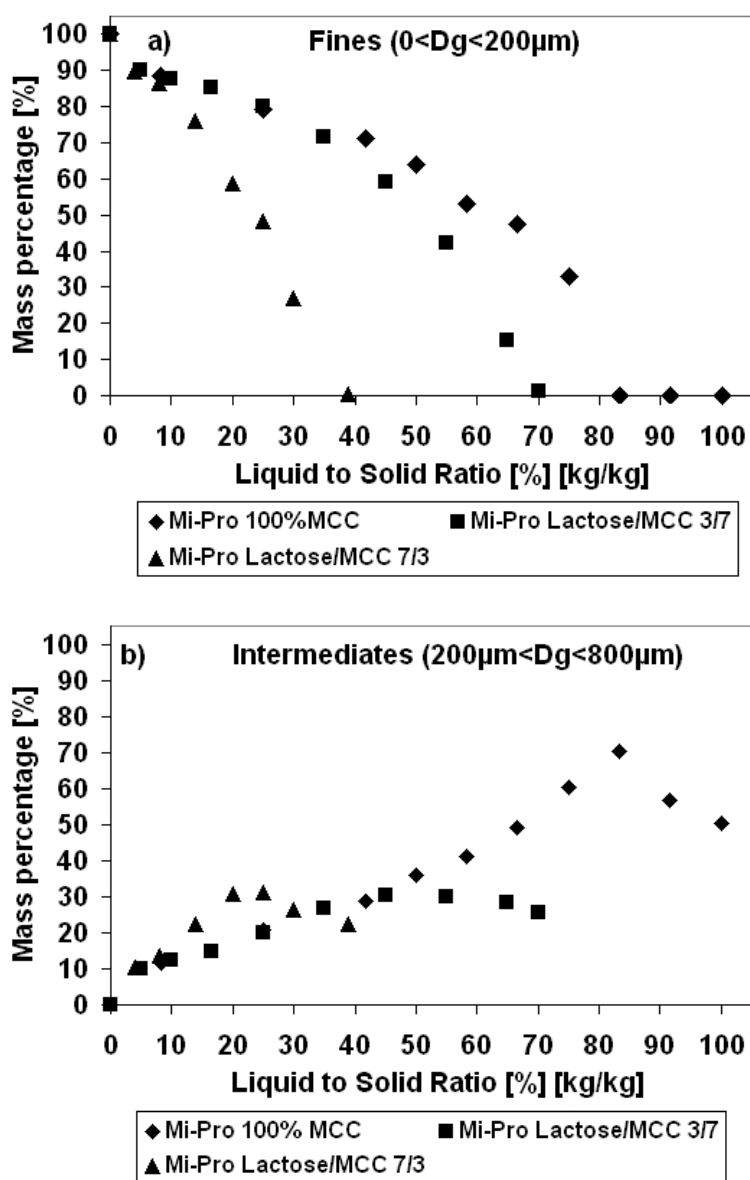


Figure 6. Torque curves on the Mi-Pro HSM for the Lactose/MCC 7/3 (a) and the Lactose/MCC 3/7 (b) formulations

Comparing the evolution of the characteristic size classes for the two studied formulations on the Mi-Pro high shear granulator and using the evolution obtained for 100% MCC as reference (Figure 7) we are able to confirm the interpretation of our torque curves: increasing lactose content in the mixtures decreases optimum water requirements and accelerates granule growth; changes in growth mechanisms occur for similar values of L/S ratio as observed in the torque curve (also confirmed by SEM observations).



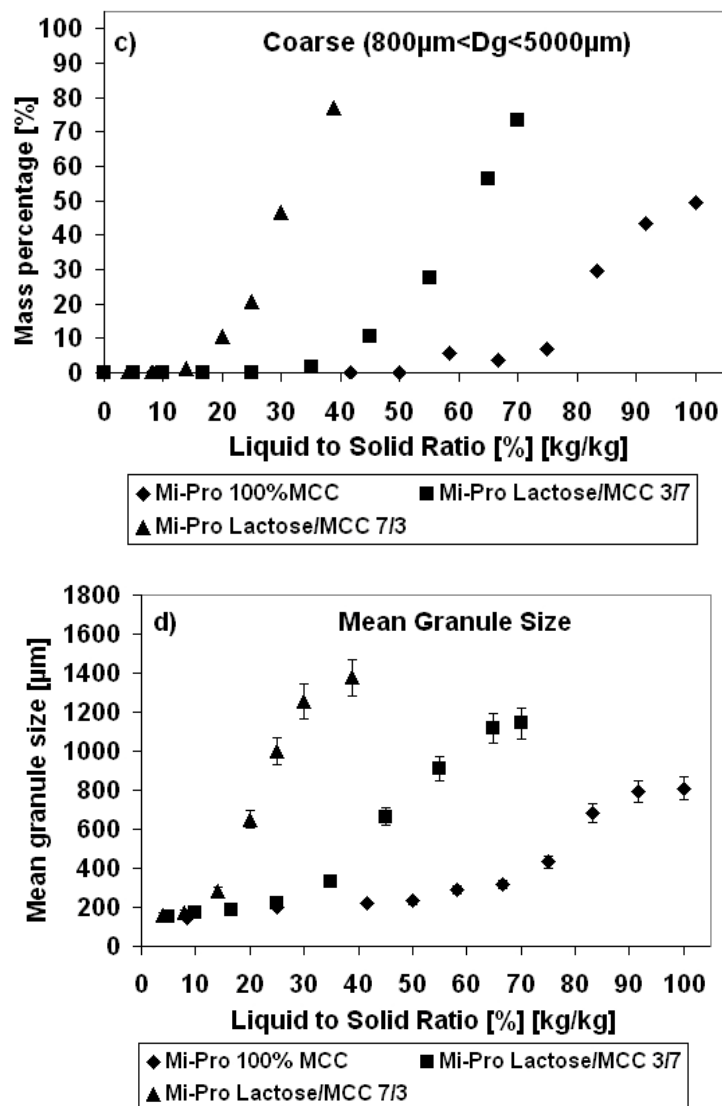


Figure 7. Evolution of fine (a), intermediate (b) and coarse(c) size classes and mean granule size for the studied formulations (d) using 100% MCC Avicel 105 as reference

After an initial wetting period ranging from 0 to 10% L/S ratio for the Lactose/MCC 7/3 formulation and from 0 to 15% for the Lactose/MCC 3/7 formulation when no significant changes in the granule size distributions are observed, nucleation occurs marked by a sudden decrease in the fine particle class mass percentage (Figure 7a) with initial particles presenting sufficient plasticity to unite into small nuclei of several initial particles.

The end of the nucleation stage can be observed as a change in the slope of the intermediate granules mass percentage (Figure 7b). For 100% MCC growth can be observed in two stages as a sudden increase in slope from 58% L/S ratio to 83% corresponding to the preferred agglomeration of fines and intermediates granules until the fines are depleted and as agglomeration between intermediates as a second stage between 83% and 100%. The intermediates particle class is never depleted as the high impeller and chopper speeds impose final granule sizes close to the upper boundary of the intermediates fraction (800 μ m).

For the Lactose/MCC 7/3 and Lactose/MCC 3/7 formulations nucleation occurs up to 20% L/S ratio and up to 40% respectively. Nucleation end can be observed as a peak in intermediate particle class (Figure 7b). This point corresponds to the beginning of the plateau region on the torque curves (Figure 6). Alternatively this point also corresponds to the apparition of the first coarse granules in the system (Figure 7c) explaining why the intermediate granules mass percentage slightly decreases and that for the mixtures growth occurs by simultaneous collision between fines and intermediates and also between intermediate granules.

For L/S ratios increasing beyond 38% for the Lactose/MCC 7/3 formulation and beyond 68% for the Lactose/MCC 3/7 formulation granules become overwettted and uncontrollable growth takes place. The optimum liquid requirement being well indicated by the end of the plateau on the torque curves. These results confirm the predictions made from torque curve analysis in terms of optimum liquid to solid ratio as well as separation between stages.

Figure 7d presents the evolution of the mean granule size as a function of L/S ratio. Given the extent of the coarse particle class (800 μ m to 4mm) the mean granule size follows a similar evolution to that of the coarse particle size class. It is also interesting to note that in order to obtain granules of a certain size less binder is necessary with decreasing MCC content. Mean granule size increases with increasing lactose percentage in the mixtures can be explained by the higher plasticity granted by the increased lactose content favoring coalescence between granules and also by the fact that upon drying granules containing MCC have been known to shrink (Kleinebudde et al [19]).

2.2.3 Morphology Evolution

SEM image analysis (Figures 8 and 9) allows us to better understand the before mentioned granulation mechanisms. For low L/S ratios we can see that no agglomerates are formed (Figure 8a and 9a). For increased L/S ratios nucleation (small agglomerates of several initial particles) can be observed, this seems to occur preferentially between MCC particles (Figures 8b and 9b) however it should also be noted the absence of fine lactose particles that most probably have went into solution.

Given the behavior observed on the water sorption isotherms with lactose presenting loosely bound water for low values of water activity it is also reasonable to suspect that nucleation is accelerated by the presence of lactose with MCC nuclei forming around lactose crystals. Figure 8c shows to that effect MCC particles sticking to the surface of the larger lactose particles. For the Lactose/MCC 3/7 formulation growth occurs in two stages that don't seem to have an impact on the characteristic sizes evolution, first we can observe the agglomeration of MCC nuclei into MCC granules (Figure 8d) for L/S ratios between 40 and 55% although they may still present a lactose core followed in a later stage by agglomeration between both MCC and lactose particles (Figure 8e). The same agglomeration between MCC granules and lactose particles can also be observed for the Lactose/MCC 7/3 formulation (Figure 8c). Final granules (Figure 8f and 9d) are spherical while initial particles, lactose crystals in particular, can still be observed.

The torque curves obtained on the Mi-Pro similar in nature to the pure MCC torque curve and SEM observations seem to imply that for both formulations MCC controls the liquid distribution in the wet mass. These findings seem to relate favorably with the findings of Kuentz and Leuenberger [20] who showed that for a binary mixture of MCC and paracetamol the percolation threshold for MCC was of about 20%, meaning that for values above 20% MCC forms a continuous network. The results also confirm the assumption made in the beginning of this study that MCC would control binder distribution based on the water sorption isotherms given the higher affinity of MCC for water.

Figure 10 shows the granule size distribution for pure MCC and the two studied formulations. No change in granule size distributions form with varying formulation is

observed. Increasing lactose content reduces the amount of finer particles and shifts the distributions to larger sizes. The larger amount of fines with increasing MCC content could also be a function of MCC shrinkage upon drying which was also observed by Kristensen et al [1].

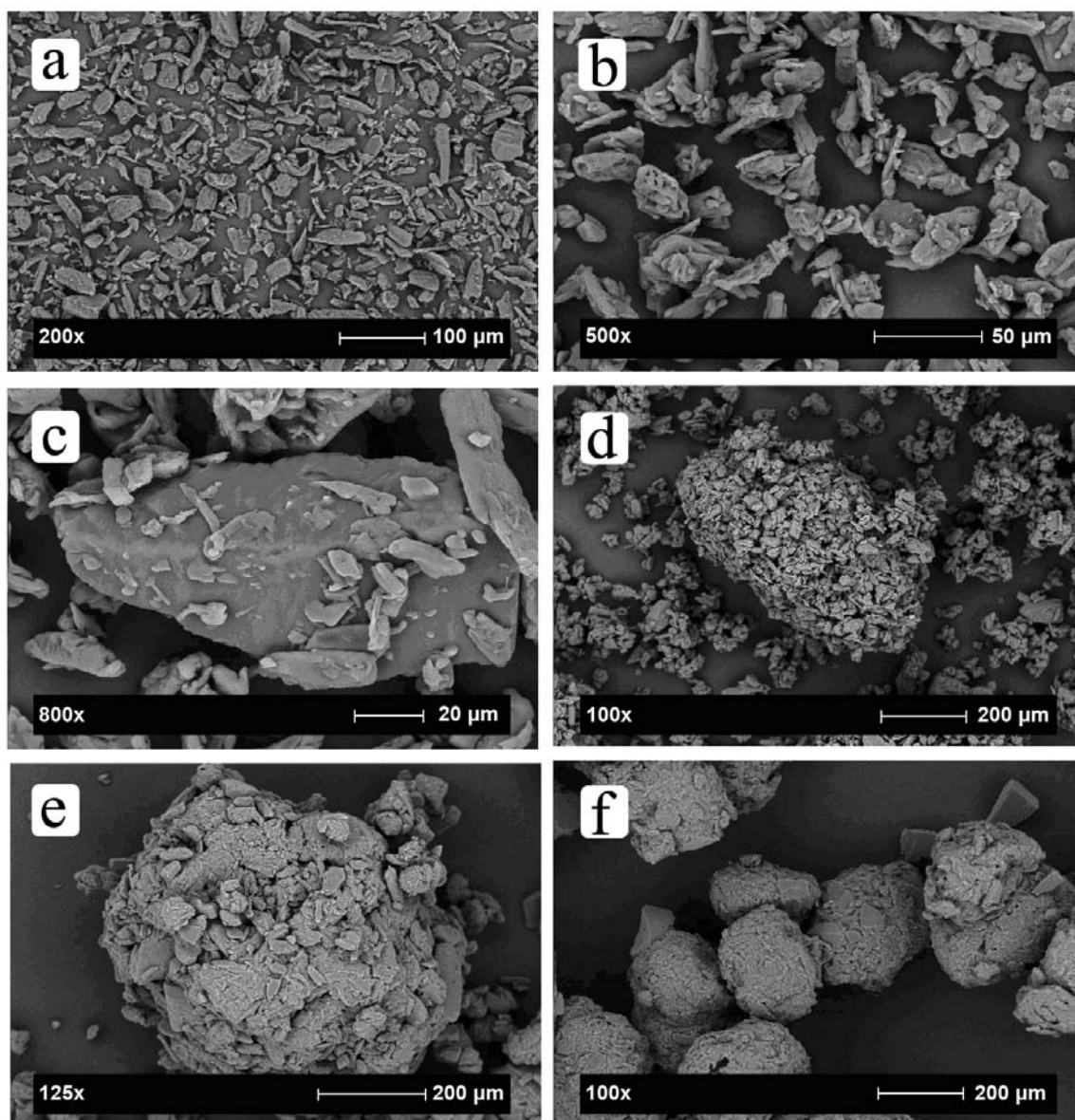


Figure 8. SEM images of agglomerates at different L/S ratios for the Lactose/MCC 3/7 formulation: (a) wetting (L/S=15%), (b) nucleation (L/S=25%), (c) MCC particles sticking on lactose particles (L/S=25%), (d) growth (L/S=40%), (e) growth (L/S=55%), (f) final granules (L/S=68%)

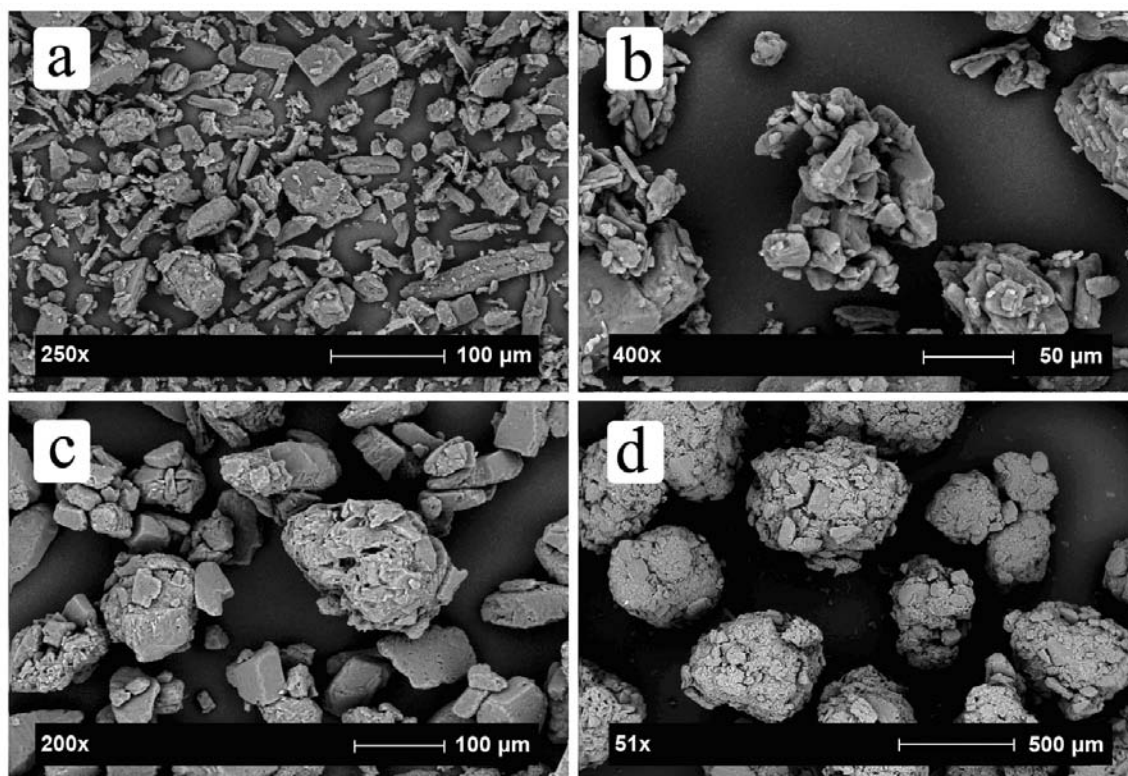


Figure 9. SEM images of agglomerates at different L/S ratios for the Lactose/MCC 7/3 formulation: (a) wetting (L/S=10%), (b) nucleation(L/S=16%), (c) growth (L/S=32%), (d) final granules (L/S=38%)

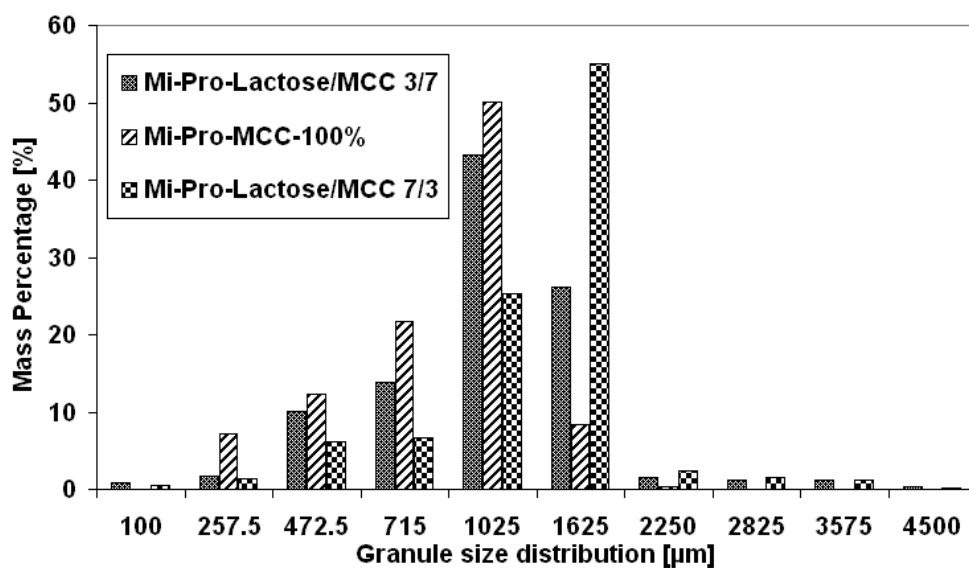


Figure 10. Granule size distribution for the two studied formulations as well as 100% MCC

2.3 Granule Strength

Granule strength has been assessed by two methods in an effort to describe both wet and dry granules: wet mass consistency measurements, for the wet end granules and uniaxial compression tests, for the end dry granules. Similar values of wet mass consistency have been obtained for the two formulations only pure MCC showing a noticeably larger wet mass consistency Table(1). In terms of granule strength we observe increase in mean dry granule strength with increasing MCC content. The opposite is observed when looking at the displacement (Figure 11) as the formulation Lactose/MCC 7/3 shows larger displacements values up to the fracture point indicating an increased plasticity of the granules.

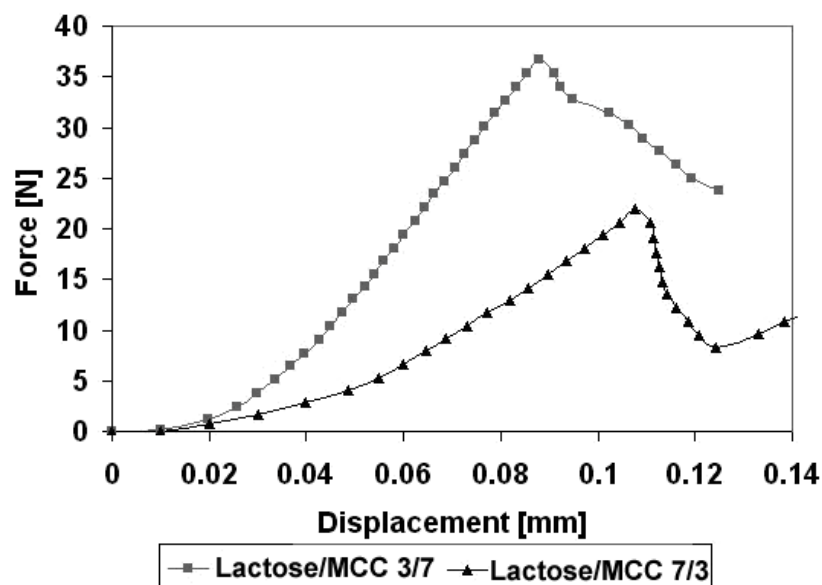


Figure 11. Force-displacement curves for the Lactose and MCC formulations

Product	Wet mass consistency [N.m/kg]	Granule strength [MPa]
Lactose/MCC 7/3	3.1 ± 0.7	18.1 ± 3.3
Lactose/MCC 3/7	4.1 ± 0.7	26.5 ± 5.5
100% MCC	8.2 ± 1.5	32.1 ± 5.8

Table 1. Wet mass consistencies and dry granule strengths for the two studied formulations and pure MCC ((Mi-Pro, $w=800$ rpm, $ch=3000$ rpm)

2.4 Effect of Mixer Design

Effect of mixer design was evaluated by applying constant impeller tip speed (Equation III-3-4) and constant Froude number (Equation III-3-5). These rules gave two corresponding impeller speeds on the Diosna: 460 rpm (impeller tip speed) and 605 rpm (Froude). The same fill ratios, granulation time, optimum L/S ratios have been kept while using a manually controlled drop by drop pump on both high shear mixers. The chopper on the Diosna has not been operated while the chopper on the Mi-Pro was turning at 3000 rpm.

In term of impeller tip speed we keep an impeller tip speed of 5.85 m/s while passing to the Diosna while the constant Froude number gives an impeller tip speed of 7.72 m/s.

Mean granule size analysis (Figure 12a and 12b) shows that both scale up rules yield lower mean granule sizes on the Diosna than on the Mi-Pro. In this Figure ITS is indicative of the scale-up rule used meaning impeller tip speed while Fr is indicative of the Froude number being used as scale-up rule. Also the granule size distributions present a more pronounced bi-modality showing a larger proportion of fine particles on the Diosna. This could be related to differences in binder addition method. While on the Mi-Pro the binder flow is directed towards the chopper in order to ensure better binder distribution on the Diosna binder addition with a capillary twice as large and binder flow can not be directed towards the chopper. The difference in granule size distribution can be explained by the formation of lumps (granules with sizes above 5 mm) representing about 10% of the mass despite the high impeller speeds on the Diosna (while on the Mi-Pro virtually no lumps are formed). The impeller tip speed yields a closer result in terms of granule size (Table 2) it shears and impacts less the wet granule reducing to a lesser extent mean granule size than when keeping the Froude number constant. It should also be noted that while for the Lactose/MCC 3/7 formulation scale-up rules produce roughly the same results with differences in final mean granule size inferior to 8%, the lactose formulation is more sensitive to changes in impeller speed: at constant impeller tip speed we observe a decrease in mean granule size of 9.2% and at constant Froude number of 17.7%. Usual variations in granule size between batches in the same operating conditions

have been between 3 and 10%. The difference in mean granule size is probably not a function of increased breakage occurring in the Diosna but rather a result of the formation of lumps giving an inhomogeneous binder distribution. From a morphological point of view, SEM observations presented in Figure 13 have not allowed us to identify differences in growth mechanisms between the two scales.

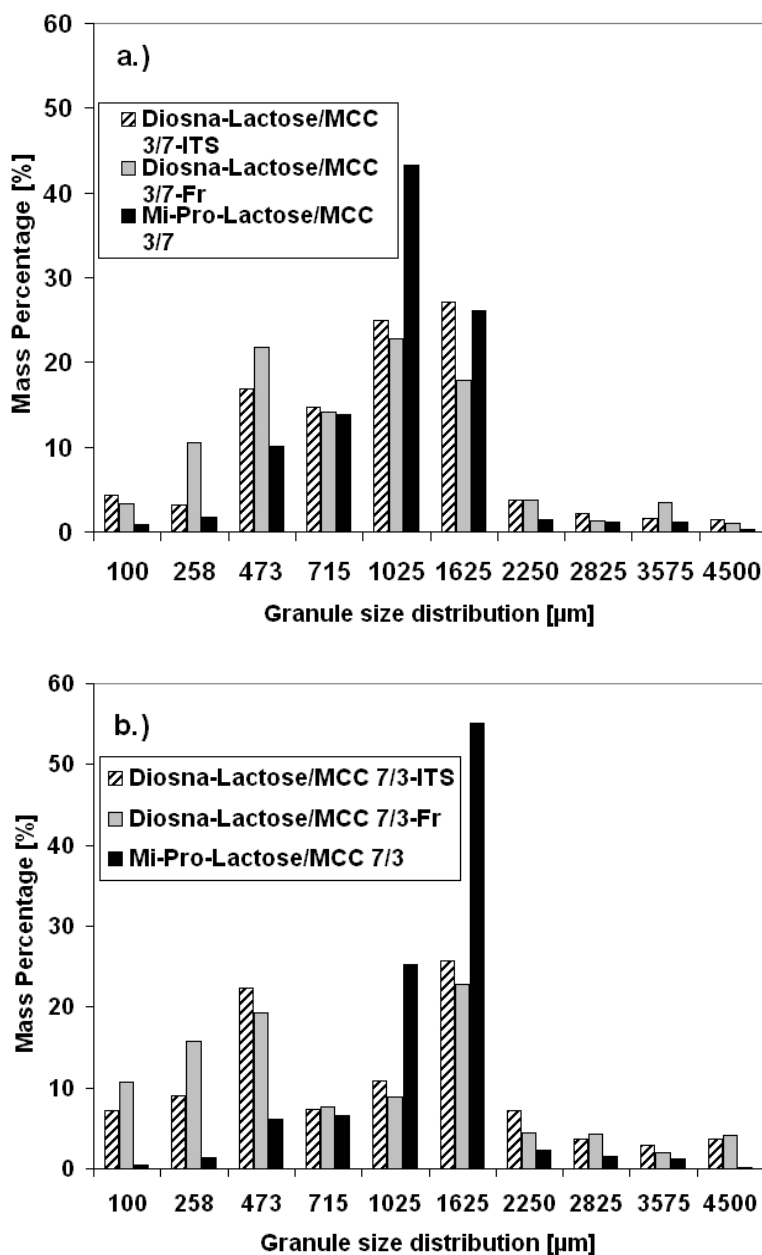


Figure 12. Granule size distributions for the (a) Lactose/MCC 3/7 formulation and (b) Lactose/MCC 7/3 formulation

Setup	D_{pm} [μm]
Mi-Pro	
Lactose/MCC 3/7	1142
Lactose/MCC 7/3	1376
Diosna - Impeller tip speed	
Lactose/MCC 3/7	1162
Lactose/MCC 7/3	1249
Diosna-Froude	
Lactose/MCC 3/7	1050
Lactose/MCC 7/3	1132

Table 2. Mean granule size for the studied formulations on the two high shear mixers: Mi-Pro and Diosna

Table 3 presents the recorded wet mass consistency values and dry granule strength measurements for the experiments on both scales for the studied formulations. We observed a higher consistency for the Lactose/MCC 3/7 formulation than the Lactose/MCC 7/3 formulation indifferent of the scale used with wet mass consistency decreasing on the large scale. For the large scale (Diosna) we observed that increasing impeller speed also increases wet mass consistency and although values remain fairly close it is not unreasonable to imagine that increased impeller speed squeezes more binder to the granule surface. Dry granule strength is found to decrease on the Diosna for both formulations regardless of scale-up rule used. However increasing impeller speed on the Diosna increases dry granule strength and as a consequence we can say that using the Froude number as scale-up rule gives a better agreement in terms of mean dry granule strength. For the case of the Lactose/MCC 7/3 formulation mean granule size is halved upon scale-up. We attributed this phenomenon to a preferential agglomeration of the MCC particles in the lumps formed on the Diosna. Because of this the granules tested poor in MCC content show lower mean granule strength.

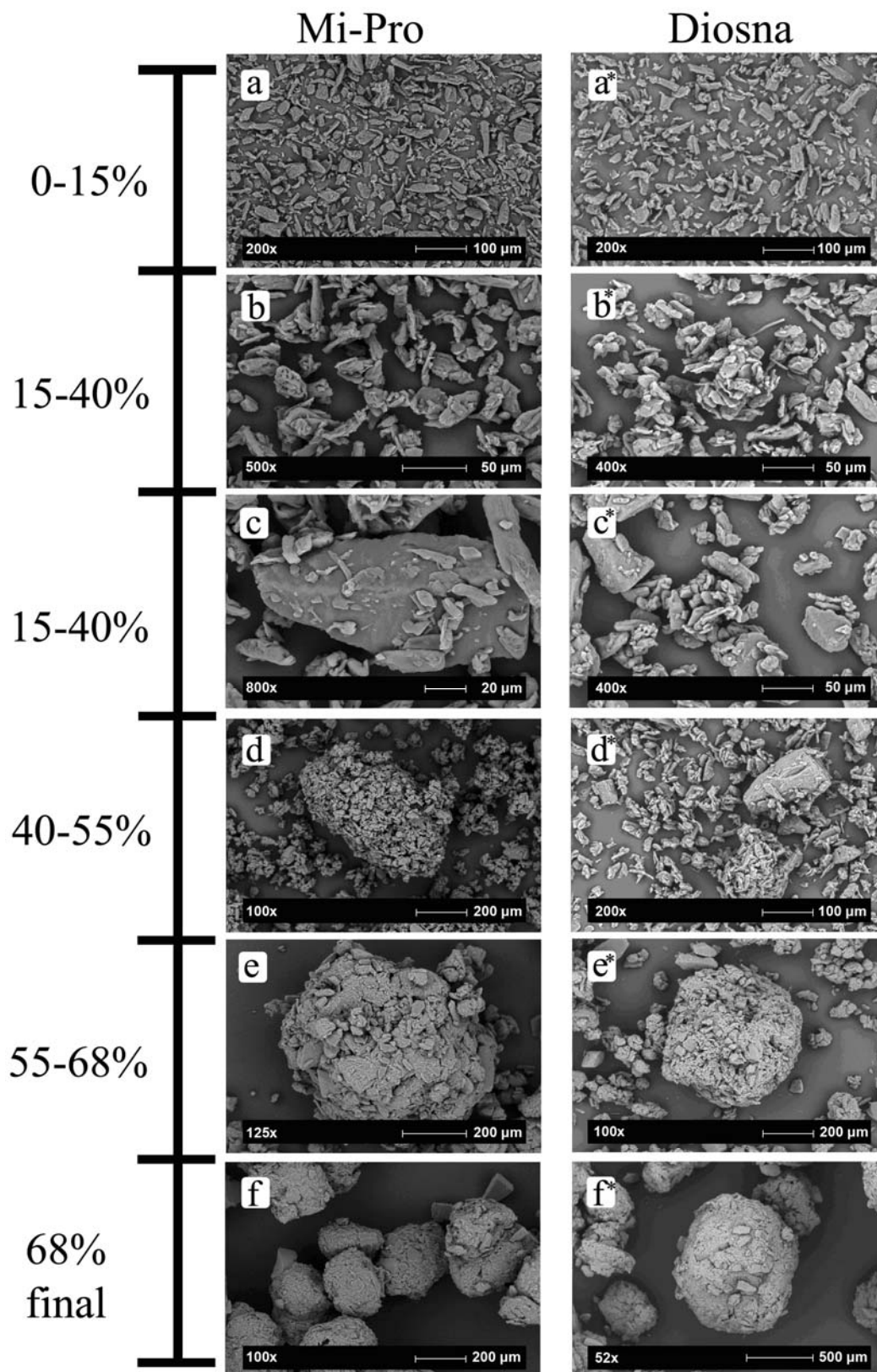


Figure 15. Growth mechanisms on the Mi-Pro (a-f) and Diosna (a*-f*) HSM for the Lactose/MCC 7/3 formulation

Product and Setup	Wet mass consistency [N.m/kg]	Granule strength [MPa]
Mi-Pro Lactose/MCC 7/3	3.1 ± 0.7	18.1 ± 3.3
Diosna (Fr=ct) Lactose/MCC 7/3	3.0 ± 0.7	10.1 ± 2.0
Diosna (ω=ct) Lactose/MCC 7/3	2.8 ± 0.7	8.9 ± 2.0
Mi-Pro Lactose/MCC 3/7	4.1 ± 0.7	26.5 ± 5.5
Diosna (Fr=ct) Lactose/MCC 3/7	3.8 ± 0.8	24.5 ± 6.0
Diosna (ω=ct) Lactose/MCC 3/7	3.6 ± 0.9	21.5 ± 4.1

Table 3. Wet mass consistencies and dry granule strengths for the different formulations on the Mi-Pro and the Diosna high shear mixers

3. Conclusion

Our study has shown that torque curves obtained during granulation can allow good control of the granulation process for the different formulations studied. Torque curves allow following agglomeration mechanisms at the macro scale which were confirmed by scanning microscope analysis and granule growth kinetics. The water sorption isotherms have shown a greater affinity of MCC for water vapor than lactose and this behavior is recognized in the granulation mechanism of the two formulations where binder distribution is conditioned by MCC. The same water sorption isotherms seem to indicate that water becomes loosely bound at particle surface quicker for lactose than for MCC. This could explain the shorter wetting periods for increasing lactose content as well as the accelerated growth associated. The proposed growth mechanism seemed to be independent of the scale used to for investigation.

From a wet mass consistency and dry granule strength the Lactose/MCC 3/7 formulation showed both higher consistencies and higher dry granule strength on both scales, with the difference being greater in terms of dry granule strength than in terms of wet mass consistency. For the Lactose/MCC 7/3 formulation dry granules are more deformable, granules supporting greater irreversible deformation until fracture appears.

The effect of mixer design studied by scaling up from the 1.9 Mi-pro to the 6L Diosna high shear mixer showed a better agreement in terms of mean granule size when using the impeller tip speed as scale-up rule. However this agreement seems of a lesser

importance when analyzing granule size distributions. Both scale-up rules yield a higher percentage of lumps and fine particles presenting significantly different granule size distributions from the ones obtained on the smaller scale. This could be explained by differences in binder addition and dispersion systems between the scales. Both wet mass consistency and dry granule strength for the studied formulations decreased upon scale-up with the difference being however more accentuated in terms of dry granule strength.

References

1. J. Kristensen, T. Schæfer, P., Kleinebudde, Direct Pelletization in a Rotary Processor Controlled by Torque Measurements. II: Effects of Changes in the Content of Microcrystalline Cellulose, *AAPS Pharmsci* 2(3) article 24 (2000)
2. J. Kristensen, P. Holm, A. Jaegerskou, T. Schæfer, Granulation in high speed mixers Part4: effect of liquid saturation on the agglomeration, *Pharm. Ind.* 46 (1984) 763-767
3. C. Vecchio, G. Bruni, A. Gazzaniga, Preparation of Indobufen Pellets by Using Centrifugal Rotary Fluidized Bed Equipment Without Starting Seeds, *Drug Dev. Ind. Pharm.* 20 (12) (1994) 1943-1956
4. P. Holm, M. Bonde, T. Wigmore, Pelletization by granulation in a roto-processor RP-2-Part 1: Effect of process and product variables on granule growth, *Pharm. Technol.* 8 (1996) 22-36
5. H.L. Leuenberger, M. Puchkov, E. Krausbacher, G. Betz, Manufacturing pharmaceutical granules: Is the granulation end-point a myth, 3rd Int. Granulation Workshop Sheffield (2007)
6. G. Betz, P. J. Burgin, H. L. Leuenberger, Power consumption profile analysis and tensile strength measurements during moist agglomeration, *Int. J. Pharm.* 252 (2003) 11–25
7. M. B. Mackaplow, L. A. Rosen, J. N. Michaels, Effect of primary particle size on granule growth and endpoint determination in high-shear wet granulation, *Powder Technol.* 108 (2000) 32-45
8. R.L. Carr, Evaluating flow properties of solids, *Chem. Eng.* 18 (1965)163-168
9. J. Schwedes, Testers for measuring flow properties of particulate solids, *Powder Handling and Processing* Vol. 12 (4) (2000) 337-354
10. R. C. Rowe, Characterization of wet powder masses using a mixer torque rheometer. 4. Effect of blade orientation, *Int. J. Pharm.* 133 (1996) 133-138
11. P. Luukkonen, T. Schæfer, L. Hellen, A. M. Juppo, J. Yliruusi, Rheological characterization of microcrystalline cellulose and silicified microcrystalline cellulose wet masses using a mixer torque rheometer, *Int. J. of Pharm.* 188 (1999) 181–192
12. P. Kleinebudde, The crystallite-gel-model for microcrystalline cellulose in wet granulation, extrusion and spheronization, *Pharm.Res.* 14 (1997) 804-809
13. J.S. Ramaker, Fundamentals of high shear pelletisation process - PhD thesis, Rijksuniversiteit Groningen (2001)
14. M.J. Adams, M.A. Mullier, J.P.K. Seville, Agglomerate strength measurement using a uniaxial confined compression test, *Pow. Tech.* 78 (1994) 5-13
15. F. Rouquerol, J. Rouquerol, S. King, Adsorption by powders and porous solids: Principles, methodology and applications, Academic Press (1999)
16. T.M. Chitu, D. Oulahna, M. Hemati, Wet granulation in a laboratory scale high shear mixer: Effect of chopper presence, design and impeller speed, 9th Int. Symposium on Agglomeration Sheffield (2009)
17. M. Benali, Prédiction des interactions substrat/liant lors de la granulation: Etude expérimentale dans un mélangeur granulateur à fort taux de cisaillement- Approches thermodynamiques par simulation moléculaire, PhD thesis, INP Toulouse (2006)
18. A; Goldszal, J. Bousquet, Wet agglomeration of powders: from physics toward process optimization, *Pow. Tech.* 117 (2001) 221-231
19. P. Kleinebudde, Shrinking and swelling properties of pellets containing microcrystalline cellulose (MCC) and low substituted hydroxypropylcellulose (L-HPC). I. Shrinking properties, *Int. J. Pharm.* 104 (1994) 209-219
20. M. Kuentz, H. Leuenberger, A new theoretical approach to tablet strength of a binary mixture consisting of a well and a poorly compactable substance, *Eur. J. of Pharm. and Biopharm.* 49 (2000) 151-159

Synopsis et Points Clés de l'Etude

Le chapitre I

Dans ce chapitre, on a présenté une synthèse bibliographique montrant les bases de la granulation humide ainsi que les derniers progrès enregistrés dans ce domaine. Nous avons décrit les connaissances à ce jour au niveau de l'influence des paramètres opératoires et des matières premières ainsi que les outils de contrôle et de suivi généralement appliqués.

À partir de cette synthèse bibliographique, on constate que:

- L'effet des paramètres opératoires sur les mécanismes de croissance est fortement dépendant du produit et du matériel utilisé et que la prédiction des comportements lors de la granulation à partir des caractéristiques physico-chimiques des constituants est peu décrit. L'effet des conditions opératoires peut être décrit par des modèles mécanistiques basés sur le couple, les bilans de population ou la carte de régimes de croissance.
- La granulation humide présente une grande complexité avec des facteurs interdépendants et difficiles à hiérarchiser et une grande variabilité des matières premières. Des mécanismes communs ont pu être définis et le processus divisé comme une succession de trois étapes: (i) mouillage et nucléation, (ii) consolidation et croissance par coalescence et (iii) rupture et attrition. Néanmoins la prédominance d'un mécanisme sur les autres est difficile à prédire et la plupart des études sont consacrés à l'investigation d'un seul mécanisme prédominant.
- Des études systémiques (Vialatte [2], Oulahna [47], Rahmanian[74], Benali [75]) permettent d'établir des liens entre les paramètres opératoires, les propriétés physico-

chimiques des matières premières et la qualité du produit final (taille, distribution de tailles, porosité, résistance mécanique).

- La définition de la quantité optimale du liant est une étape clef de la granulation. Elle dépend surtout de l'opérateur et des propriétés recherchées dans le produit final. Ce phénomène induit des grandes variations lors de la généralisation des effets observés lors de la granulation humide. Il est impératif d'avoir une définition et une optimisation robuste à mettre en place permettant ainsi de réduire l'influence d'un paramètre qui peut apporter des changements importants dans les propriétés finales du produit.
- La mesure du couple (ou de la puissance consommée) est une technique établie permettant de prédire le comportement lors de la granulation. Néanmoins, la définition selon laquelle la quantité optimale de liant (pour la granulation des produits pharmaceutiques) correspond au plateau du profil de couple (puissance) reste discutable. En plus le lien entre l'évolution du couple et les propriétés de la masse humide reste un sujet actuel. Différents auteurs ont relié l'évolution du couple (puissance consommée) à la saturation liquide, la porosité intragranulaire, la friction interparticulaire ou la résistance mécanique.
- Le rhéomètre à couple peut être employé pour apporter plus d'information au niveau d'interactions poudre - liant. Il permet de faire un lien entre les différentes échelles d'étude à travers une propriété de la masse humide appelé consistance humide ou pseudo viscosité. À notre connaissance, le lien de l'évolution du couple sur le rhéomètre MTR avec les mécanismes observés lors de la granulation n'a jamais été abordé sous l'angle "lien entre masse humide, consistance et tenue mécanique à sec".
- Les travaux bibliographiques traitant de l'influence de la viscosité du liquide (ou phase liante) sur la croissance particulaire sont controversés. Ce paramètre gouverne le temps de l'étalement du liquide à la surface du solide à granuler et affecte par ailleurs les forces d'interactions entre les particules mouillées. Sur ce dernier point, deux écoles se distinguent : la première privilégiant les propriétés de mouillage (tension de surface et angles de contact solide-liquide) et leur rôle dans les forces capillaires et la seconde école mettant en avant les phénomènes de dissipation

visqueuse lors des collisions entre particules et leur impact sur les mécanismes et cinétiques de granulation.

L'enjeu de notre travail réside dans une approche systémique basée sur le liens entre: influence des paramètres opératoires, technologie employée et propriétés physico-chimiques des matières premières grâce à un suivi rhéologique, morphologique et mécanique.

Le chapitre II

Le chapitre 2 regroupe l'ensemble des techniques de caractérisation employées, les méthodologies utilisées dans l'étude, les propriétés physico-chimiques des matières premières, les méthodes mises en place pour la caractérisation des granules issus du procédé de granulation humide ainsi que les granulateurs utilisés.

Les poudres utilisées lors de cette étude sont la cellulose microcristalline et le lactose. Ces deux excipients sont souvent rencontrés dans les opérations de mise en forme pour la fabrication des comprimés pharmaceutiques. La principale poudre de l'étude est la cellulose microcristalline « Avicel 105 » présentant une forte cohésion et un faible degré de coulabilité. Pour comparaison, certains essais sont menés avec la cellulose microcristalline « Avicel 101 » présentant une moindre cohésion et une meilleure coulabilité. Pour l'étude des mélanges binaires, le lactose a été utilisé comme deuxième excipient.

Les liants utilisés sont des solutions aqueuses de Polyvinylpyrrolidone (PVP) et hydroxyméthylpropylcellulose (HPMC), liants habituellement utilisés dans l'industrie pharmaceutique. Les concentrations en solution choisies nous ont permis de moduler la tension superficielle du liant, sa viscosité et l'angle de contact avec la poudre.

La tenue mécanique des granules peut être caractérisée soit à l'état humide en déterminant la consistance de la masse humide dans un rhéomètre à couple, soit à l'état sec par compression directe des grains individuels. La distribution granulométrique et la taille moyenne sont établies par tamisage. Trois classes granulométriques sont définies pour

décrire la cinétique de granulation : la classe de fines correspondant aux particules initiales, la classe intermédiaire avec des agglomérats de faible résistance mécanique et la classe des grosses particules.

Au niveau du procédé, l'échelle principale de l'étude est le granulateur à haut taux de cisaillement instrumenté Mi-Pro Pro-cepT[®] avec un bol de 1.9 litres. Afin d'étudier l'influence des géométries et des échelles du procédé, des essais ont été réalisés dans un Mi-Pro avec bol de 0.9 litres et dans un granulateur à haut cisaillement Diosna[®] de 6 litres.

Le chapitre III

Ce chapitre présente l'essentiel de nos essais expérimentaux. Vu la diversité des conditions opératoires étudiées et des propriétés physico-chimiques des matières premières, on a choisi de présenter dans le *sous-chapitre III.1* un exemple type de granulation humide.

Les conditions opératoires sont typiques pour un essai de granulation à haut taux de cisaillement dans le granulateur Mi-Pro de 1.9 litres sont : une vitesse de la pale d'agitation de 800 tr/min, une vitesse de l'émetteur de 3000 tr/min, une addition progressive du liant et un temps de granulation de 12 minutes pour assurer une bonne distribution du liant (addition du liant en jet à travers un tube capillaire de 400 microns vers l'émetteur). Le couple solide - liquide étudié est la cellulose microcristalline Avicel 105 granulée avec de l'eau ultra-pure.

Les mécanismes et la cinétique de croissance ainsi que l'évolution des courbes de couple sur le mixer torque rhéomètre (MTR) et le granulateur instrumenté Mi-Pro sont discutés. La caractérisation morphologique des granules (distribution de tailles, observations MEBE) nous permet d'identifier les mécanismes de croissance en fonction de la quantité de liant introduite (rapport liquide/solide) et de les relier à l'évolution du couple sur le Mi-Pro. Ainsi, on peut identifier les étapes de mouillage, nucléation et croissance : par enrobage de fines particules initialement, puis par coalescence des particules intermédiaires et sur-mouillage. Une quantité de référence de liant correspondant à un

rapport liquide solide (L/S) de 100% a été définie. La même méthodologie va être mise en place pour définir les quantités optimales de liant pour tous les autres essais.

La comparaison des évolutions du couple dans le rhéomètre (MTR) et le granulateur (Mi-Pro) montre des similitudes ainsi que des différences qui sont discutées. La partie initiale des courbes (pour de faibles valeurs du rapport liquide solide) montre une évolution similaire décrivant le mouillage et la nucléation. Pour des valeurs du rapport L/S élevées, la différence entre la conception de ces deux réacteurs devient évidente :

- sur le Mi-Pro, les granules commencent à se former et grandir par enrobage/coalescence avec des particules plus fines. Ce fait se traduit par un plateau sur l'évolution du couple. Dès que les agglomérats présentent un excès d'eau à la surface, des particules fines vont s'y déposer. Ce phénomène se traduit par une légère augmentation de la taille des agglomérats et peu d'adhésivité à la surface des grains; ce qui donne un plateau au niveau du profil rhéologique.
- sur le MTR, une agitation plus intense et un réacteur confiné imposent une accélération des mécanismes de croissance et vont unir les agglomérats dans une pâte. Ce fait, se traduit par une forte augmentation du couple vers un pic où la cohésion de cette pâte est maximale pour une valeur du rapport L/S de 150% (cas de nos poudres).

À la fin de la région du plateau (sur le Mi-Pro), la totalité des particules fines a été consommée et l'agglomération continue par coalescence des granules. Les granules présentent une couche liquide à la surface et vont s'agglomérer dans des structures de tailles plus importantes avec le risque de sur-mouiller la poudre. Il est possible de continuer la granulation jusqu'à une valeur de 100% du rapport L/S sans risquer le sur-mouillage en favorisant le pourcentage des gros agglomérats. Pour des valeurs supérieures, la prise en masse du système a lieu et des amas de produit se forment en donnant une pâte. A ce stade, on observe sur le Mi-Pro un signal du couple similaire au signal identifié au MTR pour la même valeur du rapport L/S. Pour des valeurs supérieures à 150% du rapport L/S, une pâte va se former dans les deux réacteurs étudiés. Les forces beaucoup plus grandes, présentes sur le MTR, sont observées à travers la valeur du couple normé par la masse initiale. A ce niveau, les valeurs du couple normé sont six fois plus grandes sur le MTR que sur le Mi-Pro.

L'évolution de la consistance humide des granules issus du Mi-Pro pour différents rapports L/S a été étudiée sur le MTR. Ceci nous a permis de confirmer l'augmentation de l'adhésivité des granules dans le Mi-Pro une fois que les particules fines ont été consommées. Les collisions granules-paie, granules-parois et granules-granules font ressortir une couche de liant à la surface.

Les essais de compression directe des grains individuels mettent en évidence les conclusions suivantes:

- la courbe force-déplacement permet de suivre la déformation du grain jusqu'au moment où la première rupture du grain se produit,
- à partir de cette évolution force-déplacement, on peut calculer la résistance du grain (équation d'Adams et al. 1994), le module de Young (selon la méthodologie décrite par Mangwandi et al 2007), l'énergie de compression (aire sous le pic) et l'énergie de compression spécifique (aire sous le pic divisé par la surface de contact). Les paramètres force de rupture et énergie de compression, qui ne sont pas reliés par le calcul à la taille du grain, montrent une croissance linéaire avec la taille du grain étudié (entre 450 et 1800 μm). Une relation de linéarité croissante apparaît entre la taille granulaire (de 450 à 900 μm), la résistance, le module de Young et l'énergie de compression spécifique. Pour des tailles de grain élevées, une stabilisation de ces paramètres est observé. Ceci est considéré comme indicateur d'une différence morphologique entre les grains inférieurs à 900 μm et les grains supérieurs. En effet, l'analyse morphologique de la sphéricité des granules a montré que les particules inférieures à 900 μm présentent une sphéricité plus faible. Ce phénomène peut être relié aux fortes contraintes présentes dans le mélangeur à haut cisaillement et l'hypothèse que les particules inférieures à 900 μm sont des fragments des agglomérats plus grands.

Le sous-chapitre III-2 porte sur l'effet des variables opératoires ainsi que la granulation sur deux bols différents du mélangeur à haut cisaillement Mi-Pro. Le même couple poudre-liant a été gardé: cellulose microcristalline « Avicel 105 » granulée avec de l'eau

ultra-pure. Par ailleurs, un essai a été réalisé avec la cellulose « Avicel 101 » moins cohésive.

Les variables retenues dans cette étude sont le taux de remplissage, la vitesse d'agitation et la présence et conception de l'émetteur. Le taux de remplissage et la présence et conception de l'émetteur sont des paramètres peu étudiés dans la littérature spécifique. En revanche, la vitesse d'agitation est un des paramètres les plus étudiés. La totalité des travaux référencés montrent l'influence de ce paramètre sur la qualité finale du produit et les mécanismes de croissance.

Trois taux de remplissage ont été étudiés et exprimés en pourcentage par rapport au volume occupé par la poudre initiale sèche dans le granulateur : 16, 26 et 32%. L'influence de ces taux de remplissage a été étudié pour trois valeurs d'agitations différentes : 100, 400 et 800 tr/min avec l'émetteur tournant à 3000 tr/min et un temps de granulation de 12 minutes. Les valeurs de la vitesse d'agitation ont été considérées indicatives pour conditions de faible cisaillement, intermédiaire et haut. Pour des valeurs du taux de remplissage supérieures à 32%, on rencontre une limite du granulateur au niveau du couple maximal enregistrable lors de rapports L/S supérieurs à 100%. Les valeurs, du taux de remplissage, inférieures à 16% n'ont pas été étudiées. La haute vitesse d'agitation (800 tr/min) projette du produit sur le couvercle et les parois du granulateur; ce phénomène a des effets plus importants pour les faibles taux de remplissage comme le 16% provoquant le sur mouillage du système.

L'ensemble des essais sur les différents **taux de remplissage** nous a permis de tirer les conclusions suivantes :

- pour 100tr/min, les courbes de couple montrent une différence au niveau de l'étape de mouillage et de nucléation entre le taux de remplissage de 16 et 32% en temps que le taux de remplissage (\emptyset) de 26% présente un comportement intermédiaire étape de mouillage et nucléation similaire avec $\emptyset=16\%$ et étape de croissance similaire avec $\emptyset=32\%$. Les différences peuvent être expliquées par l'effet de l'émetteur qui pour une faible vitesse d'agitation, à faibles rapports L/S, peut favoriser l'agglomération en améliorant la distribution du liant par la rupture des amas formés. Cet effet est quand même dépendant du contact entre l'émetteur et le lit de poudre. On peut imaginer ce

contact comme décroissant avec le taux de remplissage. D'une manière qualitative, on a démontré l'importance du contact entre l'émetteur et le lit de poudre lors de l'étude de la conception de l'émetteur : un émetteur légèrement plus court va favoriser la formation des particules plus grandes (même amas).

- les valeurs du couple en fin de granulation, les distributions granulométriques et la taille finale des particules, sont similaires entre les différents taux de remplissage avec une très légère augmentation avec le taux de remplissage.
- pour 400 tr/min, on n'a pas observé des effets du taux de remplissage sur les courbes de couple ou les distributions granulométriques. La même évolution croissante au niveau de la taille moyenne finale des granules avec le taux de remplissage est observée.
- pour 800 tr/min, on observe le sur-mouillage pour le taux de remplissage de 16% (aussi observable par une région de plateau plus courte sur les courbes de couple), les résultats au niveau de la taille moyenne finale sont similaires pour 26 et 32% avec une légère augmentation de la taille avec le taux de remplissage.
- les mesures de consistance humide montrent des valeurs similaires entre les différents taux de remplissage et les différentes vitesses d'agitation (sauf le couple 800 tr/min, $\emptyset=16\%$).
- les mesures de tenue mécanique, des grains individuels, montrent une augmentation de la résistance en passant du taux de remplissage 16 à 26%, puis une légère diminution de la résistance en passant de 26 à 32% pour 400 et 800 tr/min et pas d'effet pour 100 tr/min.

Au niveau de la **vitesse d'agitation, la présence et dimension de l'émetteur et géométrie de l'échelle**, on a étudié :

- l'effet de la vitesse d'agitation, avec et sans émetteur, sur la taille moyenne des granules ainsi que l'effet de la présence de l'émetteur sur la cinétique de granulation pour une vitesse d'agitation de 800 tr/min.

- l'influence de la conception de l'émoteur en utilisant un émoteur légèrement plus court sur le bol de 1.9L du Mi-Pro.
- l'influence de la vitesse d'agitation sur les courbes de couple et la cinétique de granulation avec l'émoteur tournant à 3000 tr/min.
- le cas particulier des vitesses intermédiaires (400 tr/min) pour MCC Avicel 105 et MCC Avicel 101.
- l'influence de la vitesse d'agitation sur la sphéricité et la tenue mécanique des granules.
- l'influence de la taille du bol du réacteur en comparant l'évolution de la taille moyenne des granules en fonction de la vitesse d'agitation sur les bols de 0.9 et 1.9L du Mi-Pro, influence sur la cinétique de granulation pour la même vitesse en bout de pale.

Les points clés qui ressortent de l'étude de la vitesse d'agitation et la présence et dimension de l'émoteur sont :

- sans émoteur, pour les faibles vitesses d'agitation, la formation des amas influence la granulation avec des pourcentages augmentant de 40 à 60% entre 100 et 400 tr/min. Pour des valeurs supérieures, la pale commence à rompre les amas et à 800 tr/min, on n'observe pratiquement plus d'amas et le diamètre final est similaire avec ou sans émoteur.
- la cinétique de granulation (évolution des classes caractéristiques et diamètre moyen) montre qu'à 800 tr/min, même si la taille finale de granules est similaire, l'émoteur à un effet retardateur sur la croissance des granules.
- la présence de l'émoteur à faible vitesse d'agitation (100 tr/min) va réduire la taille finale des granules et augmenter les valeurs de la courbe de couple pour les étapes de nucléation et croissance ; ce qui indique une augmentation de la densification de granules avec la présence de l'émoteur.

- pour une vitesse intermédiaire, l'utilisation d'un émotteur légèrement plus petit qui réduit le contact entre l'émotteur et le lit de poudre conduit à des granules d'une taille plus importante, moins homogènes.
- l'augmentation de la vitesse d'agitation va accélérer la croissance et réduire la taille finale des granules.
- l'investigation des courbes de couple permet de reconnaître les différentes étapes de granulation. Au niveau de la vitesse de 400 tr/min, on a observé une discontinuité au niveau de la nucléation et une chute de la courbe de couple pour la CMC Avicel 105. En réalisant le même essai avec la cellulose Avicel 101 (taille moyenne 60 μ m vs 20 μ m pour Avicel 105, même fournisseur, même indice de cristallinité), on observe une continuité de la courbe du couple. Ce phénomène peut être relié à la carte de régime de nucléation proposé par Hapgood [2003] : une taille plus faible peut donner une différence assez grande en terme de temps de pénétration, ce qui peut changer le régime de nucléation du régime intermédiaire (conditionné par les paramètres du procédé identiques pour les deux essais: même système d'addition de liant, même vitesse d'agitation) au régime de nucléation mécanique où la vitesse d'agitation va contrôler le processus de nucléation.
- la sphéricité des granules augmente avec la vitesse d'agitation jusqu' 400 tr/min puis décroît au moment où les forces d'impact et de cisaillement provoquent la rupture des agglomérats humides.
- la tenue mécanique des granules à l'état sec augmente avec la vitesse d'agitation d'une façon presque linéaire entre 100 et 800 tr/min. Pour des valeurs supérieures à 800 tr/min, on observe une légère diminution explicable par la prédominance du mécanisme de rupture sur le mécanisme de croissance et consolidation.
- la comparaison de la pression d'impact défini par Vonk et al [1997] avec la résistance à la traction des granules humide défini par Rumpf [1958] permet de prédire la vitesse d'agitation pour laquelle le mécanisme de rupture va devenir prédominant.
- D'une façon générale, l'évolution de la taille moyenne avec la vitesse d'agitation est similaire pour les deux échelles étudiées du Mi-Pro (0.9 et 1.9L). La vitesse en bout

de pale donne une bonne approximation pour la taille finale des granules entre les échelles. Néanmoins, d'un point de vue cinétique, la croissance des granules pour une vitesse en bout de pale donnée est accélérée par la granulation à l'échelle plus petite.

Le sous-chapitre III-3 traite l'influence des propriétés physico-chimiques du liant sur la rhéologie, les mécanismes et cinétiques de croissance, la consistance de la masse humide et la résistance mécanique des granules secs et l'influence de la technologie (granulation sur le Mi-Pro 1.9L et Diosna 6L). Les liants utilisés (solutions aqueuses de PVP et HPMC à différents pourcentages) nous permettent de varier la tension de surface, la viscosité et l'angle de contact. Ces caractéristiques ont été regroupées par deux termes : le travail d'adhésion et le nombre capillaire visqueux modifié.

L'influence de la technologie sur les propriétés finales des granules obtenus sur le Mi-Pro 1.9L et le Diosna 6L a été étudiée pour deux liants avec des propriétés fondamentales différentes de notre étude (eau -faible viscosité, grand travail d'adhésion et HPMC 3%-grande viscosité, travail d'adhésion plus faible). Le transfert d'échelle a été réalisé en gardant le même temps de granulation, le même débit spécifique, le même taux de remplissage et l'équivalence de la vitesse a été faite à travers le nombre de Froude ou de la vitesse en bout de pale. Néanmoins, des différences restent entre les échelles au niveau de la conception et de l'emplacement de l'émetteur et du système d'addition du liant.

Les différents faits marquants qui ressortent de cette étude d'influence des propriétés des solutions liantes sont :

- le rhéomètre décrit des évolutions similaires pour les différents liants (sauf HPMC3%). On a observé, néanmoins, que le pic augmente avec la viscosité de la solution (même au niveau des faibles viscosités). Pour la solution la plus visqueuse HPMC3%, on a observé le pic le plus grand et un passage différent avec une augmentation du couple avec une pente plus grande. Ce fait, indique qu'un sur mouillage peut se produire plus facilement avec ce liant ce qui a été confirmé avec des observations morphologiques lors des essais sur le Mi-Pro.

- la méthodologie décrite lors de l'exemple type nous a permis de définir la quantité optimale de liant pour les différents liants utilisés. D'une façon générale, même un faible ajout de polymère (PVP3%) qui ne change pas d'une manière significative la viscosité du liant va réduire le nécessaire du liant (de 100% à 83% rapport L/S). Ce qui montre que la présence de ces polymères favorise la coalescence des granules. La quantité optimale de liant reste constante à environ 83% rapport L/S pour des viscosités entre 1.3 mPa.s et 8.1 mPa.s, mais diminue à 77% pour une viscosité de 118 mPa.s.
- pour les solutions polymériques aqueuses, la fin de la région de plateau (ou zone de croissance) correspond assez bien à la quantité optimale de liant. Les courbes de couple nous ont permis de retrouver les différentes étapes de granulation et un bon contrôle du procédé. Les distributions de tailles pour les différents liants sont similaires.
- pour Ca^* inférieur à 0.8, on a observé que le travail d'adhésion est le paramètre dominant. Une réduction du travail d'adhésion réduit la tenue mécanique des granulés secs, ralentit la croissance des granules et réduit légèrement la taille des granules.
- pour Ca^* supérieur ou égal à 0.8, la viscosité est le paramètre dominant. La réduction de la viscosité ralentit la croissance des granules, réduit la taille des granules et la consistance humide.
- au niveau de la résistance mécanique des granulés secs, on a observé un effet de seuil au niveau de $Ca^* < 0.8$ pour lequel une chute de la résistance apparaît avec l'augmentation de la Ca^*
- une relation linéaire peut être établie entre la constante cinétique « K » et le travail d'adhésion pour les faibles viscosités. Une relation similaire peut être trouvée pour les grandes viscosités, mais le nombre limité des solutions visqueuses investiguées ne nous permet pas de conclure d'une manière définitive.
- Benali et al [2006] ont observé une limite similaire entre la prédominance des forces interfaciales respectivement visqueuses pour un nombre capillaire modifié autour de

l'unité. Cette différence peut être reliée à une viscosité plus faible nécessaire pour agglomérer les particules plus fines présentes dans notre étude.

- les distributions granulométriques sur le Diosna sont similaires entre elles et différentes de celles qui sont obtenues sur le Mi-Pro pour les deux liants et les deux règles de transfert d'échelle employés. La vitesse en bout de pale permet d'obtenir des tailles moyennes finales plus proches de celles qui sont obtenues sur le Mi-Pro. La résistance mécanique des granulés secs diminue avec l'augmentation de l'échelle.

Dans le *sous-chapitre III-4*, on a investigué l'effet de la formulation lors de la **granulation des mélanges des poudres hydro-solubles / hydro-insolubles**. Une caractérisation des matières de départ (CMC Avicel 105 et Lactose monohydrate) est réalisée du point de vue rhéologique et morphologique. Les isothermes de sorption montrent des différences entre ces deux matériaux pour l'interaction avec l'eau : la cellulose présente une grande affinité pour l'eau étant capable d'adsorber de grandes quantités jusqu'au moment que de l'eau libre en surface peut être identifiée. D'autre part, le lactose adsorbe moins de liquide et par conséquent présente plus rapidement du liquide en surface qui pourra favoriser le pontage entre les particules lors de l'agglomération. La CMC est insoluble avec une grande affinité pour l'eau et le lactose est soluble avec une faible affinité. De ce point de vue, il est raisonnable de s'attendre à ce que la CMC contrôle la distribution du liant dans le lit des particules lors des opérations d'agglomération des mélanges « CMC-lactose ».

La caractérisation rhéologique sur le MTR des matières premières confirme l'affinité plus grande de la CMC pour l'eau et offre une information supplémentaire sous la forme du pic de couple qui présente une cohésion beaucoup plus grande de la masse humide de CMC par rapport à la masse humide de lactose.

Au niveau de la granulation de matières premières dans le Mi-Pro, les résultats pour la CMC sont connus de l'exemple type avec une quantité optimale de liant pour un rapport L/S de 100%. Pour le lactose, on a rencontré des difficultés similaires à celles rencontrées par Mackaplow et al. [2001] avec le lactose humide présentant des grandes accumulations sur les parois du granulateur. En arrêtant l'essai et enlevant le dépôt de

matière présent sur les parois, on peut obtenir des granules pour un rapport L/S optimal d'environ 13%. Cependant, notre avis est que la granulation de lactose sur le Mi-Pro pourra être améliorée avec un ajout de toute la quantité optimale de liant en début de granulation et à faible vitesse d'agitation. Cela permettra d'obtenir une masse humide homogène qui, dans une étape suivante avec une vitesse d'agitation plus grande, pourra être dispersée et consolidée en granules.

La caractérisation rhéologique des mélanges sur le MTR a montré une dépendance linéaire et croissante entre le taux de CMC dans le mélange et le nécessaire de liant et la cohésion de la masse humide au niveau du pic. Ceci a été confirmé pour les deux types de CMC disponibles (Avicel 101 et Avicel 105) montrant que ce phénomène est indépendant de la taille de la CMC. À partir de ces essais, on a choisi deux mélanges de CMC Avicel 105 ($D_{50}=20\mu\text{m}$) et lactose ($D_{50}=60\mu\text{m}$) pour une caractérisation plus détaillée : avec 7 parts lactose et 3 parts cellulose (*Lactose/MCC 7/3*) et avec 3 parts lactose et 7 parts cellulose (*Lactose/MCC 3/7*). La granulation de ces deux mélanges avec de l'eau a été caractérisée sur deux échelles : le Mi-Pro 1.9L et le Diosna 6L.

L'ensemble de nos résultats nous permet de tirer les conclusions suivantes :

- les courbes de couple ont montré un bon contrôle du processus avec des quantités optimales de liant proches de la fin de la zone de croissance.
- un mécanisme de croissance est proposé : le lactose est vu comme le promoteur de l'étape de nucléation en favorisant le pontage entre les particules initiales et la coalescence entre les nucleus. Ceci, avec la solubilisation progressive des fines particules de lactose, on observe des agglomérats qui semblent constitués majoritairement des particules de CMC et qui, avec l'augmentation du rapport L/S, vont coalescer avec des particules de lactose de taille plus importante.
- l'étendue du plateau (et de l'étape de mouillage observables sur les courbes de couple obtenus dans le Mi-Pro) diminue avec l'augmentation du taux de lactose dans les mélanges. Ce qui est aussi confirmé au niveau des cinétiques de granulation : l'augmentation du pourcentage de lactose accélère le phénomène d'agglomération.

- la taille des granules augmente avec le pourcentage de lactose en mélange, ce qui peut être expliqué par la plus grande taille des particules initiales du lactose ainsi que par le phénomène de retraissement observé lors du séchage pour les particules de CMC (Kleinebudde [1994]).
- la consistance humide augmente faiblement entre les deux mélanges étudiés avec le contenu en CMC dans les mélanges binaires, tandis que la résistance des granulés secs augmente d'une façon plus importante avec le contenu de CMC dans les mélanges.
- comme sur les essais portant sur l'influence des propriétés de liant, les distributions granulométriques dépendent essentiellement de l'échelle utilisée. Dans le cas de la granulation de mélanges « CMC – lactose », les différences entre les échelles en terme d'addition de liant ont comme résultat une quantité plus grande des amas et des fines particules en fin de granulation.
- en terme de taille des granules, la vitesse en bout de pale permet d'obtenir une taille moyenne plus proche de celle obtenue dans le Mi-Pro. Pourtant, du point de vue de la résistance des granulés secs, le nombre de Froude constant permet d'obtenir un meilleur accord.

Conclusions et Perspectives

Conclusions

Dans cette étude, les mécanismes et les cinétiques de croissance intervenant dans la granulation humide en mélangeurs à haut taux de cisaillement ont été étudiés. Ces aspects ont été reliés au profil du couple de mélange granulaire (comme outil de suivi).

Nous avons présenté un exemple type de granulation humide et l'on a défini :

- la méthodologie nous permettant de faire le lien entre les mécanismes et cinétiques de croissance et les courbes de couple enregistrés,
- la quantité optimale de liant pour un couple poudre-liant,
- la caractérisation du point de vue des propriétés morphologiques, rhéologiques et mécaniques les granules.

Les bases émises dans l'exemple type ont été appliquées en suite pour la caractérisation de l'influence des variables opératoires, de la nature et des propriétés physico-chimiques du liant, et enfin de la formulation sur des mélanges binaires poudre hydro-soluble / hydro-insoluble.

L'étude sur l'influence des variables opératoires a permis d'identifier les conditions qui favorisent ou non l'agglomération et aussi de quantifier leur effet sur les propriétés finales de granules.

Nos essais portant sur l'influence des propriétés physico-chimiques des solutions nous permettent d'identifier deux situations en fonction de la prédominance des forces statiques ou des forces visqueuses. Le nombre capillaire visqueux Ca^* permet de définir une limite pour une valeur de (0.8). Pour des valeurs inférieures à 0.8, les forces statiques représentés par le travail d'adhésion sont dominantes et influent sur la cinétique de croissance et la résistance des granulés secs. Pour des valeurs supérieures ou égales à 0.8,

c'est les forces visqueuses qui sont dominantes et influent sur la cinétique de croissance, la taille des particules et la résistance humide des agglomérats.

Enfin la compréhension des mécanismes de croissance lors de la granulation humide des mélanges binaires des poudres hydro-solubles et hydro-insolubles peut être amélioré par la caractérisation rhéologique ainsi que par l'utilisation des isothermes de sorption. Un mécanisme de croissance a été proposé et validé par des observations microscopiques.

Perspectives

Comme perspective pour ce travail, les pistes intéressantes peuvent être séquencées comme suite:

- Étendre et généraliser à d'autres substrats solides les liens entre courbes de couple, cinétique de croissance, rhéologie et résistance mécanique des granulés secs présentés dans cette étude.
- Étude et influence de l'étape de séchage post granulation humide et son impact sur les modifications structurelles des granules secs obtenus. Ce qui permettra de lier l'évolution des structures granulaires (arrangements au sein du grain, porosité, fractures, ...) aux tenues mécaniques observées.
- Reprendre les données expérimentales développées dans cette étude avec une modélisation de type bilans de populations. Aspect que nous avons abordé lors de nos travaux de recherche mais que nous n'avons pas présenté dans ce manuscrit.
- Regarder la répartition des phases liquides liantes dans la masse granulaire humide avec d'autres moyens d'investigation que le profil rhéologique et observations microscopiques (sondes infrarouge, etc.)

Conclusions and Perspectives

Conclusions

This thesis presented the mechanisms and growth kinetics occurring during wet granulation in high shear mixers. These aspects were related to changes in the torque curve (as monitoring tool).

The presented typical wet granulation example allowed defining:

- the methodology allowing to link granulation mechanisms, granule growth kinetics and recorded torque curves,
- the optimum binder requirement for a given powder-binder couple,
- the characterization from a morphological, rheological and mechanical point of view of the granules.

On the basis of the typical example the same methodology has been applied for subsequent granulation runs investigating the influence of operating conditions, binder nature and physico-chemical properties and formulation on binary mixtures of water soluble / water insoluble powders.

The study of operating conditions allowed identifying conditions that favor agglomeration or not and quantifying the effect on end granule properties.

The experiments carried out on the influence of binder nature and physico-chemical properties describe two situations as a function of static or viscous forces dominance. The modified viscous capillary number Ca^* shows a boundary for a value of 0.8. For values below 0.8 the static forces represented by the work of adhesion are dominant influencing the granule growth kinetics and the dry granule strength. For values above 0.8 the viscous forces are dominant influencing the granule growth kinetics, granule size and wet mass consistency.

Finally the understanding of the growth mechanisms occurring for the wet granulation of water soluble / water insoluble powder mixtures can be increased by rheological characterization and water sorption isotherms of the starting materials. A growth mechanism has been proposed and validated by microscope analysis.

Perspectives

Interesting perspectives for this thesis include:

- Expanding the study of links between torque curves, granule growth kinetics, rheology and dry granule strength to other particular solids.
- Studying the influence of the granule drying stage and its impact on the structural modification of the dry granules. This would allow linking the evolution of the granular structure (inner structure, porosity, fractures etc) to the recorded granule strengths.
- Investigating the experimental results presented in this study by population balance modeling. Aspect approached during this thesis but not presented in the paper.
- The study of binder liquid distributions in the wet mass by other means than just rheological characterization and microscope observations (near infrared analysis etc)

List of Appendices

Appendix I. Dry Binder Datasheets

Appendix II. Methods

Appendix II.1 Contact Angle Measurement for MCC Avicel 105

Appendix II.2 Viscosity Determination

Appendix II.3 Flow Function Determination

Appendix III. Roundness Curves in Histograms

Appendix I. Dry Binder Datasheets

1. Hydroxy-propyl-methyl-cellulose (HPMC) - Sigma Aldrich

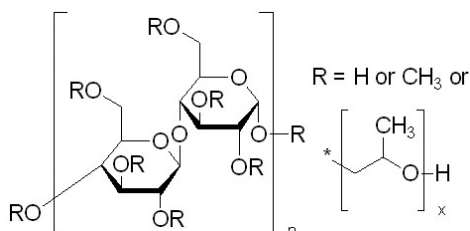


Figure 1. HPMC structure

Product Number: H8384

Product Brand: SIGMA

CAS Number 9004-65-3

Appearance (Color): White to Off-White

Appearance (Form): Powder

Solubility: 50 mg/ml

Solubility (Turbidity): Colorless to Faint Yellow at 25 G plus 500 ml of water Solubility (Color): Clear to Slightly Hazy

Apparent Viscosity: 40 - 60 cps 2% in water at 20 deg C

Preparation Instructions:

It is very important to thoroughly disperse the particles in water with agitation before they will dissolve. Otherwise, they will lump and form a gelatinous membrane around the internal particles, preventing them from wetting completely. There are four dispersion techniques commonly used to prepare solutions of hydroxypropylmethylcellulose: dispersion in hot water, dry blending, dispersion in non-solvent medium, and dispersion of surface-treated powders. (The last method is only for surface-treated powders).

Dispersion in hot water:

1. Heat approximately 1/3 the required volume of water to at least 90 °C.
2. Add the powder to the heated water with stirring or agitation.
3. Agitate the mixture until the particles are thoroughly wetted and evenly dispersed.

4. Add the remainder of the water (cold water) to lower the temperature of the dispersion. As the product cools, it will reach a temperature at which it becomes water soluble. It will then begin to hydrate and dissolve, increasing the viscosity of the solution.
5. Continue agitation for at least 30 minutes after the proper temperature is reached for solubility. The solution is now ready to use.

2. Poly-vinyl-pyrrolidone (PVP) - Sigma-Aldrich

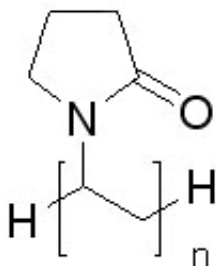


Figure 2. PVP structure

Product Name: Polyvinylpyrrolidone (average mol wt 10,000)

Product Number: PVP10

Product Brand: SIAL

CAS Number: 9003-39-8

Appearance: White To Off-White

Powder Solubility: Clear Faint to Light Yellow Solution at 100mg/ml in Water Water By
Karl Fischer: NMT 5.0%

Ir Spectrum: Consistent With Structure

Nitrogen: 11.5 To 12.8%

Ph Test: 3 To 7 (5% Solution)

K Value: 13 To 19

Recommended Retest: 4 Years

Appendix II. Methods

Appendix II.1 Contact Angle Measurement for MCC Avicel 105

The wettability of a powder by a liquid binder can be described by the surface tension or the contact angle between the powder and the liquid binder. The Washburn method is widely used technique allowing the determination of the contact angle for porous solids and powder beds (Goldszal [1], Vu[2], Galet [3]).

Washburn analyzed the capillarity driven Poiseuille flow of liquid and neglecting the effects due to initial transient flow regime and the flow of displaced air derived the differential equation (1) for which the solution is given by equation 2.

$$\frac{dl}{dt} = \frac{R_{\text{tube}}}{\mu} \frac{\gamma}{4l} \cos\theta \quad (1)$$

$$\frac{l^2}{t} = \frac{R_{\text{tube}} \gamma \cos\theta}{2\mu} \quad (2)$$

- l : capillary rise length (m)
- R_{tube} : the tube radius (m)
- μ : liquid binder viscosity (Pa.s)
- γ : liquid surface tension (mN/m)
- θ : contact angle ($^{\circ}$)

Plotting the squared length of liquid binder penetration in the bed against time gives a straight line. The slope of this linear evolution depends on the liquid binder properties (viscosity, surface tension), the radius of the capillary tube and the contact angle between powder and liquid binder. The space between the particles of the powder bed can be written as "X" capillaries with a R_c radius and by knowing the real density of the binder (ρ_L) the following equation can be written:

$$l = \frac{M_L}{\rho_L X R_c^2 \pi} \quad (3)$$

M_L : the liquid mass (kg)

X : number of capillaries (-)

R_c : capillary radius (m)

ρ_L : liquid density (kg/m³)

Thus the modified Washburn equation can be written as:

$$\frac{M_L^2}{t} = \frac{R_{\text{tube}}^5 \gamma \rho_L^2 X^2 \pi^2 \cos\theta}{2\mu} = C_w \frac{\gamma \rho_L^2}{\mu} \cos\theta \quad (4)$$

Where C_w is a constant dependant only on powder bed "geometry" and can be determined determined using a liquid known to fully wet the powder (of known ρ_L and η and with $\cos\theta=1$). Usually alkanes are used in our case hexane was used and for the microcrystalline cellulose Avicel 105 a value of $1.505 \cdot 10^{-5}$ has been obtained. The equipment used was a ILMS tensiometer produced by GBX at 25°C. Reproducibility was ensured by preparing each cell (cylindrical tube) with the same amount of powder and submitting it to centrifugation at 3500 rpm for 10 minutes in order to obtain similar packing of the particles. Figures 1 and 2 show the values of contact angles for the different studied binder solutions.

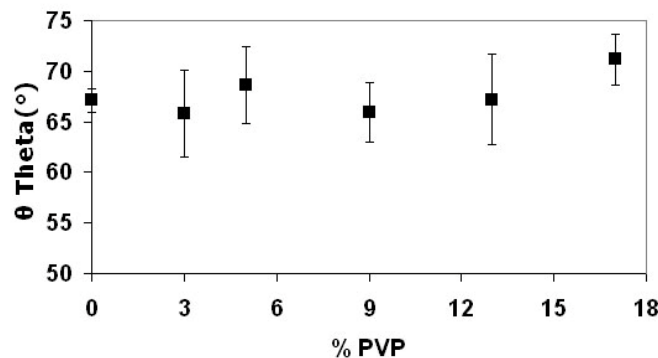


Figure 1. Contact angle values for MCC Avicel 105 and various percentages of PVP binder solutions

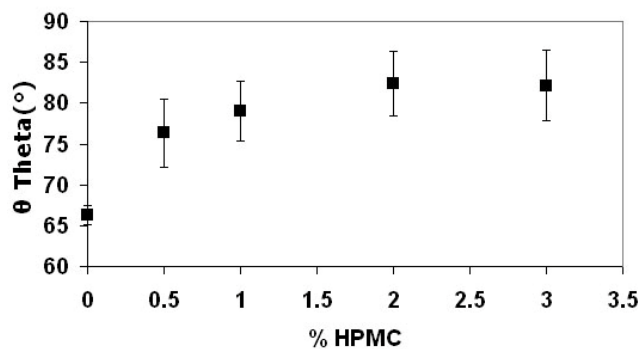


Figure 2. Contact angle values for MCC Avicel 105 and various percentages of HPMC binder solutions

References

- [1] A. Goldszal, J. Bousquet, Wet agglomeration of powders: From physics towards process optimization, Powder. Technol. 117 (2001) 221-231
- [2] T.-O. Vu, Dispersion d'une poudre dans un liquide : Caracterisation des interactions interfaciales et effets de differents facteurs sur la vitesse de dispersion, PhD thesis, Ecole Nationale Superieure des Mines de Sainte-Etienne (2002)
- [3] L. Galet, S. Patry, J. Dodds, Determination of the wettability of powders by the Washburn capillary method with bed preparation by a centrifugal packing technique, Particulate Systems Analysis Conference, Stratford, United-Kingdom (2008)

Appendix II. Methods

Appendix II.2 Viscosity Determination

The viscosity of the binder solutions used was determined on a haake Rheostress 600 rheometer. A rotating cone and plate rheometer was used for the viscosity measurements as it allowed good precision for low as well as higher viscosity liquids. The cone plate rheometer has a diameter of 35mm, a 1° cone angle and a 0.054 mm truncation (Figure 1).

Viscosity was determined at various shear rates (with the rotor turning between 200 and 2000 rpm) and at a temperature of 25°C. For all binders except the HPMC 3% solution a mean value has been calculated as the viscosity evolution has been found to be independent of shear rate. For HPMC 3% solution the value at 1047 rpm has been retained for the calculation of the modified viscous capillary number.



Figure 1. The Haake Rheostress rheometer

The shear stress can be written as::

$$\tau_d = Z \cdot M_d \quad (1)$$

Md: torque (N.m)

Z : stress factor (m^{-3})

The stress factor Z is calculated as:

$$Z = \frac{3}{2 \cdot \pi \cdot R_k^3} \quad (2)$$

R_k : the cone radius.

The shear rate is proportionally linked to the angular velocity and thus speed and a shear factor:

$$\dot{\gamma} = M \cdot \Omega$$

Ω : the angular velocity, calculated as $(2\pi/60)n$ where n is the speed of the rotor

M: shear factor, calculated as $1/\alpha$ where α is the cone angle (rad^{-1}).

Appendix II.3 Flow Function Determination

This study has been carried out on the shear cell module of the Freeman FT4 powder rheometer. Powders can flow like liquids which allow a certain ease in manipulation, continuous classification and dry mixing however internal friction and cohesion forces between particles can resist flow.

The shear cell measures rheological properties of powders at low flow rates under various consolidating pressures. There are two phases involved in the shear method: 1. consolidation and pre shear and 2. shear analysis.

The failure of the sample depends on its consolidation. Consolidation and pre-shear consists of shearing the sample under a maximal normal stress. Once steady state flow (constant shear force) has been achieved the initial normal load is removed.

The second phase consists of applying a smaller normal load. Shear travel resumes and the peak shear force corresponding to the shear normal load is noted. This step is repeated a number of times with the same consolidation load and increasing normal loads ($\sigma_{1,2,3}$) as described by Schwedes [1]. Figure 1 shows an example on a similar geometry to the Freeman FT4 (the Schulze ring shear cell). Jenike [2] offers a protocol allowing us to chose the maximum consolidation normal loads as well as the normal loads for the shear tests.

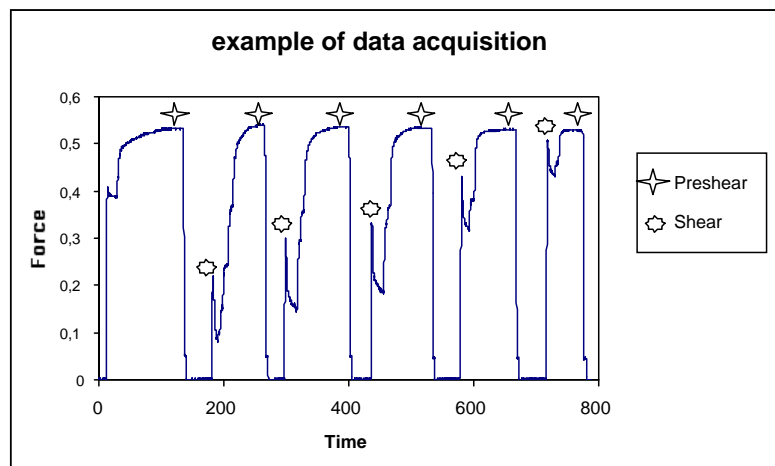


Figure 1. Example of procedure to get a yield locus from a Schulze ring shear cell

Inspired by this protocol Table 1 gives the consolidation loads as well as the normal loads retained in our study. Plotting the yield locus ($\tau=f(\sigma_{1,2,3})$, Figure 2) allows us to determine the unconfined yield strength (σ_c , Mohr circle going through the origin and tangent to the yield locus, as described by Schulze [3]) and the consolidation stress (σ_1 , obtained by drawing the largest Mohr circle tangent to the yield locus). Obtaining different yield loci for different consolidation loads allows the drawing of flow functions defined as $ffc=\sigma_c/\sigma_1$ for a material. Tables 2,3,4 and 5 give the obtained unconfined yield strength and consolidation stresses obtained for different consolidation loads for the studied powders. Similar to the classification used by Jenike [4] flow behavior can be defined as:

- not flowing for $ffc < 1$
- very cohesive for $1 < ffc < 2$
- cohesive for $2 < ffc < 4$
- easy flowing for $4 < ffc < 10$
- free flowing for $10 < ffc$

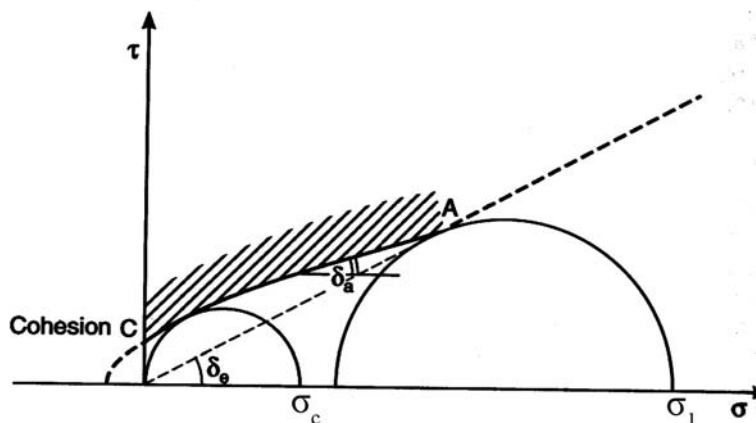


Figure 2. Example of yield locus from Bimbenet [5]

Consolidation Load (kPa)	Normal Load (kPa)
	0.5
2	0.8
	1.1
	1.4
	1.6
	1
4	1.6
	2.2
	2.8
	3.2
8	2
	3.2
	4.4
	5.6
	6.4
16	4
	6.4
	8.8
	11.2
	12.8

Table 1. Applied consolidation and normal loads

Powder	σ_c (kPa)	σ_1 (kPa)	Cohesion (kPa)	$ff_c = \sigma_1/\sigma_c$
α Lactose monohydrate	1,97	4,59	0,61	2,33
MCC Avicel 101	1,45	4,44	0,44	3,05
MCC Avicel 105	2,30	5,22	0,65	2,27

Table 2. Mechanical characterization for a consolidation load of 2 kPa

Powder	σ_c (kPa)	σ_1 (kPa)	Cohesion (kPa)	$ff_c = \sigma_1/\sigma_c$
α Lactose monohydrate	2,807	9,123	0,829	3,250
MCC Avicel 101	1,324	8,714	0,380	6,581
MCC Avicel 105	3,426	10,181	0,952	2,972

Table 3. Mechanical characterization for a consolidation load of 4 kPa

Powder	σ_c (kPa)	σ_1 (kPa)	Cohesion (kPa)	$ff_c = \sigma_1/\sigma_c$
α Lactose monohydrate	5,150	17,717	1,541	3,440
MCC Avicel 101	2,432	17,102	0,704	7,032
MCC Avicel 105	6,117	19,237	1,750	3,145

Table 4. Mechanical characterization for a consolidation load of 8 kPa

Powder	σ_c (kPa)	σ_1 (kPa)	Cohesion (kPa)	$ff_c = \sigma_1/\sigma_c$
α Lactose monohydrate	7,789	34,753	2,279	4,461
MCC Avicel 101	4,373	35,099	1,226	8,026
MCC Avicel 105	11,185	37,529	3,199	3,355

Table 5. Mechanical characterization for a consolidation load of 16 kPa

References

- [1] J. Schwedes, Measurement of flow properties of bulk solids, Powder Technol. 88 (1996) 285-290
- [2] The institution of chemical engineers, Standard shear testing technique for particulate solids using the shear cell, IchemE (1989)
- [3] D. Schulze, Powders and bulk solids : behavior, characterization, storage and flow, Springer Berlin Heidelberg (2008)
- [4] A.W. Jenike, Storage and flow of solids, (1964/1980) Bull No. 123, 20th Printing revised 1980, Univ of Utah, Salt Lake City
- [5] J.-J. Bimbenet, M. Loncin, Bases du génie des procédés alimentaires, (1995)

Appendix III Roundness Curves in Histogramms

The following figures present the distributions as histogramms for the roundness evolutions shown in represented in Chapter III.2 Influence of Operating Conditions and Equipment Geometry specifically Figures 7 (Roundness distributions by number obtained for the studied fill ratios at an impeller speed of 400 rpm for the granulation of MCC Avicel 105 with ultra-pure water) and 19 (Roundness distributions by number as a function of impeller speed for the granulation of MCC Avicel 105 with ultra-pure water).

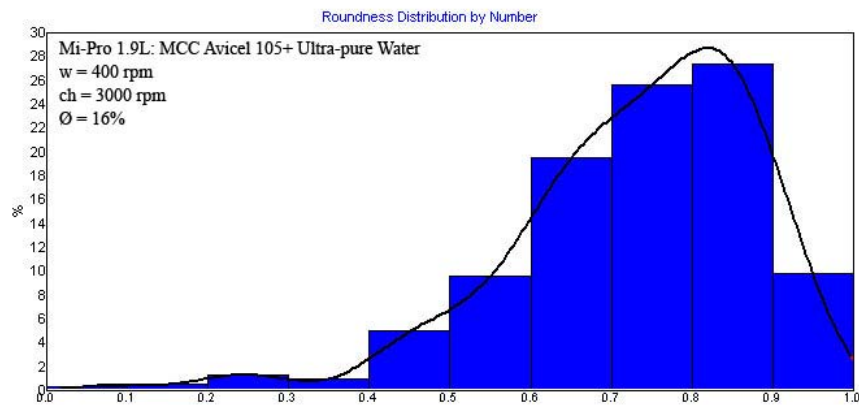


Figure 1. Roundness distribution by number obtained for a fill ratio of 16% at an impeller speed of 400 rpm for the granulation of MCC Avicel 105 with ultra-pure water

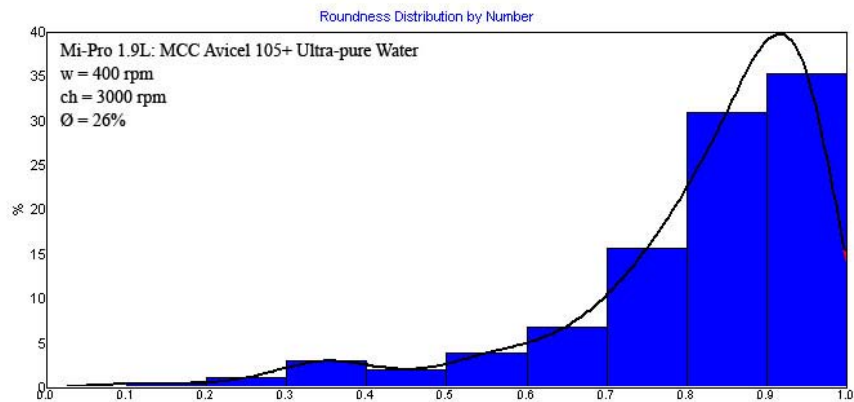


Figure 2. Roundness distribution by number obtained for a fill ratio of 26% at an impeller speed of 400 rpm for the granulation of MCC Avicel 105 with ultra-pure water

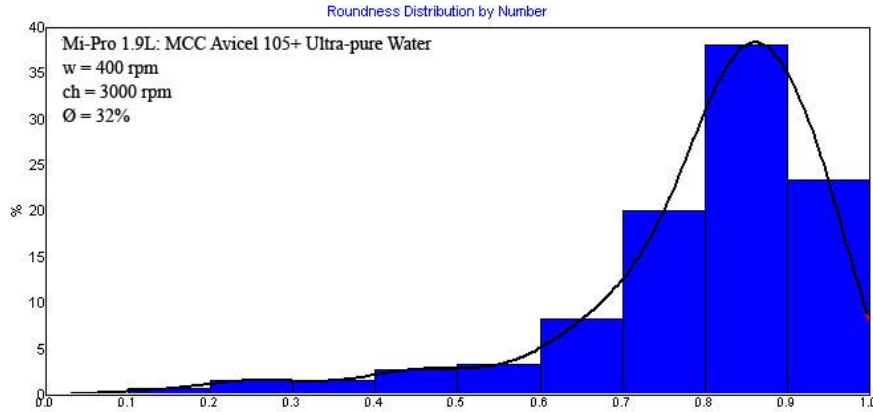


Figure 3. Roundness distribution by number obtained for a fill ratio of 32% at an impeller speed of 400 rpm for the granulation of MCC Avicel 105 with ultra-pure water

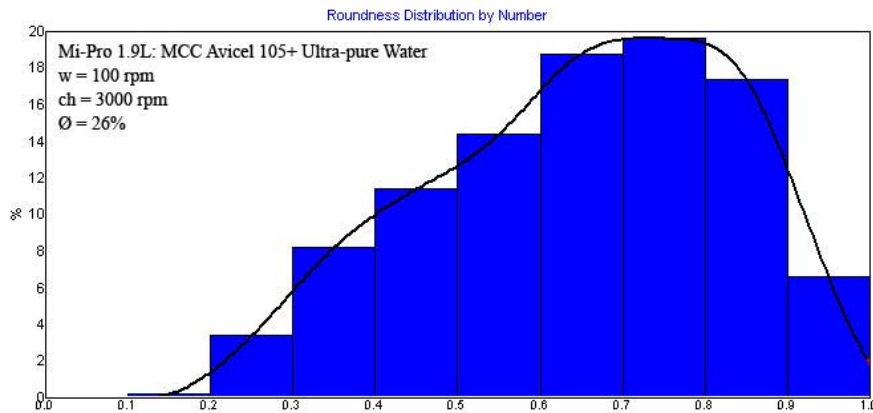


Figure 4. Roundness distribution by number obtained for a fill ratio of 26% at an impeller speed of 100 rpm for the granulation of MCC Avicel 105 with ultra-pure water

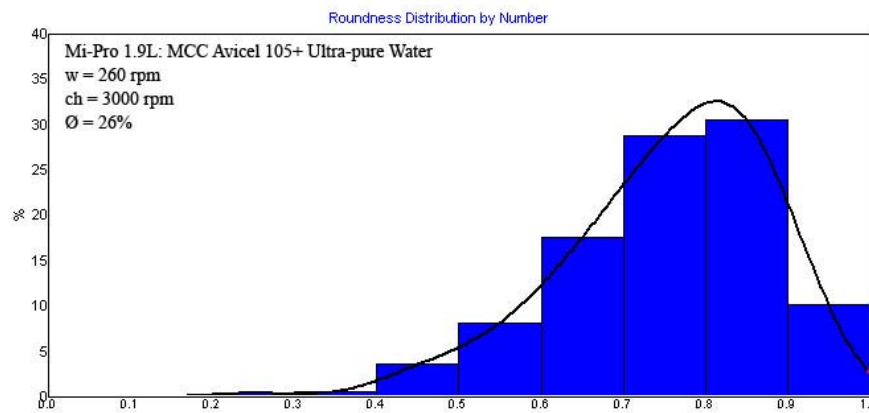


Figure 5. Roundness distribution by number obtained for a fill ratio of 26% at an impeller speed of 260 rpm for the granulation of MCC Avicel 105 with ultra-pure water

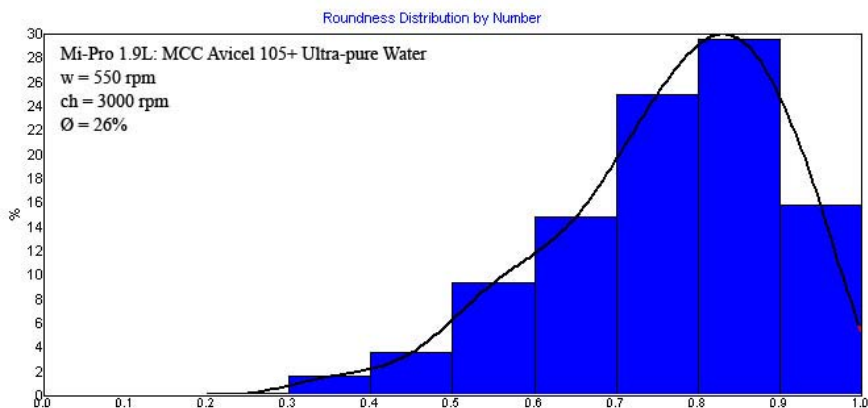


Figure 6. Roundness distribution by number obtained for a fill ratio of 26% at an impeller speed of 550 rpm for the granulation of MCC Avicel 105 with ultra-pure water

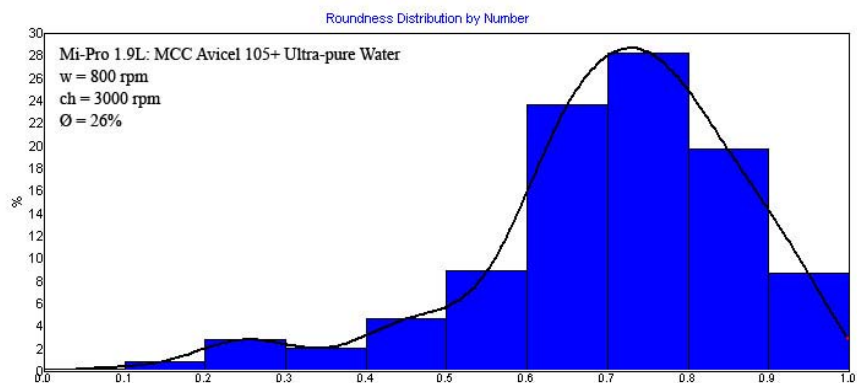


Figure 7. Roundness distribution by number obtained for a fill ratio of 26% at an impeller speed of 800 rpm for the granulation of MCC Avicel 105 with ultra-pure water

List of Symbols

a - acceleration of the granule	(m/s ²)
a _w - the water activity	(-)
A' - the area flux of powder traversing the spray zone	(m ² /s)
A - cross sectional area of the granule	(m ²)
A _g - area of the granules	(m ²)
c - flaw size in assembly	(m)
C - coordination number depending on the particle shape (C=6 for a perfect sphere)	(-)
CrI - cristallinity index	(%)
C _w - constant	(-)
D - impeller diameter	(m)
D _v - diameter of the vessel	(m)
D _g - granule diameter	(m)
d _i - mean diameter of size interval i	(m)
d _d - the droplet diameter	(m)
d _p - particle diameter	(m)
d _{pi} - initial particle diameter	(m)
d _{pm} - mean diameter	(m)
e - coefficient of restitution	(-)
E - Young's modulus	(Pa)
E _l [*] - effective Young's modulus	(Pa)
f _i - particle mass fraction of size interval i	(-)
ffc - flow function	(-)
F _a - acceleration force	(N)
F - force	(N)
g - gravitational acceleration constant.	(m/s ²)
h - thickness of the liquid surface layer	(m)
h _a - characteristic height of surface asperities	(m)

h_b - height of the blade	(m)
H - moisture content	(%)
H_r - Hausner Ratio	(-)
I_c - Carr index	(-)
I_{002}, I_{am} - intensity peaks on the X-ray diffraction curves	(-)
K - growth kinetic constant	(-)
l – capillary rise length	(m)
L - distance between two particles	(m)
L/S Ratio - liquid to solid ratio	(%)
m' - harmonic mean granule mass	(kg)
m - granule mass	(kg)
M - shear factor	(rad ⁻¹)
M_d - torque	(N.m)
M_i - initial dry powder mass	(kg)
M_L - liquid mass	(kg)
n - number of blades on the impeller	(-)
N - impeller speed	(rpm)
p - partial pressure of water vapor in the mixture	(Pa)
p_0 - saturated vapor pressure of water	(Pa)
P - power consumption	(W)
P_g - perimeter of the particles	(m)
q - mass of liquid added per unit of time	(kg/s)
r - radius of the impeller	(m)
r_d - radius of the drop footprint on the surface	(m)
R_c - capillary radius	(m)
R_g - radius of the granule	(m)
RH - relative humidity of the sample	(-)
R_k - cone radius	(m)
R_{pore} - effective pore radius based on cylindrical pores	(m)
R_{tube} - tube radius	(m)
S - the liquid saturation	(%)

t - process time	(s)
t_p - penetration time	(s)
t_c - circulation time	(s)
T_R - fill ratio	(%)
U - speed of the particles	(m/s)
U_0 - collision velocity	(m/s)
V - volume loaded with particles	(m ³)
V^* - total volume of the mixer	(m ³)
V_0 - total drop volume	(m ³)
V' - volumetric spray rate	(m ³ /s)
W_{CS} - work of cohesion for the solid	(N/m)
W_{CL} - work of cohesion for the liquid	(N/m)
W_a - work of adhesion between liquid and solid	(N/m)
X – number of capillaries	(-)
X_{fines}^0 - initial ratio of fine particles	(%)
X_{fines} - the ratio of fine particles at a given L/S ratio	(%)
Z – stress factor	(m ⁻³)

Greek Symbols

α - cone angle	(rad)
γ - liquid surface free energy	(N/m)
Γ_c - the fracture surface energy	(N/m)
Γ - equilibrium surface energy	(N/m)
Δ - displacement	(m)
Ω - angular velocity	(s ⁻¹)
ε - inter-particle porosity	(-)
θ - contact angle	(°)
λ - the spreading coefficient	(N/m)
μ - liquid viscosity	(Pa.s)
μ^* - wet mass consistency	(N.m/kg)

v_0 - relative velocity between two granules	(m/s)
ν - Poisson's ratio	(-)
ρ_{bulk} - solid bulk density	(kg/ m ³)
ρ_{tapped} - solid tapped density	(kg/ m ³)
ρ_s - solid density	(kg/ m ³)
ρ_l - liquid density	(kg/ m ³)
ρ_w - the wet mass bulk density	(kg/ m ³)
ρ - granule density	(kg/ m ³)
σ - wet agglomerate strength	(Pa)
σ_g - dry agglomerate strength	(Pa)
σ_1 - unconfined yield strength	(Pa)
σ_c - consolidation stress	(Pa)
σ_{impact} - impact pressure	(Pa)
\emptyset - solid fraction of the granular assembly	(%)
χ - the surface porosity	(%)
ω - impeller tip speed	(m/s)
ψ_a - adimensionnal spray flux	(-)
τ_h - adimensionnal penetration time	(-)
τ_d - shear stress	(Pa)

Dimensionless Groups

Ca_{vis} - viscous capillary number
Ca^* - modified viscous capillary number
Fr - Froude number
St_v - viscous Stokes number
St_v^* - critical viscous Stokes number
St_{def} - Stokes deformation number
Re - Reynolds number
RSV - relative swept volume

General Alphabetic References

- M.J. Adams, M.A. Mullier, J.P.K. Seville, Agglomerate strength measurement using a uniaxial confined compression test, *Pow. Tech.* 78 (1994) 5-13
- M.E. Aulton, M. Banks, Influence of the hydrophobicity of the powder mix on fluidised bed granulation, International Conference on Powder Technology in Pharmacy, Basel, Switzerland, Powder Advisory Centre, 1979
- M. Benali, V. Gerbaud, M. Hemati, Effect of operating conditions and physico-chemical properties on the wet granulation kinetics in high shear mixer, *Powder Technol.* 190 (2009) 160-169
- M. Benali, Prédiction des interactions substrat/liant lors de la granulation: Etude expérimentale dans un mélangeur granulateur à fort taux de cisaillement- Approches thermodynamiques par simulation moléculaire, PhD thesis, INP Toulouse (2006)
- G. Betz, P. J. Burgin, H. L. Leuenberger, Power consumption profile analysis and tensile strength measurements during moist agglomeration, *Int. J. Pharm.* 252 (2003) 11-25
- D. Bika, M. Gentzler, J. Michaels, Mechanical properties of agglomerates, *Powder Technol.* 117 (2001) 98-112.
- J.-J. Bimbenet, M. Loncin, Bases du génie des procédés alimentaires, (1995)
- T.K Bock, U. Kraas, Experience with the Diosna mini-granulator and assessment of process scalability, *Eur. J. of Pharm. and Biopharm.*, 52(3), (2001) 297-303
- A.M. Bouwman, The influence of material properties and process conditions on the shape of granules produced by high shear granulation, PhD thesis Rijksuniversiteit Groningen (2005)
- C. Capes, P. Danckwerts, Granule formation by the agglomeration of damp powders. Part I: the mechanism of granule growth, *Transactions of the Institution of Chemical Engineers* 43 (1965) 116-124
- A.L. Camara, Intrapolation du procédé de granulation humide en mélangeurs à haute vitesse, PhD thesis, Institut National Polytechnique de Lorraine (2005)
- R.L. Carr, Evaluating flow properties of solids, *Chem. Eng.* 18 (1965) 163-168
- E. Chevalier, M. Viana, C. Pouget, D. Chulia, Influence of process parameters on pellets elaborated in a Mi-Pro high-shear granulator, *Pharmaceutical development and technology* 12 (2007) 133-144
- T.M. Chitu, D. Oulahna, M. Hemati, Wet granulation in a laboratory scale high shear mixer: Effect of chopper presence, design and impeller speed, 9th Int. Symposium on Agglomeration Sheffield (2009)
- B.S. Chun, H.S. Lim, M. Sagong, K. Kim, Development of a hyperbolic constitutive model for expanded polystyrene (EPS) geof foam under triaxial compression tests, *Geotextiles and Geomembranes*, 22(4) (2004) 223-237
- M. Denesuk, G.L. Smith, B.J.J. Zelinski, N.J. Kreidl, D.R.Uhlmann, Capillary penetration of liquid droplets into porous materials, *J. Colloid Interface Sci.* 158 (1993) 114-120.

- K. van den Dries, O. de Vegt, V. Girard, H. Vromans, Granule breakage phenomena in a high shear mixer: influence of process and formulation variables and consequences on granule homogeneity, *Powder Technol.* 133 (2003) 228–236
- H. Eliassen, H. Kristensen, T. Schaefer, Growth mechanisms in melt agglomeration with a low viscosity binder, *Int. J. Pharm.* 186 (1999) 149–159
- H. Eliassen, T. Schaefer, H. Kristensen, Effects of binder rheology on melt agglomeration in a high shear mixer, *Int. J. Pharm.* 176 (1998) 73–83
- Ennis, B.J., Li, J., Tardos, G., Pfeffer, R., The influence of viscosity on the strength of an axially strained pendular liquid bridge, *Chem.Eng.Sci.* 45 (10) (1990) 3071-3088
- Ennis, B.J., Tardos, G., Pfeffer, R., A microlevel-based characterization of granulation phenomena, *Powder Technol.* 65 (1991) 257-272
- A. Faure, I. Grimsey, R. Rowe, P. York, M. Cliff, Process control in a high shear mixer-granulator using wet mass consistency: The effect of formulation variables, *J.Pharm.Sci.* 88 (1999) 191-195
- A. Faure, P. York, R. Rowe, Process control and scale-up of pharmaceutical wet granulation processes: a review, *Eur. J. Pharm. and Biopharm.* 52 (2001) 269–277
- K.E. Fielden, J.M. Newton, P. O'Brien, R.C. Rowe, Thermal studies of interaction of water and microcrystalline cellulose. *J. Pharm. Pharmacol.* 40 (1988) 674–678
- L. Galet, S. Patry, J. Dodds, Determination of the wettability of powders by the Washburn capillary method with bed preparation by a centrifugal packing technique, *Particulate Systems Analysis Conference, Stratford, United-Kingdom* (2008)
- K. Giry, Impact du changement de procede de granulation humide sur les caracteristiques pharmacotechniques des grains et des comprimés : Procédé monophasique versus procédé séquentiel, PhD thesis, Université de Limoges (2007)
- A. Goldszal, J. Bousquet, Wet agglomeration of powders: from physics toward process optimization, *Pow. Tech.* 117 (2001) 221-231
- F. Gomez, K. Saleh, P. Guigon, Étude de la granulation humide en mélangeur à taux de cisaillement élevé par rhéométrie par couple de rotation, *Congrès sur les Poudres, Nancy, France, 2001, Récents Progrès en Génie des Procédés*, 15, 77, 317-322
- J. Hamdani, A.J. Moës, K. Amighi, Development and evaluation of prolonged release pellets obtained by the melt pelletization process, *Int. J. of Pharm.* 245(1-2) (2002) 167-177
- K. Hapgood, J.D. Litster, S. R. Biggs, T. Howes, Drop penetration into porous powder beds, *Journal of Colloid and Interface Science* 253, (2002) 353–366
- K.P. Hapgood, J.D. Litster, R.Smith, Nucleation regime map for wet granulation, *AIChE J* 49 (2) (2003) 350-361
- P. W. S. Heng, O. M. Y. Koo, A Study of the Effects of the Physical Characteristics of Microcrystalline Cellulose on Performance in Extrusion Spheronization, *Pharm. Res.* 18 (4) (2001) 480-487
- P. Holm, Effect of impeller and chopper design on granulation in a high speed mixer *Drug Dev. and Ind. Pharm.* 13 (1987) 1675–1701

- P. Holm, M. Bonde, T. Wigmore, Pelletization by granulation in a roto-processor RP-2-Part 1: Effect of process and product variables on granule growth, *Pharm. Technol.* 8 (1996) 22-36
- P. Holm, O. Jungersen, T. Schaefer, H. Kristensen, Granulation in high speed mixers. Part 1. Effects of process variables during kneading, *Pharmaceutical Industry* 46, (1983) 97–101
- P. Holm, T. Schaefer, H.G. Kristensen, Granulation in High-Speed Mixers. Part V. Power Consumption and Temperature Changes During Granulation. *Powder Technol.* 43 (1985) 213-223
- F. Hoornaert, P.A.L. Wauters, G.M.H. Meesters, S.E. Pratsinis, B. Scarlett, Agglomeration behaviour of powders in a Lodige mixer granulator, *Powder Technol.* 96 (1998) 116–128.
- G. Imanidis, Untersuchungen über die Agglomerierkinetik und die elektrische Leistungsaufnahme beim Granulierprozess im Schnellmischer, PhD thesis, University of Basel (1986)
- J.N. Israelachvili, D. Tabor, Van der Waals forces: theory and experiment, *Progress of Surface and Membrane Science* 7 (1973) 1–55
- S. M. Iveson, J.D. Litster, B. Ennis, Fundamental studies of granule consolidation. Part 1. Effects of binder content and binder viscosity, *Powder Technol.* 88 (1996) 15–20
- S. M. Iveson, J.D. Litster, B. Ennis, Fundamental studies of granule consolidation. Part 2. Quantifying the effects of particle and binder properties. *Powder Technol.* 99 (1998) 243–250
- M. Iveson, J.D. Litster, Growth regime map for liquid-bound granules, *AIChE J.* 44 (1998) 1510–1518
- S. M. Iveson, J. D. Litster, K. Hapgood, B. J. Ennis, Nucleation, growth and breakage phenomena in agitated wet granulation processes: a review, *Powder Technol.* 117 (2001) 3–39
- S. M. Iveson, P. A. L. Wauters, S. Forrest, J. D. Litster, G. M. H. Meesters, B. Scarlett, Growth regime map for liquid-bound granules: further development and experimental validation, *Powder Technol.* 117 (2001) 83-97
- M. Jacob, *Handbook of Powder Technology Chapter 9 Granulation Equipment*, Elsevier (2006) 417-477
- A.W. Jenike, *Storage and flow of solids*, (1964/1980) Bull No. 123, 20th Printing revised 1980, Univ of Utah, Salt Lake City
- A. Johansen, T. Schaefer, Effects of interactions between powder particle size and binder viscosity on agglomerate growth mechanisms in a high shear mixer, *European J. of Pharm. Sciences* 12 (2001) 297–309
- K.L. Johnson, *Contact Mechanics*, Cambridge, Cambridge University Press (1985)
- S. Keningley, P. Knight, A. Marson, An investigation into the effects of binder viscosity on agglomeration behaviour, *Powder Technol.* 91 (1997) 95–103
- K. Kendall, Agglomerate strength, *Powder Metallurgy* 31 (1988) 28–31
- P. Kleinebudde, Shrinking and swelling properties of pellets containing microcrystalline cellulose (MCC) and low substituted hydroxypropylcellulose (L-HPC). I. Shrinking properties, *Int. J. Pharm.* 104 (1994) 209-219
- P. Kleinebudde, The crystallite-gel-model for microcrystalline cellulose in wet granulation, extrusion and spheronization, *Pharm.Res.* 14 (1997) 804-809

- P. Kleinebudde, M. Jumaa, F. El Saleh, Influence of degree of polymerization on behavior of cellulose during homogenization and extrusion/spheronisation, *AAPS Pharmsci* 2 (3) article 21 (2000)
- P.C. Knight, An investigation of the kinetics of granulation using a high shear mixer, *Powder Technol.* 77 (1993) 159-169
- P. Knight, Structuring agglomerated products for improved performance, *Powder Technol.* 119 (2001) 14-25
- P. Knight, T. Instone, J. Pearson, M. Hounslow, An investigation into kinetics of liquid distribution and growth in high shear mixer agglomeration. *Powder Technol.* 97 (1998) 246-257
- P. Knight, A. Johansen, H. Kristensen, T. Schaefer, J. Seville, An investigation of the effects on agglomeration of changing the speed of a mechanical mixer. *Powder Technol.* 110 (2000) 204-209.
- P.C. Knight, J.P.K. Seville, Effect of binder viscosity on agglomeration processes, *World Congr. Part. Technol.* 3 (1998)
- H.G. Kristensen, T. Schæfer, Agglomeration with viscous binders, *First International Particle Technology Forum Denver USA* (1994)
- J. Kristensen, P. Holm, A. Jaegerskou, T. Schæfer, Granulation in high speed mixers Part4: effect of liquid saturation on the agglomeration, *Pharm. Ind.* 46 (1984) 763-767
- J. Kristensen, T. Schæfer, P. Kleinebudde, Direct Pelletization in a Rotary Processor Controlled by Torque Measurements. II: Effects of Changes in the Content of Microcrystalline Cellulose - *AAPS Pharmsci* 2(3) article 24 (2000)
- M. Kuentz, H. Leuenberger, A new theoretical approach to tablet strength of a binary mixture consisting of a well and a poorly compactable substance, *Eur. J. of Pharm. and Biopharm.* 49 (2000) 151-159
- M. Landín, P. York, M.J. Cliff, R.C. Rowe, A.J. Wigmore, Scale-up of a pharmaceutical granulation in fixed bowl mixer-granulators, *Int.J.Pharm.* 133 (1996) 127-131
- H. Leuenberger, Granulation, *New Techniques*, *Pharm. Acta Helv.* 57(3) (1982) 72-82
- H. Leuenberger, H-P Bier, H. Sucker, Theory of the granulation-liquid requirement in the conventional granulation process, *Pharm.Tech.Int.* 3 (1979) 61-68.
- H. Leuenberger, M. Puchkov, E. Krausbauer, G. Betz, Manufacturing pharmaceutical granules: Is the granulation end-point a myth?, *Powder Technol.* 189 (2009) 141-148
- H.L. Leuenberger, M. Puchkov, E. Krausbacher, G. Betz, Manufacturing pharmaceutical granules: Is the granulation end-point a myth, *3rd Int. Granulation Workshop Sheffield* (2007)
- H. Leuenberger, G. Betz, *Handbook of Powder Technology Chapter 15 Granulation process control-Production of pharmaceutical Granules: The classical batch concept and the problem of scale-up*, Elsevier (2006) 705-734
- N-O Lindberg, L. Leander, L. Wenngren, H. Helgesen, R. Reenstierna, Granulation in a change can mixer. *Acta Pharm. Suec.* 11 (1974)
- L.X. Liu, S.M. Iveson, J.D. Litster, B.J. Ennis, Coalescence of deformable granules in wet granulation processes, *AIChE J.* 46 (2000) 529-539

P.Luukkonen, Rheological properties and the state of water of microcrystalline cellulose and silicified microcrystalline cellulose wet masses, Academic dissertation, Pharmaceutical Technology Division Department Pharmacy University Helsinki (2001)

P. Luukkonen, T. Maloney, J. Rantanen, H. Paulapuro, J. Yliruusi, Microcrystalline Cellulose-Water Interaction—A Novel Approach Using Thermoporosimetry, *Pharm. Res.* 18 (11) (2001) 1562-1569

P. Luukkonen, T. Schæfer, L. Hellen, A. M. Juppo, J. Yliruusi, Rheological characterization of microcrystalline cellulose and silicified microcrystalline cellulose wet masses using a mixer torque rheometer, *Int. J. of Pharm.* 188 (1999) 181–192

P. Luukkonen, T. Schæfer, K. Mäkelä, U. Södergård, L. Hellén, J. Yliruusi, Evaluation of the optimum water level for pelletisation using a mixer torque rheometer. *AAPS PharmSci* 1148 (1999), New Orleans, USA

M. B. Mackaplow, L. A. Rosen, J. N. Michaels, Effect of primary particle size on granule growth and endpoint determination in high-shear wet granulation, *Powder Technol.* 108 (2000) 32-45

Mangwandi, C., Y.S. Cheong, M.J. Adams, M.J. Hounslow, A.D. Salman, The coefficient of restitution of different representative types of granules. *Chem. Eng. Sci.* 62 (2007), 437 – 450

J. N. Michaels, L. Farber, G. S. Wong, K. Hapgood, S. J. Heidel, J. Farabaugh, J-H Chou, G. I. Tardos, Steady states in granulation of pharmaceutical powders with application to scale-up, *Powder Technol.* 189 (2009) 295-303

P.J.T. Mills, J.P.K. Seville, P.C. Knight, M.J. Adams, The effect of binder viscosity on particle agglomeration in a low shear mixer/agglomerator, *Powder Technol.* 113 (2000)140–147

P.R. Mort, *Handbook of Powder Technology Chapter 19 Scale-up of high shear binder-agglomerate processes*, Elsevier (2006) 853-896

D.M. Newitt, J.M.A. Conway-Jones, A contribution to the theory and practice of granulation *Trans.Instr.Chem.Engrs.* 36 (1958) 422-442.

K. Niishi, M. Horio, *Handbook of Powder Technology Chapter 6 Dry Granulation*, Elsevier (2006) 289-323

J. Nordström, K. Welch, G. Frenning, G. Alderborn, On the physical interpretation of the Kawakita and Adams parameters derived from confined compression of granular solids, *Pow. Tech.* 182 (2008) 424–435

D. Oulahna, F. Cordier, L. Galet, J. A. Dodds, Wet granulation: the effect of shear on granule properties, *Powder Technol.* 130 (2003) 238-246

M.D. Parker, P.York, R.C. Rowe, Binder-substrate interactions in wet granulation 1: The effect of binder characteristics, *Int.J.Pharm.* 64 (1990) 207-216

M.D. Parker, P.York, R.C. Rowe, Binder-substrate interactions in wet granulation. 2: The effect of binder molecular weight, *Int.J.Pharm.* 72 (1991) 243-249

M.D. Parker, R.C. Rowe, Source variation in the wet massing (granulation) of some microcrystalline celluloses. *Powder Technol.* 65 (1991) 273-281

J. Pearson, M. Hounslow, T. Instone, Tracer studies of high-shear granulation: I. Experimental results. *A.I.Ch.E. Journal* 47 (2001) 1978–1983

- X. Pepin, S. Blanchon, G. Couarraze, Power Consumption Profiles in High-Shear Wet granulation. I: Liquid distribution in Relation to Powder and Binder Properties, *J.Pharm.Sci.* 90 (2001) 322-331
- W. Pietsch, *Size enlargement by agglomeration*, Wiley (1991)
- N. Rahmanian, M. Ghadiri, Y. Ding, Effect of scale of operation on granule strength in high shear granulators, *Chemical Engineering Science* 63 (2008) 915 – 923
- J.S. Ramaker, *Fundamentals of high shear pelletisation process - PhD thesis*, Rijksuniversiteit Groningen (2001)
- J. Ramaker, M. Albada Jelgersma, P. Vonk, N. Kossen, Scaledown of a high shear pelletisation process: flow profile and growth kinetics. *International Journal of Pharmaceutics* 166 (1998) 89–97
- G.K. Reynolds, P.K. Le, A.M. Nilpawar, *Handbook of Powder Technology Chapter 1 High Shear Granulation*, Elsevier (2006) 1-23
- J.Ribet, *Fonctionnalisation des excipients : Application a la comprimabilité des celluloses et des saccharoses*, Thèse Université de Limoges, Faculté de Pharmacie
- M. Ritala, P. Holm, T. Schæfer, H.G. Kristensen, Influence of liquid bonding strength on power consumption during granulation in a high shear mixer, *Drug Dev.Ind.Pharm.* 14 (1988) 1041-1060
- M. Ritala, O. Jungersen, P. Holm, A comparison between binders in the wet phase of granulation in a high shear mixer, *Drug Dev. And Ind; Pharm.* 12 (1986) 1685-1700
- A. Royce, M. Mecadon, J. Holinej, A. Karnachi, S. Valazza and W. Wei, Process control and scale-up of high shear wet granulation, *The Journal of Process Analytical Technology* 2 (2005) (2) 8–16
- F. Rouquerol, J. Rouquerol, S. King, *Adsorption by powders and porous solids: Principles, methodology and applications*, Academic Press (1999)
- R.C. Rowe, Adhesion of film coating to tablet surfaces: a theoretical approach based on solubility parameters, *International Journal of Pharmaceutics* 41 (1988a) 219-222
- R. C. Rowe, Characterization of wet powder masses using a mixer torque rheometer. 4. Effect of blade orientation, *Int. J. Pharm.* 133 (1996) 133-138
- H. Rumpf, *Die Wissenschaft des Agglomerierens.*, *Chemie-Ingenieur-Technik* 46 (1974) 1–11
- H. Rumpf, *Methoden des granulieren*, *Chem. Eng. Technol.* 30 (1958) 144-158
- H. Rumpf, *Grundlagen und Methoden des Granulierens*, *Chemie-Ingenieur-Technik* 30 (1958) 144–158
- H. Rumpf, *Agglomeration: the strength of granules and agglomerates*, W.A. Keppner (1962)
- K. Saleh, L. Vialatte, P. Guigon, Wet granulation in a batch high shear mixer, *Chemical Engineering Science* 60 (2005), 3763-3775
- T. Schaefer, Growth mechanisms in melt agglomeration in high shear mixers, *Powder Technol.* 117 (2001) 68–82
- T. Schaefer, P. Holm, H. Kristensen, Melt pelletization in a high shear mixer. Part i. Effects of process variables and binder, *Acta Pharmaceutica Nordica* 4 (1992) 133–140

- T. Schæfer, C. Mathiesen, Melt pelletization in a high shear mixer: IX. Effects of binder particle size, *Int. J. Pharm.* 139 (1996) 139–148
- T. Schaefer, B. Taagegaard, L. Thomsen, H. Kristensen, Melt pelletization in a high shear mixer. Part V. Effects of apparatus variables. *European J. Pharm. Science* 1 (1993) 133–141
- H. Schubert, Grundlagen des Agglomerierens. *Chemie-Ingenieur-Technik* 51 (1979) 266–277
- Schubert, H., Tensile strength of agglomerates, *Powder Technol.* 11 (1975) 107-119
- D. Schulze, *Powders and bulk solids : behavior, characterization, storage and flow*, Springer Berlin Heidelberg (2008)
- J. Schwedes, Measurement of flow properties of bulk solids, *Powder Technol.* 88 (1996) 285-290
- J. Schwedes, Testers for measuring flow properties of particulate solids, *Powder Handling and Processing* 12 (4) (2000) 337-354
- A.C. Scott, M.J. Hounslow, T. Instone, Direct evidence of heterogeneity during high-shear granulation, *Powder Technol.* 113 (2000) 205–213
- D. K. Sidiras, D. P. Koullas, A. G. Vgenopoulos, E. G. Koukios, Cellulose crystallinity as affected by various technical processes, *Cellulose Chemistry and Technology* 24 (1990) 309–317
- R.H. Snow, T.Allen, J.D. Litster, B.J. Ennis, Size Reduction Size Enlargement, in R.H. Perry, D.W. Green (Eds), *Perry Chemical Engineers Handbook* (1997) McGraw-Hill, USA
- J.J. Sousa, A. Sousa, F. Podczek, J.M. Newton, Factors influencing the physical characteristics of pellets obtained by extrusion-spheronization, *Int. J. Pharm.* 232 (2002) 91-106
- C. Souto, R. Alvarez, R. Duro, A. Concheiro, J.L. Gomez-Amoza, R. Martinez-Pacheco, Versatility of mixer torque rheometry predictions in extrusion-spheronization, *Proc. 2nd World Meeting APGI/APV* (1998), 447-448
- T. Suzuki, H. Kikuchi, S. Yamamura, K. Terada, K. Yamamoto, The change in characteristics of microcrystalline cellulose during wet granulation using a high-shear mixer, *J. Pharm. Pharmacol.* 53 (2001) 609–616
- G. Tardos, Wet-granulation research with application to scale-up, *China Particuology*, 3 (3) (2005) 191-195
- The institution of chemical engineers, Standard shear testing technique for particulate solids using the shear cell, *IchemE* (1989)
- F. Thielmann, M. Naderi, M. A. Ansari, F. Stepanek, The effect of primary particle surface energy on agglomeration rate in fluidised bed wet granulation, *Powder Technol.* 181 (2008) 160–168
- R. Thies, P. Kleinebudde, Melt pelletisation of a hygroscopic drug in a high shear mixer: Part 1. Influence of process variables, *Int. J. of Pharm.* 188(2) (1999) 131-143
- J. Tomas, H. Schubert, Modeling of the strength and flow properties of moist soluble bulk materials, *Proceedings of International Symposium on Powder Technology '81 Kyoto* (1981), 118–124

J. Tomas, Adhesion of ultra fine particles-A micromechanical approach, *Chemical Engineering Science* 62 (2007) 1997-2010

J. Tomas, Zum Verfestigungsprozeß von Schüttgütern - Mikroprozesse, Kinetik-modelle und Anwendungen., *Chemie-Ingenieur-Technik* 69 (1997) 455-467

D.N. Travers, A.G. Rogerson, T.M. Jones, A torque arm mixer for studying wet massing, *J.Pharm.Pharmacol.* 27 Suppl. 3P (1975)

Z. Tüske, G. Regdon, Jr. Eris, I.S. Srčić, K. Pintye-Hódi, The role of the surface free energy in the selection of a suitable excipient in the course of wet-granulation method
Powder Technology 155 (2005) 139-144

C. Vecchio, G. Bruni, A. Gazzaniga, Preparation of Indobufen Pellets by Using Centrifugal Rotary Fluidized Bed Equipment Without Starting Seeds, *Drug Dev. Ind. Pharm.* 20 (12) (1994) 1943-1956

L. Vialatte, Mécanismes de granulation. Application à la granulation par agitation mécanique, PhD Thesis Université Technologique de Compiègne (1998)

P. Vonk, C.P.F. Guillaume, J.S. Ramaker, H. Vromans, N. Kossen, Growth mechanisms of high-shear pelletisation, *Int.J.Pharm.* 157 (1997) 93-102

T.-O. Vu, Dispersion d'une poudre dans un liquide : Caractérisation des interactions interfaciales et effets de différents facteurs sur la vitesse de dispersion, PhD thesis, Ecole Nationale Supérieure des Mines de Saint-Etienne (2002)

Résumé

Cette étude est dédiée à la compréhension du processus de granulation humide en mélangeurs à haut taux de cisaillement. Une étude systémique et méthodologique a été menée permettant l'investigation de l'influence des paramètres opératoires, de la technologie employée et des propriétés physico-chimiques des matières premières. Cette investigation est réalisée à travers des techniques de caractérisation morphologiques, rhéologiques et mécaniques. En reliant les courbes de couple enregistrés lors de la granulation humide à la cinétique de croissance des granules, aux caractérisations microscopiques et aux propriétés mécaniques des granules la prédiction du comportement lors de la granulation devient possible. La caractérisation des propriétés mécaniques des granules a été étudiée à deux échelles: à l'échelle du milieu humide la consistance a été caractérisée par un rhéomètre à torque et à l'échelle de l'agglomérat sec la résistance mécanique a été caractérisée par des mesures de compression directe des grains individuelles. Cette approche permet d'avoir des informations complémentaires permettant de mieux décrire l'évolution des courbes de couple dépendantes de propriétés de la masse humide et la compétition entre les forces interfaciales et visqueuses conditionnant la qualité des grains secs résultés. Les paramètres investigués par cette approche sont l'effet du taux de remplissage du réacteur, l'effet de la vitesse d'agitation, de la présence et de la conception de l'émoteur, de la conception du réacteur employé, des propriétés physico-chimiques de la solution liante et des propriétés des mélanges binaires des poudres hydro-solubles / hydro-insolubles.

Mots clés: Granulation humide, haut taux de cisaillement, mécanismes et cinétiques de croissance, rhéologie, résistance des granules, excipients pharmaceutiques

Abstract

This study is dedicated to the understanding of the wet granulation process in high shear mixers. A systematic study has been carried out that allows the investigation of the influence of operating conditions, technology and physico-chemical properties of the starting materials. This investigation is achieved by morphological, rheological and mechanical characterization methods. By linking recorded torque curves during the granulation process to granule growth kinetics, microscope characterizations and to the end-granule properties granulation outcome prediction becomes possible. The characterization of the mechanical properties has been done at two scales: at the granule bed scale the bulk wet mass consistency has been determined on a mixer torque rheometer, at the granule scale single dry granule direct compression tests were carried out. This approach gives complementary information allowing better description of the torque curves directly related to the wet mass properties and the competition between static and viscous forces conditioning the dry end granule quality. The factors investigated in this study are: the effect of fill ratio, impeller speed, chopper presence and design, mixer design, binder physico-chemical properties and formulation properties for binary water-soluble / water insoluble powder mixtures.

Keywords: wet granulation, high shear mixers, growth mechanisms and kinetics, rheology, granule strength, pharmaceutical excipients